RISK-BASED APPROACH FOR BRIDGE SCOUR PREDICTION

FINAL REPORT

Prepared for:

National Cooperative Highway Research Program
Transportation Research Board
National Research Council
Washington, D.C.

Dr. P.F. Lagasse (PI)
Ayres Associates
Fort Collins, Colorado

Dr. M. Ghosn (Co-PI)
CCNY/CUNY
New York, New York

Dr. P.A. Johnson (Co-PI)
Pennsylvania State University
University Park, Pennsylvania

Dr. L.W. Zevenbergen
Ayres Associates
Fort Collins, Colorado

Mr. P.E. Clopper
Ayres Associates
Fort Collins, Colorado

October 2013

RISK-BASED APPROACH FOR BRIDGE SCOUR PREDICTION

FINAL REPORT

Prepared for:

National Cooperative Highway Research Program
Transportation Research Board
National Research Council
Washington, D.C.

Dr. P.F. Lagasse (PI)
Ayres Associates
Fort Collins, Colorado

Dr. M. Ghosn (Co-PI)
CCNY/CUNY
New York, New York

Dr. P.A. Johnson (Co-PI)
Pennsylvania State University
University Park, Pennsylvania

Dr. L.W. Zevenbergen
Ayres Associates
Fort Collins, Colorado

Mr. P.E. Clopper
Ayres Associates
Fort Collins, Colorado

AYRES ASSOCIATES

P.O. Box 270460
Fort Collins, Colorado 80527
(970) 223-5556, FAX (970) 223-5578

Ayres Project No. 32-1508.00
24-34-PDFR-TXT10-REV-10-21-13.docx

October 2013

TABLE OF CONTENTS

LIST OF FIGURES

LIST OF TABLES

(page intentionally left blank)

ACKNOWLEDGMENTS

This work was sponsored by the American Association of State Highway and Transportation Officials, in cooperation with the Federal Highway Administration (FHWA), and was conducted through the National Cooperative Highway Research Program (NCHRP), which is administered by the Transportation Research Board (TRB) of the National Research Council (NRC).

The research reported herein was performed under NCHRP Project 24-34 by Ayres Associates, Fort Collins, Colorado. Dr. P.F. Lagasse, Senior Vice President, served as Principal Investigator. Dr. Michel Ghosn (CCNY/CUNY) and Dr. Peggy Johnson (Pennsylvania State University) served as Co-Principal Investigators. They were assisted by Dr. L.W. Zevenbergen, Manager of River Engineering at Ayres Associates (currently Program Manager/Hydraulic Engineer, Tetra Tech) and Mr. P.E. Clopper, Senior Water Resources Engineer at Ayres Associates.

The authors wish to acknowledge the contributions of Mr. Will deRosset of Ayres Associates and Dr. David Zachmann, Consultant in developing the rasTool© software that links the U.S. Army Corps of Engineers 1-Dimensional hydraulic model with Monte Carlo simulation techniques. This linkage was integral to achieving project objectives. A Technical Advisory Team consisting of Dr. D.T. Williams, Dr. R. Ettema, Mr. Arun Shirole, and Mr. Harry Capers provided input at the outset of the project and/or periodic review of draft project documents. The participation, advice, and support of NCHRP Panel members throughout this project are gratefully acknowledged.

Panel member Dennis D. Stuhff, who passed away suddenly on June 27, 2012, is respectfully acknowledged for his contributions to this project. Mr. Stuhff was known for his depth of knowledge of bridge structures, hydraulics, and environmental engineering; for his commitment to improving highway safety for the people of Utah; and for contributing to advancing the state of practice in his chosen disciplines through activities such as serving on the panel for NCHRP Project 24-34. The research team would like to dedicate this report to Mr. Stuhff.

DISCLAIMER

(page intentionally left blank)

ABSTRACT

This report documents the results of an investigation of risk-based approaches for bridge scour prediction. The uncertainties associated with bridge scour prediction, including hydrologic, hydraulic, and model/equation uncertainty were identified and evaluated. An essential element of the research was the development of software that links the most widely used 1-Dimensional hydraulic model (HEC-RAS) with Monte Carlo simulation techniques. A set of tables of probability values (scour factors) is presented that allow associating an estimate of scour depth with a conditional (single event) probability of exceedance when a bridge meets certain criteria for hydrologic uncertainty, bridge size, and pier size. The tables address pier scour, contraction scour, abutment scour, and total scour. For complex foundation systems and channel conditions, a step-by-step procedure is presented to provide scour factors for site-specific conditions. An integration technique that incorporates the uncertainties associated with the conditional probability of a limited number of return period flood events provides a reliability analysis framework for estimating the unconditional probability of exceeding a design scour depth over the service life of a bridge. A set of detailed illustrative examples demonstrate the full range of applicability of the methodologies. A stand-alone Reference Guide (NCHRP Report 761) is available to aid the practitioner in the application of the probability-based methodologies presented in this report.

(page intentionally left blank)

RISK-BASED APPROACH FOR BRIDGE SCOUR PREDICTION

SUMMARY

Overview

This research accomplished its basic objectives of developing a risk/reliability-based methodology that can be used in calculating bridge pier, abutment, contraction, and total scour at waterway crossings so that scour estimates can be linked to a probability. The developed probabilistic procedures are consistent with LRFD approaches used by structural and geotechnical engineers.

Load and Resistance Factor Design (LRFD) incorporates state-of-the-art analysis and design methodologies with load and resistance factors based on the known variability of applied loads and material properties. These load and resistance factors are calibrated from actual bridge statistics to ensure a uniform level of safety over the life of the bridge. LRFD allows a bridge designer to focus on a design objective or limit state, which can lead to a similar probability of failure in each component of the bridge. Bridges designed with the LRFD specifications should have relatively uniform safety levels, which should ensure superior serviceability and long-term maintainability.

There is wide-spread belief within the bridge engineering community that unaccounted- for biases, and input parameter and hydraulic modeling uncertainty lead to overly conservative estimates of scour depths. The perception is that this results in design and construction of costly and unnecessarily deep foundations. This research project closed the gap between perception and reality and provides risk/reliability-based confidence bands for bridge scour estimates that align the hydraulic design approach with the design procedures currently used by structural and geotechnical engineers. Hydraulic engineers now have the option of and ability to perform scour calculations that incorporate probabilistic methods into the hydraulic design of bridges.

Research Approach

The research approach involved the following steps:

1. Completion of a literature review and evaluation of current practice in the areas of hydrologic and hydraulic analyses for bridge scour prediction, including the use of probabilistic methods in hydrologic and hydraulic engineering. The review included other disciplines where risk and reliability analyses have been incorporated into engineering design, with emphasis on LRFD approaches used by structural and geotechnical engineers.

2. Investigation of the application of reliability theory to the determination of bridge scour prediction and the quantity and quality of data available to support the objectives of this project.

3. Identification and evaluation of uncertainty associated with the variables and approaches used in bridge scour prediction, including hydrologic, hydraulic, and model/equation uncertainty.

4. Development of a conceptual approach for the implementation phase of the research and production of research-level software the links the most widely used 1-Dimensional hydraulic model (HEC-RAS) with Monte Carlo simulation techniques.

5. Development of a set of tables of probability values (scour factors) that can be used to associate an estimate of scour depth with a conditional (single event) probability of exceedance when a bridge meets certain criteria for hydrologic uncertainty, bridge size, and pier size. In total, more than 300,000 HEC-RAS/Monte Carlo simulations were required to produce the statistics on which the 27-element matrix in Appendix A is based. In addition, more than 300,000 scour calculations for each of the scour equations were completed off-line (i.e., more than 1.2 million off-line scour calculations).

6. For complex foundation systems and channel conditions, development of a step-by-step procedure that provides an approach for developing probability-based estimates and scour factors for site-specific conditions.

7. Development of an integration technique that incorporates the uncertainties associated with a conditional probability prediction into a reliability analysis framework to estimate the unconditional probability of exceedance for a selected service life of a bridge. Both a direct Monte Carlo approach and a fitted distribution approach are presented.

8. Providing a set of detailed illustrative examples to demonstrate the full range of applicability of the methodologies.

9. Production of a stand-alone Reference Guide to aid the practitioner in the application of the probability-based methodologies developed by this research.

10. Identification of additional research that would expand the findings of this project and suggestions for implementing the results of this research.

Appraisal of Research Results

The primary purpose of this project was to analyze the probability of scour depth exceedance, not the probability of bridge failure. The latter requires advanced analyses of the weakened foundation under the effects of the expected applied loads which was beyond the scope of this project.

This research project developed and implemented a work plan that produced significant results of practical use to the bridge engineering community. The final outcome of this project was the development of a "Level I" approach that consists of a set of tables of probability values or scour factors that can be used to associate an estimated scour depth provided by the hydraulic engineer with a probability of exceedance for simple pier and abutment geometries. For complex foundation systems and channel conditions, or for cases requiring special consideration, this project provided a "Level II" approach that consists of a step-by-step procedure that hydraulic engineers can follow to provide probability-based estimates of site-specific scour factors. In order to develop the probability-based estimates or scour factor tables for each scour component and to develop the Level II approach, an understanding of the uncertainties associated with the prediction of individual scour components was required.

In addition, these uncertainties were incorporated into a reliability analysis framework to estimate the probability of scour level exceedance for the service life of a bridge. The reliability analysis for scour is consistent with the reliability analysis procedures developed and implemented by AASHTO LRFD/LRFR for calibrating load and resistance factors for bridge structural components and bridge structural systems as well as foundations.

The goals of this study were achieved. A methodology is now available that can be used to link scour depth estimates to a probability and determine the risk associated with scour depth exceedance for a given design event. The probability linkage considers the propagation of uncertainties among the parameters that are used to quantify the confidence of scour estimates for a design event (e.g., a 100-year flood) based on uncertainty of input parameters and considering model uncertainty and bias. In addition, this methodology has been extended to provide an initial estimate of target reliability for the design life of a bridge consistent with LRFD approaches used by structural and geotechnical engineers. This Final Report is supplemented by a separate "Reference Guide" to aid practitioners in applying the results of this research (NCHRP Report 761 2013).

(page intentionally left blank)

CHAPTER 1

1. INTRODUCTION AND RESEARCH APPROACH

1.1 Scope and Research Objectives

1.1.1 Scope

Load and Resistance Factor Design (LRFD) incorporates state-of-the-art analysis and design methodologies with load and resistance factors based on the known variability of applied loads and material properties. These load and resistance factors are calibrated from actual bridge statistics to ensure a uniform level of safety over the life of the bridge. LRFD allows a bridge designer to focus on a design objective or limit state, which can lead to a similar probability of failure in each component of the bridge. Bridges designed with the LRFD specifications should have relatively uniform safety levels, which should ensure superior serviceability and long-term maintainability. Bridge hydraulic engineers should have the option of and ability to perform scour calculations that incorporate similar probabilistic methods.

There is wide-spread belief within the bridge engineering community that unaccounted- for biases, and input parameter and hydraulic modeling uncertainty lead to overly conservative estimates of scour depths. The perception is that this results in design and construction of costly and unnecessarily deep foundations. This research project offered a unique opportunity to close the gap between perception and reality and provide risk/reliability-based confidence bands for bridge scour estimates that will align the hydraulic design approach with the design procedures currently used by structural and geotechnical engineers.

1.1.2 Objectives

The primary objective of this research was to develop a risk/reliability-based methodology that can be used in calculating bridge pier, abutment, and contraction scour at waterway crossings so that scour estimates can be linked to a probability. The developed probabilistic procedures should be consistent with LRFD approaches used by structural and geotechnical engineers.

1.2 Research Approach

1.2.1 Overview

The challenge of this research project was to develop and implement an effective work plan that produced significant results of practical use to the bridge engineering community. The final outcome of this project was the development of a "Level I" approach that consists of a set of tables of probability values or scour factors that can be used to associate the estimated scour depth provided by the hydraulic engineer with a probability of exceedance for simple pier and abutment geometries. For complex foundation systems and channel conditions, or for cases requiring special consideration, this project provided a "Level II" approach that consists of a step-by-step procedure that hydraulic engineers can follow to provide probability-based estimates of site-specific scour factors. In order to develop the probability-based estimates or scour factor tables for each scour component and to develop the Level II approach, an understanding of the uncertainties associated with the prediction of individual scour components was required.

The goals of this study were to develop a methodology that can be used to link scour depth estimates to a conditional probability of exceedance and extend this methodology to provide a preliminary approach for determining an unconditional target reliability for the service life of a bridge. In this study, the probability linkage considers the propagation of uncertainties among the parameters that are used to quantify the confidence of scour estimates for a specific design event (for this study, a 100-year flood) based on uncertainty of input parameters and considering model uncertainty and bias. In addition, these uncertainties were incorporated into a reliability analysis framework to provide an initial estimate of a target reliability for the design life of a bridge consistent with LRFD approaches used by structural and geotechnical engineers. This Final Report is supplemented by a separate "Reference Guide" to aid practitioners in applying the results of this research.

The primary purpose of this project was to analyze the probability of scour depth exceedance, not the probability of bridge failure. The latter requires advanced analyses of the weakened foundation under the effects of the expected applied loads which is beyond the scope of this project.

1.2.2 Research Tasks

The following specific tasks were completed to accomplish the project objectives:

PHASE I

Task 1 – Review the Technical Literature
Task 2 – Define and Discuss Application of Reliability Theory to Scour Prediction
Task 3 – Identify and Evaluate Uncertainty Associated with Scour Prediction
Task 4 – Develop Conceptual Approach and Phase II Work Plan
Task 5 – Interim Report and Panel Meeting

PHASE II

Task 6 – Execute Approved Work Plan
Task 7 – Prepare Detailed Report on Task 6 Results
Task 8 – Recommend Future Research Needs
Task 9 – Develop Detailed Illustrative Examples
Task 10 – Submit Final Report

1.2.3 Organization of the Final Report

Chapter 2 of this report provides a discussion of the various types and sources of uncertainty that must be considered in the assessment of bridge scour. In each section of this chapter, relevant citations from the literature are discussed to provide background information on the current state of practice. The three components of scour addressed in this study (pier, contraction, and abutment scour) are fundamentally linked to both the hydrologic estimation of the magnitude of a design flood event and the anticipated hydraulic conditions associated with that event. Hydrology (Section 2.2) and hydraulics (Section 2.3) both introduce uncertainties in the determination of the variables that are subsequently used as input to the various scour equations. The scour equations themselves have uncertainty, as evidenced by the fact that even under controlled laboratory conditions, the equations do not precisely predict the observed scour (Section 2.5). Lastly, framing the scour problem within the context of the AASHTO LRFD statistical methods and procedures used in bridge structural design is discussed in Section 2.6.

Chapter 3 describes an approach to evaluating the uncertainty of the three scour components. The approach is based on Monte Carlo Simulation (MCS) linked directly with the most common and widely-accepted hydraulic model used in current practice, HEC-RAS, and is described in Section 3.2. For each individual scour component, the parameters that were allowed to vary in the MCS are discussed in Section 3.3, along with a listing of other factors and/or considerations which were not addressed in this study. The chapter concludes with Section 3.4 which discusses how the model Bias and Coefficient of Variation (COV) were incorporated into the scour predictions using the results of the MCS.

Chapter 4 presents a summary of the data sets used in developing model bias and COV for each of the three individual scour components, the data screening and analysis procedures, and the results of the analyses. For pier scour (Section 4.1), both the HEC-18 and Florida Department of Transportation (FDOT) equations were assessed using comprehensive data sets from both laboratory and field studies. Contraction scour (Section 4.2) used the HEC-18 equation for clear-water scour with laboratory data only. Abutment scour (Section 4.3) used the NCHRP 24-20 approach (which is also recommended in the most recent edition of HEC-18) with laboratory data only.

Chapter 5 presents a description of the HEC-RAS hydraulic model, and a detailed discussion of the linkage between the hydraulic model HEC-RAS and the Monte Carlo Simulation software. The calibration and testing of the linked model using data from a bridge on the Sacramento River is described, along with a discussion of the results for pier, contraction, and abutment scour considering hydrologic uncertainty, hydraulic uncertainty, and scour prediction (model) uncertainty.

Chapter 6 provides two approaches for assessing the conditional probability that the design scour depth will be exceeded for a given design flood event. Either approach can be used to estimate this probability for each of the three individual scour components. The first approach ("Level I") assumes that the practitioner can categorize a bridge based on three general conditions: (1) the size of the bridge, channel, and floodplain (small, medium or large), (2) the size of the piers (small, medium, or large), and (3) the hydrologic uncertainty (low, medium, or high). The Level I approach provides scour factors which can be used to multiply the estimated scour depth to achieve a desired level of confidence based on the reliability index β, commensurate with standard LRFD practice. Scour factors are provided in tabular format for each of the individual scour components for all 27 combinations of the three category conditions for simple pier and abutment geometries (Appendix A). On the other hand, when the practitioner cannot match a particular site to the categories described above, a Level II approach is required. The Level II approach is necessarily site-specific and is summarized in this chapter. The Level II approach is identical to the procedure used on the Sacramento River bridge as described in Chapter 5.

Chapter 7 provides five illustrative examples using the Level I approach to: (1) categorize a bridge site; (2) estimate pier, contraction, abutment, and total scour; and (3) identify the appropriate scour factors for a desired level of confidence using the results provided in Chapter 6 and the information in Appendix A. Examples are presented for a range of bridge configurations and hydrologic/geomorphic settings where hydraulic input is developed from both 1-D and 2-D models.

Chapter 8 presents a methodology to determine the unconditional probability that a scour estimate will not be exceeded over the remaining service life of an existing bridge, or the design life of a new bridge. It is recognized that over the remaining life of a bridge, it will be exposed

to a wide range of flows. Most of these flows will be less than the design event; however, there is a small but finite chance that some will be larger. The proposed methodology uses the conditional probabilities of the design scour depth being exceeded for a limited number of return period flood events. The conditional probabilities are then integrated to determine the unconditional probability of exceedance over the entire service life (Section 8.1). In Section 8.2, the results from five case studies (using pier scour as an example) are presented in detail to validate the proposed approach. In Section 8.3, the integration method is implemented for pier scour (both HEC-18 and FDOT methods), contraction scour (HEC-18 method), combined pier and contraction scour, and abutment scour. Section 8.4 concludes this chapter with a summary of scour factors for a 75-year service life for various target levels of the reliability index β. Both a direct Monte Carlo approach and a fitted distribution approach are presented.

Chapter 9 identifies and discusses research needs that involve topics beyond the scope of this study that would extend the results and usefulness of this research.

Chapter 10 presents conclusions, observations, and recommendations related to issues, considerations, and results encountered during the conduct of this research project. An implementation plan for the results of the this research is outlined.

Chapter 11 presents the References Cited in the Final Report.

Appendix A presents a summary of scour factors in tabular and graphical form for use with the Level I approach described in Chapter 6.

Appendix B is a Detailed Problem Statement for a laboratory contraction scour study.

Appendix C provides a Glossary of terms used in this report. The Glossary is presented in two parts: (1) Hydrologic, Hydraulic, and Geomorphic terms, and (2) Probability and Statistical terms.

Additional guidance in applying the results of this research can be found in the "Reference Guide for Applying Risk and Reliability-Based Approaches for Bridge Scour Prediction" published as NCHRP Report 761 (Lagasse et al. 2013).

CHAPTER 2

2. UNCERTAINTY IN HYDRAULIC DESIGN

2.1 Introduction

As a basis for providing bridge hydraulics engineers the ability to perform scour calculations that incorporate probabilistic methods, the relevant literature, practice, and research findings in the areas of hydrologic and hydraulic analysis and bridge scour prediction were reviewed. The results of this review are summarized in the following sections. Other disciplines related to bridge design and safety evaluation where risk and reliability approaches are being integrated into engineering design were also explored and documented.

2.2 Hydrologic Uncertainty

2.2.1 Overview

The majority of hydrologic phenomena, such as droughts and floods, precipitation, dewpoint, etc. are stochastic processes, which can be characterized as processes governed by laws of chance. Strictly speaking, there are no pure deterministic hydrologic processes in nature; hydrologic phenomena have traditionally been understood and described using methods of probability theory (Yevjevich 1972).

Scour prediction is typically associated with a design hydrologic event that has a given likelihood of recurrence, e.g., the 100-year flood. Hydraulic conditions from such an event, in terms of the depth and velocity of flow corresponding to the peak rate of flow, are used to predict local and contraction scour at the bridge using methods described in HEC-18 (Arneson et al. 2012). This scour prediction is in turn used for determining structural stability for the case where all the soil material in the scour prism is removed. Usually the time rate of scour is ignored and scour is assumed, in effect, to occur instantaneously in response to the peak hydraulic load for the event of interest.

Practitioners understand that the 100-year flood is defined as the discharge rate that has a 1% chance of being equaled or exceeded in any given year; the 50-year flood has a 2% probability of exceedance, etc. Typically, the discharge is estimated based on flow records from stream gaging stations upstream or downstream of the bridge, and are adjusted to the bridge location using area-weighting and other techniques. Where gaging station records on the particular stream or river are not available, data from stations in nearby watersheds of similar size and nature to the watershed of interest are used. In many cases, regional regression relationships are available for use, and typically include watershed area and a rainfall index (such as the 2-year, 24-hour rainfall depth) as input values to the regression equations.

While practitioners understand that the magnitude of any recurrence-interval event is an *estimate*, the current state of practice in bridge scour prediction places no emphasis on quantifying the *reliability* of that estimate. Typically, when scour assessments are performed for a new or existing bridge, it is almost never the case that we consider and incorporate the *confidence* we have in our estimates of flood discharge. However, it has been standard practice to report the 95% confidence limits as part of Bulletin 17B, U.S. Geological Survey (1981) methodology for nearly half a century. As with any probability-based estimate, confidence in the predicted value of the 100-year flood increases with the number of observations from the population of discharges. Regional regression relationships often include a measure of uncertainty about the predicted recurrence-interval values.

NCHRP Report 717, "Scour at Bridge Foundations on Rock," (Keaton et al. 2012) provides an example to illustrate this issue. For that project, four field sites were investigated where the erodibility of rock at bridge pier foundations was assessed. One site, State Route 22 over Mill Creek in western Oregon, has exhibited approximately 7 feet of scour over the period from December 1945 to August 2008. Data from the USGS gaging station upstream of the bridge is available from its installation in 1958 until the station was discontinued in 1973, so only 15 years of mean daily flows and annual instantaneous peaks are available from that location. The time series was extended by regression analysis using data from stations on the South Yamhill River, located further downstream. This technique provided additional data necessary to assess the cumulative hydraulic loading experienced by the bridge to the present time. The resulting time series of mean daily flows is provided in **Figure 2.1**.

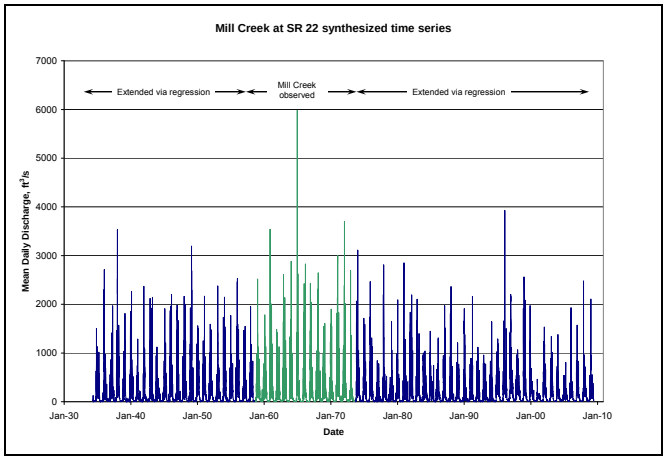

Figure 2.1. Mean daily flows, Mill Creek at SR 22 showing observed and extended records.

The data from other gaging stations allowed the period of record to be extended from 1935 through 2008 (74 years) for purposes of quantifying the cumulative hydraulic loading from the time the bridge was built to the present. Figure 2.1 clearly shows that the single largest flood event in the entire period of record (mean daily flow of 5,980 ft^3/s, with an instantaneous peak of 7,320 ft^3/s) occurred during the period of time when the Mill Creek gaging station was active. All other mean daily flows for the 74-year period are less than 4,000 ft^3/s.

The USGS flood frequency analysis software PKFQWin (Flynn et al. 2006) was used to estimate the magnitudes of various recurrence-interval floods using Bulletin 17B methodology, assuming a Log-Pearson Type III probability distribution. The generalized skew of 0.086 at this location was combined with the observed station skew to produce a weighted skew for use with this probability distribution, for both the 15- and 74-year periods of record. **Table 2.1** presents the results of these flood frequency analyses.

Figure 2.2 presents the predicted frequency curves and associated 95% confidence limits for the 15 years of observed annual peaks and also for the entire 74-year extended period of record. As seen in this figure, the estimates of the recurrence-interval flood magnitude, and the corresponding confidence limits, are quite different for the two periods of record considered.

Table 2.1. Flood Frequency Analyses for SR 22 Over Mill Creek, Oregon.						
Recurrence Interval (yrs)	15-Year Period Weighted Skew = 0.159			74-Year Period Weighted Skew = 0.253		
	Discharge (ft^3/s)	95% Confidence		Discharge (ft^3/s)	95% Confidence	
		Lower	Upper		Lower	Upper
1.5	3,142	2,633	3,629	2,806	2,653	2,954
2	3,630	3,116	4,220	3,138	2,981	3,302
5	4,858	4,182	5,995	3,946	3,734	4,205
10	5,686	4,811	7,384	4,472	4,197	4,827
25	6,752	5,562	9,344	5,132	4,761	5,634
50	7,561	6,102	10,940	5,622	5,171	6,247
100	8,384	6,633	12,650	6,113	5,575	6,871
500	10,380	7,860	17,120	7,275	6,514	8,383

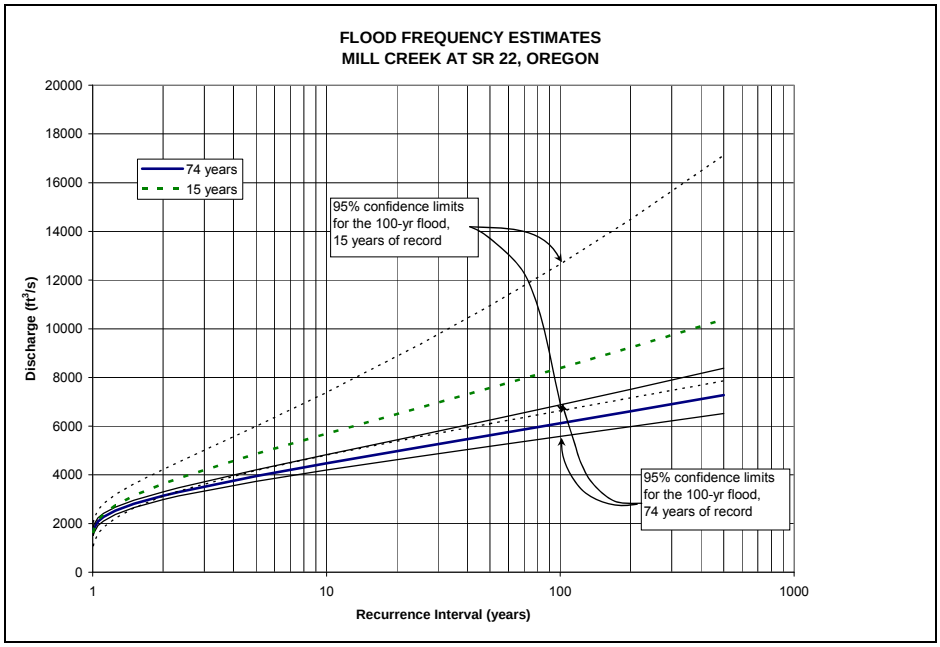

Figure 2.2. Flood frequency estimates for 15- and 74-year periods of record, SR 22 over Mill Creek, Oregon.

Table 2.1 and Figure 2.2 illustrate how the confidence limits associated with a Log-Pearson Type III probability distribution are sensitive to the number of observations, and how the confidence interval becomes wider as the recurrence interval increases. For smaller, more frequent events, the reliability of the discharge estimate is greater than for larger, less frequent floods.

For purposes of predicting scour, flow discharge in and of itself is not a meaningful variable. What is important is the hydraulic load associated with the discharge. For example, the calculation of pier scour using the HEC-18 equation uses the depth and velocity of flow as the only hydraulic variables. Depth and velocity are both related to discharge through transform functions that are usually derived from HEC-RAS modeling (USACE 2010), or in some cases, 2-dimensional models. The depth and velocity transforms for SR 22 over Mill Creek in Oregon were developed using a HEC-RAS model of the bridge reach, and are shown in **Figure 2.3**.

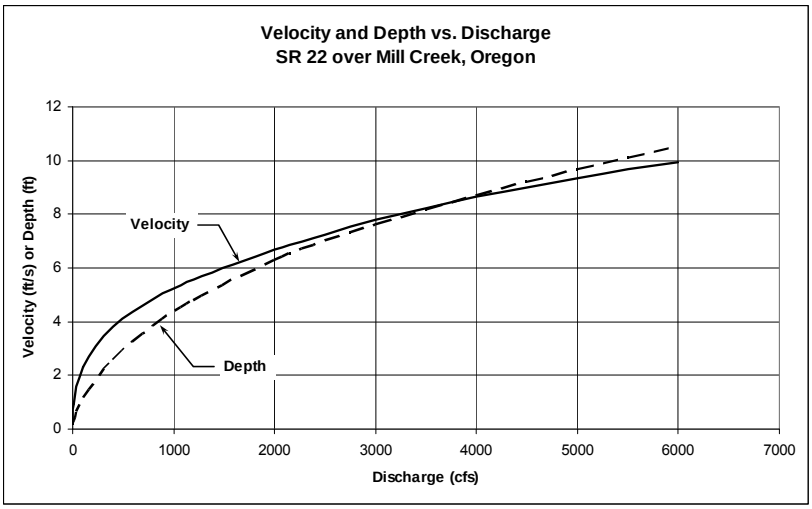

Figure 2.3. Depth and velocity vs. discharge, SR 22 over Mill Creek, Oregon.

The HEC-18 pier scour equation is:

$$y_s = 2y_1K_1K_2K_3\left(\frac{a}{y_1}\right)^{0.65} F_r^{0.43} \qquad (2.1)$$

where:

y_s	=	Scour depth
y_1	=	Approach flow depth, a is the pier width normal to the flow velocity
K_1, K_2, K_3	=	Coefficients that are independent of hydraulic conditions
F_r	=	Froude number given by:

$$F_r = \frac{V}{\sqrt{gy_1}} \qquad (2.2)$$

where:

g	=	Gravitational acceleration constant
V	=	Mean velocity of flow directly upstream of pier

The predicted depth of pier scour is seen to be directly proportional to $(\text{depth})^{0.135}$ times $(\text{velocity})^{0.43}$. Given the transform functions for a particular site, the relationship of hydrologic uncertainty to estimated scour uncertainty can be explored (assuming that the HEC-18 model is accurate and that the uncertainties are only in the hydrologic input).

From Figure 2.3, at higher discharges on Mill Creek the rate of change of both depth and velocity are relatively insensitive to a change in discharge. For example, at the estimated 100-year discharge of 6,113 ft^3/s, a 10% change in discharge results in a 5.7% change in depth and a 4.9% change in velocity. Therefore, a 10% increase in discharge would produce only a 2.8% increase in the predicted pier scour at this location.

In summary, the characteristics of the probability distribution typically used in flood frequency analyses (Log-Pearson Type III) are well known and described. The sensitivity of predicted scour to uncertainty in discharge is also well characterized. This result is well suited to LRFD procedures for establishing a probability-based characterization of scour using standard

practices in hydrologic analysis. Clearly, an understanding of and ability to characterize sources of hydrologic uncertainty are central to probability-based bridge scour predictions.

2.2.2 Evaluating Hydrologic Uncertainty

Flood Frequency Estimates From Gaging Station Data. As discussed above, characteristics of the probability distribution typically used in flood frequency analyses (Log-Pearson Type III) are well known and described. Uncertainty in hydrologic estimates can, therefore, be easily incorporated within the framework of existing LRFD procedures to establish a probability-based characterization of scour using standard practices in hydrologic analysis.

The USGS software package PKFQWin can be used to determine hydrologic uncertainty when dealing with data from gaged sites. The software is a public-domain, Windows-based program that allows the user to access annual peak flow records in standard USGS format. Flood frequency estimates, as well as the 95% confidence limits about the estimated values, are part of the PKFQWin output files. From the USGS gaging station identifier, PKFQWin identifies the generalized skew based on location (latitude and longitude) and computes the actual station skew using the observed record from the site. These values are then used to compute a weighted skew value in accordance with USGS Bulletin 17B procedures.

Flood Frequency Estimates From Regional Regression Equations. The USGS has developed and published regression equations for every State, the Commonwealth of Puerto Rico, and a number of metropolitan areas in the United States. The National Streamflow Statistics (NSS) software compiles all current U.S. Geological Survey (USGS) regional regression equations for estimating streamflow statistics at ungaged sites in an easy-to-use interface that operates on computers with Microsoft Windows operating systems. NSS expands on the functionality of the USGS NFF Program, which it replaces.

The regression equations included in NSS (Ries 2007) are used to transfer streamflow statistics from gaged to ungaged sites through the use of watershed and climatic characteristics as explanatory or predictor variables. Generally, the equations were developed on a statewide or metropolitan-area basis as part of cooperative study programs. The NSS output also provides indicators of the accuracy of the estimated streamflow statistics. The indicators may include any combination of the standard error of estimate, the standard error of prediction, the equivalent years of record, or 90% prediction intervals, depending on what was provided by the authors of the equations.

NSS is a public-domain software program that can be used to:

- Obtain estimates of flood frequencies for sites in rural (non-regulated) ungaged basins.
- Obtain estimates of flood frequencies for sites in urbanized basins.
- Estimate maximum floods based on envelope curves.
- Create hydrographs of estimated floods for sites in rural or urban basins and manipulate the appearance of the graphs.
- Create flood-frequency curves for sites in rural or urban basins and manipulate the appearance of the curves.
- Quantify the uncertainty of flood frequency estimates.
- Obtain improved flood-frequency estimates for gaging stations by weighting estimates obtained from the systematic flood records for the stations with estimates obtained from regression equations.

- Obtain improved flood-frequency estimates for ungaged sites by weighting estimates obtained from the regression equations with estimates obtained by applying the flow per unit area for an upstream or downstream gaging station to the drainage area for the ungaged site.

2.3 Hydraulic Uncertainty

2.3.1 Overview

As discussed in the previous section on hydrologic uncertainty, hydraulic conditions associated with the design event must be determined in order to estimate scour depths. At a particular location, such as a pier, the hydraulic parameters of flow depth and velocity are related through the Manning n resistance factor and the local energy slope. From these basic parameters, other hydraulic variables such as Froude Number, shear stress, shear velocity, stream power, etc. are calculated. The distribution of flow and velocity within the main channel or between the main channel and overbank (floodplain) is highly sensitive to the river reach geometry and the choice of Manning n used to characterize these areas.

Figure 2.4 shows a bridge opening approach cross section and the associated velocity distributions from a HEC-RAS model (USACE 2010), which bases flow distribution on conveyance. A change in geometry or in Manning n would result in a different flow distribution between channel and floodplain (impacting the contraction scour) and the magnitudes of the computed velocities (impacting local pier and abutment scour).

However, whether simple models (e.g., Manning's equation) or more sophisticated approaches (HEC-RAS, FESWMS, etc.) are used to estimate the hydraulic conditions at a particular site and at a particular discharge, such estimates necessarily result from a simplification of the complex physical processes involved with open-channel flow. There are several broad categories of uncertainty that are common to any design process. These can be described as follows:

Model Uncertainty. This results from attempting to describe a complex physical process or phenomenon through the use of a simplified mathematical expression. Model uncertainty in scour analysis is the result of selecting a particular scour equation to estimate scour. Each equation has bias that causes it (on average) to over- or under-predict scour for certain situations.

Parameter Uncertainty. This type of uncertainty results from difficulties in estimating model parameters. For example, Manning's roughness coefficient and design discharge are two common parameters that cannot be measured directly; therefore, they must be estimated or assumed. The result is parameter uncertainty. Examples of hydraulic models used in bridge designs include HEC-RAS (USACE 2010) and FESWMS-FST2DH (Froehlich 2003). Each of these models has strengths and weaknesses that can lead to more or less parameter uncertainty based on the particular bridge, road embankment and river conditions. Parameter uncertainty can be reduced by using more sophisticated models, such as 2-D models, for more complex situations or by calibrating the model to measured conditions. **Figure 2.5** shows velocity contours from a complex hydraulic location (I-35W crossing the Mississippi River in Minneapolis, Minnesota). The more complete representation of the physics of flow in the 2-D model made it possible to simulate flow releases from the gates of the lock and dam upstream of the bridge. The 2-D model reduced parameter uncertainty (including angle of attack) for the scour analysis.

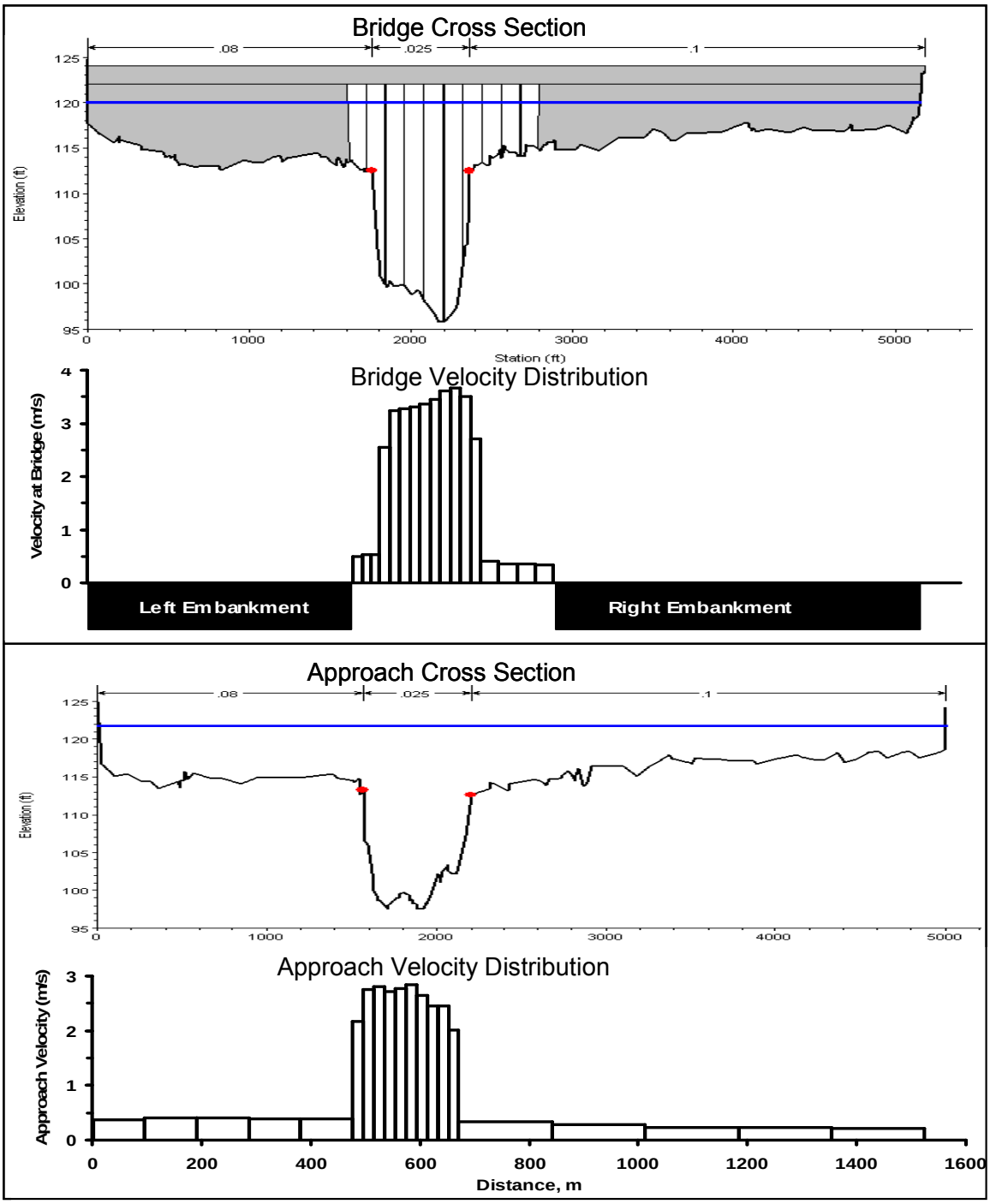

Figure 2.4. Flow distribution from 1-D hydraulic modeling.

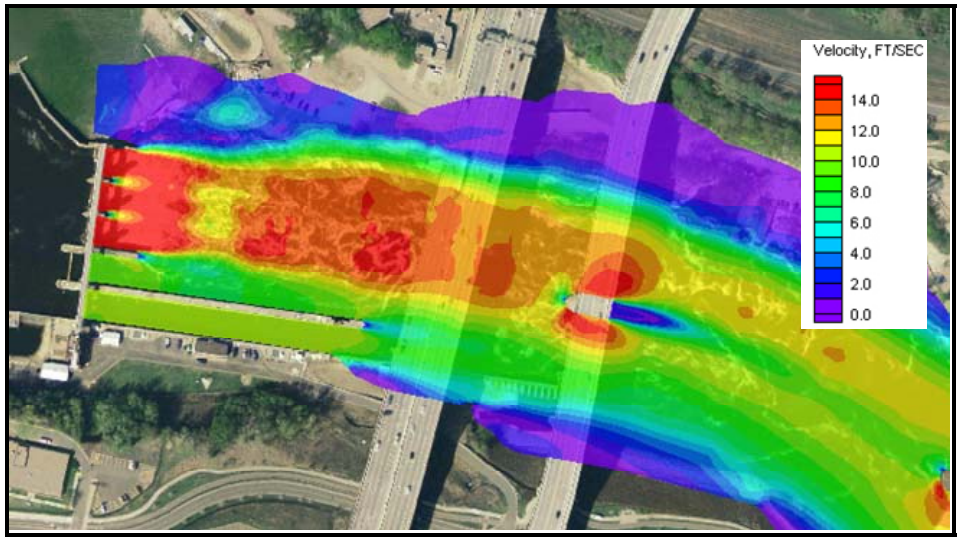

Figure 2.5. Velocity contours from 2-D modeling (I-35W Mississippi River).

Randomness. Natural (or inherent) randomness is a source of uncertainty that includes random fluctuation in parameters, such as flow discharges and velocities. Other types of randomness may be changes to floodplain vegetation that occur over time (seasonally or over the life of the bridge).

Human Error. There is always potential for human error in design and in the actual implementation of a design. This type of uncertainty includes calculation and construction errors. Human errors are not usually considered in current reliability-based calculation of load and resistance factors, but their possible occurrence may be considered during the selection of the target reliability levels in the code calibration process.

2.3.2 Evaluating Hydraulic Uncertainty

Hydraulic parameters, such as roughness coefficient, channel or energy slope, and critical shear stress, common to many hydraulic engineering problems, are known to contain considerable uncertainty. A common way to express uncertainty is through the coefficients of variation and associated distributions of parameters. Johnson (1996a) quantified uncertainty in common hydraulic parameters based on data from the scientific literature, experiments, and field observations.

The study resulted in **Table 2.2**, which provides the coefficient of variation, distribution, and reference or method by which these data were determined. In the table, where two values are included, the values represent either a different assumed probability distribution or a different situation. Of course, in a hydraulic model used for bridge design, several Manning n values will be used, including channel, left overbank and right overbank. These Manning n values have their own uncertainty which may be different. The channel Manning n may be calibrated for frequent bankfull flows and the overbank Manning n values may be selected based on experience or by comparison with published values. This table has been cited numerous times in risk, reliability, and other studies since the time it was published, and has been the basis for parameter input for bridge scour, levee and dam overtopping, and other hydrodynamic studies.

Table 2.2. Uncertainty of Hydraulic Variables (Johnson 1996a).			
Variable	Coefficient of Variation	Distribution	Reference or Method
Manning n	0.1, 0.15	Normal	Cesare 1991
Manning n	0.2, 0.053	Normal	Mays and Tung 1992
Manning n	0.08	Triangular	Yeh and Tung 1993
Manning n	0.10, 0.055	Triangular, gamma	Tung 1990
Manning n	0.20-0.35	Lognormal	HEC 1986
Manning n	0.28, 0.18	Uniform	Johnson 1996a
Channel Slope	0.3, 0.068	Normal	Mays and Tung 1992
Channel Slope	0.12, 0.164	Triangular	Tung 1990
Channel Slope	0.25	Lognormal	Johnson 1996a
Particle size	0.02	Uniform	Yeh and Tung 1993
Particle size	0.05	Uniform	Johnson and Ayyub 1992b
Friction slope	0.17	Uniform	Yeh and Tung 1993
Sediment sp. weight	0.12	Uniform	Yeh and Tung 1993
Flow velocity[a]	0.008x[b]	Triangular	Meter manufacturer;
Flow velocity	0.12x[b]	Uniform	Johnson 1996a
[a]Measured using electromagnetic meter [b]x = average velocity			

Hydraulic parameters are typically input to hydraulic models such as HEC-RAS to estimate flood elevations and velocities. Uncertainty in the parameters will propagate through the model to create uncertainty in the resulting calculation. In addition, uncertainty in the model itself will combine with the parameter uncertainty to create additional uncertainty. As an example of uncertainty propagation, Manning's equation for uniform flow is given by:

$$Q = \frac{c}{n} A R^{2/3} S^{1/2} \tag{2.3}$$

where:

Q = Discharge
c = Constant (1.49 for US units, 1.0 for S.I. units)
n = Manning roughness coefficient
R = Hydraulic radius
S = Channel bed slope (uniform flow)

Assuming that the area and, thus, hydraulic radius, contain relatively minor uncertainty, then the uncertainty in Q based on the uncertainty in n and S is given by (Mays 2005):

$$\Omega_Q^2 = \Omega_n^2 + 0.25\Omega_S^2 \tag{2.4}$$

where:

Ω = Coefficient of variation

Assuming that flow depth is determined from the standard step method (as in HEC-RAS), the uncertainty in flow depth can be calculated based on the results of uncertainty analyses conducted by the U.S. Army Corps of Engineers (Hydrologic Engineering Center 1986):

$$\Omega_y = 0.76 y^{0.6} S^{0.11} (5N_r)^{0.65} \tag{2.5}$$

where:

N_r = Reliability estimate for *n*, $0 \le N_r \le 1$

Uncertainties in hydraulic conditions can be reduced when measured data are available to calibrate the model. For example, high water marks or other observations of water surface elevation, combined with a discharge measurement, can be extremely valuable in adjusting Manning n values in the main channel and overbank areas so that the hydraulic model matches observed conditions. In addition, discharge measurements made using the velocity-area method provide useful information on the velocity distribution across the channel.

However, channels and floodplains change through time. These changes include maturing vegetation, land-use change, and channel aggradation, degradation, migration and width adjustment. These future conditions, while often difficult to estimate, introduce considerable uncertainty, and should not be neglected during the hydraulic analysis because they impact flow velocity and depth directly, and they impact the distribution of flow and velocity, each of which impact scour estimates.

As with the hydrologic uncertainty, incorporating hydraulic uncertainty into bridge design is not a trivial matter. However, there is considerable information on the subject of hydraulic uncertainty, and through the use of hydraulic models the levels of uncertainty in velocity, depth and flow distribution can be quantified both in general and in any specific application.

2.4 Evaluating Uncertainty Associated With Channel Instability

Alluvial channels are dynamic landscape features that can readily adjust aspects of their morphology, hydraulics, and sedimentology in response to altered environmental conditions or disturbances. If an alluvial channel is modified by straightening, widening, clearing, or dredging, resulting in increased flow-energy conditions, the channel will adjust toward a lower energy state by degrading upstream, widening, and aggrading downstream (Simon 1992). Knowledge of the spatial and temporal trends of channel adjustment is central to the protection and maintenance of bridges. Degradation of the channel bed can undermine piers and abutments. Aggradation can reduce the size of the bridge opening, cause debris to become trapped on the upstream side of the bridge and increase contraction and local scour. Bank erosion can undermine abutments and pier foundations in the floodplain and can lead to a contracted opening at the bridge, resulting in contraction scour. As the channel degrades and widens in response to imposed channel modifications, the likelihood that the bridge foundations will be undermined increases. At some point, critical conditions may develop at the bridge such that the bridge may become unstable and fail. Few studies have focused on the reliability of bridges in unstable channels.

Many alluvial channels experience long-term degradation; however, the engineer is concerned only with that portion which occurs over the life of the bridge. Prediction of channel degradation requires the use of a mathematical model or years of data showing trends in channel bed changes. There is considerable uncertainty in all sediment transport and channel degradation models (e.g., Richardson et al. 2001). The long-term degradation process can be accelerated considerably by human activities, such as channel straightening and urbanization. This often causes the channel to become unstable and incise. In this case it is sometimes possible to predict the near term bed degradation using a regression equation based on bed elevation data collected at the site.

Johnson and Simon (1995; 1997) assessed bridge reliability in an alluvial stream channel by combining an analysis of channel adjustment processes during channel evolution with a reliability analysis to determine the likelihood of failure. They provided a case study in western Tennessee in which annual bed elevation data were used to calibrate a regression equation that predicted bed elevation as a function of time. The probability of failure was then computed as a function of both simulated bed elevations and local scour, the margin of safety, and a modified Monte Carlo simulation. The resulting information can be used to determine maintenance or mitigation needs, and the appropriate depth for a new pier footing. In addition,

the information can be used to assess the vulnerability of piers in the floodplain to erosional events as the channel widens. Of course, channel degradation can change channel slope and both degradation and widening affect flow distribution. Changes to these factors then alter contraction, pier, and abutment scour potential, so developing the uncertainty of total scour can be a complex and involved process.

The Federal Highway Administration recommends that local scour, contraction scour and long-term bed degradation be assumed to be independent (Arneson et al. 2012). Based on this assumption, the total vertical erosion at the bridge is then simply the sum of the three scour components. This assumption provides a conservative estimate for a complex set of processes. Johnson (1999) used fault tree analysis to determine the probability of failure of a bridge due to these components of scour as well as other geomorphic channel instabilities.

This analysis permits an examination of a very complex system of interactions and processes that are not well understood. Minimal knowledge regarding the actual processes of scour and channel instability is required for a fault tree analysis. Johnson provided three examples of analyses for actual bridges demonstrating different combinations of scour (local and contraction) and geomorphic instabilities (channel widening and degradation) at both the abutments and piers. Riprap placed at the abutments for protection is also included in the analyses.

More recently, Johnson and Whittington (2010) developed a methodology to systematically document the factors related to risk of bridge failure due to stream channel instability and provide justification for the need for a HEC-20 Level II analysis (Lagasse et al. 2012). They determined the relative risk as a function of vulnerability and criticality. Vulnerability was based on a stream stability assessment and the National Bridge Inventory (NBI) ratings for channel condition for a particular bridge. Criticality was determined indirectly as a function of the bridge importance, using data extracted from the NBI. Relative risk is then qualitatively determined by combining vulnerability and criticality. An example at a bridge over Bentley Creek in north-central Pennsylvania was provided in which the relative level of risk was used to determine the need for a Level II analysis.

Additional data on channel degradation are reported by Keefer et al. (1980) where it is noted that degradation is a more common problem than aggradation and, in general, has a more severe impact on highway river crossings. Although gradation changes do occur naturally, human activities are responsible for the most severe cases. An assessment of applicable technology, from simple analysis procedures based on critical shear stress of the bed material to more complex computer solutions is provided. The documented data base on gradation problems nationwide includes 110 case histories of which 81 provide data on degradation. These case histories demonstrate that bridge footings, piles, and abutments can be undermined, and that channel widening frequently accompanies degradation.

2.5 Uncertainty in Bridge Scour Estimates

2.5.1 Overview

Scour at bridges is a very complex process. Scour and channel instability processes, including local scour at the piers and abutments, contraction scour, channel bed degradation, channel widening, and lateral migration, can occur simultaneously. The sum and interaction of all of these river processes create a very complex phenomenon that has, so far, eluded definitive mathematical modeling. To further complicate a mathematical solution, countermeasures, such as riprap, grout bags, and gabions, may be in place to protect abutments and piers from scour. A complete mathematical model would have to account for these structures as well.

Considerable uncertainty exists in estimating all components of scour at the piers and abutments. Sources of uncertainty include model, parameter, and data uncertainties. For some bridges, the uncertainty is much greater than for other bridges due to unusual circumstances and difficulties in estimating parameters. For example, Oben-Nyarko and Ettema (2011) point out that scour located close to an abutment is determined predominantly by scour at the abutment and, therefore, may substantially exceed the depth estimated for an isolated pier. When the prototype conditions differ significantly from the conditions under which the model was calibrated, the model uncertainty is increased and may overshadow all other types of uncertainty. A number of studies have been aimed at developing probabilistic estimates of bridge scour, particularly for piers, for the purpose of design and mitigation. These studies are summarized in this section.

Hopkins et al. (1980) used field data from four bridges in Mississippi and Texas to compare a large number of pier scour equations. They concluded that although laboratory studies have been beneficial in examining the process of local scour, the lack of scaling factors for sediment transport have limited the success of equations developed from laboratory data. Jones (1984) also compared numerous pier scour equations using laboratory data and limited field data. He found that the HEC-18 equation tended to give reasonable, although conservative, results. Johnson (1991) listed four primary concerns with bridge pier scour prediction methods, including the inability to determine the impact of future storms on the scour depth or on the probability that the bridge will fail or survive.

Johnson (1995) collected 515 field data points for bridge pier scour from existing literature in the U.S., Russia, and China and analyzed the data to determine the model (equation) uncertainty for seven scour equations under three different conditions: flow depth to pier width ratio (y/a), Froude number (F), and the ratio of flow velocity to critical velocity for sediment movement (V/Vc). The uncertainty was presented in terms of a bias factor **(where Johnson defined bias as the computed scour to observed scour ratio)** and the coefficient of variation. For the HEC-18 pier scour equation, the bias factor ranged from 1.21 (for $V/Vc \geq 3$) to 4.39 for $0.7 \leq V/Vc \leq 0.9$. It is not surprising that the bias factor is greater than 1.0 for all cases, given the conservative nature of the equation. A bias factor greater than 1 is desirable for this type of design equation if underestimation of scour is to be avoided. The coefficient of variation (COV) was very high for all cases, ranging from COV = 0.49 for $2 < y/b < 3$ to 1.04 for $0.7 \leq V/Vc \leq 0.9$. Such high values of COV indicate considerable uncertainty in the bridge pier scour model.

Few studies have been conducted on scour using a probabilistic approach. Laursen (1970) used a return period method to determine the economic risk associated with the potential for scour. He concluded that all bridge pier foundations should be designed for the probable maximum flood, because the likelihood of the probable maximum flood is sufficient to justify the relatively small additional cost for a deeper pier foundation; however, he states that the practicability of this event compared to the design life of the bridge seems somewhat excessive.

Using a return period or exceedance probability to estimate risk involves accounting for the statistical characteristics of floods by using a frequency analysis. The probability that a flood of a given magnitude is exceeded in any year is equal to the reciprocal of the return period. Although the return period method is simple, it does not account for uncertainties in estimating parameters, such as the estimate of flow depth, velocity, effective pier width, and angle of attack, or uncertainty in the scour model itself. Johnson and Ayyub (1992a and b) developed a method of determining the probability of failure due to scour around a bridge pier based on a time-dependent scour model developed by Johnson and McCuen (1991).

The analysis involved simulating pier scour for a period of time and determining the probability that the bridge will fail at various points in time during that period. Johnson (1992) developed a relationship between the probability of failure due to pier scour and safety factors. A best-fit version of the HEC-18 pier scour model was used and, thus, model uncertainty was not considered, since a best-fit model has a model correction factor of 1.0. Years later, Yanmaz and Ustun (2001), Yanmaz and Cicekdag (2001), and Yanmaz (2002) developed a dynamic reliability model based on a resistance-loading methodology that also produced safety factors as a function of service life, return period and pier size, similar to the Johnson (1992) paper. They also used a best-fit version of the HEC-18 model and so did not consider model uncertainty. Barbe et al. (1992) developed a very different approach that was based on a method of evaluating the probability of failure due to pier scour based on an entropy-based velocity distribution used to estimate local scour.

Johnson and Heil (1996) developed a probabilistic approach to provide a stochastic estimate of scour and the corresponding reliability or probability of failure based on the scour estimate and the depth of the bridge foundations. Two case studies, in Delaware and west Tennessee, were used to illustrate the procedure for computing the probability of failure. The results showed the use of reliability analyses and simulation techniques as important tools in assessing the implications of uncertainties in the prediction of bridge scour. The probability of failure is a quantifiable estimate that may be used to identify the extent, type, and urgency of remedial repair activities required due to the potential for scour at existing bridge sites. In each of the two examples, the probabilities of failure computed from the simulations were on the order of 10^{-3} to 10^{-5}. As a comparison, the probability of failure for major structures, such as bridges, should be less than about 10^{-5}. The U.S. Army Corps of Engineers (1992) determined that probabilities of failure (or unsatisfactory conditions) for inland navigation structures greater than 0.001 will require frequent outages for repair, and at a probability of failure of 0.07, extensive rehabilitation is required. For structures with even greater probabilities of failure, emergency action is required to alleviate risks. The results showed that probabilistic methodologies could be used in the design of new bridge structures as they relate to scour and have the potential to provide an accountable means of comparing different foundation types and sizes for new structures as a cost savings measure without compromising the integrity (as measured by the probability of failure) of the structure due to scour. An assessment of the probability of failure could also be used to prioritize mitigation needs for existing structures.

Ideally, a good scour prediction model would have a bias of 1.0 and a COV close to zero. However, even if modeling bias and uncertainties are eliminated, additional safety factors would still be needed to account for parametric and data uncertainties when using the model for design purposes. Because the data used in the Johnson (1995) study were field data, there is also uncertainty in the measured scour amounts (in the measurement, whether ultimate scour was reached, and other factors such as the presence of debris) and in the associated hydraulic parameters used to test the models (velocity, depth, angle of attack, etc.). NCHRP Report 653, "Effects of Debris on Bridge Pier Scour" provides an approach to computing the increased scour potential at piers with debris (Lagasse et al. 2010). This study also provides an extensive data base from laboratory studies of debris clusters with a range of shapes, geometry, and locations in the water column.

Johnson and Ayyub (1996) used fuzzy regression to investigate the modeling uncertainty in the prediction of bridge pier scour. Fuzzy bias factors, which describe the bias between observed field data and scour estimates based on equations developed from laboratory data, were estimated. The bias exists because of the use of small-scale laboratory results to model large-scale, real-world problems. Fuzzy regression is a method of calibrating fuzzy numerical coefficients in a linear equation. Since the regression coefficients are fuzzy parameters, the output, in this case scour depth, is also a fuzzy number. The fuzzy bias factors developed from the fuzzy regression equations were compared for a variety of input data. For example, they found that the model uncertainty ranged from less than 0.05 for small piers in low flow depths and large sediment gradations, to more than 1.0 for large piers in low flow and a well-sorted sediment. In general, they found that the model uncertainty for the bridge pier scour equation was less for larger sediment gradations (well graded), greater for situations involving larger bridge piers, and less as flow depth increased. Fuzzy bias factors provide useful information in the application of bridge pier scour equations currently available to engineers. The results of this study can be used to guide experimenters in their interpretation of small-scale laboratory test results. The fuzzy bias can be incorporated into laboratory-based models in the form of multiplicative correction factors to provide engineers with a more realistic estimate of the predicted variable for field applications.

A similar analysis of the bias and the modeling uncertainties was performed by Ghosn et al. (2003) based on data assembled by Landers and Mueller (1996) (see **Tables 2.3 and 2.4**). They observed that the ratio of measured scour to scour predicted by the HEC-18 equation (the inverse of the bias as defined above), as well as the COV of that ratio vary with the foundation geometry and dimension, as well as the soil type, flow depth and velocity with values similar to those reported by Johnson (1995). Using a Chi-Squared goodness of fit test, they found that the ratio can be reasonably well represented by a Lognormal distribution. Ghosn et al. (2003) used these data in a probabilistic analysis which also accounted for the randomness in other hydraulic parameters and input variables to study the reliability of hypothetical bridge foundation designs and reported low levels of reliability when compared to those for bridges subjected to other extreme events. The results were used to propose an approach for calibrating scour factors for local scour and the combination of local scour with other extreme events.

Table 2.3. Summary of Mean and COV of the Ratio of Observed to Estimated Local Pier Scour Based on Data of Landers and Muller (1996) assembled by Ghosn et al. (2003).

Flow and Channel Material Type	Pier Shape	Mean	Standard Deviation	COV	Number of Observations	Stand. Deviat. of Mean
All Cases		0.412	0.266	0.646	374	0.0138
Channels with live-bed conditions only		0.429	0.247	0.576	240	0.0159
All channel bed material	Rounded	0.400	0.231	0.577	126	0.0206
	Sharp	0.523	0.292	0.558	32	0.0516
	Cylinder	0.383	0.204	0.532	30	0.0372
	Square	0.432	0.246	0.570	52	0.0341
Non-Cohesive soils	All shapes	0.417	0.237	0.569	195	0.0170
Unknown soil type	All shapes	0.479	0.283	0.593	45	0.0422
Single piers	All shapes	0.405	0.223	0.550	191	0.0161
Pier Groups	All shapes	0.535	0.310	0.580	49	0.0443
Pile foundation	All shapes	0.421	0.256	0.607	158	0.0204
Poured foundation	All shapes	0.419	0.185	0.442	67	0.0226
Unknown foundation	All shapes	0.547	0.361	0.660	15	0.0932
Non-cohesive soils, poured	Rounded	0.405	0.181	0.446	48	0.0261
Non-cohesive soils, poured	Cylinder	0.355	0.132	0.371	18	0.0311

Table 2.4. Summary of Mean and COV for Contraction Scour Based on Report of Hong (2005).			
Reference	Observed Contraction Scour (ft)	Estimated Scour (ft)	Observed/Estimated
Fischer (1995)	19.68	29.85	0.66
Brabtes (1994)	10.80	13.40	0.81
	7.80	8.10	0.96
Norman (1975) Mueller, D.S. and Wagner, C.R. (2005)	15.68	16.30	0.96
	18.01	20.50	0.88
	18.40	20.80	0.88
	10.30	9.81	1.05
	15.38	16.70	0.92
Hong (2005)	3.06	5.01	0.61
	3.69	5.58	0.66
	4.73	6.03	0.78
		Average	0.83
		COV	17%

In an effort to use probabilistic estimates as a tool in decision making, Johnson and Dock (1998) developed a probabilistic framework for estimating scour using deterministic methods given in HEC-18. Uncertainties in the HEC-18 model, in determination of the parameters, and in estimating the hydraulic variables for a large event storm, were included in the analysis. The probabilistic framework can then be used as the basis for determining the likelihood of achieving various scour depths, probabilities of failure for various foundation designs, pile depths necessary to achieve a specified probability of failure for a design bridge life span, and for comparing designs based on various storm events. The Bonner Bridge in North Carolina was used as an example. Pile depths appropriate for various design life spans were calculated based on both 100- and 500-year storm events. The following assumptions were made: (1) the failure event was defined as the point at which the scour reached the base of the piles; (2) the arrival of hurricanes is a Poisson process; and (3) the piles can be placed at a depth y_p with a small coefficient of variation and follow a normal distribution. The first assumption can be readily changed to reflect different design criteria. **Figure 2.6** shows the resulting frequency histogram of 1,000 simulated scour depths. Based on this resulting normal distribution, and a mean scour depth of 53.2 ft (16.21 m), and a standard deviation of 4.8 ft (1.46 m), the probability that a scour depth of less than 68.9 ft (21 m) will occur is 97.4%. The scour depth that has a 90% nonexceedance probability of occurrence is 63.5 ft (19.36 m).

Stein et al. (1999) developed a method for assessing the risk associated with scour threat to bridge foundations as a function of the cost associated with failure and the probability of scour failure. Data were taken from the National Bridge Inventory. The risk was calculated from Equation 2.6:

$$R = KP\,[C_{Re} + C_{Rc} + C_T] \qquad (2.6)$$

where:

- R = Risk of scour failure in dollars for 1 year given the current physical condition
- K = Risk adjustment factor based on foundation type and type of span (NBI Item 43)
- P = Probability of failure for 1 year (NBI Items 26, 60, 61, and 71) and the C parameters are replacement cost, running cost, and time cost, respectively

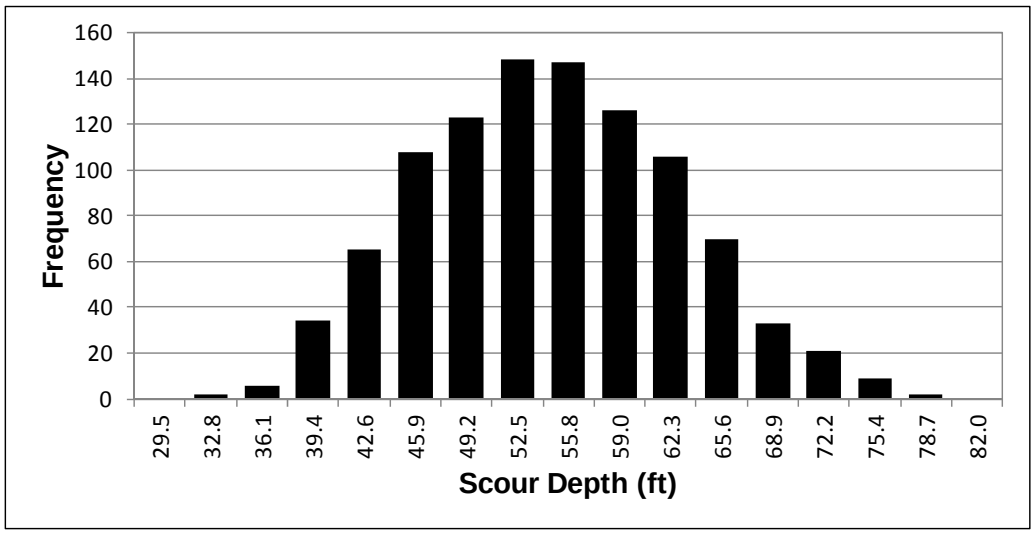

Figure 2.6. Frequency histogram for 1000 simulated scour depths.

As stated by Stein et al., the risks calculated using this method are appropriate as a relative measure for prioritization, rather than as an absolute value.

Briaud et al. (2007) developed a site specific method to estimate the probability that a threshold scour depth would be exceeded over the life of a bridge based on uncertainties associated with the randomness of hydrologic conditions. They did not include any of the uncertainties in the hydraulic or geotechnical parameters or the scour model uncertainty. Given the significance of these other uncertainties, the results of the Briaud et al. study are limited. However, the results may be useful in considering scenarios in which hydrologic conditions are expected to change.

Muzzammil and others (Muzzammil, Siddiqui, and Siddiqui 2006 and 2008 and Muzzammil, Siddiqui, and Anwar 2009) applied a first order reliability method (FORM) and Monte Carlo simulation, including correlation among the design variables, to develop a simplified relationship between safety factor and reliability index. They considered the effects of flow discharge and sediment size on bridge pier reliability against scour. A case study was presented in which the reliability of Elgin Bridge over the Ghagra River in India was estimated. The estimated reliability was then used to explain the root cause behind a sequence of problems faced by this bridge since its construction.

There are few reliability studies related to abutment scour. The uncertainty in abutment scour models is well known in engineering practice; thus, the omission of model uncertainty in the design and safety assessment of abutments brings the results into question. The model and parameter uncertainty can also be estimated for these types of scour when looked at independently. However, there remains the question of interaction between the scour types (contraction scour and local scour at an abutment). For example, based on hydrologic uncertainty, a larger event typically increases the scour potential for all types of scour. Yanmaz and Celebi (2004) attempted to develop a reliability-based model for abutment scour based on resistance-loading interference. They used the statistical randomness of laboratory data to represent the joint probability density function of dependent resistance and loading. Other sources of uncertainty, which are very significant in abutment scour equations, particularly model uncertainty, were omitted. They compared the results of the proposed model with a Monte Carlo simulation; however, no comparisons with field data were made.

Contraction scour results in a lower local velocity, which would tend to decrease pier scour. Another example of scour interaction is that a lower channel Manning n changes the flow distribution by increasing the channel discharge. The resulting contraction scour would be less (in live-bed conditions) and the resulting pier scour would be greater. These types of scour interactions must be addressed by incorporating the overall hydrologic and hydraulic uncertainties at the bridge site.

The use of bridge scour countermeasures can introduce additional uncertainty due to a lack of systematic testing and unknown potential for failure. Johnson and Niezgoda (2004) developed a risk-based method for ranking, comparing, and choosing the most appropriate scour countermeasures using failure modes and effects analysis and risk priority numbers (RPN). Failure modes and effects analysis (FMEA) incorporates uncertainty in the selection process by considering risk in terms of the likelihood of a component failure, the consequence of failure, and the level of difficulty required to detect failure. Risk priority numbers can provide justification for selecting a specific countermeasure and the appropriate compensating actions to be taken to prevent failure of the countermeasure. Failure modes and effects analysis is an appealing method because it considers risk in terms of the consequences of failure, the likelihood of a component failure, and the level of difficulty required to detect failure. With a "design-not-to-fail" philosophy, FMEA is implemented to determine failure modes and remove their causes before the design is implemented (McCollin 1999). Thus, the preventative action in the FMEA implies modification of the system design for risk reduction before the design is in place.

Fault tree analysis provides one method that can be used to combine the effects of uncertainty in all of the scour components, as well as scour countermeasures that are present, on the overall scour condition at the bridge. Johnson (1999) examined the interactions and sequences of events that could lead to a bridge failure due to scour at the piers or abutments or channel instabilities. Coefficients of variation and probability distributions were based on previous studies (e.g., see Johnson (1992, 1995, 1996a and b); Johnson and Ayyub (1992a and b); and Johnson and Dock (1998)). Model and parameter uncertainty were both accounted for in the study. Three examples showing a range of scenarios from abutment scour with riprap protection to pier scour combined with channel degradation are provided.

Pearson et al. (2000) extended the risk based approach developed by Stein et al. (1999) to the design of bridge scour countermeasures. They used a modification of the HYRISK model to develop a decision tool to select various levels of countermeasure protection for a bridge that has already been evaluated and determined to be scour critical for some probability flood event. The model is based on information that can be read from the National Bridge Inventory and accounts for average daily traffic, detour lengths, value of lost time, risks associated with scour at various types of foundations, bridge condition, bridge geometry, and bridge age. From the model, an optimum level of protection for the bridge and the maximum expenditures can be estimated to increase the level of protection.

The uncertainty in a scour estimate can be computed in several different ways. First-order analyses are frequently used to perform uncertainty analyses. For first-order methods no distribution is required, but the underlying assumption is that the variables are all normally distributed and the function being analyzed is linear. This assumption can introduce large errors in some cases where the variable distributions are significantly different than normal and the function or equation is highly nonlinear. To overcome these issues, advanced First Order Reliability (FORM) algorithms perform an iterative optimization where non-Normal distributions are mapped into equivalent Normal distributions and nonlinear equations are

linearized at the design point (most likely failure point) to vastly improve the estimate of the probability of failure and the reliability.

A second method of assessing uncertainty in scour estimates is to use simulation techniques, such as Monte Carlo simulation or modifications of the Monte Carlo simulation technique. The benefit of using simulation is that the uncertainty in scour can be quantified as a function of the uncertainty in the hydraulic model and its parameters. Unlike the first-order method, any distribution can be used directly. The result is a probabilistic scour estimate, i.e., one that has a mean, standard deviation, and probability distribution associated with it. The drawback of Monte Carlo simulations is the large number of calculations that are needed, particularly when dealing with large numbers of random variables and low probabilities. Johnson and Dock (1998) used Monte Carlo simulation to generate random samples of the parameters in the HEC-18 pier scour equation based on the associated coefficients of variation and distributions described above. They also accounted for model uncertainty using a model correction factor and its coefficient of variation and distribution. Using the example of a 500-year storm at the Bonner Bridge in North Carolina, they generated the scour distribution shown in Figure 2.6, with a mean scour depth of 53.2 ft (16.21 m), a coefficient of variation of 0.090, and a normal distribution. Following this process, probabilistic statements can then be made regarding the likelihood of obtaining a specified scour depth. These types of results, based on the uncertainty in the hydrologic input, hydraulic parameters, and model uncertainty, are the basic input for risk and reliability analyses.

2.5.2 FHWA Guidance - Incorporating Risk in Bridge Scour Analyses

As additional background, this section presents FHWA's latest guidance on risk analysis as applied to bridge scour (see the Fifth Edition of HEC-18 published in April 2012). Bridge foundations for **new** bridges should be designed to withstand the effects of scour caused by hydraulic conditions from floods larger than the design flood. In 2010, the U.S. Congress recommended that FHWA apply risk-based and data-driven approaches to infrastructure initiatives and other FHWA bridge program goals. This included the FHWA Scour Program. Risk-based approaches factor in the importance of the structure and are defined by the need to provide safe and reliable waterway crossings and consider the economic consequences of failure. For example, principles of economic analysis and experience with actual flood damage indicate that it is almost always cost-effective to provide a foundation that will not fail, even from very large events. However, for smaller bridges designed for lower frequency floods that have lower consequences of failure, it may not be necessary or cost effective to design the bridge foundation to withstand the effects of extraordinarily large floods. Prior to the use of these risk-based approaches, all bridges would have been designed for scour using the Q_{100} flood magnitude and then checked with the Q_{500} flood magnitude. **Table 2.5** presents FHWA's recommended **minimum** scour design flood frequencies and scour design check flood frequencies based on hydraulic design flood frequencies (Arneson et al. 2012).

Table 2.5. Hydraulic Design, Scour Design, and Scour Design Check Flood Frequencies.

Hydraulic Design Flood Frequency, Q_D	Scour Design Flood Frequency, Q_S	Scour Design Check Flood Frequency, Q_C
Q_{10}	Q_{25}	Q_{50}
Q_{25}	Q_{50}	Q_{100}
Q_{50}	Q_{100}	Q_{200}
Q_{100}	Q_{200}	Q_{500}

The Hydraulic Design Flood Frequencies outlined in Table 2.5 assume an inherent level of risk. There is a direct association between the level of risk that is assumed to be acceptable at a structure as defined by an agency's standards and the frequency of the floods they are designed to accommodate.

Discussion of Design Flood Frequencies

The Scour Design Flood Frequencies presented in Table 2.5 are larger than the Hydraulic Design Flood Frequencies because there is a reasonably high likelihood that the hydraulic design flood will be exceeded during the service life of the bridge. For example, using **Table 2.6** on "Probability of Flood Exceedance of Various Flood Levels" it can be seen that during a 50-year design life there is a 39.5% chance that a bridge designed to pass the Q_{100} flood will experience that flood or one that is larger. Similarly, there is a 63.6% chance that a bridge that is designed to pass the Q_{50} flood will experience that or a larger flood during a 50-year design life. Using the larger values for the Scour Design Flood Frequency for the 200-year flood and a 50-year design life reduces the exceedance value to 22.2%. This is considered to be an acceptable level of risk reduction. In other words, a bridge **must** be designed to a higher level for scour than for the hydraulic design because if the hydraulic design flood is exceeded then a greater amount of scour will occur which could lead to bridge failure. Also, designing for a higher level of scour than the hydraulic design flood ensures a level of redundancy after the hydraulic design event occurs. The Scour Design Check Flood Frequencies are larger than the Scour Design Flood Frequencies using the same logic and for the same reasons as outlined above.

Table 2.6. Probability of Flood Exceedance of Various Flood Levels.

Flood Frequency	Probability of Exceedance in N Years (or Assumed Bridge Design Life)						
Years	N = 1	N = 5	N = 10	N = 25	N = 50	N = 75	N = 100
10	10.0%	41.0%	65.1%	92.8%	99.5%	100.0%	100.0%
25	4.0%	18.5%	33.5%	64.0%	87.0%	95.3%	98.3%
50	2.0%	9.6%	18.3%	39.7%	63.6%	78.0%	86.7%
100	1.0%	4.9%	9.6%	22.2%	39.5%	52.9%	63.4%
200	0.5%	2.5%	4.9%	11.8%	22.2%	31.3%	39.4%
500	0.2%	1.0%	2.0%	4.9%	9.5%	13.9%	18.1%

If there is a flood event greater than the Hydraulic Design Flood but less than the Scour Design Flood that causes greater stresses on the bridge, e.g., overtopping flood, it should be used as the Scour Design Flood. For this condition there would not be a Scour Design Check Flood since the overtopping flood is the one that causes the greatest stress on the bridge. Similarly, if there is a flood event greater than the Scour Design Flood but less than the Scour Design Check Flood that causes greater stresses on the bridge, it should be used as the Scour Design Check Flood. Balancing the risk of failure from hydraulic and scour events against providing safe, reliable, and economic waterway crossings requires careful evaluation of the hydraulic, structural, and geotechnical aspects of bridge foundation design.

Flood Exceedance Probabilities

A flood event with a recurrence interval of T years has a 1/T probability of being exceeded in any one year. The 100-year recurrence interval flood is often used as a hydraulic design value and to establish other types of flooding potential. Regardless of the flood design level, there is a chance, or probability, that it will be exceeded in any one year and the probability increases

depending on the life of the structure. The probability that a flood event frequency will be exceeded in N years depends on the annual probability of exceedance as defined by:

$$P_N = 1-(1-P_a)^N \qquad (2.7)$$

where:

P_N = Probability of exceedance in N years
P_a = Annual probability of exceedance (1/T)
N = Number of years
T = Flood event frequency of exceedance

The number of years, N, can be assumed to equal the bridge design life or remaining life. Table 2.6 shows the probability of exceedance of various flood frequencies for time periods (that may be assumed to equal the bridge design life) ranging from 1 to 100 years. For example a 100-year flood has an annual (N = 1) probability of exceedance of 1.0%, but has a 39.5% chance of exceedance in 50 years. A 200-year flood has a 22.2% chance of being exceeded in 50 years and a 31.3% chance of being exceeded in 75 years.

FHWA notes that the probability of exceedance may be applied to an individual bridge or for a population of similar bridges. Therefore, if a 200-year design flood condition is used for a population of bridges with expected design lives of 75 years, then that flood condition will be exceeded at approximately 31.3% of the bridges over their lives. Because design flood conditions are exceeded at many bridges during their useful lives, factors of safety, conservative design relationships, and LRFD are used to provide adequate levels of safety and reliability in bridge design.

2.6 LRFD Approaches for Structural Uncertainty

2.6.1 Introduction

Load and Resistance Factor Design (LRFD) incorporates state-of-the-art analysis and design methodologies with load and resistance factors based on the known variability of applied loads and material properties. These load and resistance factors are calibrated from actual bridge statistics to ensure a uniform level of reliability. LRFD allows a bridge designer to focus on a design objective or limit state, which can lead to a similar probability of failure in each component of the bridge. Bridges designed with the LRFD specifications should have relatively uniform safety levels, which should ensure superior serviceability and long-term maintainability.

Scour of earth materials from around bridge foundation elements does not represent a load, but a loss of resistance. Hydraulic engineers are tasked with estimating scour depths for different types of scour processes (e.g., pier, contraction, and abutment scour). Scour estimates are typically associated with a design flood event, for example a 100-year flood. Structural and geotechnical engineers then use this information for developing a bridge design to maintain structural stability that accommodates the loss of resistance due to scour.

2.6.2 Structural Reliability

The aim of structural reliability theory, as incorporated in LRFD methodology, is to account for the uncertainties encountered while evaluating the safety of structural systems or during the calibration of load and resistance factors for structural design codes. More detailed explanations of the principles discussed in this section can be found in published texts on structural reliability and risk (e.g., Thoft-Christensen and Baker 1982; Nowak and Collins 2000; Melchers 1999; Ayyub 2003; Ayyub and McCuen 2003).

The uncertainties associated with predicting the load carrying capacity of a structure, the intensities of the loads expected to be applied, and the effects of these loads may be represented by random variables. The value that a random variable can take is described by a probability distribution function. That is, a random variable may take a specific value with a certain probability and the ensemble of these values and their probabilities are described by the distribution function. The most important characteristics of a random variable are its mean value or average, and the standard deviation that gives a measure of dispersion or a measure of the uncertainty in estimating the variable. A dimensionless measure of the uncertainty is the coefficient of variation (COV) which is the ratio of standard deviation divided by the mean value. For example the COV of the random variable R is defined as V_R such that:

$$V_R = \frac{\sigma_R}{\overline{R}} \tag{2.8}$$

where:

σ_R = Standard deviation and $\overline{R}$ is the mean value
$\overline{R}$ = Mean value

Codes often specify nominal values for the variables used in design equations. These nominal values are related to the means through bias values. The bias is defined as the ratio of the mean to the nominal value used in design. For example, if R is the resistance, the mean of R, namely, $\overline{R}$, can be related to the nominal or design value R_n using a bias factor such that:

$$\overline{R} = b_r R_n \tag{2.9}$$

where:

b_r = Resistance bias
R_n = The nominal value as specified by the design code

For example, A36 steel has a nominal design yield stress of 36 ksi (248,220 kPa) but coupon tests show an actual average value close to 40 ksi (275,800 kPa). Hence the bias of the yield stress is 40/36 or 1.1. **See Section 3.4 for definitions of Bias and COV as used in this study**. In addition to the material properties, the bias and the COV in member resistance account for fabrication errors and modeling uncertainties reflecting the existing lack of precision in our ability to model the actual strength of structural members even when the material properties and dimensions are precisely known.

In structural reliability, safety may be described as the situation where capacity (e.g., strength, resistance, fatigue life, foundation depth) exceeds demand (e.g., load, moment, stress ranges, scour depth). Probability of failure, i.e., probability that capacity is less than load demand, may be formally calculated; however, its accuracy depends upon detailed data on the probability

distributions of load and resistance variables. Since such data are often not available, approximate models are often used for calculation.

The reserve margin of safety of a bridge component can be defined as, Z, such that:

$$Z = R - S \tag{2.10}$$

where:

R = Capacity
S = Total demand

The probability of failure, P_f, is the probability that R is less than or equal to the total applied load effect S or the probability that Z is less or equal to zero. This is symbolized by the equation:

$$P_f = P_r [R \leq S] \tag{2.11}$$

where:

P_r is used to symbolize the term probability

If R and S follow independent normal distributions then:

$$P_f = \Phi\left(\frac{0-\overline{Z}}{\sigma_Z}\right) = \Phi\left(-\frac{\overline{R}-\overline{S}}{\sqrt{\sigma_R^2+\sigma_S^2}}\right) \tag{2.12}$$

where:

Φ = Normal probability function that gives the probability that the normalized random variable is below a given value
$\overline{Z}$ = Mean safety margin
σ_Z = Standard deviation of the safety margin

Equation 2.12 gives the probability that Z is less than 0. The reliability index, β, is defined such that:

$$P_f = \Phi(-\beta) \tag{2.13}$$

which for the normal distribution case gives:

$$\beta = \frac{\overline{Z}}{\sigma_Z} = \frac{\overline{R}-\overline{S}}{\sqrt{\sigma_R^2+\sigma_S^2}} \tag{2.14}$$

Thus, the reliability index, β, which is often used as a measure of structural safety gives in this instance the number of standard deviations that the mean margin of safety falls on the "safe" side.

The reliability index β defined by Equation 2.14 provides an exact evaluation of risk (failure probability) if R and S follow normal distributions. Although β was originally developed for normal distributions, similar calculations can be made if R and S are lognormally distributed (i.e., when the logarithms of the basic variables follow normal distributions). Other methods have been developed to obtain the reliability index for the cases when the basic variables are not normal. These methods, often referred to as FORM (First Order Reliability Methods) or FOSM (First Order Second Moment) involve an iterative calculation to obtain an estimate to the failure probability. This is accomplished by approximating the failure equation (i.e., when Z = 0) by a tangent multi-dimensional plane at the point on the failure surface closest to the mean value. When the random variables are not Normal, they are mapped into equivalent Normal distributions to provide good approximations to the probability of failure P_f and the reliability index β.

More advanced techniques including SORM (Second Order Reliability Methods) have also been developed to improve the estimates when the failure function is highly nonlinear. On the other hand, Monte Carlo simulations can be used to provide estimates of the probability of failure. Monte Carlo simulations are suitable for any random variable distribution type and failure equation. In essence, a Monte Carlo simulation creates a large number of "experiments" through the random generation of sets of resistance and load variables. Estimates of the probability of failure are obtained by comparing the number of experiments that produce failure to the total number of generated experiments. Given values of the probability of failure, P_f, the reliability index, β is calculated from Equation 2.13 and used as a measure of structural safety even for non-normal distributions.

2.6.3 LRFD Code Calibration

The reliability index has been used by many groups throughout the world to express structural risk (e.g., AASHTO LRFD (2007); AASHTO MBE (2008); AISC (2005); ACI (2005); Can/CSA (2006); Eurocode (1992); ASCE 7(2010)). A value of β in the range of 2 to 4 is usually specified for different structural applications. For example, $\beta = 3.5$ was used for the calibration of the Strength I limit state in AASHTO LRFD Specifications (2007) for the design of new bridges. The calibration process as described by Nowak (1999) and Kulicki et al. (2007) is based on the reliability of bridge members subject to random truck loads within a 75-year design life. On the other hand, the LRFR provisions in the AASHTO MBE (2008) were calibrated to meet a target reliability index $\beta = 2.5$ for checking the safety of existing bridges under random truck loads for a rating period of 5 years (Moses 2001).

The difference between the two return periods and target reliability values in the AASHTO LRFD and LRFR is justified based on a strict inspection process for existing bridges and a qualitative cost-benefit analysis. Although demanding higher reliability levels for new designs will imply a marginal increase of bridge construction costs, the replacement of existing bridges would lead to major construction as well as other tangible and intangible economic and other costs associated with the disruption of traffic. A qualitative evaluation of the costs and benefits had to be followed since efforts to implement analytical methods are being hampered by the lack of data (Aktas et al. 2001).

The reliability index values used in the AASHTO LRFD and LRFR calibrations correspond to the failure of a single component following the approach outlined in other code calibration efforts (see for example, Ravindra and Galambos 1978, Ellingwood et al. 1980). If there is adequate redundancy, overall system reliability indices will be higher as indicated by Ghosn and Moses (1998) and Liu et al. (2001) who proposed the application of system factors calibrated to meet system reliability criteria rather than component criteria. A slightly different

approach taken in ASCE 7-10 (2010) recommends the use of different member reliability targets based on the consequences of a member's failure. Thus, the target reliability to be used for the design of a connection must be higher than that of a beam in bending.

Generally speaking, the reliability index β is not used in practice for making decisions regarding the safety of a particular design or an existing structure, but instead is used by code writing groups for recommending appropriate load and resistance safety factors for new structural design or evaluation specifications. One commonly used calibration approach is based on the principle that each type of structure should have uniform or consistent reliability levels over the full range of applications. For example, in the calibration of the AASHTO LRFD and LRFR Bridge Design and Rating codes, load and resistance factors were chosen to produce β values that uniformly match a target reliability level β_{target} for bridges of different span lengths, number of lanes, simple or continuous spans, roadway categories, strength, etc. (Nowak 1999, Moses 2001, Kulichi et al. 2007). Ideally, a single target β is achieved for all applications. A similar approach had been followed for the calibration of the fatigue limit state under cyclic truck loads (Moses et al. 1987).

This reliability-based calibration approach is being adhered to while extending the design specifications to new bridge types and materials subjected to truck live loads (Rizkalla et al. 2007; Nowak and Ibrahim 2009; Tse and Ibrahim 2009; Nowak 2009; Kulicki et al. 2006; Nowak et al. 2006). However, current reliability models do not account for the effects of material degradation under environmental factors or the expected changes in truck loading conditions over time. A significant amount of theoretical research work has been ongoing over the last two decades to develop time-dependent reliability models to account for the deterioration of concrete beams and the corrosion of steel bridge girders and their influence on member, as well as system strength. These efforts, however, have not matured yet to a level where they can be applied in the LRFD specifications to help extend the useful life of the next generation of bridges and obtain good estimates of the safety and reliability of existing bridges subjected to harsh environments (Mori and Ellingwood 1994; Enright and Frangopol 1998; Kayser and Nowak 1989; Czarnecki and Nowak 2008; Akgul and Frangopol 2004).

The same is true with regard to the design for extreme events other than live loads. A probabilistic model for the consideration of ship collisions is based on calculating a nominal annual probability of failure that should not exceed 0.001 (AASHTO Specifications for Vessel Collisions 2009). However, the design criteria limit states associated with other types of extreme events are based on previous generations of codes that were not based on reliability principles. In these cases, emphasis was placed on the hazard analysis of the load events without explicitly considering the uncertainties in the response of the bridge to these events and the ability of the bridge to withstand their effects. For example, recent proposals recommend using for design the earthquakes corresponding to a 1000-year return period, without explicitly accounting for the uncertainties associated with estimating the dynamic bridge response or the ability of a bridge system to resist the applied seismic ground motions (Imbsen 2007). Threats from floods are based on probabilistic models of flood occurrence without considering other modeling uncertainties (e.g., the bias and COV of scour prediction equations) and the parametric uncertainties associated with estimating discharge, flow depth, flow velocity, and so forth as discussed in Sections 2.2 and 2.3. Probabilistic models for analyzing bridges subjected to vessel and ship collisions have not been extended to collisions by trucks or trains. Reliability models for ice load effects on bridge substructures are still under development, and no consensus has yet evolved on how best to model the threats from fire or blast (Ghosn 2010).

Furthermore, existing bridge design codes propose different return periods and consequently various levels of conservatism (or safety factors) for different hazards. For example, the calibration of the live load factors in the AASHTO LRFD is based on the 75-year maximum load effect, the wind maps use 50-year maximum wind speeds, a 1000-year return period has been proposed for seismic hazards, while scour predictions are based on flood events having various return periods based on bridge size and level of service (see Table 2.5). In addition, existing bridge design specifications provide equations to model bridge behavior and member/system capacities under these various threats that are necessarily presented in a somewhat similar format that blurs the implicit levels of conservatism to the end users. For example, the use of the force method in traditional seismic bridge design ignores the uncertainties associated with determining the actual response modification factor as compared to the code specified value (Hwang and Shinozuka 1988; Takada et al. 1989; Mechakhchekh and Ghosn 2007). Thus, current methods for estimating bridge vulnerability to each hazard are also inconsistent.

Given that structural safety is related to both the magnitude of the hazard and the vulnerability of the bridge elements to the hazard, the discrepancies in the current methods may not lead to consistent levels of reliability for the different hazards that a bridge may be subjected to. To account for many of these uncertainties, some specification writers have recommended the design of bridges for hazard levels corresponding to very high return periods. For example a 2500-year return period was recommended for seismic hazards when using the traditional force based design methods, while recent proposals have recommended the use of a 1000-year return period in conjunction with a performance-based design approach (ATC/MCEER 2002, Imbsen 2007). Although the use of different return periods to account for the different levels of conservatism and uncertainties associated with the analysis and design approaches is a valid approach for developing design codes, the determination of the code-specified design return period must be supported using probabilistic analyses of the overall safety of the structure.

During the calibration of a new design code, the average reliability index from typical "safe" designs is used as the target reliability value for the new code. That is, a set of load and resistance factors as well as the nominal loads (or return periods for the design loads) are chosen for the new code such that bridges designed with these factors will provide reliability index values equal to the target value as closely as possible. For example, Nowak (1999) used a reliability index $\beta = 3.5$ for the design of new bridge members. Moses (2001), on the other hand, used a reliability index $\beta = 2.5$ for the load capacity evaluation of existing bridges.

Both targets are based on a generic set of load and member capacity statistical databases that are believed to represent the most typical loading conditions and material properties. The differences between the $\beta = 3.5$ (new bridges) and $\beta = 2.5$ (existing bridges) are justified based on cost implications, given that the design of new bridges to higher safety standards would only marginally increase the cost of construction, while increasing the load capacity criteria for an existing bridge may require its replacement and lead to considerable costs. The lower safety criteria for existing bridges is, however, associated with strict requirements for regular inspection. Ghosn et al. (2003) found that existing design criteria for extreme events (other than scour) are associated with reliability index values that vary between $\beta = 2.0$ to 3.5.

Ghosn and Moses (1986) found that the load and resistance factors obtained following a calibration based on existing "safe designs" are relatively insensitive to errors in the statistical data base as long as the same statistical data and criteria are used to find the target reliability index and to calculate the load and resistance factors for the new code. Thus, a change in the load and resistance statistical properties (e.g., in the standard deviations) would affect the

computed β values. Specifically, the change will affect the β values for all the bridges in the sample population of "typical safe designs" and consequently the average β (which is set as the target β). Assuming that the performance history of these bridges is satisfactory, then the target reliability index would be changed to the new "average" and the final calibrated load and resistance factors would remain approximately the same.

The calibration process described above does not contain any pre-assigned numerical values for the target reliability index. This approach that has traditionally been used in the calibration of LRFD criteria (e.g., AISC, AASHTO) has led code writers to choose different target reliabilities for different types of structural elements or for different types of loading conditions. For example, in the AISC LRFD, a target β equal to 3.5 was chosen for the reliability of beams in bending under the effect of dead and live loads, while a target β equal to 4.0 was chosen for the connections of steel frames under dead and live loads, and a target β equal to 2.5 may be chosen for the main members of a structure subjected to earthquakes. A reliability index β = 3.5 corresponds to a probability of limit state exceedance equal to 2.3×10^{-4}, while a β = 2.5 corresponds to a probability of exceedance equal to 6.2×10^{-3}.

Similarly, the U.S. Army Corps of Engineers (1992) determined that probabilities of unsatisfactory conditions for inland navigation structures greater than 0.001 will require frequent outages for repair, and at a probability of 0.07, extensive rehabilitation is required. For structures with even greater probabilities of limit state exceedance, emergency action is required to alleviate risks. Such differences in the target reliability index and associated probabilities clearly reflect the economic costs associated with the selection of the target β and the consequences of exceeding a limit state.

In summary, this section shows that much progress has been made over the last 3 decades to apply reliability methods during the development of bridge design and evaluation specifications. However, current bridge design specifications and the equations used to model bridge behavior and member/system capacities under various threats are inconsistent and are presented in a format that blurs the implicit levels of conservatism to the end users. Existing discrepancies in the design return periods and the methods used by the specifications to treat the different hazards, including scour, have to be overcome in order to address issues related to multi-hazard risk management and life cycle engineering principles (Ghosn et al. 2003).

CHAPTER 3

3. EVALUATING UNCERTAINTY ASSOCIATED WITH SCOUR PREDICTION

3.1 Introduction

Bridge scour processes, including pier, abutment, and contraction scour, have been well researched over the past several decades and equations have been developed to estimate scour depths for each of the scour components. The vulnerability of a bridge to scour is due to the existence of a weakness or design that can lead to an unexpected, undesirable event compromising the bridge safety. By assessing and quantifying all sources of uncertainty in the parameters and equations used in the design estimation for scour, the reliability of a bridge scour estimate and the probability that the design estimate will be exceeded over the design life of the bridge can be determined, thus reducing the vulnerability to an undesirable event.

3.2 Determining Individual Scour Component Uncertainty

The current practice for determining the total scour prism at a bridge crossing generally involves summing individually calculated scour components. The scour components include local scour (pier and abutment), contraction scour (live-bed or clear-water), and long-term channel change (degradation, lateral migration, and channel widening). Uncertainty is not directly addressed in the determination of any of the scour components, so current practice establishes a design amount of scour that is generally recognized as conservative, although the level of conservatism is undefined. For scour at bridge abutments HEC-18 (Arneson et al. 2012) now recommends a methodology developed under NCHRP Project 24-20 (Ettema et al. 2010) which provides an estimate of abutment and contraction scour combined.

Pier, abutment and contraction scour uncertainty are each comprised of two types of uncertainty; parameter (aleatory) uncertainty and model (epistemic) uncertainty. This is because each type of scour is defined by an equation (model) that includes variables (parameters) that must be estimated. Monte Carlo simulation was used to assess parameter uncertainty and observed data (lab and field) was used to assess model uncertainty. Each of the variables (discharge, velocity, flow depth, particle size, etc.) used in scour calculations possesses a probability density function defined by the distribution type (normal, log-normal, etc.), and distribution properties (mean, standard deviation, skew, etc.).

Monte Carlo simulation was used to address the parameter uncertainty for the local and contraction scour equations or in the case of abutment scour, local scour and contraction scour combined. The Monte Carlo simulation included a hydraulic modeling step where a hydraulic model was run for a large number of scenarios to develop the input variables for the scour computations. HEC-RAS was used for this step (see USACE 2010). Each run provided data to be used to compute both local and contraction scour. The HEC-RAS input parameters that were varied are discharge, boundary condition (energy slope), channel Manning n, and floodplain Manning n. HEC-RAS produced the hydraulic variables for the scour components which are velocity, flow depth, and flow distribution between the channel and the overbank areas.

3.3 Parameter Uncertainty

The Monte Carlo simulations included the following random variables:

Hydraulic Modeling

- Hydrologic uncertainty (Log-Pearson Type III)
- Channel Manning n
- Floodplain Manning n
- Boundary condition (energy slope)

Pier Scour

- Equation (HEC-18 and FDOT (Sheppard et al. 2011))
- Velocity and flow depth

Abutment Scour

- Equation and methodology for total scour (NCHRP 24-20 (Ettema et al. 2010))
- Obstructed flow area, discharge, velocity, and depth

Contraction Scour

- Upstream flow distribution (Q_1)
- Bridge flow distribution (Q_2, Q_{left}, Q_{right})
- Flow depths (Y_1, Y_o)

There are two categories of factors that were not included in the Monte Carlo simulation. One category is composed of parameters that would be known in a bridge design, such as pier dimensions or road elevation. Therefore, these parameters would be constants and thus be considered deterministic instead of random. The other category that was excluded from the Monte Carlo simulation includes factors that would overly complicate the analysis. Examples of these types of variables are multiple bridge openings and time rate of scour.

The Monte Carlo simulations did not include the following:

Hydraulic Modeling

Deterministic variables:

- Bridge or embankment skew
- Pier size, shape and skew
- Varying road elevation
- Abutment shape

Over-complicating factors:

- Non-stationary aspects of hydrologic uncertainty (climate change, sea level rise/fall)
- Multiple bridge openings
- 2-D modeling or complex hydraulic situations

Pier Scour

Deterministic variables:

- Pier shape
- Width
- Length
- Skew angle

Over-complicating factors:

- Material erodibility (clay, rock)
- Complex pier geometry
- Debris or ice
- Time rate of scour
- Armoring

Abutment Scour

Deterministic variables:

- Abutment shape
- Embankment skew

Over-complicating factors:

- Material erodibility (clay, rock)
- Time rate of scour
- Change in abutment shape during scour

Contraction Scour

Deterministic variables:

- Embankment length
- Abutment setback
- Approach channel width
- Contracted channel width

Over-complicating factors:

- Relief bridge scour
- Time rate of scour
- Material erodibility (clay, rock, or vegetation) other than particle size
- Pressure scour (vertical contraction scour)
- Channel bed forms for live-bed conditions

Scour Interaction

Over-complicating factors:

- Overlapping scour holes (pier-to-pier or abutment-to-pier)

Long-term channel changes

Over-complicating factors:

- Aggradation, degradation, or headcuts
- Lateral migration
- Channel width adjustments

3.4 Model Uncertainty

Model (equation) uncertainty depends on how well a given scour equation predicts scour. It can be evaluated by comparing observed scour to predicted scour, comparing simulated scour to predicted scour, or by expert knowledge. **For this study model uncertainty is represented by the statistical properties of the ratio of observed scour to predicted scour for a given scour equation. The mean of the ratios is the bias (λ) and the standard deviation of the ratios divided by the bias is the coefficient of variation (COV)**.

As discussed in Chapter 4, the bias and COV for each of the scour equations were evaluated based on available laboratory and field data, and the reliability index (β) was determined for each scour equation. Because the determination of bias and COV requires observed data, the limitations of each data source need to be addressed. Laboratory data have the disadvantages of small scale, inconsistent length scales (geometric and sediment), and a predominance of clear-water conditions. Field data have the disadvantages of being uncontrolled, large parameter uncertainty, difficulties associated with measuring scour, difficulties in separating types of scour, unmeasured scour hole refill, highly variable bed materials, and non-ultimate scour levels.

Contraction scour is widely accepted as a sediment transport problem. However, finding reliable laboratory and field contraction scour data was a problem (see Section 4.2). Ultimate live-bed contraction scour is reached when the rate of sediment transport in the bridge opening matches the supply of sediment from the upstream channel. Ultimate clear-water contraction scour is reached when the flow can no longer erode the bed. Most bridge waterway openings are, in reality, short contractions. However, the HEC-18 contraction scour equations were derived using a long contraction assumption, thus introducing additional uncertainty.

Long-term channel changes are components of total scour that need to be considered in bridge design, although they cannot be addressed in the same manner as local and contraction scour. Degradation and lateral migration often contribute significantly to total scour at bridges, although aggradation and channel widening may also cause problems. Future degradation and aggradation may be estimated in several ways, including bridge inspection profiles, rating curve shifts, equilibrium slope, sediment continuity, sediment transport modeling, and headcut analysis. Future amounts of channel migration can be estimated by comparing historic aerial photos as described in NCHRP Report 533, "Handbook for Predicting Meander Migration" (Lagasse et al. 2004).

Rather than developing uncertainty parameters related to long-term vertical and lateral channel change, standard design approaches were used. The standard approach currently used in bridge design is to establish a conservative estimate of future channel change (Arneson et al. 2012, Lagasse et al. 2012). Uncertainty and reliability approaches for predicting long-term channel change were not considered in this study.

CHAPTER 4

4. DATA SCREENING AND ANALYSIS

4.1 Pier Scour Data

4.1.1 Pier Scour Laboratory Data - Compilation, Screening, and Analysis

Pier scour data obtained under controlled laboratory conditions were assembled from 22 sources, yielding 699 independent measurements of pier scour in cohesionless soils. All data sets consisted of studies where the following information was documented: (1) scour depth y_s, (2) approach flow depth y, (3) approach flow velocity V, (4) median sediment size d_{50}, (5) pier width a, and (6) pier shape (e.g., cylindrical, square, rectangular, etc.). Seventeen of the 22 data sources were obtained from NCHRP Report 682 (Sheppard et al. 2011) which provided 569 data points. Data from five additional studies were also acquired, which contributed another 130 data points.

To determine whether an individual test run was conducted under clear-water or live-bed conditions, the procedure presented in Hydraulic Engineering Circular 18 (HEC-18), Fifth Edition (Arneson et al. 2012) uses the critical velocity for particle motion given by the following relationship in (U.S. customary units):

$$V_c = \frac{y^{1/6}\sqrt{K_s(S_s - 1)}d_{50}}{n} \qquad (4.1)$$

where:

V_c = Critical velocity for particle motion, ft/s
y = Approach flow depth, ft
K_s = Dimensionless Shields parameter for sediment motion (0.03 for gravel, 0.047 for sand)
S_s = Specific gravity of solid particle (assumed equal to 2.65 unless otherwise indicated)
d_{50} = Median particle diameter, ft
n = Manning resistance coefficient, estimated as $n = 0.034(d_{50})^{1/6}$ (d_{50} in ft)

The critical velocity equation as given in NCHRP Report 682 (Sheppard et al. 2011) is:

$$V_c = (u_{*c})\ 5.75 \log\left(1685\frac{y}{d_{50}}\right) \qquad (4.2)$$

where:

V_c = Critical velocity for particle motion, ft/s
u_{*c} = Shear velocity for 0.1 mm < d_{50} < 1 mm given by: $0.0377 + 0.0410(d_{50})^{1.4}$, ft/s
u_{*c} = Shear velocity for 1 mm < d_{50} < 100 mm given by: $0.1(d_{50})^{0.5} - 0.0213(d_{50})^{-1}$, ft/s
y = Approach flow depth, ft
d_{50} = Median particle diameter, mm

Nearly all of the laboratory tests involved cylindrical piers; only 36 tests (about 5% of the data points) used square, rectangular, or multiple-column piers. These 36 tests with non-cylindrical piers all used an orientation aligned with the flow such that a skew angle was not introduced. **Table 4.1** provides a summary of the laboratory data sources.

Table 4.1. Summary of Laboratory Pier Scour Data Sets												
Source	No. data points	Pier shape[1]	V (ft/s)	y (ft)	d_{50} (mm)	a (ft)	y_s (ft)	V/V_c (HEC18)	V/V_c (FDOT)	y/a	y_s/a	a/d_{50}
Chabert & Engeldinger (1956)	93	C	0.6 to 1.9	0.3 to 1.2	0.3 to 3.0	0.2 to 0.5	0.2 to 0.8	0.5 to 1.0	0.5 to 1.3	0.7 to 7.0	1.1 to 2.2	17 to 385
Chee (1982)	38	C	0.8 to 3.9	0.3	0.2 to 1.4	0.2 to 0.3	0.2 to 0.5	0.7 to 3.8	0.9 to 4.3	1.0 to 2.0	1.3 to 3.0	36 to 425
Chiew (1984)	101	C	0.7 to 5.3	0.6 to 1.1	0.2 to 3.2	0.1 to 0.2	0.1 to 0.3	0.7 to 2.7	0.8 to 3.1	2.4 to 7.5	1.7 to 4.2	10 to 188
Coleman (unpub.)	6	C	1.0	0.1 to 0.3	0.8	1.0 to 2.5	0.6 to 1.1	0.7 to 0.8	0.9 to 1.0	0.1 to 0.3	0.3 to 0.7	378 to 911
Dey, Bose & Sastry (1995)	18	C	0.6 to 0.9	0.1 to 0.2	0.3 to 0.6	0.2 to 0.3	0.2 to 0.3	0.6 to 0.9	0.7 to 1.0	0.5 to 0.9	0.9 to 1.4	98 to 292
Ettema (1976)	19	C	1.2 to 3.1	2.0	0.6 to 4.1	0.3	0.1 to 0.7	1.7 to 3.3	1.0	6.0	1.8 to 2.8	24 to 182
Ettema (1980)	97	C	0.5 to 4.0	0.1 to 2.0	0.2 to 7.8	0.1 to 0.8	0.1 to 1.2	0.4 to 1.0	0.7 to 1.0	0.2 to 20.9	0.6 to 4.7	4 to 999
Ettema et al. (2006)	6	C	1.5	3.3	1.1	0.2 to 1.3	0.4 to 1.5	0.7	0.9	2.5 to 15.6	1.3 to 2.5	61 to 387
Graf (1995)	3	C	1.9 to 2.0	0.6 to 0.8	2.1	0.3 to 0.5	0.6 to 0.9	0.9	0.9	1.5 to 2.3	1.7 to 2.0	48 to 71
Hancu (1971)	3	C	1.0 to 4.9	0.2 to 0.3	0.5 to 5.0	0.4	0.4 to 0.6	0.9 to 2.1	0.9 to 2.2	0.4 to 0.8	1.1 to 2.2	26 to 260
Jain & Fischer (1980)	34	C	1.6 to 4.9	0.3 to 0.8	0.3 to 2.5	0.2 to 0.3	0.2 to 0.6	0.8 to 4.1	0.8 to 4.7	1.0 to 4.9	1.6 to 3.6	20 to 406
Jones (unpub.)	17	C	1.0 to 2.6	0.9	0.3 to 5.0	0.5	0.3 to 0.9	0.5 to 0.9	0.6 to 1.1	1.8	1.3 to 2.0	30 to 506
Kothyari et al. (1992)	67	C	0.7 to 4.2	0.1 to 0.8	0.2 to 7.8	0.1 to 2.3	0.1 to 0.8	0.6 to 1.7	0.7 to 1.2	0.1 to 5.1	0.3 to 2.5	9 to 2500
Lagasse et al. (2007)	2	S	2.4 to 2.9	1.0	0.8	0.7	1.1 to 1.2	1.4 to 1.7	1.9 to 2.3	1.5	1.9 to 2.1	254
Lagasse et al. (2009)	19	S, R, M	0.9 to 1.6	1.0 to 1.1	0.7	0.1 to 0.3	0.2 to 1.0	0.5 to 1.0	0.7 to 1.2	3.0 to 25.0	1.6 to 3.7	18 to 145
Melville (1997)	17	C	0.6 to 1.1	0.2 to 0.8	0.8 to 0.9	0.1 to 2.5	0.1 to 1.4	0.4 to 0.8	0.6 to 1.0	0.1 to 12.6	0.4 to 2.7	18 to 901
Melville & Chiew (1999)	27	C	0.5 to 1.1	0.2 to 0.7	1.0	0.1 to 0.2	0.1 to 0.5	0.3 to 0.7	0.5 to 0.9	0.7 to 5.2	1.1 to 2.1	40 to 73
Oliveto & Hager (2002)	22	C	0.6 to 2.6	0.2 to 1.0	0.6 to 4.8	0.2 to 1.6	0.1 to 0.7	0.5 to 1.0	0.7 to 1.1	0.1 to 4.7	0.4 to 2.5	13 to 467
Shen (1969)	24	C	0.5 to 3.3	0.4 to 2.2	0.2 to 0.5	0.5 to 3.0	0.1 to 2.3	0.5 to 3.5	0.9 to 3.9	0.7 to 1.8	0.6 to 1.9	331 to 1988
Sheppard & Miller (2006)	24	C	0.6 to 7.1	0.7 to 1.6	0.3 to 0.8	0.5	0.4 to 1.0	0.5 to 4.4	0.6 to 5.4	1.3 to 3.2	1.1 to 3.1	181 to 564
Sheppard et al. (2004)	14	C	1.0 to 2.5	0.6 to 6.2	0.2 to 2.9	0.4 to 3.0	0.6 to 4.6	0.6 to 1.0	0.7 to 1.2	0.2 to 11.1	0.6 to 2.0	142 to 4159
Yanmaz & Altinbilek (1991)	48	C, S	0.5 to 1.2	0.2 to 0.5	0.8 to 1.1	0.2	0.1 to 0.5	0.4 to 0.7	0.5 to 0.9	0.7 to 3.5	1.0 to 2.2	44 to 80
ALL DATA	699	C, S, R, M	0.5 to 7.1	0.1 to 6.2	0.2 to 7.8	0.1 to 3.0	0.1 to 4.6	0.3 to 4.4	0.5 to 5.4	0.1 to 6.0	0.3 to 4.7	9 to 4159

Notes: [1] S = square, R = rectangular, M = multiple cylindrical columns, C = cylindrical

HEC-18 Pier Scour Equation – Laboratory Data

Using the laboratory data, pier scour for each test was predicted using the HEC-18 equation as presented in Hydraulic Engineering Circular 18 (HEC-18), Fifth Edition (Arneson et al. 2012). The HEC-18 equation, normalized to pier width, is:

$$\frac{y_s}{a} = 2.0\, K_1 K_2 K_3 K_w \left(\frac{y}{a}\right)^{0.35} (Fr)^{0.43} \quad \text{subject to the following limits:} \tag{4.3}$$

$$\frac{y_s}{a} = 2.4 \quad \text{for } Fr < 0.8$$

$$\frac{y_s}{a} = 3.0 \quad \text{for } Fr > 0.8$$

The coefficients and variables of the HEC-18 equation are:

y_s	=	Scour depth, ft (m)
a	=	Pier width normal to flow, ft (m)
K_1	=	Correction factor for shape of pier nose
K_2	=	Correction factor for skew angle (= 1.0 for piers aligned with the flow)
K_3	=	Correction factor for bedforms
K_w	=	Correction factor for very wide piers
y	=	Depth of approach flow, ft (m)
Fr	=	Froude number of the approach flow

The correction factor K_w for very wide piers is:

$$K_w = 2.58\left(\frac{y}{a}\right)^{0.34} Fr^{0.65} \quad \text{for } V/V_c < 1.0 \tag{4.4}$$

$$K_w = 1.0\left(\frac{y}{a}\right)^{0.13} Fr^{0.25} \quad \text{for } V/V_c \geq 1.0$$

$$K_w \leq 1.0$$

The correction factor K_w is only applied when <u>all</u> of the following conditions are met:

- $y/a < 0.8$
- $a/d_{50} > 50$
- $Fr < 1.0$

Based on the estimated critical velocity using the HEC-18 procedure described above, 495 data tests were conducted under clear-water scour conditions; the remaining 204 tests were conducted with live-bed conditions. The evolution of scour depth over time was not investigated in many of the studies; therefore, the data collection required introducing assumptions regarding the maturity of the scour hole at the end of each test. The 699 data points represent test runs that had a duration of 4 hours or more, and all data were subjected to a data quality examination as discussed later in this section.

The HEC-18 pier scour equation applied to all 699 data points in the laboratory data set is presented graphically in **Figure 4.1**. From this figure, it is clear that the limiting values of y_s/a = 2.4 for Froude numbers less than 0.8 and y_s/a = 3.0 for Froude numbers greater than 0.8 were met by some of the test data. The figure also indicates the line of perfect prediction as well as the best-fit linear regression through the origin (0,0).

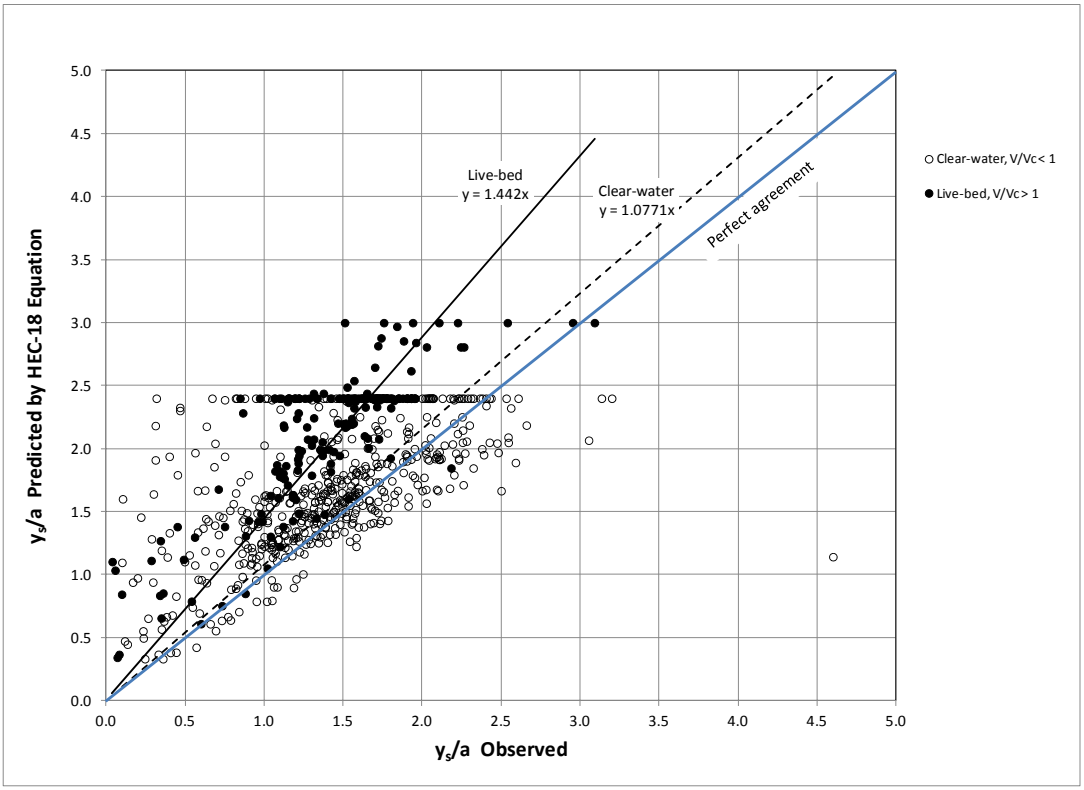

Figure 4.1. HEC-18 pier scour prediction vs. observed scour for clear-water and live-bed conditions, all data.

The bias of the HEC-18 pier scour prediction equation was determined to be 0.80 as the mean value of the ratio y_s (observed) to y_s (predicted) for all 699 data points. The Coefficient of Variation (COV) of the data is the standard deviation divided by the mean, and was determined to be 0.34 for this data set. Further partitioning the data into clear-water and live-bed subsets was performed; the results are shown in **Table 4.2** (see Section 2.6.2 for a discussion of the reliability index as a measure of bridge safety).

Table 4.2. Bias and Coefficient of Variation of the HEC-18 Pier Scour Equation with Laboratory Data, all data.

Data set	No. data points	Bias	COV	Percent under-predicted	Reliability β	
					Normal	Log-normal
All data	699	0.80	0.34	20.0%	0.72	0.83
Clear-water subset	495	0.86	0.34	27.7%	0.48	0.63
Live-bed subset	204	0.66	0.24	1.5%	2.14	1.87

Assessment of Laboratory Pier Scour Data Quality

Following the initial analysis of all 699 data points from the 22 data sources, a method was developed and used to identify and remove outliers, as described in this section. The data quality assessment method developed for this purpose relies only on variables that were directly measured during each test; no predictive techniques were used to discriminate among data points. Comments and suggestions from the Panel were incorporated in the screening procedure used to identify and remove outliers.

Three independent variables in non-dimensional form were identified as fundamental descriptors of physical processes causing scour at bridge piers. The first step of the data quality assessment procedure involves plotting these variables against measured pier scour normalized to pier width (y_s/a). The dimensionless variables (log a/d_{50}, V/V_c, and y/a) were used in NCHRP Report 682 (Sheppard et al. 2011) in their assessment of data quality, albeit in a manner different than that presented here. In this screening procedure, V_c as determined using the HEC-18 approach was used, as we determined that for the 43 data points where the two methods differ in distinguishing between clear-water vs. live-bed conditions, all data points are for borderline conditions where V/V_c is very nearly equal to 1.0.

Observed normalized scour depths y_s/a for all 699 tests were plotted against each of the three dimensionless variables described above. The data were then partitioned so that 90% of the data points fell within a band parallel to the linear regression line through the data scatter. The partitioning approach was structured such that 5% of the points fell above the band, and 5% below it. Data points outside the band were identified were considered outliers and removed from the data set.

This procedure resulted in 119 data points being eliminated from the laboratory pier scour data set, leaving 580 points for further analysis. This compares to the final data set used in NCHRP Report 682 which consisted of 441 data points. **Figures 4.2 through 4.4** present the results of the outlier screening process described above. In these figures, outliers are presented as data points falling above or below the dashed lines.

With the outliers removed, the final data set was re-plotted and used to re-analyze the bias and COV of the HEC-18 pier scour prediction equation. **Table 4.3** provides the final results of the analysis. **Figure 4.5** presents the final data graphically.

The data quality assessment procedure described in this section eliminated 17% of the data points, resulting in a significant improvement (decrease) in the Coefficient of Variation for all data in the final data set, as well as the clear-water and live-bed subsets. The reliability index β also improved significantly as can be seen by comparing Tables 4.2 and 4.3. Figure 4.5 presents the final data analysis graphically.

Florida DOT (FDOT) Pier Scour Equation – Laboratory Data

The pier scour approach in NCHRP Report 682 (Sheppard et al. 2011) is referenced as the Florida DOT (FDOT) Pier Scour Methodology in the 5th edition of HEC-18. The method is referred to as the FDOT pier scour equation in this report.

As with the HEC-18 equation, the FDOT pier scour equation includes flow velocity, depth and angle of attack, pier geometry and shape, but also includes particle size. The FDOT equation combines pier geometry, shape, and angle of attack to compute an effective pier width, a*. In contrast to the HEC-18 equation, the FDOT pier scour equation also distinguishes between clear-water and live-bed flow conditions.

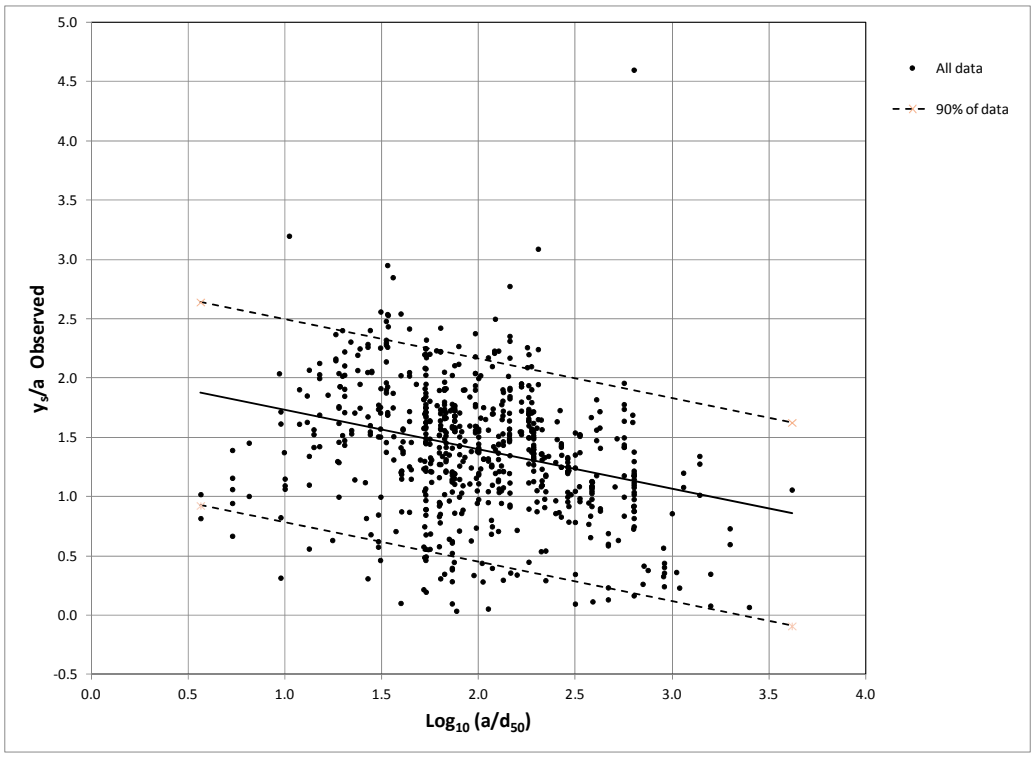

Figure 4.2. Observed scour vs. $\log_{10}(a/d_{50})$ showing outliers.

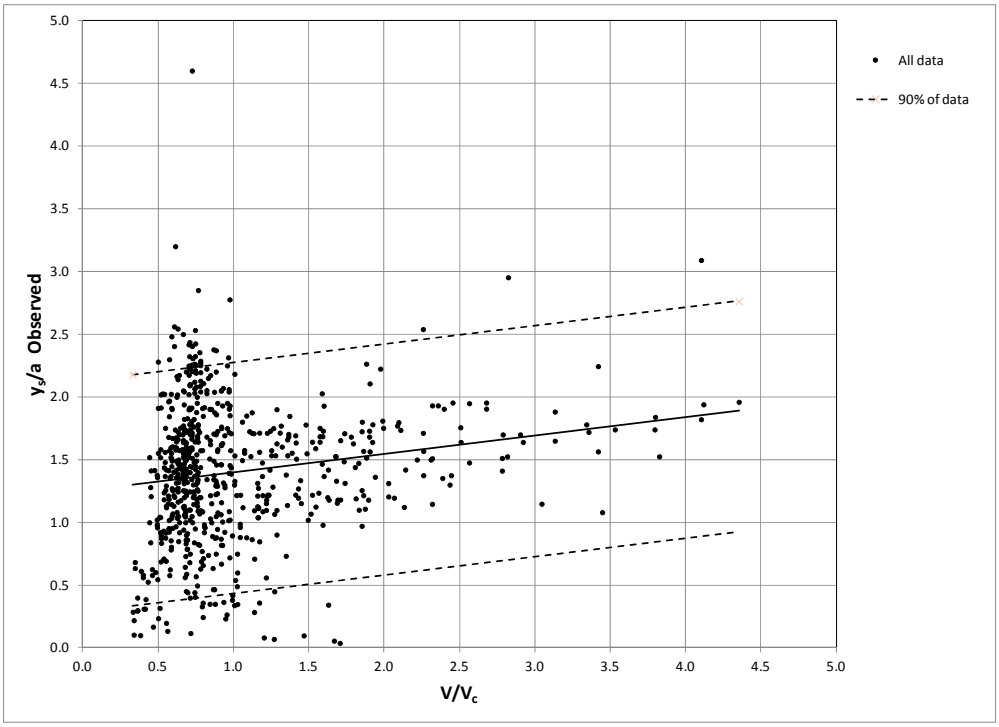

Figure 4.3. Observed scour vs. V/V_c showing outliers.

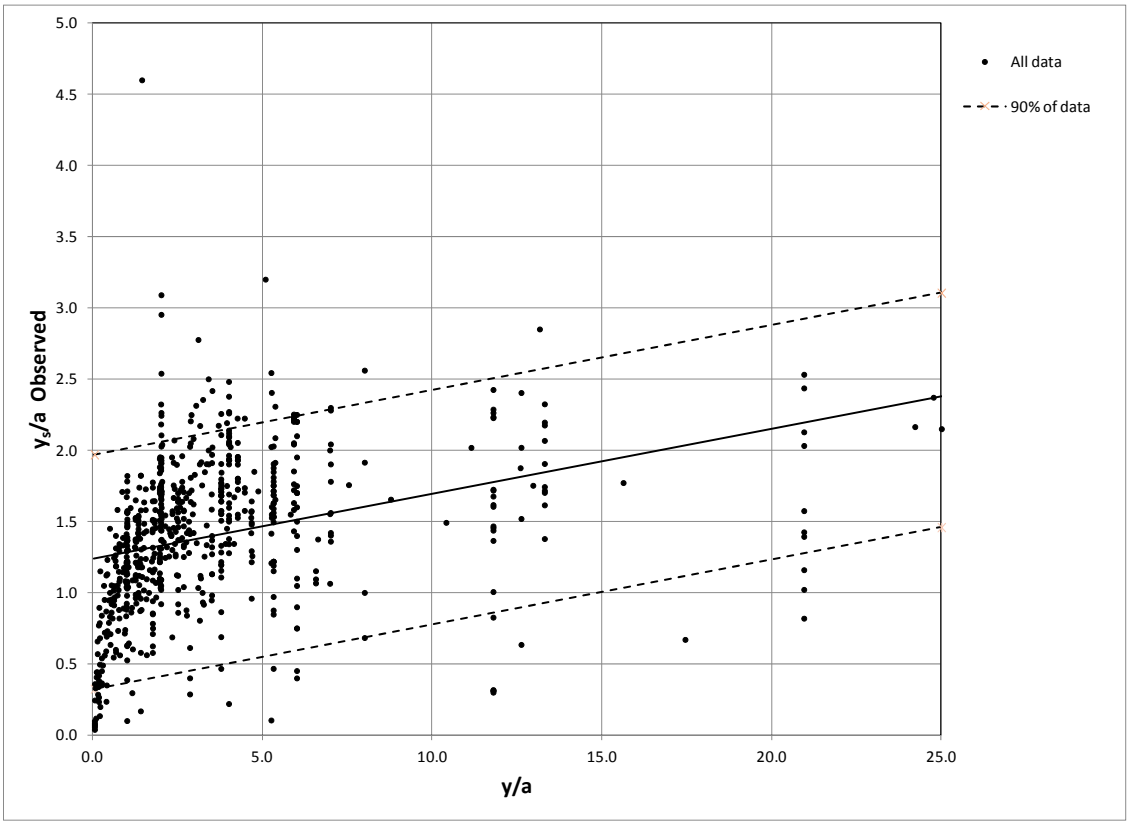

Figure 4.4. Observed scour vs. y/a showing outliers.

Table 4.3. Bias and Coefficient of Variation of the HEC-18 Pier Scour Equation with Laboratory Data, outliers removed.						
Data set	No. data points	Bias	COV	Percent under-predicted	Reliability β	
					Normal	Log-normal
All data	580	0.82	0.23	17.2%	0.97	1.00
Clear-water subset	402	0.88	0.21	24.6%	0.66	0.73
Live-bed subset	178	0.68	0.16	0.6%	2.92	2.49

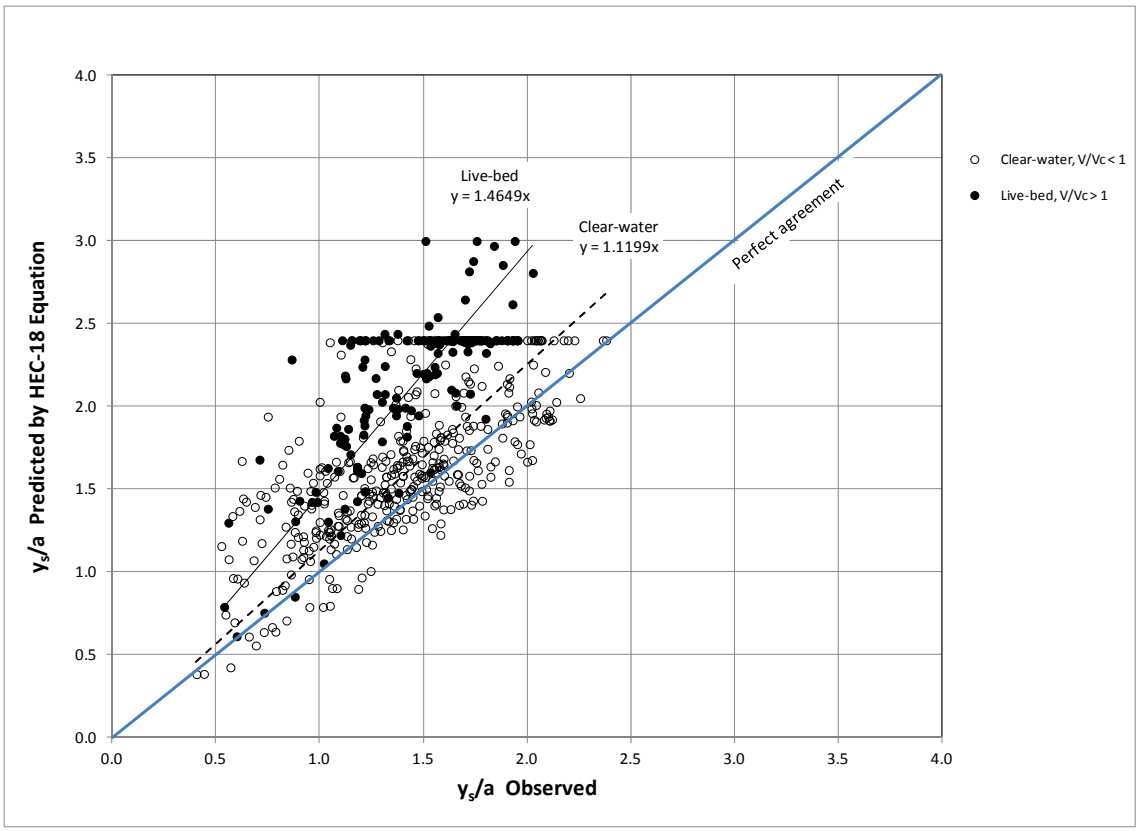

Figure 4.5. HEC-18 pier scour prediction vs. observed scour for clear-water and live-bed laboratory conditions (outliers removed).

Although the HEC-18 equation provides good results for most applications, the FDOT equation should be considered as an alternative, particularly for wide piers (y/a < 0.2) (Arneson et al. 2012). The FDOT methodology includes the following equations:

$$\frac{y_s}{a^*} = 2.5 f_1 f_2 f_3 \qquad \text{for } 0.4 \le \frac{V_1}{V_c} < 1.0 \tag{4.5}$$

$$\frac{y_s}{a^*} = f_1 \left[2.2 \left(\frac{\frac{V_1}{V_c} - 1}{\frac{V_{lp}}{V_c} - 1} \right) + 2.5 f_3 \left(\frac{\frac{V_{lp}}{V_c} - \frac{V_1}{V_c}}{\frac{V_{lp}}{V_c} - 1} \right) \right] \qquad \text{for } 1.0 \le \frac{V_1}{V_c} \le \frac{V_{lp}}{V_c} \tag{4.6}$$

$$\frac{y_s}{a^*} = 2.2 f_1 \qquad \text{for } \frac{V_1}{V_c} > \frac{V_{lp}}{V_c} \tag{4.7}$$

$$f_1 = \tanh\left[\left(\frac{y_1}{a^*} \right)^{0.4} \right] \tag{4.8}$$

$$f_2 = \left\{1 - 1.2\left[\ln\left(\frac{V_1}{V_c}\right)\right]^2\right\} \quad (4.9)$$

$$f_3 = \left[\frac{\left(\frac{a^*}{D_{50}}\right)^{1.13}}{10.6 + 0.4\left(\frac{a^*}{D_{50}}\right)^{1.33}}\right] \quad (4.10)$$

where:

y_s = Pier scour depth, ft (m)
a^* = Effective pier width, ft (m)
V_1 = Mean velocity of flow directly upstream of the pier, ft/s (m/s)
V_{lp} = Velocity of the live-bed peak scour, ft/s (m/s)
V_c = Critical velocity for movement of D_{50} as defined above, ft/s (m/s)
D_{50} = Median particle size of bed material, ft (m)

$$V_{lp} = 5V_c \text{ or } 0.6\sqrt{gy_1} \text{ (whichever is greater)} \quad (4.11)$$

where V_c is computed using Equation 4.2.

The effective pier width, a*, is the projected width of the pier times the shape factor, K_{sf}.

$$a^* = K_{sf}a_{proj} \quad (4.12)$$

The shape factor for a circular or round nosed pier is 1.0 and for a square end pier the shape factor depends on the angle of attack.

$$K_{sf} = 1.0 \quad \text{for circular or round nosed piers} \quad (4.13)$$

$$K_{sf} = 0.86 + 0.97\left(\left|\frac{\pi\theta}{180} - \frac{\pi}{4}\right|\right)^4 \quad \text{for square nosed piers} \quad (4.14)$$

where:

θ = flow angle of attack in degrees.

The projected width of the pier is:

$$a_{proj} = a\,\mathrm{Cos}\theta + L\,\mathrm{Sin}\theta \quad (4.15)$$

where:

a_{proj} = Projected pier width in direction of flow, ft (m)
a = Pier width, ft (m)
L = Pier length, ft (m)

The methodology can be accessed through a spreadsheet available at the Florida Department of Transportation website. It can also be computed from the equations presented above or by following the following steps.

1. Calculate V_c using Equation 4.2
2. Calculate V_{lp} using Equation 4.11
3. Calculate a* using Equation 4.12
4. Calculate f_1 using Equation 4.8
5. Calculate f_3 using Equation 4.10
6. Calculate $\frac{y_{s-c}}{a^*}$ and y_{s-c} (defined below)
7. Calculate $\frac{y_{s-lp}}{a^*}$ and y_{s-lp} (defined below)
8. If $V_1 < 0.4V_c$, then $y_s = 0.0$
9. If $0.4V_c < V_1 \leq V_c$, then calculate f_2 using Equation 4.9, and $y_s = f_2 y_{s-c}$
10. If $V_1 \geq V_{lp}$, then $y_s = y_{s-lp}$
11. If $V_c < V_1 < V_{lp}$, then calculate y_s from:

$$y_s = y_{s-c} + \frac{(V_1 - V_c)}{(V_{lp} - V_c)}(y_{s-lp} - y_{s-c}) \qquad (4.16)$$

Note that Equation 4.16 is an equivalent, but simplified version of Equation 4.6. y_{s-c} is the scour at critical velocity for bed material movement (V_c) and is equal to $2.5f_1f_3a^*$. y_{s-lp} is the scour at live-bed peak velocity (V_{lp}) and is equal to $2.2f_1a^*$. The FDOT spreadsheet uses y_{s-c} as the design scour value when it is greater than y_{s-lp}.

The FDOT methodology for pier scour includes four regions as shown in **Figure 4.6**.

- Scour Region I (Step 8, above) is for clear-water conditions with velocity too low to produce scour, which occurs for velocities less than $0.4V_c$. However, field data in NCHRP Report 682 include observed scour for this condition, although it was only observed on one occasion for laboratory data.
- Scour Region II is for clear-water conditions with flow velocity large enough to produce pier scour ($V_c > V_1 > 0.4V_c$) as defined by Step 9, above.
- Scour Region IV is defined by the live-bed peak velocity (V_{lp}), where the maximum live-bed scour occurs at $5V_c$ or greater. Any velocity greater than V_{lp} is assigned the scour, y_{s-lp}, computed for V_{lp} (Step 10).
- Live-bed scour that occurs for flow velocities between critical velocity and the live-bed peak velocity ($V_c < V_1 < V_{lp}$) occurs in scour Region III as defined by Step 11 and Equation 4.16.

Pier scour was predicted using the FDOT methodology on the same 580 laboratory data points previously analyzed with the HEC-18 equation. It should be noted that HEC-18 uses a different method than the FDOT equation for differentiating clear-water from live-bed. Using the HEC-18 method, 178 of the data points are live-bed and 402 are clear-water. Using the FDOT method, 221 data points are live-bed and 359 are clear-water. All of the points identified as clear-water by the HEC-18 method are clear-water using the FDOT method. Of the 43 points where the two methods differ (all are clear-water according to HEC-18), the two methods differ only for borderline cases of distinguishing live-bed versus clear-water conditions.

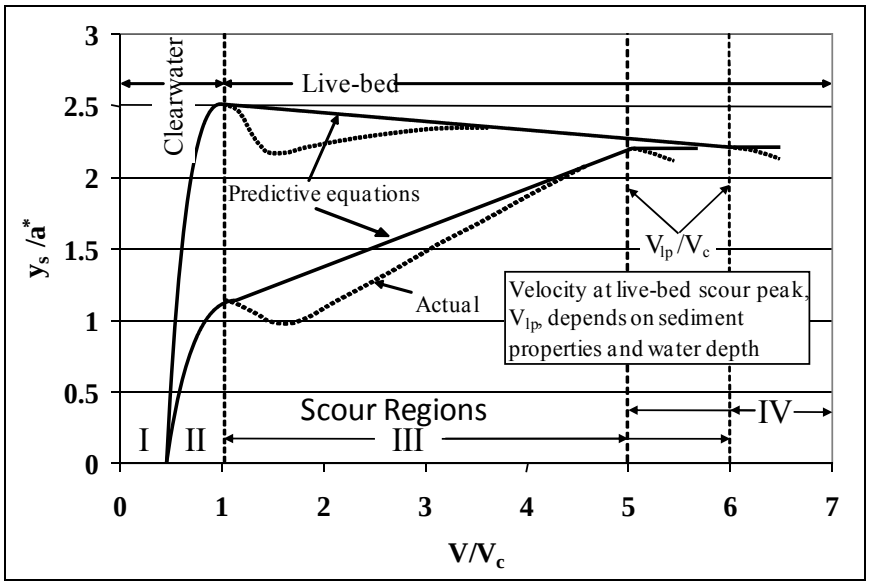

Figure 4.6. Scour regions for FDOT pier scour methodology.

Table 4.4 provides the final results of the pier scour prediction for the laboratory data using the FDOT methodology. **Figure 4.7** presents the final data graphically.

Table 4.4. Bias and Coefficient of Variation of the FDOT Pier Scour Methodology with Laboratory Data, outliers removed.

Data set	No. data points	Bias	COV	Percent under-predicted	Reliability β	
					Normal	Log-normal
All data	580	0.78	0.20	6.7%	1.42	1.29
Clear-water subset	359	0.80	0.20	9.5%	1.26	1.55
Live-bed subset	221	0.75	0.18	2.3%	1.78	1.58

Discussion of HEC-18 and FDOT Pier Scour Predictions – Laboratory Data

Live-bed conditions are predominant for bridge design for piers in the main channel. Clear-water conditions occur most frequently for piers in the overbank. For live-bed conditions, the HEC-18 equation provides an equation reliability (Beta) of 2.92 while the FDOT equation provides a reliability of 1.78; both equations have a better reliability assuming the variability in predictions are normally distributed. For clear-water data, both equations do not perform as well; the HEC-18 equation provides a reliability (Beta) of 0.73 while the FDOT equation provides a reliability of 1.55. In the case of the clear-water data, the variability in prediction is better described assuming a log-normal distribution for both equations.

One possibility is that the large number of under predictions by the HEC-18 equation for clear-water conditions is related to the 43 data points where the two approaches differ in identifying critical velocity. If these 43 data points are included as live-bed in the HEC-18 data set, there is only one additional under prediction (2 versus 1). Therefore, the large group of clear-water under predictions by the HEC-18 equation is identified by either method as clear-water. **Figure 4.8** presents the scour predicted by the HEC-18 equation vs. the scour predicted by the FDOT methodology. In this figure, the distinction between live-bed vs. clear-water conditions was determined using the FDOT procedure. It is clear that either equation can predict more or less scour than the other, depending on the particular combination of hydraulic conditions, and it does not matter if the conditions are live-bed or clear-water.

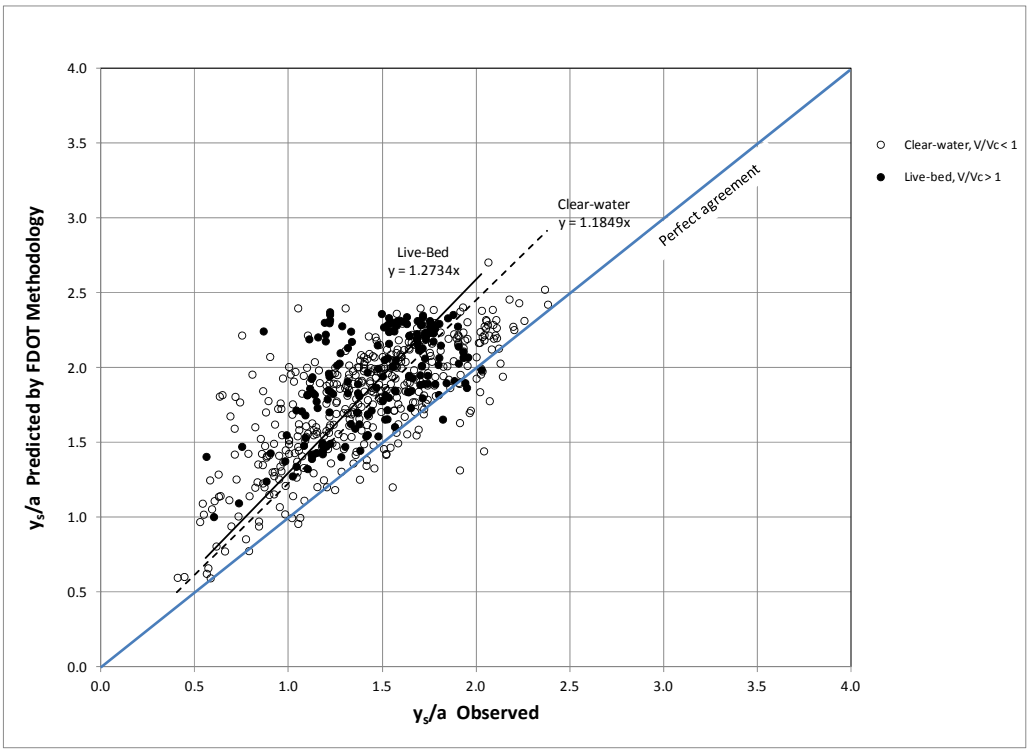

Figure 4.7. FDOT pier scour prediction vs. observed scour for clear-water and live-bed laboratory conditions (outliers removed).

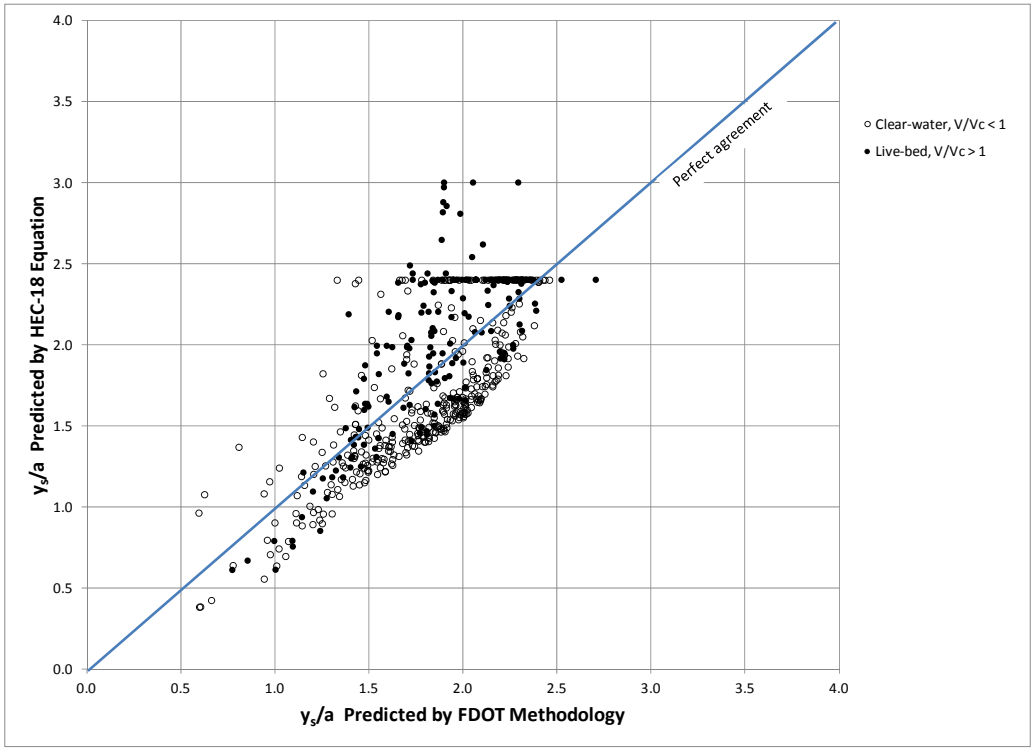

Figure 4.8. HEC-18 vs. FDOT pier scour predictions using laboratory data.

These results indicate that there may be value using one equation (FDOT) for clear-water conditions and the other (HEC-18) for live-bed and that different scour factors could be applied based on the bed condition and the desired reliability. It should be noted that the equation reliability is not the final reliability for bridge design because many other factors and types of uncertainty must be included with evaluating the reliability for the design life of a structure.

4.1.2 Pier Scour Field Data - Compilation and Analysis

Pier scour data from field studies were obtained from NCHRP Report 682 (Sheppard et al. 2011) which provided 943 data points from four sources. From the data screening performed by that study, 183 data points were identified as outliers and the remaining 760 data points were used in their analyses. No additional data were added to this data set, i.e., an independent screening was not performed. The analysis for this study simply used the same 760 data points reported by Sheppard et al. (2011). **Table 4.5** provides a summary of the range of variables associated with the field data sets.

Table 4.5. Summary of Field Pier Scour Data Sets (from NCHRP Report 682).

Source	No. data points	V (ft/s)	y (ft)	a (ft)	d_{50} (mm)	y_s obs(ft)
Mueller and Wagner (2005)	409	0.3 – 14.8	0.3 – 73.8	1.6 – 55.2	0.1 – 108	0 – 25.3
Gao et al. (1993)	234	1.1 – 15.4	0.4 – 38.1	3.3 – 29.7	0.2 - 70	0.3 – 17.7
Zhuravlyov (1978)	52	1.1 – 5.3	1.0 – 56.1	0.7 – 33.5	0.2 – 1.8	0.6 – 18.9
Froehlich (1988)	65	0.5 – 12.0	1.4 – 61.7	3.0 – 33.1	0.3 - 90	0.5 – 25.6
ALL DATA (outliers removed)	760	0.3 – 15.4	0.3 – 73.8	0.7 – 55.2	0.1 - 108	0 – 25.6

HEC-18 Pier Scour Equation – Field Data

The HEC-18 pier scour equation (Equation 4.3) applied to all 760 data points in the field data set is presented graphically in **Figure 4.9**, partitioned into clear-water and live-bed conditions in accordance with the critical velocity equation used with the HEC-18 method. The figure also indicates the line of perfect prediction as well as the best-fit linear regression through the origin (0,0). **Table 4.6** presents the summary statistics for the HEC-18 equation using the field data set.

The COVs associated with the pier scour field data (both live-bed and clear water subsets) are significantly larger than those for the laboratory data. This reflects the difficulty in estimating the hydraulic conditions associated with the creation of a scour hole at an actual bridge site compared to a controlled laboratory setting, as well as the uncertainty regarding the maturity of the scour hole with respect to equilibrium depth.

Florida DOT (FDOT) Pier Scour Equation – Field Data

Figure 4.10 and **Table 4.7** present the results of the FDOT methodology applied to the field data set. It should be noted that for critical velocity ratios V/V_c less than 0.4, the FDOT method predicts zero scour. Of the 760 field data points, 27 exhibited measurable scour when the velocity ratio was less than 0.4, where the FDOT procedure predicts no scour.

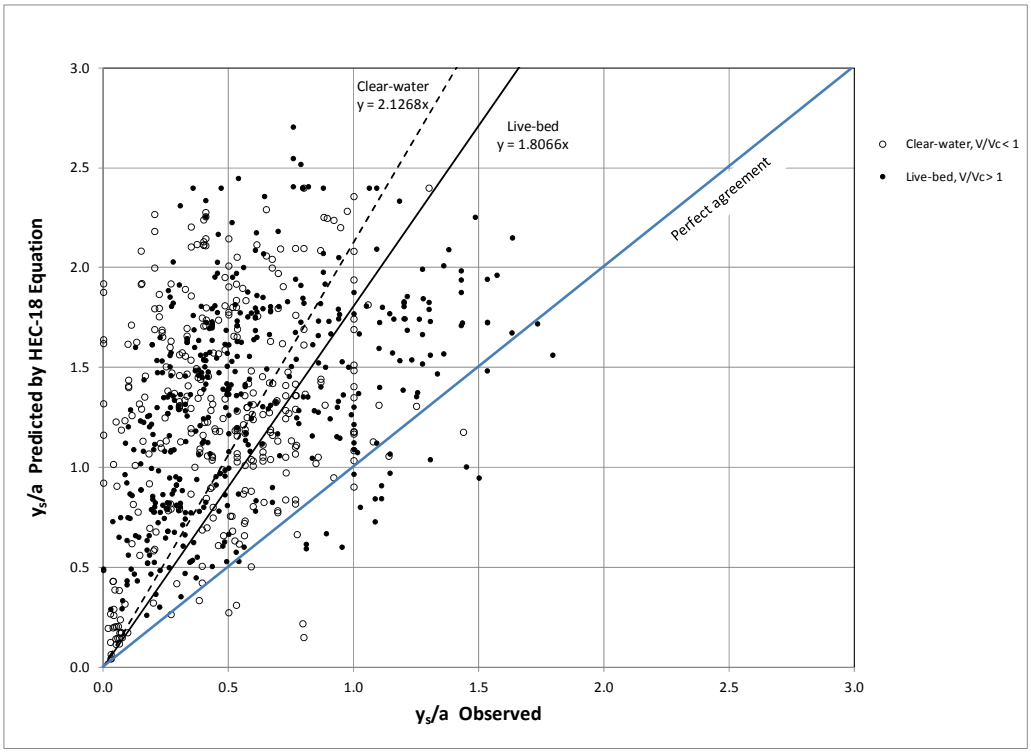

Figure 4.9. HEC-18 pier scour prediction vs. observed scour for clear-water and live-bed field data (outliers removed).

Table 4.6. Bias and Coefficient of Variation of the HEC-18 Pier Scour Equation with Field Data, outliers removed.

Data set	No. Data points	Bias	COV	Percent Under-predicted	Reliability β	
					Normal	Log-normal
All data	760	0.44	0.79	4.0%	1.61	1.52
Clear-water subset	325	0.44	0.97	3.4%	1.33	1.43
Live-bed subset	435	0.45	0.62	4.4%	1.99	1.70

Therefore, when calculating bias and COV for FDOT methodology using ($y_{s\ obs}/y_{s\ calc}$), these 27 points give a divide by zero and were therefore eliminated. However, for purposes of reporting the percent of underpredictions, these 27 clear-water points are included. Also, as with the laboratory data set, the partitioning of live-bed vs. clear-water data subsets conditions is different than that for the HEC-18 approach, because the critical velocity equations are different.

Discussion of HEC-18 and FDOT Pier Scour Predictions – Field Data

Live-bed conditions were much more predominant in the field data set compared to the laboratory data, presumably reflecting more monitoring and reporting of piers in the main channel compared to overbank areas. Overall, the conclusions from the analyses of the field data are similar to those for the laboratory data, with the exception that the HEC-18 equation exhibited fewer underpredictions for both live-bed and clear-water subsets compared to the FDOT methodology.

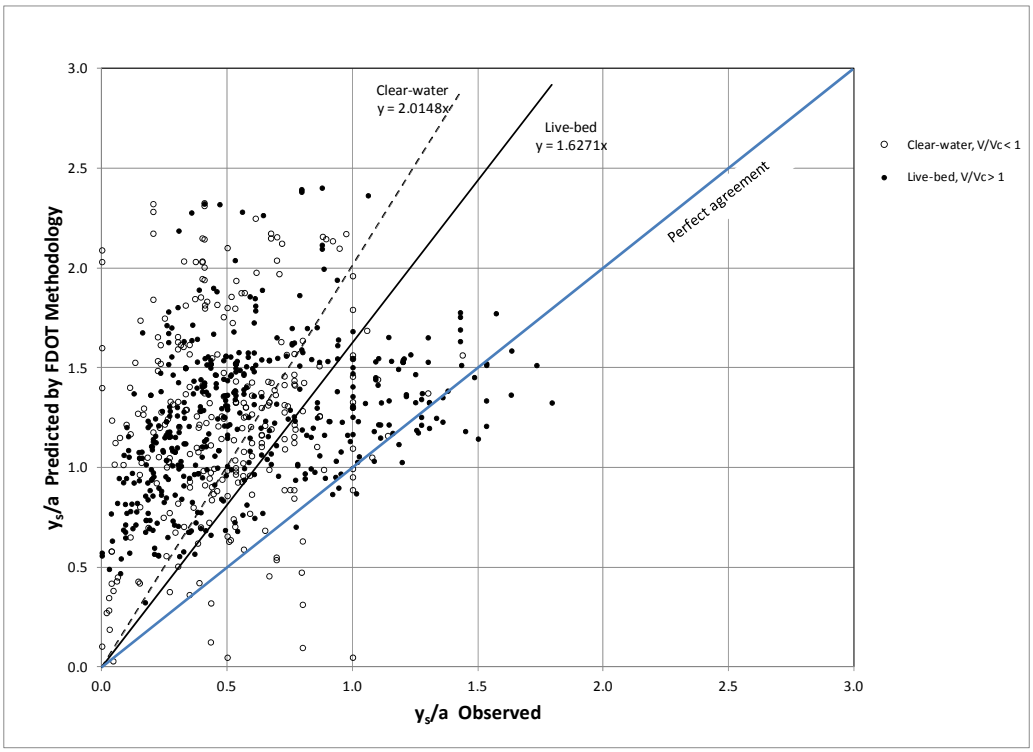

Figure 4.10. FDOT pier scour prediction vs. observed scour for clear-water and live-bed field data (outliers removed).

Table 4.7. Bias and Coefficient of Variation of the FDOT Pier Scour Methodology with Field Data, outliers removed.

Data Set	No. Data Points	Bias	COV	Percent Under-predicted (Note 2)	Reliability β	
					Normal	Log-normal
All data	733 (Note 1)	0.51	1.83	9.1%	0.53	1.17
Clear-water subset	275 (Note 1)	0.59	2.51	14.2%	0.28	1.08
Live-bed subset	458	0.46	0.61	5.7%	1.91	1.66
Note 1: 27 data points eliminated where predicted scour was zero and observed scour was nonzero. Note 2: 27 data points included in the calculation of percent underpredicted						

For live-bed conditions, the HEC-18 equation provides an equation reliability (Beta) of 1.99 while the FDOT equation provides a reliability of 1.91; both equations have a better reliability assuming the variability in predictions are normally distributed. For clear-water field data, both equations do not perform as well; the HEC-18 equation provides a reliability (Beta) of 1.43 while the FDOT equation provides a reliability of 1.08. In the case of the clear-water data, the variability in prediction is better described assuming a log-normal distribution for both equations, similar to the laboratory data set.

Figure 4.11 presents the scour predicted by the HEC-18 equation vs. the scour predicted by the FDOT methodology. In this figure, the distinction between live-bed vs. clear-water conditions was determined using the FDOT procedure. Similar to the laboratory data set, the field data show that either equation can predict more or less scour than the other, depending on the particular combination of hydraulic conditions, and does not matter if the conditions are live-bed or clear-water.

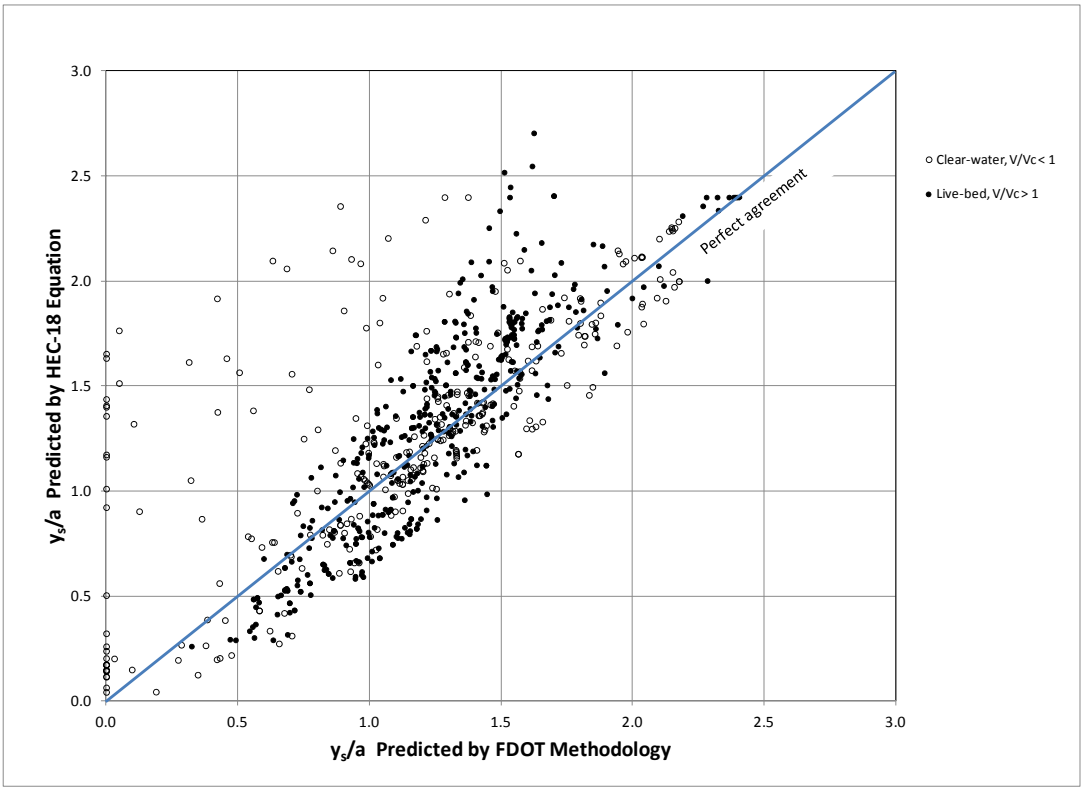

Figure 4.11. HEC-18 vs. FDOT pier scour predictions using field data.

4.2 Contraction Scour

4.2.1 Clear-Water Contraction Scour Laboratory Data - Compilation and Screening

The HEC-18 clear-water contraction scour equation was not developed from laboratory or field data, but instead was derived from sediment transport concepts and theory (Richardson et al. 2001). In U.S. customary units, the HEC-18 clear-water contraction scour equation is:

$$y_2 = \left[\frac{K_u Q^2}{D_m^{2/3} W^2}\right]^{3/7} \quad (4.17)$$

$$y_s = y_2 - y_0 \quad (4.18)$$

where:

y_2 = Depth of flow in contracted section after scour has occurred, ft (m)
K_u = Conversion factor equal to 0.0077 for U.S. customary units (0.025 for SI units)
Q = Discharge in contracted section, ft^3/s (m^3/s)
D_m = Representative particle size equal to 1.25 times d_{50}, ft (m)
W = Width of contracted section, ft (m)
y_s = Depth of scour in contracted section, ft (m)
y_0 = Depth of flow in contracted section before scour occurs, ft (m)

A definition sketch showing these variables is provided as **Figure 4.12**.

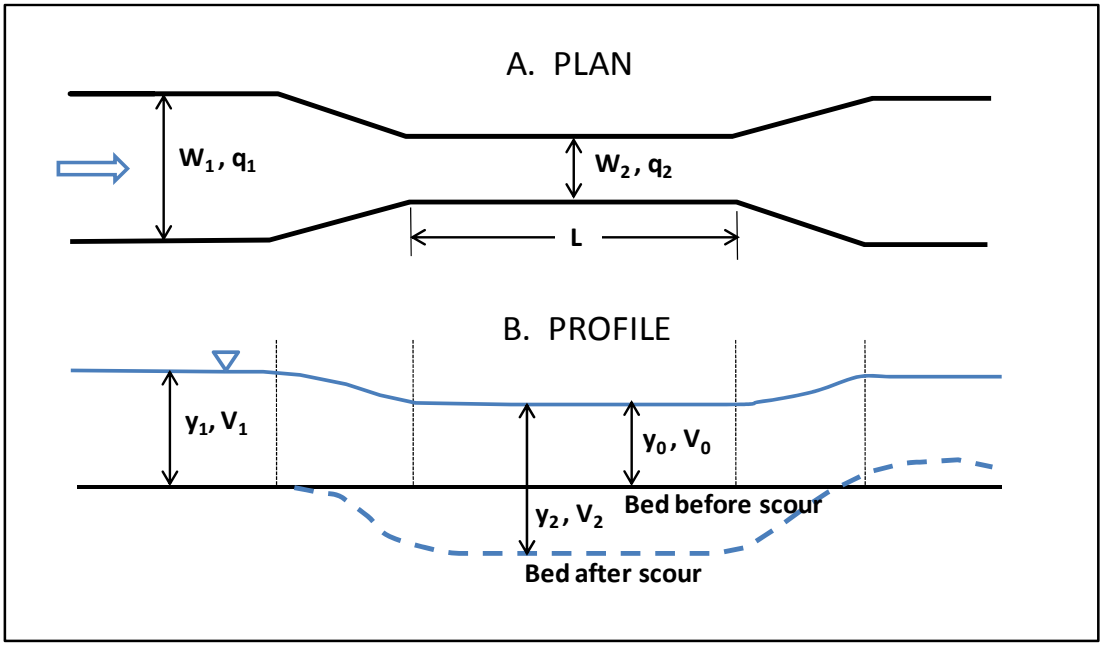

Figure 4.12. Definition sketch for HEC-18 clear-water contraction scour equation.

Contraction scour data obtained under controlled laboratory conditions were assembled from eight sources, yielding 182 independent measurements of contraction scour in cohesionless soils. Only long contractions were considered, because short contractions include an abutment scour effect in addition to the contraction scour. A contraction is considered to be long if the length L of the contracted section is greater than the width W_1 of the approach section as shown in Figure 4.12 (Raikar 2004). However, comprehensive studies by Webby (1984) suggest that a long contraction is defined when the length, L, is twice the width of the approach section W_1.

All data sets consisted of studies where the following information was documented: (1) scour depth y_s, (2) approach flow depth y_1, (3) approach flow velocity V_1, (4) median sediment size d_{50}, (5) approach width W_1, (6) width of contracted section W_2, and (7) length of contracted section L. Data from 182 test runs are summarized in Dey and Raikar (2005) and were obtained from that reference. In that publication, data from other researchers (Komura 1966, Gill 1981, Webby 1984, and Lim 1993) were included along with the tests actually performed by Dey and Raikar.

All 182 tests involved clear-water conditions in the approach flow ($V_1/V_c < 1.0$), where V_c is the critical velocity for each test estimated using the relationship presented in HEC-18 (Arneson et al. 2012):

$$V_c = \frac{y^{1/6}\sqrt{K_s(S_s - 1)}d_{50}}{n} \qquad (4.19)$$

where:

V_c = Critical velocity for particle motion, ft/s
y = Approach flow depth, ft
K_s = Dimensionless Shields parameter (0.03 for gravel, 0.047 for sand)
S_s = Specific gravity of particle (assumed equal to 2.65 unless otherwise indicated)

d_{50} = Median particle diameter, ft
n = Manning resistance coefficient, estimated as $n = 0.034(d_{50})^{1/6}$ (d_{50} in ft)

Table 4.8 provides a summary of the laboratory contraction scour data compiled for this project (U.S. customary units are shown, with the exception of particle diameter in millimeters).

Table 4.8. Summary of Laboratory Clear-Water Contraction Scour Data Sets

Source	No. Data Points	d_{50} (mm)	V_1 (ft/s)	V_1/V_c	Y_1 (ft)	W_1 (ft)	W_2 (ft)	$y_{s\ observed}$ (ft)
Dey & Raikar, 2005 uniform sand	24	0.81 – 2.54	1.02 – 1.86	0.79 – 0.95	0.28 – 0.43	1.97	0.79 – 1.38	0.08 – 0.51
Dey & Raikar, 2005 uniform gravel	75	4.1 – 14.25	1.89 – 3.05	0.83 – 0.95	0.22 – 0.45	1.97	0.79 – 1.38	0.07 – 0.47
Dey & Raikar, 2005 well graded sand	12	0.81 – 2.54	1.09 – 1.86	0.81 – 0.95	0.41 – 0.43	1.97	1.18	0.05 – 0.21
Dey & Raikar, 2005 well graded gravel	20	4.1 – 14.25	2.16 – 2.98	0.86 – 0.93	0.40 – 0.45	1.97	1.18	0.05 – 0.24
Komura 1966	12	0.35 – 0.55	0.57 – 0.81	0.66 – 0.88	0.09 – 0.28	1.31	0.33 – 0.66	0.11 – 0.26
Gill 1981	22	0.92 – 1.53	0.67 – 1.26	0.54 – 0.88	0.09 – 0.27	2.49	1.64	0.03 – 0.16
Webby 1984	11	2.15	0.70 – 1.22	0.38 – 0.68	0.29 – 0.43	5.20	1.72	0.15 – 0.38
Lim 1993	6	0.47	0.68 – 0.73	0.81 – 0.84	0.08 – 0.09	1.31	0.39 – 0.85	0.03 – 0.17
Total	**182**	**0.35 – 14.25**	**0.57 – 3.05**	**0.38 – 0.95**	**0.08 – 0.45**	**1.31 – 1.97**	**0.33 – 1.72**	**0.03 – 0.51**

Figure 4.13 presents measured data taken during a contraction scour experiment (Webby 1984) that clearly shows that there is a significant difference between y_0 and y_1 as scour begins to take place during the early stages of a test.

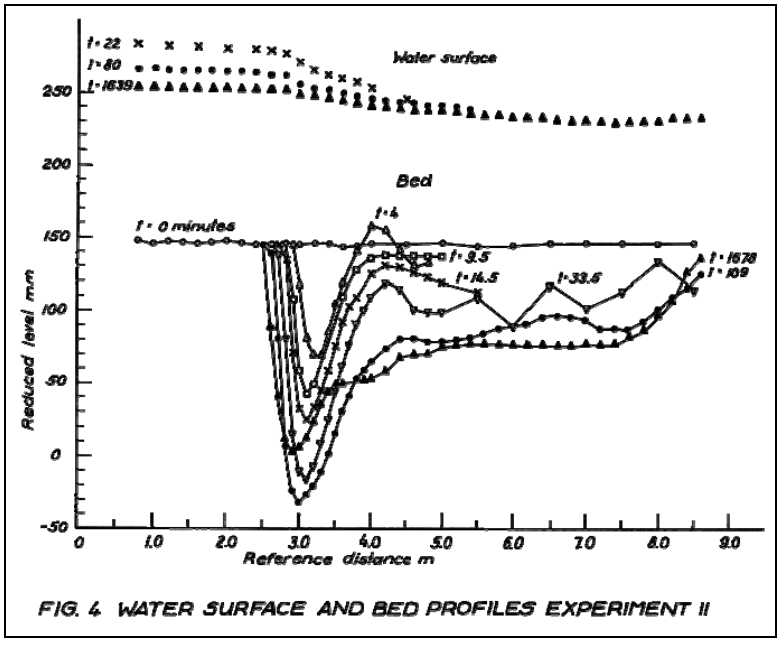

Figure 4.13. Water surface and bed elevations at different times during a clear-water contraction scour experiment (from Webby 1984).

Assessment of Data Quality

Because of questions regarding the accuracy of some of the data provided in the Dey and Raikar (2005) table during the screening and assessment of the contraction scour data, the original work from all previous studies was obtained and reviewed.

A detailed review of previous studies found that Dey and Raikar (2005) incorrectly interpreted the results of the tests conducted by Komura (1966), Gill (1981), and Lim (1993). Specifically, those studies did not actually measure the depth of scour in the contracted section, but instead assumed that the depth of scour was equal to the difference in flow depths, $y_2 - y_1$.

Dey and Raikar reported those results as "observed scour." As discussed above, this assumption is not valid because the drawdown effect on the water surface in the contracted section is not accounted for. Therefore, it was concluded that the scour "measurements" from the studies by Komura (1966), Gill (1981), and Lim (1993) are unreliable, and those data points were discarded from further analysis.

The Dey and Raikar tests that utilized well-graded bed materials were also re-examined. Although Dey and Raikar do not provide the grain size curves for the materials, they do provide the d_{50} grain size and the geometric standard deviation σ_g, defined as

$$\sigma_g = \sqrt{\frac{d_{84}}{d_{16}}} \tag{4.20}$$

For the Dey and Raikar tests using well-graded bed materials, σ_g ranged from 1.46 to 3.60. Further investigation revealed that when σ_g is greater than 1.9, there is a sufficient number of larger particles present in the bed material to create a self-armoring condition that limits the depth of scour. Therefore, the Dey and Raikar tests that used well-graded bed material for which σ_g was greater than 1.9 were eliminated.

After screening the 182 data points as discussed above, 119 data points remained with which to assess the HEC-18 clear-water scour equation.

4.2.2 Clear-Water Contraction Scour Laboratory Data - Analysis

In practice, the depth of flow y_0 in the contracted section before scour occurs is typically determined by use of a water surface profile model such as HEC-RAS. However, because the laboratory data did not include a direct measurement of this flow depth (presumably because in the laboratory, scour occurs before the target flow conditions are established), y_0 must be estimated from available data. As a first approximation, the velocity V_0 and flow depth y_0 in the contracted section before scour occurs are estimated as:

From continuity,

$$V_0 = \frac{Q}{A} \approx \frac{Q}{y_1 W_2} \tag{4.21}$$

Assuming no energy losses, the specific energy in the contracted section is equal to that in the approach section, so:

$$y_0 = y_1 + \frac{V_1^2}{2g} - \frac{V_0^2}{2g} \tag{4.22}$$

V_0 is then recalculated as:

$$V_0 = \frac{Q}{A} = \frac{Q}{y_0 W_2} \tag{4.23}$$

For the laboratory data, this approach yielded estimates of y_0 which in many cases were unreasonably small and, for a significant number of data points, negative values of y_0 were obtained using this first approximation. Further investigation revealed that the contraction ratios W_2/W_1 in the laboratory tests were severe enough to create a "choked" condition at the entrance to the contraction. The threshold of choking occurs when the actual contraction ratio is less than the critical ratio σ, defined by (Wu and Molinas 2005):

$$\sigma = \left(\frac{3}{(2 + F_1^2)} \right)^{3/2} F_1^2 \tag{4.24}$$

It was found that 113 of the 119 tests were conducted with some degree of choking. **Figure 4.14** presents the dimensionless choking ratio $\sigma W_2/W_1$ plotted versus the unit discharge in the contracted section. To resolve this issue, the estimate of y_0 was refined by comparing the initial depth ratio y_0/y_1 to the contraction ratio W_2/W_1. If the depth ratio from the initial approximation was less than the contraction ratio, the depth y_0 was re-estimated as y_1 times the contraction ratio as a limiting condition. This second iteration yielded more reasonable values for assessing the HEC-18 clear-water contraction scour prediction. Three additional data points were identified as outliers, leaving a final data set of 116 points for analysis.

Figure 4.15 shows the results of the analysis with the reduced data set. The bias of the HEC-18 clear-water contraction scour equation was determined to be 0.92 as the mean value of the ratio y_s (observed) to y_s (predicted). The Coefficient of Variation (COV) of the data is the standard deviation divided by the mean, determined to be 0.21 for this data set. The clear-water scour equation underpredicted the observed scour for 23.3% of the data points (27 tests out of 116).

The reliability index β for the clear-water contraction scour equation was determined to be 0.44 and 0.52 for normal and log-normal distributions, respectively. These relatively low values of β are not surprising, considering that the HEC-18 clear-water contraction scour equation was not developed from laboratory or field data, but instead was derived from sediment transport concepts and theory. It is therefore a predictive equation, not a design equation, and as such does not have built-in conservatism. Values of β near zero indicate that on average, observed scour is underpredicted by about the same magnitude and frequency as it is overpredicted. **Table 4.9** provides a summary of the prediction statistics for the HEC-18 clear-water contraction scour equation.

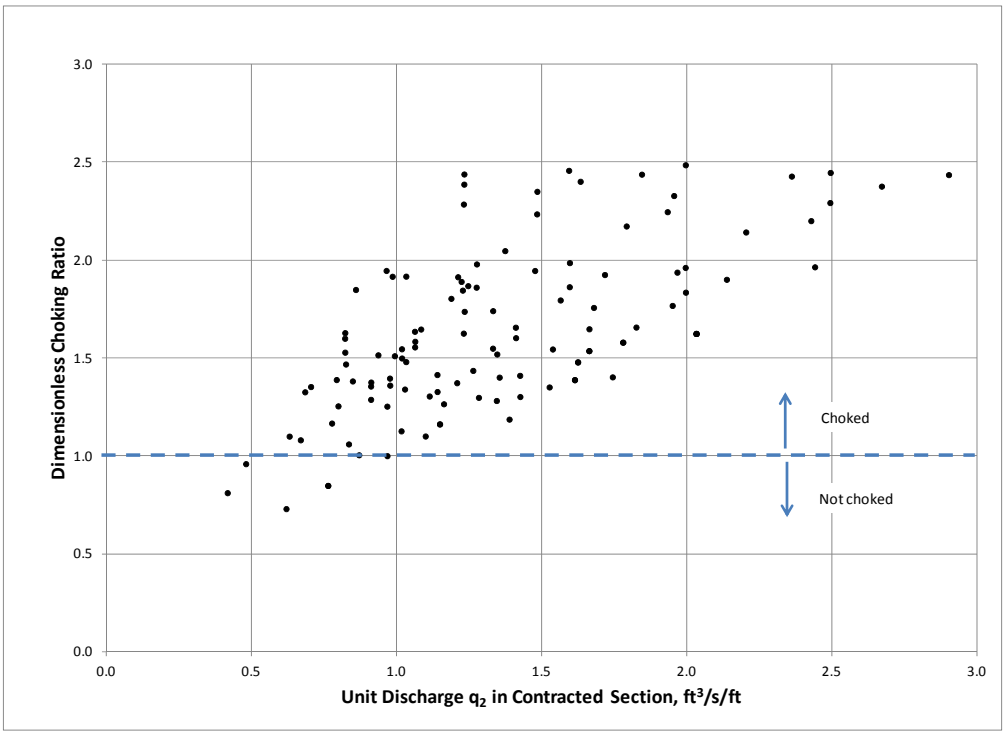

Figure 4.14. Dimensionless choking ratio vs. unit discharge in the contracted section for 119 laboratory tests.

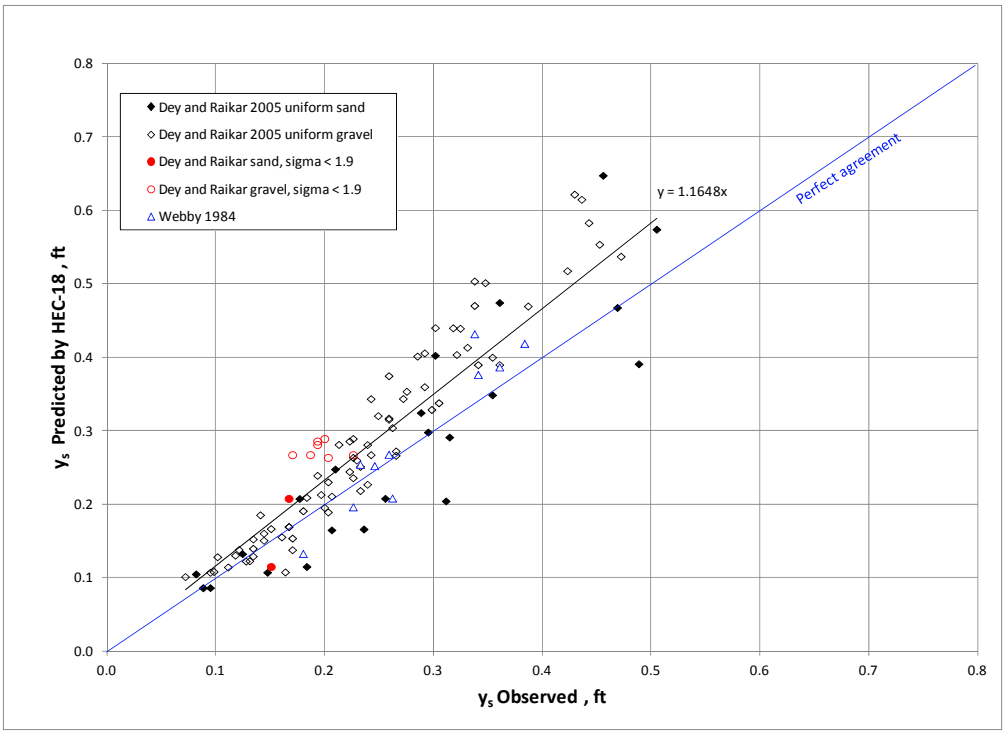

Figure 4.15. Predicted vs. observed clear-water contraction scour, 116 laboratory tests (outliers removed).

Table 4.9. Bias and Coefficient of Variation of the HEC-18 Clear Water Contraction Scour Equation with Laboratory Data, outliers removed.						
Data Set	No. Data Points	Bias	COV	Percent Under-predicted	Reliability β	
					Normal	Log-normal
All data (clear-water)	116	0.92	0.21	23.3%	0.44	0.52

4.3 Abutment Scour Data

4.3.1 Abutment Scour Laboratory Data - Compilation

In the initial research work plan for this project, it was recommended that two equations from the then-current HEC-18 (4th Edition, Richardson and Davis 2001) be investigated (the Froehlich and the HIRE equations), but also that results and recommendations from on-going NCHRP research on abutment scour be considered, if available in a timely fashion.

Final reports were available from both NCHRP 24-20 "Estimation of Scour Depth at Bridge Abutments," (Ettema et al. 2010), and NCHRP Project 24-27(2) "Evaluation of Bridge Scour Research: Abutment and Contraction Scour Processes and Prediction," (Sturm et al. 2011). Both NCHRP reports were reviewed and all laboratory data from the NCHRP 24-20 study was acquired. This study combines contraction and abutment scour processes to provide an estimate of the total scour at an abutment. This section presents the results of the screening and analysis of the NCHRP 24-20 data and includes a similar abutment scour data set (Ballio et al. 2009).

Rather than analyzing abutment scour data related to the Froehlich and HIRE equations (local scour only at an abutment), the predictive capability of the approach taken by NCHRP Project 24-20 (which was subsequently endorsed by NCHRP Project 24-27(02)) was investigated. Although the Froehlich and HIRE equations still appear in the 5th Edition of HEC-18 (Arneson et al. 2012), FHWA guidance suggests that the NCHRP 24-20 methodology will provide a better estimate of the combined effects of contraction scour and local scour at an abutment.

NCHRP 24-20 developed abutment scour equations considering a range of abutment types, abutment locations, flow conditions, and sediment transport conditions. These equations use contraction scour as the starting calculation for abutment scour and apply an amplification factor to account for large-scale turbulence that develops in the vicinity of the abutment tip. One important distinction regarding the contraction scour calculation is that the abutment creates a non-uniform flow distribution in the contracted section. The flow is more concentrated in the vicinity of the abutment and the contraction scour component is greater than for average conditions in the constricted opening. NCHRP 24-20 defines three abutment scour conditions:

Scour Condition A: Scour occurring when the abutment is in, or close to, the main channel.

Scour Condition B: Scour occurring when the abutment is on the floodplain and set well back from the main channel.

Scour Condition C: Scour occurring when the embankment breaches and the abutment foundation acts as a pier. NCHRP study 24-20 concluded that there is a limiting depth of abutment scour when the geotechnical stability of the roadway embankment or channel bank is reached.

Abutment scour conditions A, B, and C are illustrated in **Figure 4.16**. For purposes of this research project, scour condition C (in which the approach embankment is breached) is a special case and is not considered here. Note that the abutment scour computed from the NCHRP approach is total scour at the abutment; it is not added to contraction scour because it already includes contraction scour. The advantages of using the NCHRP abutment scour equations include: (1) not using an "effective" embankment length, L', which is difficult to determine in many situations, (2) the equations are more physically representative of the abutment scour process, and (3) the equations predict total scour at the abutment rather than an abutment scour component that is then added to a separate contraction scour estimate.

4.3.2 NCHRP 24-20 Abutment Scour Approach

The NCHRP approach for calculating the depth of scour at abutments uses contraction scour as the starting calculation for abutment scour and applies an amplification factor to account for large-scale turbulence that develops in the vicinity of the abutment. One important distinction regarding the contraction scour calculation is that the abutment creates a non-uniform flow distribution in the contracted section. The flow is more concentrated in the vicinity of the abutment and the contraction scour component is greater than for average conditions in the constricted opening.

The equations for scour conditions A and B are:

$$y_{max} = \alpha_A \, y_c \text{ or } y_{max} = \alpha_B \, y_c \tag{4.25}$$

$$y_s = y_{max} - y_0 \tag{4.26}$$

where:

y_{max} = Maximum flow depth resulting from abutment scour, ft (m)
y_c = Flow depth including live-bed or clear-water contraction scour, ft (m)
α_A = Amplification factor for live-bed conditions
α_B = Amplification factor for clear-water conditions
y_s = Total scour depth at abutment, ft (m)
y_0 = Flow depth prior to scour, ft (m)

Scour Condition A:

If the projected length of the embankment, L, is 75% or greater than the width of the floodplain (B_f), scour condition A in Figure 4.16 is assumed to occur and the contraction scour calculation is performed using a live-bed scour calculation. The contraction scour equation presented in NCHRP 24-20 is a simplified version of the HEC-18 live-bed contraction scour equation. The equation combines the discharge and width ratios due to the similarity of the exponents because other uncertainties are more significant. By combining the discharge and width, the live-bed contraction scour equation simplifies to the ratio of two unit discharges. Unit discharge (q) can be estimated either by discharge divided by width or by the product of velocity and depth. The contraction scour equation for scour condition A is:

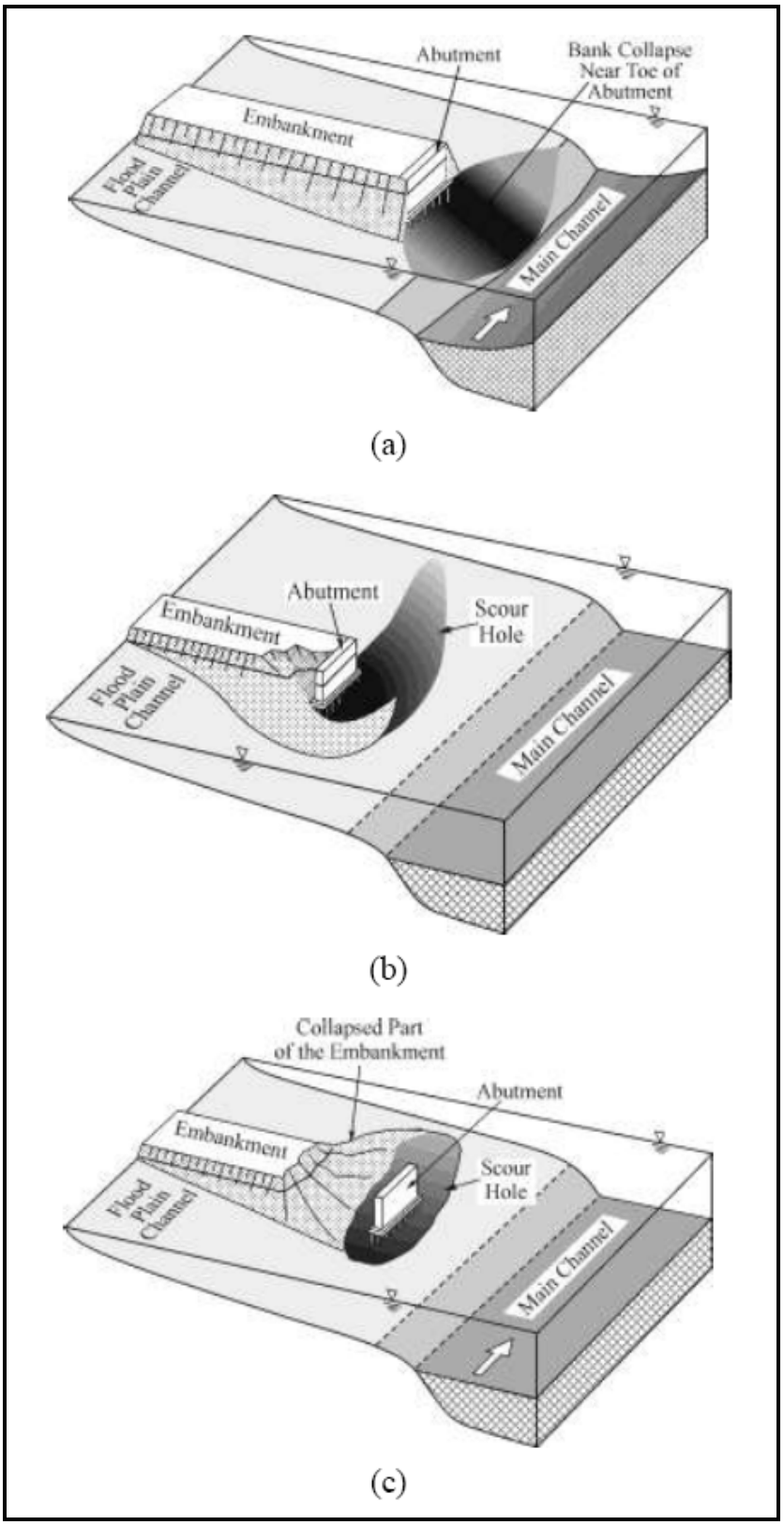

Figure 4.16. Abutment scour conditions NCHRP 24-20 (Ettema et al. 2010).

$$y_c = y_1\left(\frac{q_2}{q_1}\right)^{6/7} \qquad (4.27)$$

where:

y_c = Flow depth including live-bed contraction scour, ft (m)
y_1 = Upstream flow depth, ft (m)
q_1 = Upstream unit discharge, ft^2/s (m^2/s)
q_2 = Unit discharge in the constricted opening accounting for non-uniform flow distribution, ft^2/s (m^2/s)

The value of q_2 can be estimated as the total discharge in the bridge opening divided by the width of the bridge opening. The value of y_c is then used in Equation 4.25 to compute the total flow depth at the abutment. The value of α_A is selected from **Figure 4.17** for spill-through abutments and **Figure 4.18** for wingwall abutments. The solid curves should be used for design. The dashed curves represent theoretical conditions that have yet to be proven experimentally.

For low values of q_2/q_1, contraction scour is small, but the amplification factor is large because flow separation and turbulence dominate the abutment scour process. For large values of q_2/q_1, contraction scour dominates the abutment scour process and the amplification factor is small.

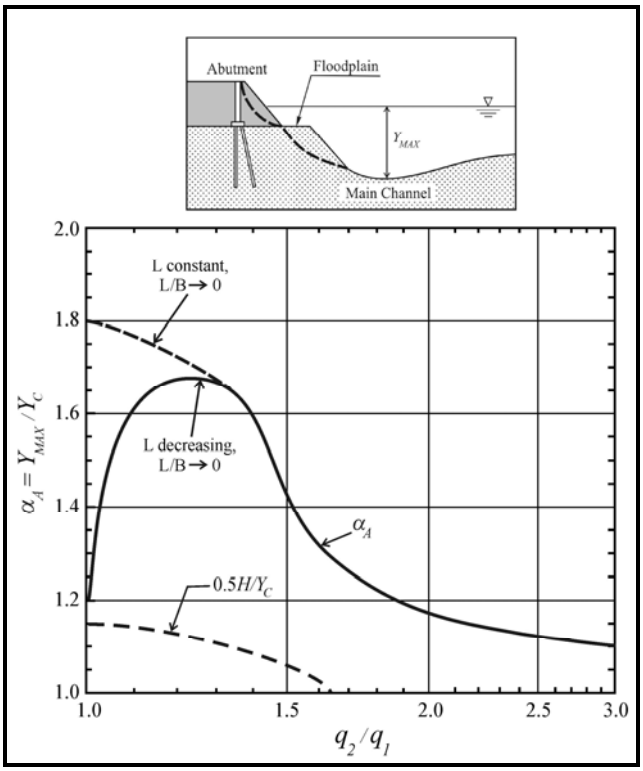

Figure 4.17. Scour amplification factor for spill-through abutments and live-bed conditions (Ettema et al. 2010).

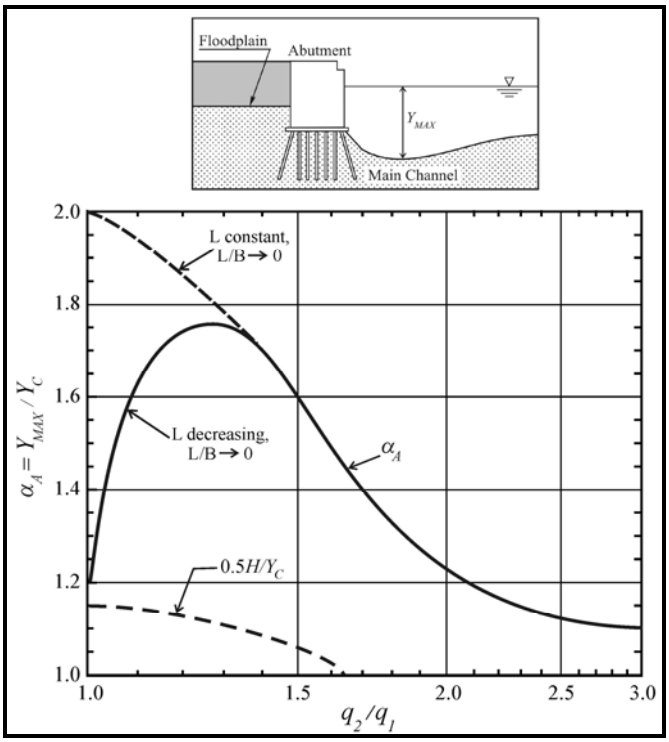

Figure 4.18. Scour amplification factor for wingwall abutments and live-bed conditions (Ettema et al. 2010).

Scour Condition B:

If the projected length of the embankment, L, is less than 75% of the width of the floodplain (B_f), scour condition B in Figure 4.16 occurs and the contraction scour calculation is performed using a clear-water scour calculation. The clear-water contraction scour equation also uses unit discharge (q), which can be estimated either by discharge divided by width or by the product of velocity and depth. Two clear-water contraction scour equations may be applied. The first equation is the standard equation based on particle size:

$$y_c = \left(\frac{q_{2f}}{K_u D_{50}^{1/3}} \right)^{6/7} \qquad (4.28)$$

where:

y_c = Flow depth including clear-water contraction scour, ft (m)

q_{2f} = Unit discharge in the constricted opening accounting for non-uniform flow distribution, ft^2/s (m^2/s)

K_u = 11.17 English units

K_u = 6.19 SI

D_{50} = Median particle diameter with 50% finer, ft (m)

A lower limit of particle size of 0.2 mm is a reasonable limitation on the use of Equation 4.28 because cohesive properties increase the critical velocity and shear stress for cohesive soils that have finer grain sizes. If the critical shear stress is known for a floodplain soil, then an alternative clear-water scour equation can be used:

$$y_c = \left(\frac{\gamma}{\tau_c}\right)^{3/7}\left(\frac{nq_{2f}}{K_u}\right)^{6/7} \qquad (4.29)$$

where:

n	=	Manning n of the floodplain surface material under the bridge
τ_c	=	Critical shear stress for the floodplain surface material, lb/ft^2 (Pa)
γ	=	Unit weight of water, lb/ft^3 (N/m^3)
K_u	=	1.486 English Units
K_u	=	1.0 SI

The value of q_{2f} should be estimated including local concentration of flow at the bridge abutment. The value of q_f is the floodplain flow upstream of the bridge. The value of y_c is then used in Equation 4.25 to compute the total flow depth at the abutment. The value of α_B is selected from **Figure 4.19** for spill-through abutments and **Figure 4.20** for wingwall abutments. The solid curves should be used for design. The dashed curves represent theoretical conditions that have yet to be proven experimentally. For low values of q_{2f}/q_f, contraction scour is small, but the amplification factor is large because flow separation and turbulence dominate the abutment scour process. For large values of q_{2f}/q_f, contraction scour dominates the abutment scour process and the amplification factor is small.

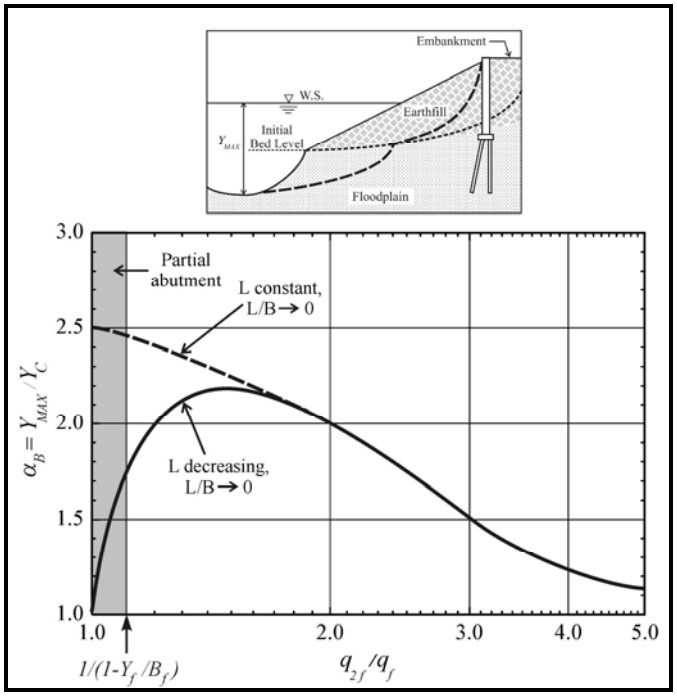

Figure 4.19. Scour amplification factor, spill-through abutments, and clear-water conditions (Ettema et al. 2010).

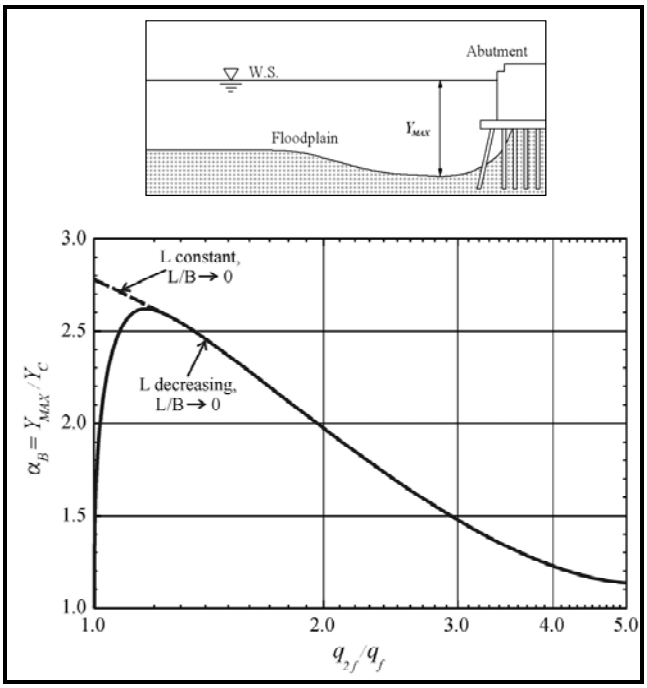

Figure 4.20. Scour amplification factor, wingwall abutments, and clear-water conditions (Ettema et al. 2010).

Unit discharge can be calculated at any point in the two-dimensional flow field by multiplying velocity and depth. Although two-dimensional modeling is strongly recommended for bridge hydraulic design, HEC-18 (Arneson et al. 2012) includes a method for estimating the velocity at an abutment. This method is used to size abutment riprap, but can also be used to determine the unit discharge at an abutment.

4.3.3 Abutment Scour Data Screening and Analysis

Fifty tests of abutment scour under live-bed conditions (scour condition A) and 12 clear-water tests (scour condition B) were conducted under NCHRP 24-20. An additional 19 clear-water tests were conducted by Ballio et al. (2009). Of the 50 live-bed tests, 6 were considered outliers where the ratio q_2/q_1 is less than 1.05 and the scour amplification factor is ambiguous. Of the 31 clear-water tests, 5 tests from the Ballio 2009 data set (Ballio's "test series D") were also considered outliers because they were conducted in a different flume and used very small particle sizes (d_{50} < 0.2 mm) near the silt size range, causing severe underprediction. After this screening, 70 data points remained for analysis using the NCHRP 24-20 abutment scour method. The data sets are summarized in **Table 4.10**.

Table 4.10. Summary of Laboratory Abutment Scour Data Sets.

Source	No. Data Points	d_{50} (mm)	L/B_f	q_2/q_1	Flow depth y_c (ft)	Flow depth y_{max} (ft)	y_{max}/y_c	Scour depth $y_{s\ observed}$ (ft)
Ettema et al., 2010 live-bed (Condition A)	44	0.45	0.50 – 2.13	1.06 – 2.49	1.03 – 2.02	1.56 – 2.29	1.05 – 1.71	0.22 – 1.20
Ettema et al., 2010 clear-water (Condition B)	12	0.45	1.89 – 3.05	1.16 – 3.18	0.52 – 1.21	1.08 – 1.74	1.34 – 2.50	0.59 – 1.23
Ballio et al., 2009 clear-water (Condition B)	14	5.0	1.09 – 1.86	1.05 – 2.00	0.33 – 0.88	0.94 – 2.52	2.40 – 3.17	0.44 – 1.12
Total	**70**	**0.45 – 5.0**	**0.50 – 3.05**	**1.05 – 2.00**	**0.33 – 2.02**	**0.94 – 2.52**	**1.05 – 3.17**	**0.22 – 1.23**

Figure 4.21 shows the results of the analysis. The bias of the NCHRP 24-20 abutment scour equation was determined to be 0.74 as the mean value of the ratio y_s (observed) to y_s (predicted). The Coefficient of Variation (COV) of the data is the standard deviation divided by the mean, determined to be 0.23 for this data set. The NCHRP 24-20 abutment scour equation underpredicted the observed scour for 2.9% of the data points (2 tests out of 70).

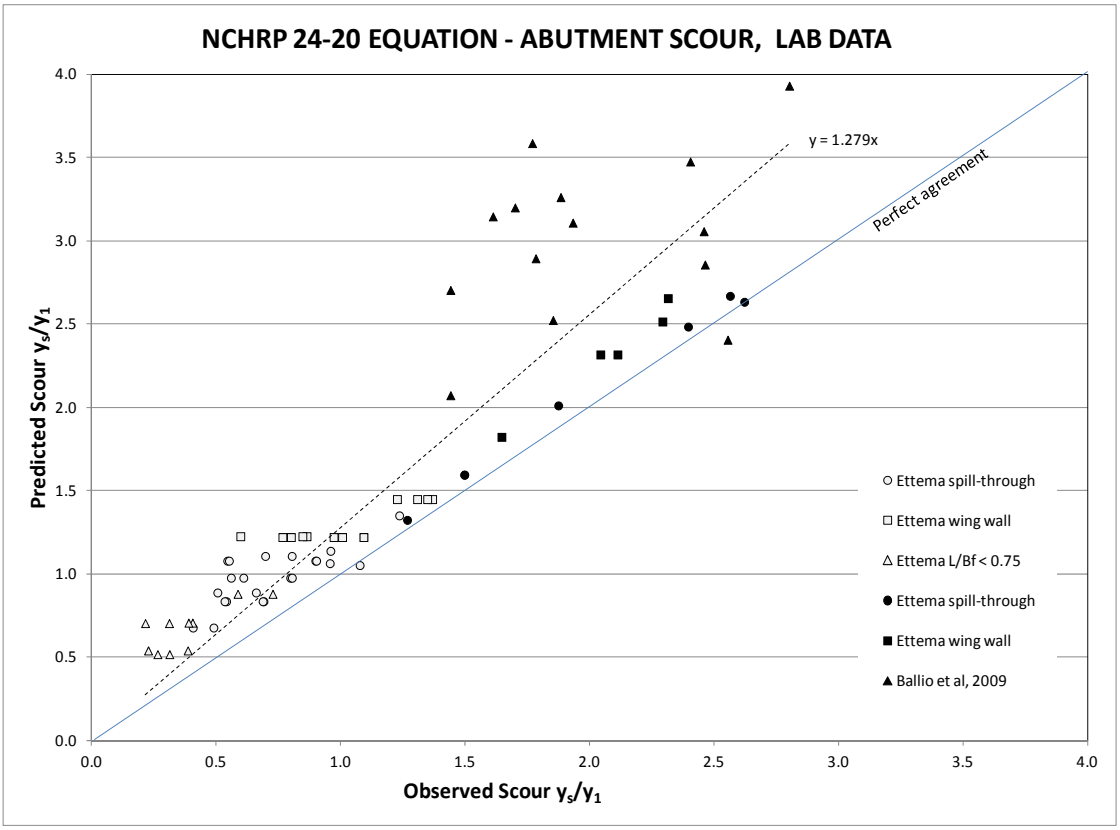

Figure 4.21. Predicted vs. observed abutment scour, 70 laboratory tests (outliers removed).

The reliability index β for the NCHRP 24-20 abutment scour equation was determined to be 1.53 and 1.44 for normal and log-normal distributions, respectively. These relatively high values of β reflect the fact that the curves for the amplification factors α_A and α_B for both spill-through and wingwall abutments (Figures 4.17 through 4.20) were developed by Ettema et al. (2010) as envelope curves for design. Although the Ballio data tend to be overpredicted by the NCHRP 24-20 method, it was important to include an independent data set and not rely solely on Ettema's data. **Table 4.11** provides a summary of the prediction statistics for the NCHRP 24-20 abutment scour procedure.

Table 4.11. Bias and Coefficient of Variation of the NCHRP 24-20 Abutment Scour Equations with Laboratory Data, outliers removed.

Data Set	No. Data Points	Bias	COV	Percent Under-predicted	Reliability β	
					Normal	Log-normal
All data	70	0.74	0.23	2.9%	1.53	1.44

(page intentionally left blank)

CHAPTER 5

5. DEVELOPMENT OF SUPPORTING SOFTWARE

5.1 HEC-RAS

For each bridge type analyzed, a representative HEC-RAS model was developed to assess the hydraulic conditions at the bridge given the hydrologic and other input variable uncertainties.

Models were developed representing small, medium, and large bridges to support the Level I and Level II analyses (see Chapter 6). Each consists of:

- A single reach of four cross-sections plus the automatically-generated (by HEC-RAS) Bridge Upstream and Bridge Downstream sections. These cross-sections include ineffective flow areas and flow transition reach lengths, determined using standard engineering methods, appropriate to capture the full effect of flow contraction and expansion at the bridge.
- Manning roughness (n) values are assigned with a channel Manning n value and a single overbank Manning n value for all four cross-sections for each realization.
- Design Discharge (100-year) was set for each bridge.
- The downstream boundary condition was determined by HEC-RAS using a normal depth computation, driven by friction slope. No supercritical simulations were performed; consequently, no upstream water surface elevation (WSEL) computation was required.
- Neither overtopping (relief) nor internal pier geometry was directly represented. All flow was forced through the bridge opening. Pier and abutment geometry was considered in the (post-process) scour computations.

5.2 Integration of HEC-RAS and Monte Carlo

5.2.1 Approach

To analyze the probability of scour depth exceedance, it was necessary to perform a large number of Monte Carlo realizations (cycles) using the HEC-RAS model. This precluded the use of HEC-RAS through its standard Graphical User Interface (GUI). Consequently, the HEC-RAS Application Programming Interface (API) was used to integrate HEC-RAS simulations with the Monte Carlo simulation software.

Research software (the rasTool©) was developed to automate the running of HEC-RAS. This software included specifying input variables for HEC-RAS geometric and flow files. Results from each run were then appended to a summary output file. **Figure 5.1** presents a screen shot of the rasTool© interface. This section provides a description of the final rasTool© software and its application to scour risk analysis.

The steps to use rasTool© to perform a Monte Carlo simulation are:

1. Select a HEC-RAS project file (see Figure 5.1)
2. Press the Open Project button
3. Press the Run RAS button (opens HEC-RAS GUI and performs a single HEC-RAS model run using the base hydraulic and geometric variables
4. Press the Monte Carlo button (runs multiple Monte Carlo realizations as specified by the user in the input table)

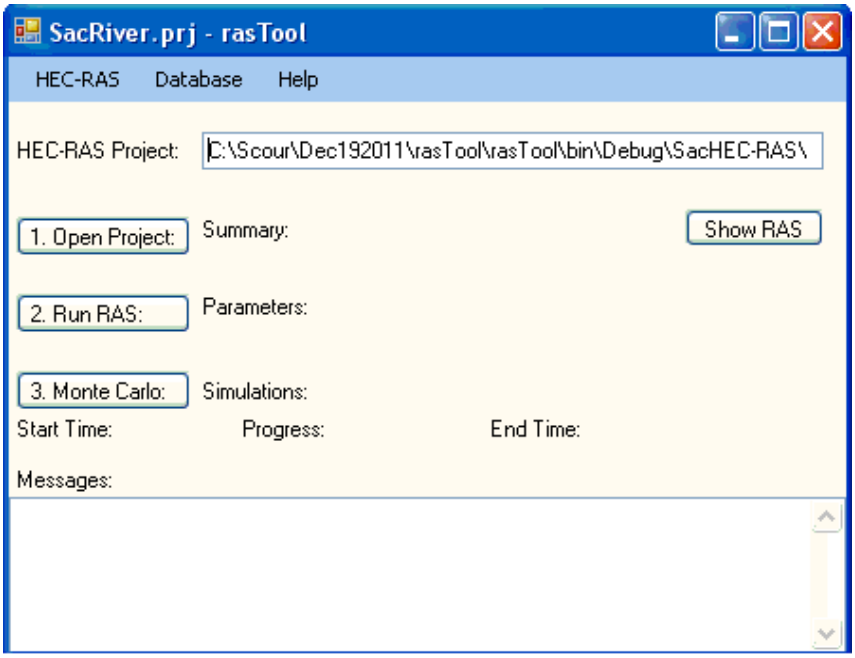

Figure 5.1. The rasTool© Graphical User Interface (GUI).

The rasTool© was developed using Microsoft Visual Studio 2010, using the VB.NET language. The program is compatible with Windows XP or Windows 7. **The rasTool© interface is a research-level software engine requiring considerable insight on the part of the user for application. The application process used in this study is described in the following paragraphs**.

The rasTool© requires a tab-delimited text input file in the executable directory, "settings.txt", containing simulation settings (number of realizations, the HEC-RAS model path and project name, and variable distribution functions and summary statistics for each independent input variable for a Monte Carlo simulation). These data are loaded into a table in rasTool© prior to simulation and may be modified and saved using the rasTool© interface. The rasTool© also requires Interop.RAS41.dll be present in the executable directory or specified in the system path to support the HEC-RAS API.

When rasTool© is started, rasTool© initializes a double-precision random number generator (RNG), seeded with the computer clock time, to generate a large (~10^{55}), uniformly-distributed pseudo-random number string. The uniformly distributed pseudo-random number string values generated by the RNG are transformed as necessary during the Monte Carlo realizations into Gaussian-distributed Z-values using the polar form of the Box-Muller transform and used for all subsequent random numbers required by the simulation (eight per realization). Four of the random numbers are used in the HEC-RAS modeling (discharge, channel Manning n, floodplain Manning n, and energy slope) and four are used in computing scour (HEC-18 pier scour, FDOT pier scour, contraction scour, and abutment scour).

Once the Monte Carlo realizations are launched (Step 4, above), the rasTool© performs Monte-Carlo realizations as follows:

1. Randomized input variables (described below) are determined for a realization using the input probability density function type, summary statistics, and generated randomized Z-values for each input variable.

2. These input variables are assigned to the HEC-RAS model using the Interop.RAS41 API for geometric variables and direct assignment to input text files for flow and boundary condition variables. The direct assignment of flow variables proved necessary as the Interop.RAS41 API allowed asynchronous updates of flow variables, geometric variables, and simulations, resulting in interleaved updates and inconsistent hydraulic simulation of the desired input variables. Direct assignment of flow and boundary condition variables eliminated this conflict and ensured fully synchronous simulations.
3. HEC-RAS is run for the given geometric, flow, and boundary condition variables assigned.
4. Input variables and detailed hydraulic results are retrieved from the completed HEC-RAS model using the Interop.RAS41.dll API and stored in a results matrix. These results are sufficiently detailed to support contraction scour, abutment scour, and pier scour computations.
5. Steps 1-4 are iterated until the user-assigned number of realizations have been performed. From testing, it was determined that 10,000 realizations were sufficient to generate a fully-descriptive dataset.
6. The Monte Carlo hydraulic results matrix is written to a text file (OutputMC.txt), along with four standard-normal (Gaussian) random variables per realization to support randomization of the scour results. Scour computations (using HEC-18 and FDOT pier methods, contraction and abutment scour) were performed as a post-processing step in a spreadsheet.

A 10,000-realization simulation required between one and two hours of computer time, depending on the machine used.

The rasTool© requires input data from the user to perform its simulation. For each independent input variable, summary statistics and assumed distributions about expected value are required. This effort randomized discharge, channel Manning n, overbank Manning n, and friction slope for normal depth boundary condition computation. The rasTool© supports normal and lognormal distributions. The rasTool© requires a representative HEC-RAS model of the bridge simulated. Simulation parameters (number of realizations, Z limit) were also required.

Four assumed-independent random geometric and hydraulic variables for each bridge type analyzed were considered for this effort. They were discharge, Manning roughness (overbanks and main channel), and friction slope. The application of these variables is described below.

5.2.2 Discharge

A Lognormal discharge distribution about its expected value (mean in logarithm transform) was assumed. The expected value discharge was constant for all hydrologic uncertainty scenarios for a given annual exceedance probability and bridge type (small, medium, and large) as presented in **Tables 5.1** and **5.2** (see also Section 6.1.3). The expected value discharge parameter (in natural logarithm space, A) was determined for each bridge type using Bulletin 17B methods for the relevant period of record and normalized to a N=50-year period of record (see Section 2.2). Note that the Bulletin 17B predicted discharge for a given exceedance probability represents the mode in linear space, not the mean (expected) value in logarithmic space. The expected value discharge (in natural logarithmic space) is the statistical mean discharge parameter of interest for the Monte Carlo realizations.

Table 5.1. 100-Year Discharge Parameters for Lognormal Distribution (Natural Log Space).				
Bridge	A μ[ln (Q)]	B σ[ln (Q)]		
		Hydrologic Uncertainty		
		Low	Medium	High
Large	11.8791	0.1282	0.1865	0.2448
Medium	10.3015	0.1111	0.1617	0.2123
Small	7.5175	0.0811	0.1180	0.1549

Table 5.2. Illustrative Example: Low Hydrologic Uncertainty; A and B Based on Gage Analysis N = 49 Years.			
Event		A	B
p(X>x)	T(years)	μ[ln (Q)]	σ[ln (Q)]
0.04	25	11.64920308	0.115282339
0.02	50	11.77682701	0.125057456
0.01	100	11.88793137	0.133901695
0.002	500	12.10459348	0.151400894

COV values for a given hydrologic uncertainty scenario were based on a qualitative review of Bulletin 17B Flood Frequency analyses performed at eight USGS gaged sites to assess the observed range of discharge COV as a function of period of record and regional variation. COV was constant for a given hydrologic uncertainty and annual exceedance probability, as presented in **Table 5.3**.

Table 5.3. Hydrologic Uncertainty as Function of Annual Exceedance Probability.				
Annual Exceedance		Discharge COV (lognormal)		
p(X>x)	T(years)	Low	Medium	High
0.04	25	0.009	0.014	0.018
0.02	50	0.010	0.015	0.019
0.01	100	0.011	0.016	0.021
0.005	200	0.012	0.017	0.022
0.002	500	0.013	0.018	0.023

The COV values in Table 5.3 were multiplied by the expected value discharge in natural logarithm space to determine discharge lognormal standard deviation values for each bridge type (small, medium, large) and hydrologic uncertainty scenario (low, medium, high). Natural log space expected value discharge (A) and Standard deviation (B) were input to the Monte Carlo realizations described above. Input parameters to the Monte Carlo simulation were constant for each bridge type and hydrologic uncertainty scenario, and are presented in Table 5.1.

5.2.3 Manning Roughness Coefficient

Manning roughness values were randomized assuming a lognormal distribution. Overbank roughness and main channel roughness were considered independent random variables for this analysis. They were held constant for a given Monte Carlo realization (e.g., all cross-sections were assigned the same, independently randomized, overbank roughness and main channel roughness). The linear-space mean values were estimated for each bridge type using standard engineering methods for estimating Manning roughness coefficients and were converted into natural logarithmic input variables using the variable transforms presented below (see Equations 5.10 and 5.11). A constant COV was assumed for all bridge types and hydrologic scenarios. The final natural-log space variables are presented in **Table 5.4** (see Section 5.3.3 for a discussion of initial estimates, testing, and refinement of these variables).

Table 5.4. Manning Roughness Coefficients Assuming Lognormal Distribution.			
Linear	Natural Log Space		
Manning n	COV	A μ[ln (n)]	B σ[ln (n)]
0.025	0.015	-3.690411607	0.055356174
0.035	0.015	-3.353672518	0.050305088
0.045	0.015	-3.102175432	0.046532631
0.09	0.015	-2.40859826	0.036128974
0.1	0.015	-2.303181866	0.034547728
0.12	0.015	-2.120769523	0.031811543

5.2.4 Downstream Boundary Friction Slope

The downstream boundary friction slope was assumed to be normally distributed about the expected (mean) value. Expected values were estimated in the field for each bridge type (see Section 6.1.3). Standard deviation values were determined using COV values developed as discussed below. The final values of downstream boundary friction slopes for each of three bridge types (small, medium, large) as defined in Table 6.1 are presented in **Table 5.5** (see Section 5.3.3 for a discussion of initial estimates, testing, and refinement of these variables).

Table 5.5. Friction Slopes Assuming Normal Distribution.		
Linear		
μ	COV	σ
0.0048	0.1	0.00048
0.0024	0.1	0.00024
0.005	0.1	0.0005

5.2.5 Summary

Each Monte Carlo realization generated a set of randomized input variables based on the underlying input variables and summary statistics discussed in this section. These variables were assigned to the HEC-RAS model as described above, and a HEC-RAS model run performed for each realization. Once this run was complete, input variables and hydraulic results for the realization to support pier scour (HEC-18 and FDOT methods), contraction scour (HEC-18 methods), and Ettema abutment scour (as presented in HEC-18) were accessed using the rasTool© software and tabulated in a tab-delimited text file for post-processing. Four additional double-precision normally distributed random variable values were recorded for each realization to support randomization of the (post-processed) scour predictions based on the scour prediction component bias and COV from the data analysis in Chapter 4.

5.3 Implementation and Testing

5.3.1 Approach

A four cross section HEC-RAS bridge hydraulic model was developed for each Monte Carlo simulation. The base-model input parameters including discharge, Manning n (channel and overbank), and downstream energy slope and the corresponding uncertainties in these

parameters were specified in the input file of the rasTool© program. The rasTool© output included hydraulic results for the base condition (expected values) and output for each of the randomly generated input parameter values. RasTool© does not make scour calculations but does create a table of output. This output table is then copied and pasted into an Excel spreadsheet that performs the scour calculations. For each simulation, pier (HEC-18 and FDOT), contraction (HEC-18), and abutment scour (NCHRP 24-20 method) are computed from the MCS output. The rasTool© software also includes four normally distributed random numbers (μ = 0.0 and σ = 1.0) for each simulation. The model (equation) bias and COV from the laboratory data analysis in Chapter 4 are then applied to each of the computed scour values to compute the expected distribution of each scour component for the specified event.

5.3.2 Hydraulic Parameter Uncertainty

The HEC-RAS Monte Carlo analysis requires that uncertainty in the input parameters be quantified in order to compute the range of hydraulic conditions and scour that can occur at a bridge. The input parameters selected for HEC-RAS simulations were discharge, channel Manning n, overbank Manning n, and the energy slope downstream boundary condition. Each of these parameters has a value that is either determined or selected during the bridge hydraulic design process, which then results in the design value of scour. By incorporating the hydraulic parameter uncertainty and the model (scour equation) uncertainty, the statistical characteristics of the individual scour components (pier, contraction, and abutment), and total scour can be evaluated.

Hydrologic Uncertainty (Discharge): Flood frequency analysis provides estimates of discharge versus exceedance probability. The Bulletin 17B procedure uses the Log-Pearson Type III distribution to develop the "Bulletin 17B Estimate" over the range of annual exceedance probabilities ranging from 0.95 to 0.002, which are the recommended discharges for flood mapping, hydraulic structure design, and other types of analysis (see Section 2.2). The results of the 17B procedure also include 95% confidence limits and an "Expected Probability" estimate of discharge. As defined by Bulletin 17B, the confidence limits are one sided, so 95% of the estimates of discharge are greater than the lower bound and 95% less than the upper bound.

The probability distribution of a discharge estimate is established by the expected probability value and the two confidence limits of the log-transformed values. Therefore:

$$\ln(Q_{p\text{-}ex,0.95}) = \mu + 1.645\sigma \quad (5.1)$$

$$\ln(Q_{p\text{-}ex,0.05}) = \mu - 1.645\sigma \quad (5.2)$$

$$\sigma = \frac{1}{3.29}\ln\left(\frac{Q_{p-ex,0.95}}{Q_{p-ex,0.05}}\right) \quad (5.3)$$

$$\mu = 0.5\ln(Q_{p-ex,0.95}Q_{p-ex,0.05}) \quad (5.4)$$

$$COV_{ln} = \sigma/\mu \quad (5.5)$$

Where $Q_{p\text{-}ex,0.05}$ and $Q_{p\text{-}ex,0.95}$ are the lower and upper one-sided 95% confidence limits for a particular exceedance probability (p-ex), μ is the log-transformed expected probability discharge value, and σ is the standard deviation of the normally distributed probability density

function of the particular exceedance probability. For example, the 100-year Bulletin 17B flow estimate (p-ex = 0.01) for the test Monte Carlo/HEC-RAS analysis of the Sacramento River bridge (see Section 5.3.3) is 140,000 cfs with expected probability flow of 145,500 cfs and 95% confidence limits of 115,800 cfs and 179,900 cfs. These values result in $\sigma = 0.134$ and $\mu = 11.888$, which are entered as the discharge values for the Monte Carlo simulation flagged as a log-transformed variable.

Regional Regression Equations

Where gaging station data is unavailable, the use of regression relationships is a common method for estimating flood magnitudes for various return-period events. These relationships utilize watershed and climatologic characteristics specific to a physiographic region to estimate the 2-year, 5-year, … up to the 500-year peak discharge at any location within the region of interest. Typical relationships often take the form $Q_i = A(X_1)^b(X_2)^c.....(X_n)^n$. In these equations, Q_i is the estimated discharge for an i-year flood, A is a region-specific coefficient, X_1, X_2 … X_n are watershed and climatologic characteristics such as drainage area, mean annual precipitation, percent forest cover, mean basin elevation, etc. and *b, c, … n* are region-specific exponents.

The standard error of prediction (SE) in percent is typically reported for each equation and is a measure of the predictive accuracy of the equation for each return period Q_2, Q_5, … Q_{500} as compared to actual streamflow measurements and gaging station data in that physiographic region. Approximately two-thirds of the estimates obtained from a regression equation for ungaged sites will have errors less than the standard error of prediction (Helsel and Hirsch 1992).

For purposes of assigning a level of hydrologic uncertainty to ungaged sites where regional regression equations are used to estimate flood magnitudes, the following standard error limits are suggested for the applications in this document:

- **Low hydrologic uncertainty:** **SE < 15%**
- **Moderate hydrologic uncertainty:** **15% < SE < 30%**
- **High hydrologic uncertainty:** **30% < SE**

Manning n Uncertainty: As described in Johnson (1996a), numerous methods have been used to describe the uncertainty in Manning n estimates. The "data" provided in USACE (1986) are the most comprehensive and are used in this study. The USACE study included nine natural channels throughout the U.S. with a wide range of conditions. A group of 77 engineers were shown pictures of the channels and asked to estimate the Manning n for a 100-year flow at each location. The engineers could base their estimates on experience, tables, or pictures found in the scientific literature. Outliers were removed from the estimates so that the individual number of estimates ranged from 71 to 77 at each site for a total number of estimates of 675 and an average of 75 per site. The USACE concluded that the distribution of Manning n was log-normal, but did not provide the statistical properties of the log-transformed data.

For this study the USACE estimates were normalized by dividing by the mean estimate for each site and grouping the data into a single data set. The 675 normalized data were then log transformed to evaluate the suitability of using a log-normal distribution. The results are shown in **Figure 5.2** and indicate the suitability of using the log-normal distribution on Manning n for these data. **Figure 5.3** shows the complete PDF and CDF of the normalized Manning n

data. With this distribution, 93% of the Manning n values fall between 0.5 and 1.5 of the expected Manning n. The assumption for applying the results in the HEC-RAS Monte Carlo simulation is that the mean estimate of the 77 engineers corresponds well to the expected Manning n for the nine rivers at 100-year flood stage.

The COV of the log-transformed data was 0.082. Therefore, an estimate of a channel (or overbank) Manning n (n used in design) can be used to estimate μ and σ of the log-transformed variable using the following equations:

$$n = \exp(\mu + 0.5\sigma^2) = \exp[\mu + 0.5(\mu COV)^2] \quad (5.6)$$

$$\mu = \frac{-1 + \sqrt{1 + 2\ln(n)COV^2}}{COV^2} = \frac{-1 + \sqrt{1 + 2\ln(n)0.082^2}}{0.082^2} \quad (5.7)$$

$$\sigma = \mu COV = \mu 0.082 \quad (5.8)$$

The values of σ and μ are entered for the Monte Carlo simulation flagged as a log-transformed variable. Because the value of COV of the log-transformed data is 0.082, only the expected channel or overbank Manning n value is required to develop the input for the HEC-RAS/Monte Carlo simulation (see Section 5.3.3).

Energy Slope Uncertainty: Although energy slope and channel slope appear to be relatively simple parameters to estimate, Johnson (1996a) found this variable to have relatively significant uncertainty that should not be ignored. Johnson found that several types of distributions have been used to describe channel and friction slope, including uniform, normal, triangular, and log-normal. For this study, a normal distribution with COV = 0.17 was used initially (see Section 5.3.3). This distribution and value was selected such that plus or minus three standard deviations would result in 99.8% of the starting energy slope values between 0.5 and 1.5 times the expected value.

5.3.3 Testing the Software

The Sacramento River bridge (Example Bridge #3 in Chapter 7) was used to test the HEC-RAS/Monte Carlo software. For the initial runs, the hydraulic parameter uncertainty values for discharge, Manning n (channel and overbank), and energy slope as discussed in Section 5.2 were used. The Monte Carlo analysis was compared with data from a gage near the Sacramento River bridge site for flows in the range of the discharges in the Monte Carlo analysis. This was done to test the reasonableness of the Monte Carlo runs. It was determined that the HEC-RAS modeling compared well with the discharge variation at the gage, and that the recommended energy slope parameter uncertainty (normal distribution and COV = 0.17) produced slightly greater variation in water surface and depth as compared to the gage data. The recommended Manning n parameter uncertainty produced extreme variability in water surface. Therefore, the energy slope and Manning n parameter uncertainties were reduced until the combined effects of Manning n and energy slope produced similar variability as the water surface measurements at the gage.

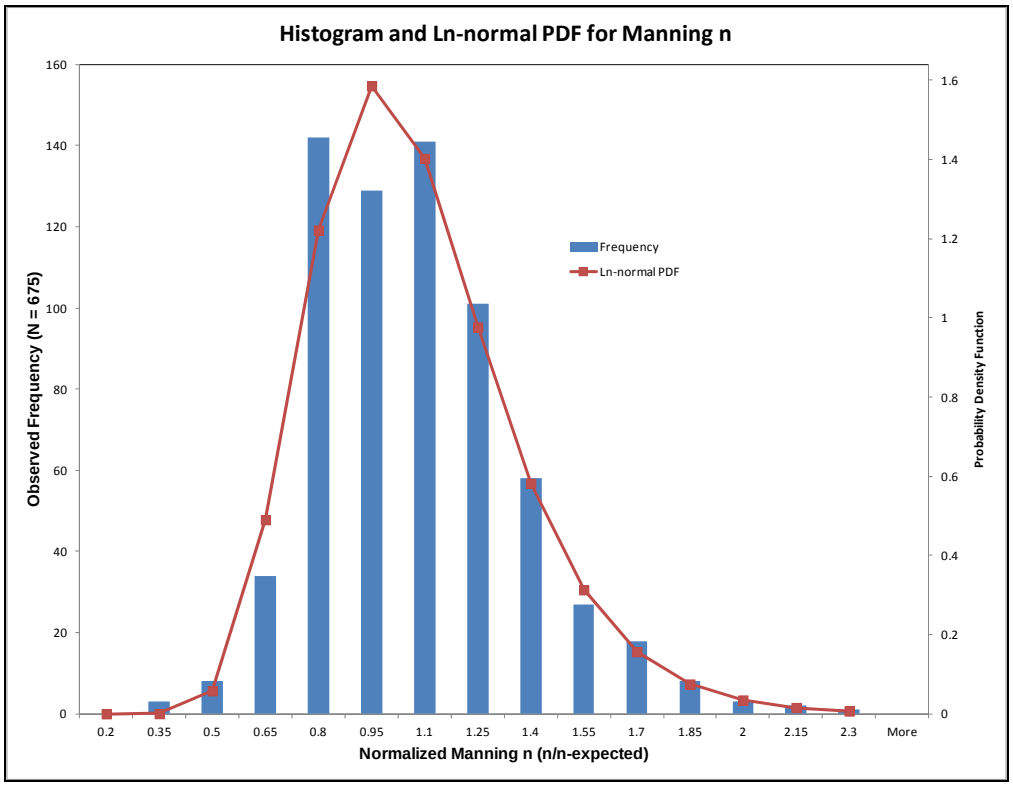

Figure 5.2. USACE (1986) Manning n data.

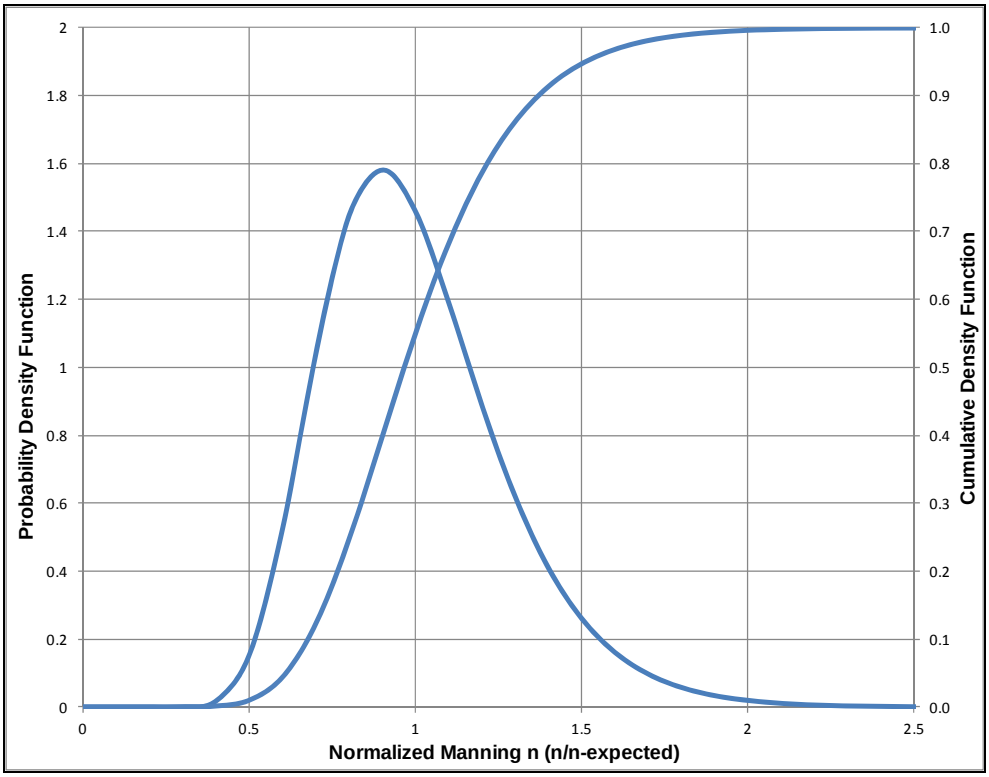

Figure 5.3. Normalized Manning n PDF and CDF.

Given the large range in discharge as represented by the 5% and 95% confidence limits (see discussion of Hydrologic Uncertainty in Section 5.2.2), it was expected that there would be a large range in water surface elevation and flow depth at the bridge in the Monte Carlo simulation. The Monte Carlo simulation includes flows much further out on the tails of the distribution, so the smallest and largest simulated flows for the 100-year discharge were well under 100,000 to well over 200,000 cfs. Over this range of flows the HEC-RAS model computed water surface varied by nearly 7 feet when Manning n and energy slope were held constant. **Figure 5.4** shows gage heights for extreme flows at the Butte City gage (11389000) on the Sacramento River, which is approximately 11 miles downstream of the bridge site. For flows in the range of 100,000 to 144,000 cfs the gage water surface varies by approximately 3.0 feet and the HEC-RAS water surface varies by 3.3 feet. Therefore, the variations in water surface and flow depth with changing discharge in the HEC-RAS model are reasonable.

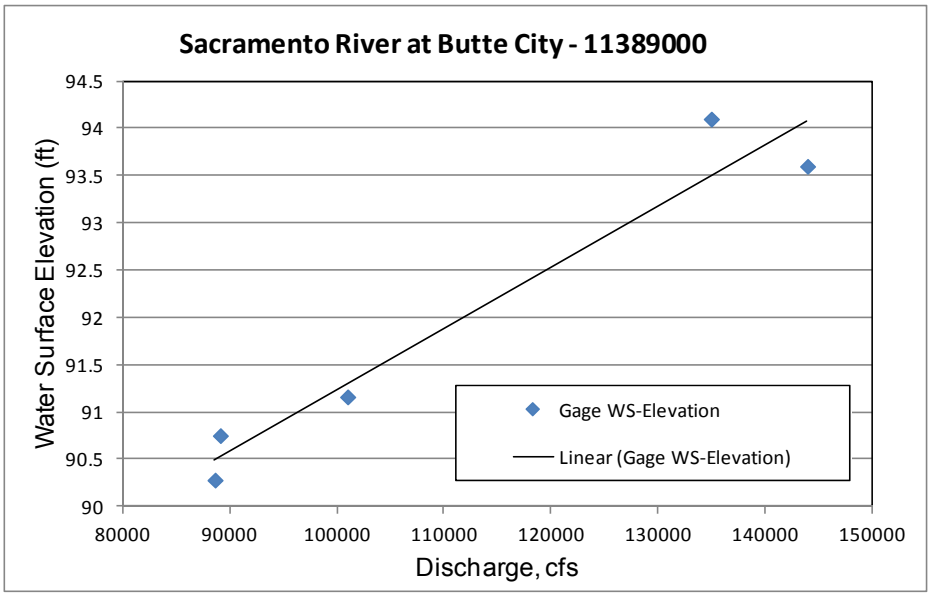

Figure 5.4. Gage heights versus discharge at Sacramento River Butte City Gage.

The data in Figure 5.4 also illustrate the variability in water surface measurements at the Butte City gage. The standard deviation of the differences in the observed values versus the trend line is 0.49 feet. Therefore, this value was used to assess the reasonableness of the parameter uncertainties of Manning n and energy slope because these parameters will create variability in water surface for a given discharge.

Energy Slope Uncertainty: As noted in Section 5.3.2, Johnson (1996a) found that several types of distributions have been used to describe channel and friction slope, including uniform, normal, triangular, and log-normal. Initially, a normal distribution with COV = 0.17 was used for this study. This produced a standard deviation in water surface of 0.66 ft, which is greater than the observed value of 0.49 ft at Butte City gage. Therefore, COV was reduced to 0.10, which resulted in a water surface standard deviation of 0.37 ft.

Manning n Uncertainty: When the 675 data points of the USACE (1986) study were evaluated, a COV of 0.082 for the log-transformed data fit the data well (see Section 5.3.2). However, when this COV was used in the HEC-RAS Monte Carlo Simulation, the standard deviation in water surface was 2.5 feet, which was twice the standard deviation created by discharge uncertainty and much greater than the observed variability in water surface for a

given discharge. Therefore, the COV was adjusted until the variability in water surface was more consistent with observed amounts. The COV of the log-transformed Manning n variable of 0.015 yielded a standard deviation in water surface of 0.47. Therefore, an estimate of a channel (or overbank) Manning n can be used to estimate μ and σ of the log-transformed variable using the following equations:

$$n = \exp(\mu + 0.5\sigma^2) = \exp[\mu + 0.5(\mu COV)^2] \quad (5.9)$$

$$\mu = \frac{-1+\sqrt{1+2\ln(n)COV^2}}{COV^2} = \frac{-1+\sqrt{1+2\ln(n)0.015^2}}{0.015^2} \quad (5.10)$$

$$\sigma = \mu \, x \, COV = \mu \, x \, 0.015 \quad (5.11)$$

The large difference in COV (0.082 based on selection of Manning n versus 0.015 based on impacts on water surface variability) indicates that Manning n is an important parameter that may often be difficult to reliably estimate. Therefore, calibration of Manning n to observed conditions is an important practice whenever possible.

5.4 Scour Computations

5.4.1 HEC-RAS/Monte Carlo Simulation Results for Pier Scour

The HEC-RAS model for the Sacramento River bridge was run for 20,000 cycles to evaluate the range of hydraulic conditions and scour that result from the parameter uncertainty described in Section 5.3.3. For this application, 20,000 cycles were run to fully test the Monte Carlo application and to produce results at the extremes of the input parameters. Subsequent evaluations revealed that 10,000 MCS cycles provide virtually identical probability distributions.

The results of NCHRP Project 24-32 (Sheppard et al. 2011) were evaluated and expanded into a pier scour analysis methodology by the Florida Department of Transportation (FDOT). FDOT has incorporated this methodology in its Bridge Scour Manual and developed supporting spreadsheets for a wide range of pier scour applications using this procedure. The NCHRP 24-32 pier scour equations are now referred to as the FDOT pier scour methodology in the most recent edition of HEC-18 (Arneson et al. 2012). Pier scour was evaluated using both the HEC-18 and FDOT procedures.

The design condition of Q=140,000 cfs, channel Manning n of 0.025, floodplain Manning n of 0.09, and starting energy slope of 0.00035 produced a design depth and velocity at the bridge of 24.5 feet and 12.1 ft/s. The computed HEC-18 scour for the 6 ft diameter circular pier was 13.7 ft and the FDOT equation resulted in 11.2 ft of scour for 2.0 mm bed material size. The sediment transport condition is live-bed for these conditions.

In the 20,000 cycle Monte Carlo simulation, discharge ranged from 87,000 to 245,000 cfs and dominated the hydraulic conditions at the bridge. Energy slope, which ranged from 0.00022 to 0.00049, had the smallest impact on hydraulic conditions. Manning n ranged from 0.021 to 0.030 for the channel and from 0.074 to 0.108 for the floodplain. At the bridge, the design depth ranged from 19.5 to 30.2 feet and design velocity ranged from 9.4 to 16.4 ft/s.

The results for pier scour in the Monte Carlo simulation are summarized in **Table 5.6**. Although the simulated discharge varied by more than a factor of 2.5 and velocity varied significantly, the computed range of pier scour was 4 ft for the HEC-18 equation and was only 1.6 ft for the FDOT equation. For this range of hydraulic conditions, the range of computed scour from the FDOT equation is very small, indicating that the FDOT equation is less sensitive to hydraulic conditions. It should be noted that the maximum computed scour from the HEC-18 equation exceeds 2.4 times the pier width, which is an expected upper limit based on a circular pier and Froude number less than 0.8 (Arneson et al. 2012). See Section 4.1.1 for detailed information on the FDOT method.

Table 5.6. Pier Scour Results from 20,000 Cycle Sacramento River Bridge HEC-RAS.

Variable	HEC-18 Equation	FDOT Equation
Design Scour (ft)	13.7	11.2
Mean Scour (ft)	13.8	11.3
Standard Deviation (ft)	0.49	0.21
COV	0.036	0.019
Minimum Computed Scour (ft)	12.1	10.6
Maximum Computed Scour (ft)	16.0*	12.2
Results after applying Bias and COV		
Mean Scour (ft)	9.4	8.5
Standard Deviation (ft)	1.56	1.59
COV	0.166	0.189
Minimum Computed Scour (ft)	3.5	2.6
Maximum Computed Scour (ft)	15.8*	14.1
Beta (design result)	2.75	1.81
Scour Factor for Beta = 3.0	1.04	1.17
Scour required for Beta = 3.0 (ft)	14.2	13.1
*Computed scour greater than 2.4 times the circular pier width.		

The pier scour results are also shown in **Figures 5.5 and 5.6**. In Figure 5.5, the direct results of the FDOT and HEC-18 equations are shown for the computed velocity and depth from the HEC-RAS models. The design value for each of these equations is shown, and in each case the design value is very close to the mean of the calculated values. This is expected because in the Monte Carlo simulation velocity and depth are distributed around the base model results. Figure 5.5 illustrates that for this particular bridge hydraulic condition, the FDOT equation and the HEC-18 equation have no overlap, although the actual magnitude of scour is not significantly different. The FDOT equation is less sensitive to the hydraulic conditions resulting in a spread of only 1.6 feet versus a spread of 4 feet for the HEC-18 equation.

Figure 5.6 shows the results after each equation's bias and COV are introduced. From the analysis of laboratory pier sour data, the Bias and COV of the observed versus computed scour is 0.68 and 0.16 for the HEC-18 equation and 0.75 and 0.18 for the FDOT equation.

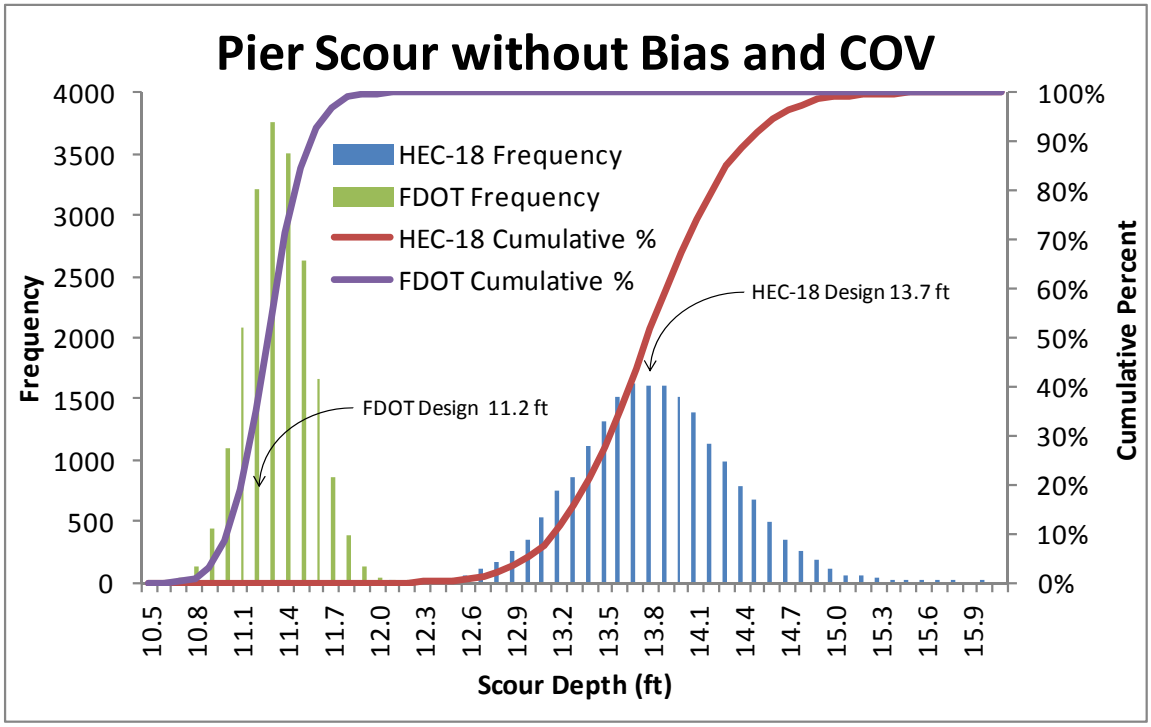

Figure 5.5. Direct pier scour results for the HEC-RAS Monte Carlo simulations.

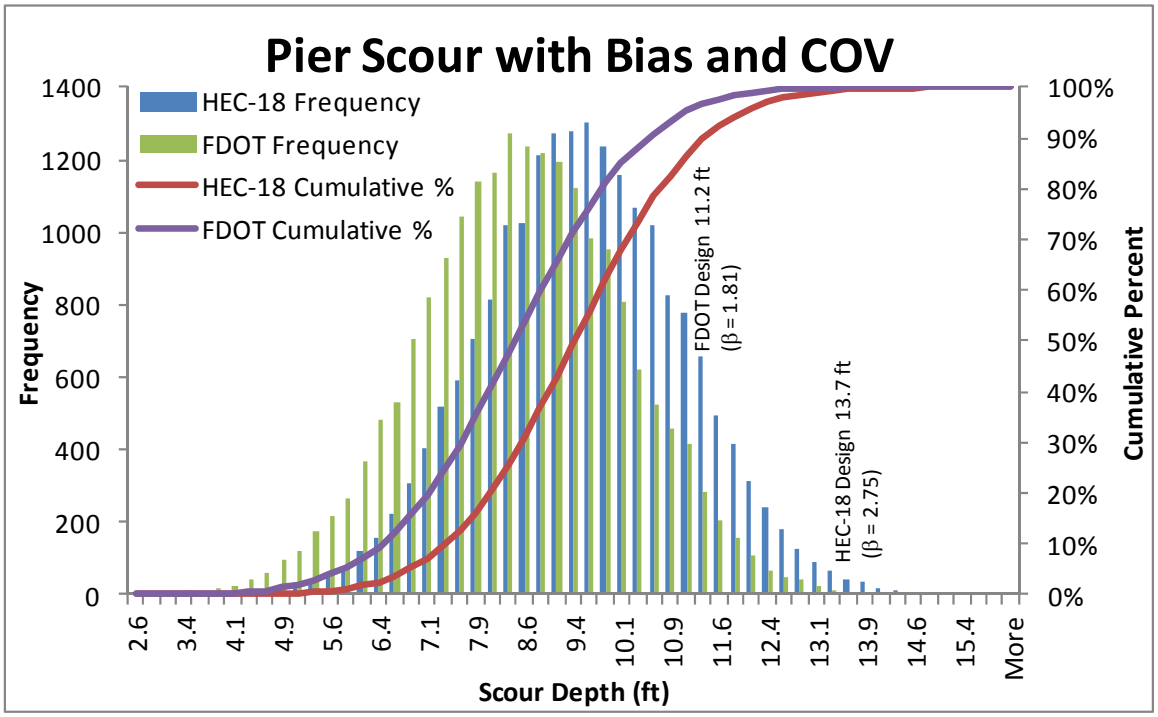

Figure 5.6. Pier scour results for the HEC-RAS Monte Carlo simulations after including equation bias and COV.

Assuming a normal distribution, these values result in an estimated conditional reliability (β) of 2.92 and 1.78 for the HEC-18 and FDOT equations (see Section 2.6.2 for a discussion of the reliability index as a measure of structural safety). The computed scour was then multiplied by normally distributed random values with mean equal to the bias, and standard deviation based on the COV for each equation. As shown in Figure 5.6, because the HEC-18 equation has a smaller bias and COV than the FDOT equation, the resulting distributions are similar with only a small offset. From these results the value of (β) can be determined for each equation. The computed values of β from the Monte Carlo analysis (HEC-18 β = 2.75, FDOT β = 1.81) are essentially the same as those originally estimated from the live-bed laboratory data bias and COV assuming a normal distribution, which indicates that the implementation of the Monte Carlo simulation is reliable. If a target β of 2.5 is desired, then the FDOT design value of 11.2 ft would need to be increased to 12.4 ft (multiplied by a factor of 1.11) and the HEC-18 equation design value of 13.7 ft would need to be decreased to 13.4 ft (multiplied by a factor of 0.98).

Table 5.6 also shows the pier scour results after applying the Bias and COV for each equation based on live-bed laboratory data. For this 100-year flow condition, the HEC-18 equation provides a β of 2.75, while the results of the FDOT equation would need to be increased to provide the same level of reliability. The scour factors to achieve a β of 3.0 are shown, and in this case both equations would require greater design scour to achieve this level of reliability. Use of the FDOT equation for this bridge and hydraulic condition does result in less required scour (11.2 x 1.17 = 13.1 ft) to achieve the same reliability as the HEC-18 equation (13.7 x 1.04 = 14.2 ft) as shown in Table 5.6 for a β of 3.0. This is due primarily to the fact that the FDOT equation is less sensitive over a wide range of velocity and depth.

This type of simulation, though with fewer than 20,000 cycles, was performed for other discharges, pier sizes, and bridge configurations (see Chapter 6). Subsequent analyses revealed that 10,000 MCS cycles are sufficient to establish a consistent β value for each of the scour components.

5.4.2 HEC-RAS/Monte Carlo Simulation Results for Contraction Scour

Contraction scour is caused by a change in flow distribution from upstream of the bridge (Approach cross section) to the bridge. At the Approach, flow is distributed throughout the overall cross section among the channel, left, and right floodplains based on the conveyance of these sub areas. At the bridge, flow is concentrated in the bridge opening entirely in the channel if the abutments are set at the channel bank or into the channel. If the abutments are set back from the channel banks, then some of the flow is conveyed in the setback areas between the channel banks and the abutments. The Monte Carlo simulations vary discharge, starting energy slope (downstream boundary condition), and channel and overbank Manning n values. Each of these parameters affects flow distribution at the Approach and at the bridge. As with pier scour, contraction scour was computed for the 20,000 cycle simulation of the Sacramento River Bridge to fully accommodate the extremes of the input parameters.

The design condition produced a design contraction scour of 5.3 feet. Although the largest computed contraction scour was generated from the highest discharges, other combinations of conditions also produced significantly more (or less) contraction scour than the design value. For example, if the channel Manning n value is high and the floodplain Manning n is low, then more flow is conveyed in the floodplain. This condition results in a much greater amount of flow constriction and much greater contraction scour. Conversely, a low channel Manning n combined with a high floodplain Manning n concentrates flow in the channel, results in less flow constriction at the bridge and much less contraction scour. The range of computed contraction scour was from 0.55 to 14.0 feet.

Another process that affects contraction scour is road overtopping. It has been standard practice to limit scour analyses to flow up to the point of road overtopping (Arneson et al. 2012). The rationale is that once road overtopping commences flow through the bridge will not increase due to the significant amount of relief provided by the weir flow over the road. To keep the HEC-RAS model stable over the full range of flow and other input parameters, road overtopping was eliminated from the model and all flow was conveyed through the bridge opening. It is also better to exclude road overtopping for the general Monte Carlo analyses because the elevation where road overtopping initiates will be highly bridge specific. In the spreadsheet used to compute scour, however, adjustments were made to assess the impacts of road overtopping for this bridge. To develop **Figure 5.7**, the road elevation was set at a reasonable height relative to the design water surface elevation. The lower limit of computed contraction scour was, of course, unchanged. The upper limit was 9.2 feet and occurred with slight road overtopping flow (3,000 cfs of a total 181,000 cfs in that run).

A comparison of contraction scour estimates with and without road overtopping is shown in Figure 5.7. The majority of the simulations (16,907 cycles) did not generate road overtopping flow. The remaining simulations (3,093 cycles) generated up to 77,400 cfs of road overtopping flow. In Figure 5.7, the computed contraction scour is plotted versus the road overtopping discharge whether or not road overtopping was considered. This illustrates that for small amounts of road overtopping the scour is relatively unaffected by the relief flow, but that for the largest amounts road overtopping scour can be minimal (2 ft versus 14 ft). Generally road overtopping is undesirable, but from this analysis it is clear that it can greatly reduce contraction scour potential.

Contraction scour results from the Monte Carlo simulation are shown in **Figures 5.8 and 5.9**. Figure 5.8 shows the contraction scour computed directly from the hydraulic results with and without road overtopping flow. The design scour is 5.3 ft, which is centered within the distributions. Road overtopping shifts the most extreme amounts of contraction scour to lower values.

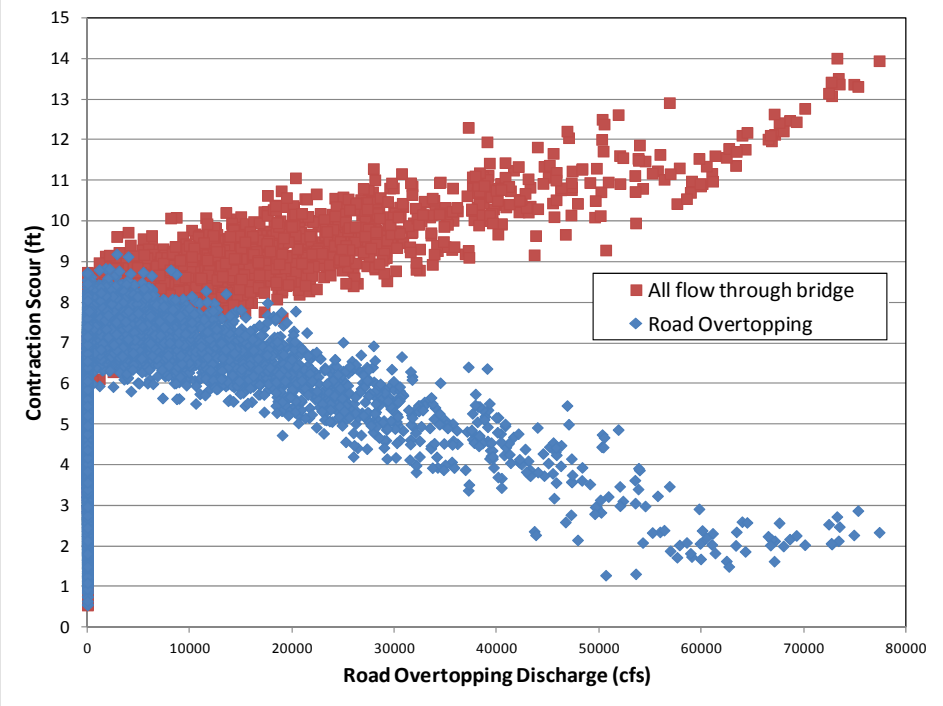

Figure 5.7. Contraction scour with and without road overtopping.

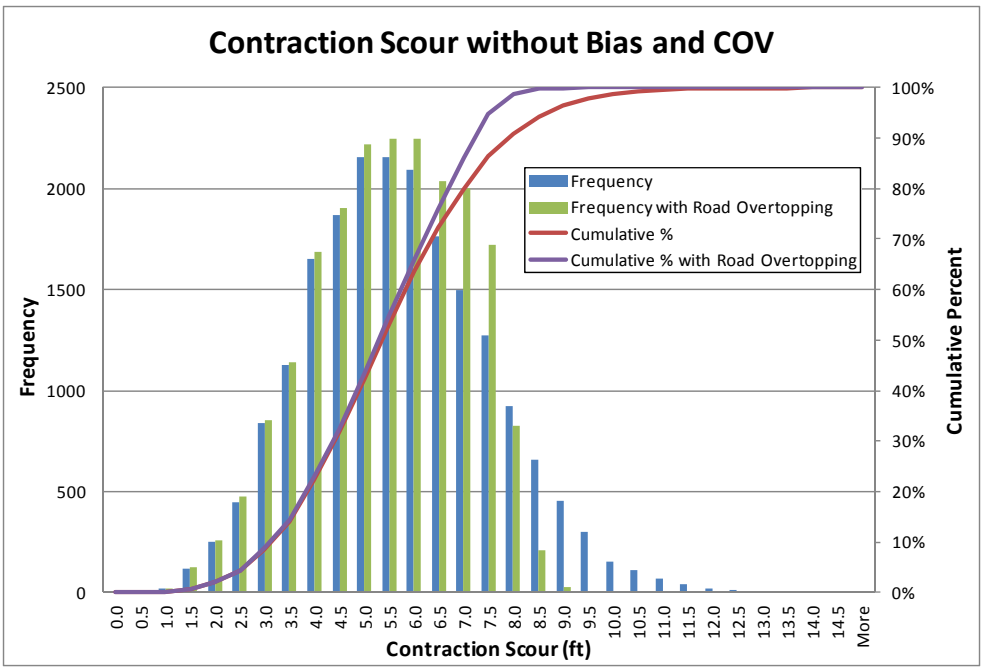

Figure 5.8. Computed live-bed contraction scour results from the HEC-RAS Monte Carlo Simulations.

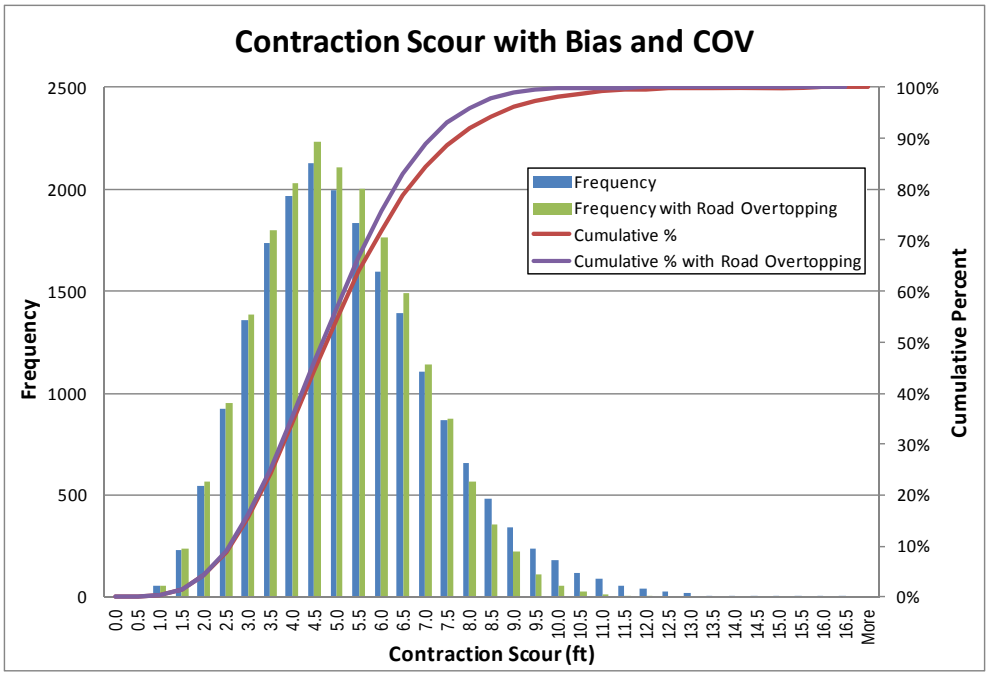

Figure 5.9. Live-bed contraction scour results for the HEC-RAS Monte Carlo simulations after including equation bias and COV.

Unlike the HEC-18 and FDOT equations, the contraction scour equations are predictive and do not include conservative factors for design. The clear-water contraction scour equation is developed from sediment incipient motion criteria and the live-bed contraction scour equation is developed from sediment transport relationships. The HEC-18 and FDOT pier scour equations have bias values of 0.68 and 0.75 based on comparisons to the laboratory data, which indicates a level of conservatism. The clear-water contraction scour equation has a bias of 0.92 based on comparisons with laboratory data (see Chapter 4), which indicates very little bias (i.e., no built-in conservatism as expected in a predictive equation). Contraction scour laboratory data has a higher COV than pier scour (0.16 for HEC-18 and 0.18 for FDOT). This indicates greater variability in contraction scour. Although the bias and COV are for clear-water conditions, these values were applied to the live-bed equation to produce Figure 5.9. Both equations are derived based on sediment transport relationships and are predictive so this is justifiable, though not ideal. From a practical standpoint, there is insufficient live-bed data to develop independent bias and COV for the live-bed equation. Therefore, clear-water values were applied to the live-bed results.

With bias close to 1.0, the contraction scour equation has very low reliability with β close to zero. As shown in Figure 5.9, for the larger COV the range of computed contraction scour increases significantly as compared to Figure 5.8, though the mean scour is relatively unchanged from the design value of 5.3 ft. It also made relatively little difference whether road overtopping was included.

Table 5.7 summarizes results from this set of bridge-specific simulations. Based on these results, scour factors are shown for various target levels of reliability. For example, a β of 2 would require that contraction scour be multiplied by a factor of 1.8 resulting in a design scour of 9.7 feet if road overtopping is not considered. With road overtopping at this bridge, a β of 2 would require multiplying contraction scour by 1.6 giving 8.5 feet of scour to be used for design. This is considerably greater than the 5.3 feet that would currently be used.

Table 5.7. Contraction Scour Results from 20,000 Cycle Sacramento River Bridge HEC-RAS.

Variable	All Flow Through Bridge					Road Overtopping				
Design Scour (ft)	5.4					5.3				
Mean Scour (ft)	5.5					5.2				
Standard Deviation (ft)	1.85					1.53				
COV	0.338					0.293				
Minimum Computed Scour (ft)	0.55					0.55				
Maximum Computed Scour (ft)	14.0					9.2				
Results After Applying Bias and COV										
Mean Scour (ft)	5.00					4.78				
Standard Deviation (ft)	2.02					1.74				
COV	0.404					0.364				
Minimum Computed Scour (ft)	0.41					0.41				
Maximum Computed Scour (ft)	16.3					11.7				
β (design scour)	0.26					0.33				
Target β	1	1.5	2	2.5	3	1	1.5	2	2.5	3
Scour Factor for Target β	1.3	1.6	1.8	2.1	2.4	1.2	1.4	1.6	1.0	2.0
Scour required for Target β (ft)	7.0	8.3	9.7	11.3	12.9	6.6	7.5	8.5	9.4	10.4

5.4.3 HEC-RAS/Monte Carlo Simulation Results for Abutment Scour

As described in Section 4.3, abutment scour is both a contraction and local scour process. The constriction of flow in the bridge opening that produces contraction scour also concentrates flow at the abutments. Therefore, the starting point for abutment scour is a contraction scour calculation. The obstruction of the abutment produces vortices and turbulence that amplify the contraction scour. The equations and figures in Section 4.3 present this approach to computing abutment scour for various hydraulic and sediment conditions and abutment configurations (Ettema et al. 2010).

The 20,000 cycle Monte Carlo simulation results were used to compute abutment scour at the Sacramento River bridge. The computed abutment scour for the base condition was 11.0 feet, but ranged from less than 1.0 feet to more than 30 feet depending on the hydraulic conditions computed in HEC-RAS. This variability is similar to the variability of computed contraction scour. This is expected because of the similarities of the two scour processes. As with the other scour components, the abutment scour equation bias and COV were applied to the computed scour values to determine the reliability of the design scour amount. For abutment scour the bias and COV values are 0.74 and 0.23 from the data analysis in Chapter 4. The bias is lower than the contraction scour bias because the amplification values were developed to envelop the laboratory results.

Figure 5.10 shows the distributions of computed abutment scour and abutment scour after including equation bias and COV. **Table 5.8** summarizes the results and shows scour factors needed to achieve various levels of reliability (β). For example, to achieve a target β value of 2.0, the design abutment scour of 11.0 ft (rounded from 10.94 ft) would have to be increased by a factor of 1.6 to 17.5 ft. These results are based on the hydraulic variables computed without adjusting for road overtopping. As with contraction scour, it is expected that abutment scour potential would be reduced when road overtopping occurs.

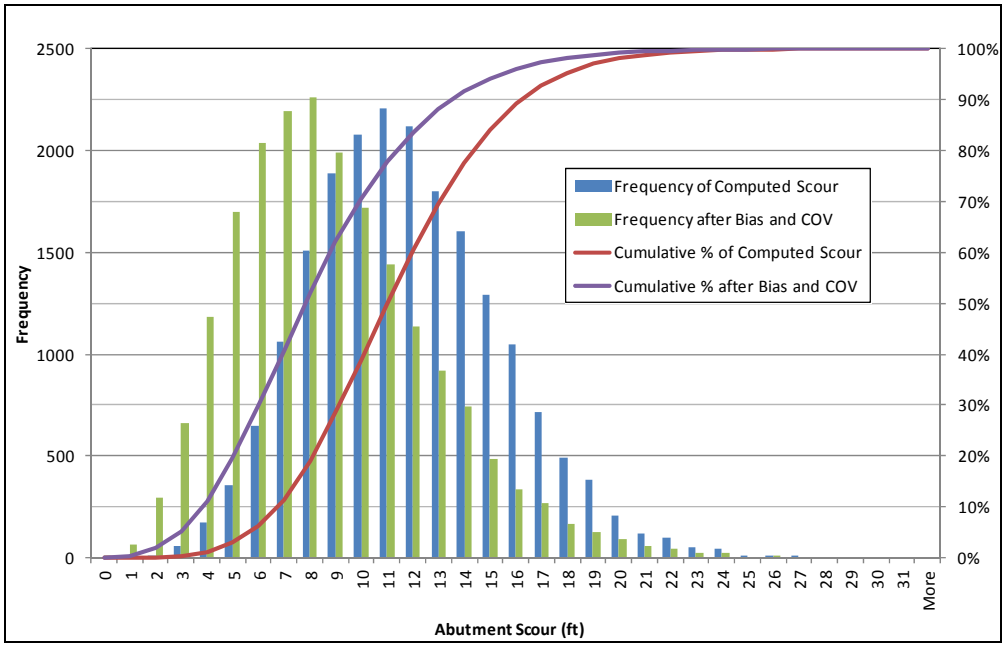

Figure 5.10. Abutment scour results from the HEC-RAS Monte Carlo Simulations.

Table 5.8. Abutment Scour Results from 20,000 Cycle Sacramento River Bridge HEC-RAS.					
Variable	Value				
Design Scour (ft)	11.0				
Mean Scour (ft)	11.3				
Standard Deviation (ft)	3.7				
COV	0.33				
Minimum Computed Scour (ft)	0.35				
Maximum Computed Scour (ft)	30.4				
Results after applying Bias and COV					
Mean Scour (ft)	8.3				
Standard Deviation (ft)	3.9				
COV	0.46				
Minimum Computed Scour (ft)	-1.4 (0.0)				
Maximum Computed Scour (ft)	30.4				
β (design scour)	0.78				
Target β	1.0	1.5	2.0	2.5	3.0
Scour Factor for Target β	1.1	1.3	1.6	1.9	2.2
Scour required for Target β (ft)	12.1	14.6	17.5	20.9	24.0

(page intentionally left blank)

CHAPTER 6

6. PROBABILITY-BASED SCOUR ESTIMATES

6.1 Approach

6.1.1 Background

The primary objective of this research is to develop a methodology that can be used to estimate the probability that the design scour level will be exceeded. The goal is to check whether the probability of design scour exceedance will meet an acceptable level of risk. The developed probabilistic procedures are consistent with LRFD approaches used by structural and geotechnical engineers.

This objective was achieved by providing a set of tables of probability values and scour factors for a given design event that can be used to associate the estimated scour depth with a conditional probability of exceedance, **i.e., that probability is conditional based on the hydrologic design event selected**. The probability values and scour factors were calibrated for typical bridge foundations and river channel geometries and hydraulic conditions. A 100-year return period was used for the design event.

This approach is identified as Level I analysis. For complex foundation systems and channel conditions, or for cases requiring special consideration, a Level II approach that consists of a step-by-step procedure that hydraulic engineers can follow to provide site-specific probability estimates was developed. Providing a second level option is similar to what the AASHTO LRFR Guide Manual for Bridge Condition Evaluation (2005) proposes when a refined evaluation is deemed necessary.

6.1.2 Calibration of Level I Statistical Parameters

The object of the Level I approach was to provide an easy to apply method to allow the engineer to control the level of safety to use when designing a foundation for scour. The calibration of the probability values and scour factors requires knowledge of the appropriate bias and COV values which may depend on the bridge foundation and channel geometric and site conditions. These two parameters must account for all the levels of uncertainties and conservative assumptions that are intentionally or unintentionally embedded in the scour estimation process.

Two types of uncertainties must be accounted for:

(1) Aleatory uncertainties (natural uncertainties due to inherent parameter variability and randomness)
(2) Epistemic uncertainties (modeling uncertainties)

Aleatory uncertainties are due to random variations in the variables that control the parameter being estimated. For example, a 100-year river discharge rate used for design is only an estimated value that is calculated from previous discharge rates. Such estimates are associated with various levels of uncertainties. Similarly, estimated values of soil properties even when measured in laboratory tests are associated with various levels of uncertainties that are due to local spatial variations in the soil profile but also due to uncertainties in the accuracy of the test devices.

The calibration of the probability values and scour factors account for the uncertainties inherent in the scour analysis process. These include modeling (epistemic) uncertainties as well as parametric (aleatory) uncertainties as described above. The availability of probability

values and scour factors that represent "typical" or "standard" conditions provide an engineer with the flexibility of selecting the level of scour risk appropriate for the particular bridge being analyzed for a given design event. That level of risk is represented by a reliability index β (see Section 2.6.2 for a discussion of the reliability index as a measure of structural safety).

Section 6.1.3 and Section 6.2 outline the development of the scour factor tables, describe a representative table, and summarize the bias and COV values for the individual scour components. Chapter 7 provides illustrative examples applying the Level I approach to determine the conditional probability of exceedance for estimated scour depths for bridges selected from different physiographic regions of the U.S.

6.1.3 Level I Applications for Typical Site Conditions

The Level I approach to providing probability values and scour factors for typical or standard bridge configurations is shown in **Table 6.1**. A 3 x 3 matrix based on bridge size (bridge length) and pier size is considered as shown in Table 6.1. The analysis includes a small, medium, and large bridge each with small, medium and large piers. The size of the piers increased proportionately with each bridge.

Table 6.1. Bridge and Pier Geometry for Typical Bridges.

	Bridge Length (ft)		Pier Size (ft)		
Bridge Size	Range	Monte-Carlo	Small	Medium	Large
Small	< 100	50	1	2	3
Medium	100 – 300	180	1.5	3	4.5
Large	> 300	1200	3	6	9

Bridge, channel, and floodplain size scale together and each must be represented by a Monte Carlo simulation. In addition, the typical bridge matrix was expanded by including three levels of hydrologic uncertainty. The values in **Table 6.2** show the 100-year discharges used for the typical bridges and correspond to the values shown in Tables 5.1 and 5.3. Thus, a total of 27 scour permutations were considered for the Level I analysis.

Table 6.2. Bridge Discharges for Typical Bridges.

		Hydrologic Uncertainty					
		Low		Medium		High	
Bridge Size	Q_{100} (cfs)	5%	95%	5%	95%	5%	95%
Small	1,840	1,610	2,100	1,520	2,230	1,430	2,370
Medium	29,800	24,800	35,700	22,800	38,900	21,000	42,200
Large	144,000	117,000	178,000	106,000	196,000	96,400	216,000

6.1.4 Level II Probabilistic Evaluation of Scour Depth

The application of the 27 tables calibrated for the Level I approach can be executed on a regular basis for the probability-based analyses of "typical" or "standard" scour site conditions. However, the calibration of the Level I statistical parameters will average the model biases for pier, abutment, and contraction scour (λ_p, λ_a, and λ_c) and associated COV values and distributions for random variables at similar sites (see Section 3.4).

When a bridge site does not fit any of the categories identified, or when the bridge is unique or is classified as being critically important for economic, societal or security reasons, it would be more appropriate to execute site-specific (Level II) probabilistic or reliability analyses of scour depths using site-specific statistical data for each variable that is used as input in the scour model (see Section 6.3).

6.2 Level I Analysis and Results

The results of each of the 27 Monte Carlo scour simulations (3 bridge sizes x 3 pier sizes x 3 hydrologic uncertainties) were analyzed to compute pier scour (HEC-18 and FDOT), contraction scour (HEC-18), and abutment scour (NCHRP-24-20) for representative 100-year design events (see Table 6.2). Total scour, the sum of pier and contraction scour, was also computed using each of the pier scour equations. Each simulation included a computation of design scour for the base condition. With every Monte Carlo realization, the computed amounts of each scour component were adjusted with the laboratory bias and COV applied as normally distributed random numbers. This produced data sets of 10,000 scour values that include model (equation) uncertainty and hydraulic uncertainty, where hydraulic uncertainty is the combination of hydrologic, Manning n, and boundary condition uncertainties. From each Monte Carlo simulation (10,000 runs), the expected scour (mean of the data set), bias (expected/design), standard deviation, and COV (standard deviation/expected) were computed. **In total, more than 300,000 HEC-RAS/Monte Carlo simulations were required to produce the statistics on which the 27 tables in Appendix A are based. In addition, more than 300,000 scour calculations for each of the scour equations were completed off-line (i.e., more than 1.2 million off-line scour calculations).**

For each of the types of scour the bias from the Monte Carlo simulation was essentially equal to the model bias. This is expected because the hydraulic uncertainties result in scour conditions more and less severe than the base hydraulic condition. For pier scour (both HEC-18 and FDOT) the COV from the Monte Carlo simulations was also essentially the same as the model COV. This indicates that the model bias and COV are the primary factors for the extreme conditions represented by the Monte Carlo simulations, which were computed for 100-year events. For contraction and abutment scour, although the bias from the Monte Carlo simulations was essentially equal to the model bias from the laboratory data, COV was greater in the Monte Carlo simulations. Although the hydraulic conditions were both more and less severe than the base condition, the variability of hydraulic conditions produced highly variable contraction scour results. Because abutment scour depends on contraction scour, the increased variability was also seen in the abutment scour results.

Table 6.3 is the summary table from one Monte Carlo simulation. Appendix A includes 27 summary tables from the Monte Carlo simulations (see also Tables 6.1 and 6.2). Table 6.3 represents a medium bridge with a medium pier size, and medium hydrologic uncertainty (see Table A.14). Each of the types of scour is shown. For pier scour, the HEC-18 equation results in design scour of 7.20 feet. Design contraction scour is 8.02 ft for a total design scour of 15.22 ft. Considering the bias in the scour equations, the results of the Monte Carlo simulation indicate expected scour of 4.89 feet of pier scour, 7.42 feet of contraction scour and 12.31 feet of total scour. Although the sum of the expected component scour values equal the total expected scour, the expected total scour was actually calculated as the average of the 10,000 computed total scour amounts. This very consistent result indicates that the expected total scour can be computed from the expected values of pier and contraction scour.

In Table 6.3, the HEC-18 pier scour equation reliability index β is calculated as (7.20-4.89)/0.77 = 3.0 (Equation 2.14), which compares to the table value of 2.99. The difference is due to the number of significant figures displayed in the table. Contraction scour has a very low reliability based on the expected scour only slightly less than the design scour and a very large value of COV, which was 0.21 from the model (equation) and increased to 0.37 for this bridge associated with hydraulic uncertainty.

Table 6.3. Medium Bridge - Medium Hydrologic Uncertainty - Medium Pier (3 ft).						
	Pier Scour (HEC-18)	Pier Scour (FDOT)	Contraction Scour	Total Scour (HEC-18)	Total Scour (FDOT)	Abutment Scour
Design Scour (ft)	7.20	5.94	8.02	15.22	13.95	15.12
Expected Scour (ft)	4.89	4.45	7.42	12.31	11.87	11.35
Bias	0.68	0.75	0.93	0.81	0.85	0.75
Std. Dev. (ft)	0.77	0.79	2.74	2.86	2.89	3.18
COV	0.16	0.18	0.37	0.23	0.24	0.28
Design Scour β	2.99	1.89	0.22	1.01	0.72	1.18
Non-Exceedance	0.9986	0.9706	0.5857	0.8444	0.7648	0.8818
Scour non-exceedance (ft) based on Monte Carlo results						
β = 0.5 (0.6915)	5.29	4.85	8.60	13.58	13.13	12.77
β = 1.0 (0.8413)	5.68	5.24	10.17	15.18	14.76	14.55
β = 1.5 (0.9332)	6.05	5.63	11.89	16.90	16.47	16.38
β = 2.0 (0.9772)	6.44	6.01	13.56	18.69	18.28	18.21
β = 2.5 (0.9938)	6.73	6.37	15.50	20.73	20.21	20.54
β = 3.0 (0.9987)	6.96	6.62	17.24	22.54	22.19	22.31
Scour factors based on Monte Carlo results						
β = 0.5 (0.6915)	0.73	0.82	1.07	0.89	0.94	0.84
β = 1.0 (0.8413)	0.79	0.88	1.27	1.00	1.06	0.96
β = 1.5 (0.9332)	0.84	0.95	1.48	1.11	1.18	1.08
β = 2.0 (0.9772)	0.89	1.01	1.69	1.23	1.31	1.20
β = 2.5 (0.9938)	0.94	1.07	1.93	1.36	1.45	1.36
β = 3.0 (0.9987)	0.97	1.11	2.15	1.48	1.59	1.48
Scour non-exceedance (ft) based on scour mean and standard deviation						
β = 0.5 (0.6915)	5.28	4.84	8.79	13.75	13.31	12.94
β = 1.0 (0.8413)	5.66	5.23	10.16	15.18	14.75	14.53
β = 1.5 (0.9332)	6.05	5.63	11.53	16.61	16.20	16.12
β = 2.0 (0.9772)	6.43	6.02	12.91	18.04	17.64	17.72
β = 2.5 (0.9938)	6.82	6.42	14.28	19.48	19.08	19.31
β = 3.0 (0.9987)	7.20	6.81	15.65	20.91	20.53	20.90
Scour factors based on scour mean and standard deviation						
β = 0.5 (0.6915)	0.73	0.82	1.10	0.90	0.95	0.86
β = 1.0 (0.8413)	0.79	0.88	1.27	1.00	1.06	0.96
β = 1.5 (0.9332)	0.84	0.95	1.44	1.09	1.16	1.07
β = 2.0 (0.9772)	0.89	1.01	1.61	1.19	1.26	1.17
β = 2.5 (0.9938)	0.95	1.08	1.78	1.28	1.37	1.28
β = 3.0 (0.9987)	1.00	1.15	1.95	1.37	1.47	1.38

Also included in Table 6.3 is an estimate of the design equation non-exceedance β value and percentile computed from the design scour, expected scour, and scour standard deviation assuming a normal distribution. As indicated in Table 6.3, a β value of 0.5 (for example) results in a probability of scour depth non-exceedance of 69.15%, or conversely, an exceedance probability of 30.85% for this bridge during a 100-year event. Note that Table 6.3 provides scour non-exceedance depths and corresponding scour factors derived directly from the Monte Carlo simulation (based on Monte Carlo results), and also with the assumption that the 10,000 predicted scour depths are normally distributed (based on scour mean and standard deviation). The fact that the scour depths and scour factors are similar but not identical indicates that the probability distribution based on Monte Carlo results is not precisely normal.

The HEC-18 pier scour standard deviation for this simulation was 0.77 ft (COV = 0.16). Contraction scour was much more variable with a standard devation of 2.74 ft (COV = 0.37). The total scour standard deviation from the Monte Carlo results was 2.86 ft (COV = 0.23) and can be estimated from the pier and contraction component values as the square root of the sum of the squares $(0.77^2 + 2.74^2)^{0.5}$=2.85 ft (Equation 2.14).

As shown in Table 6.3, HEC-18 and FDOT pier scour results have the highest level of realibility, contraction scour has the lowest level of reliability, and abutment scour has an intermediate level of reliability. Because total scour is used in design at a pier, the high reliability of the pier scour compensates for the lower level of reliability in the contraction scour value. This cannot, however, be considered a general result because of cases where there is small pier scour and large contraction scour.

Table 6.3 also shows non-exceedance scour amounts for β ranging from 0.5 to 3.0. These are computed in two ways for comparison. The first is directly from the Monte Carlo results and the second is based on the expected scour and standard deviation. The two methods are generally within plus or minus 5% for all scour components; however, the contraction scour amounts tend to be greater with the Monte Carlo results than from the statistics for β of 2.0 to 3.0.

From the non-exeedance scour values, the scour factors for each scour component are also shown. For this bridge and pier size, and hydrologic uncertainty, the Monte Carlo results show that the HEC-18 pier scour equation provides a β of 3.0 without any increase whereas the FDOT equation would require a small scour factor (1.11) to achieve a β of 3.0. Based on the Monte Carlo results the current design values of contraction and abutment scour would have to be increased by factors of 2.15 and 1.48 to achieve this level of reliability.

The scour factors for each component can be used for that component individually, but cannot be combined individually to arrive at the scour factor for total scour. Abutment scour is total scour based on the development of the NCHRP 24-20 equation. Total scour at a pier includes pier and contraction scour. Although the scour factors for total scour (pier plus contraction) are shown, they depend on the relative amounts of the two types of scour. Therefore, the β value for total scour should include calculation of the design scour components and total scour, expected scour components and total scour, and the standard deviation of the scour components and total scour. Simply adding the scour components for a specific β value would be overly conservative. For example, using a β of 2.5 and the statistical results in Table 6.3, FDOT pier scour is 6.42 ft and contraction scour is 14.28 ft, which combines to 20.70 ft. The total scour for β = 2.5 is 19.08 ft. Using the expected scour and standard deviations of the scour components, the total scour of β = 2.5 is 19.0 ft, which is very close to the desired result. The value of 19.0 ft comes from expected scour of 11.87 ft (4.45 ft pier + 7.42 ft contraction) and standard devation of 2.85 ft $(0.79^2+2.74^2)^{0.5}$, with a 2.5 multiplier for β (11.87 + 2.5 x 2.85 = 19.00 ft). This approach is general in that it accounts for any relative range of pier and contraction scour.

Figure 6.1 shows the scour factors for HEC-18 pier scour for all 27 bridge, pier, and hydrologic uncertainty combinations of Appendix A (see Figure A.1). In the legend SB, MB, and LB represent small, medium and large bridges, LH, MH, and HH represent low, medium and high hydrologic uncertainty, and SP, MP, and LP represent small, medium and large piers.

Figure 6.1a shows the scour factors directly from the results of the Monte Carlo simulations and Figure 6.1b shows the scour factors from the bias and COV of each of the simulations. For pier scour, whether the HEC-18 or FDOT equation is used, there is very little difference in the scour factors among the 27 simulations. At a β of 3, the range from the Monte Carlo results is 0.97 to 1.04 with an average of 0.99. From the statistical results the range is 1.00 to 1.03 with an average of 1.01. The two highest scour factors were computed for the large bridge, large pier, medium and high hydrologic uncertainty runs. Although the bias for these runs was consistent with the other runs the COV for these runs was 0.17 compared with 0.16 for all the other runs.

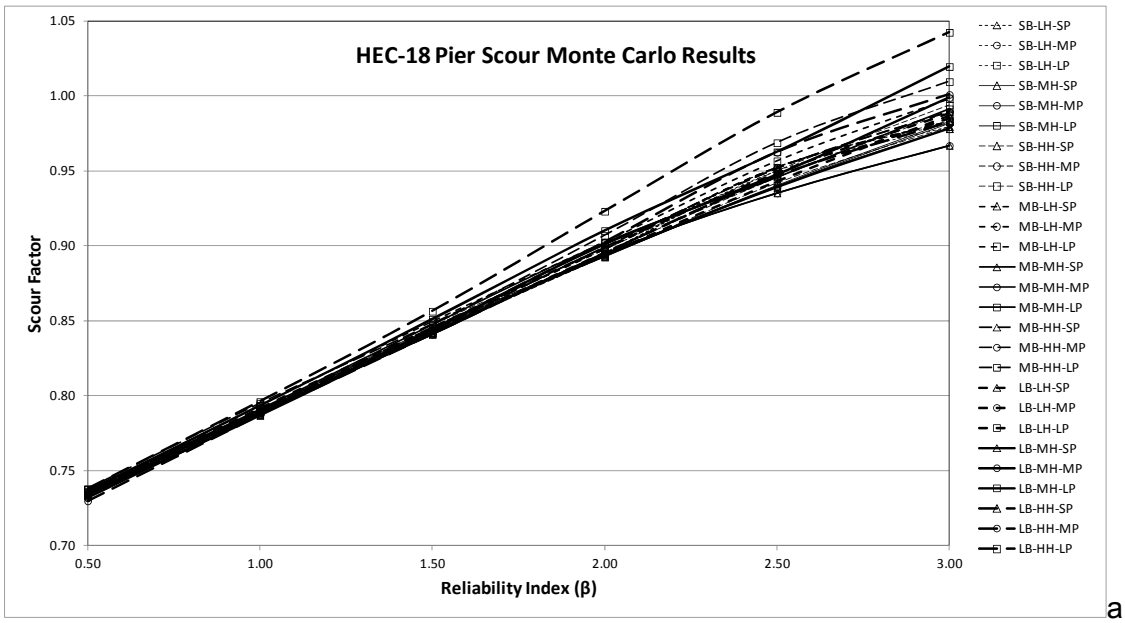

a

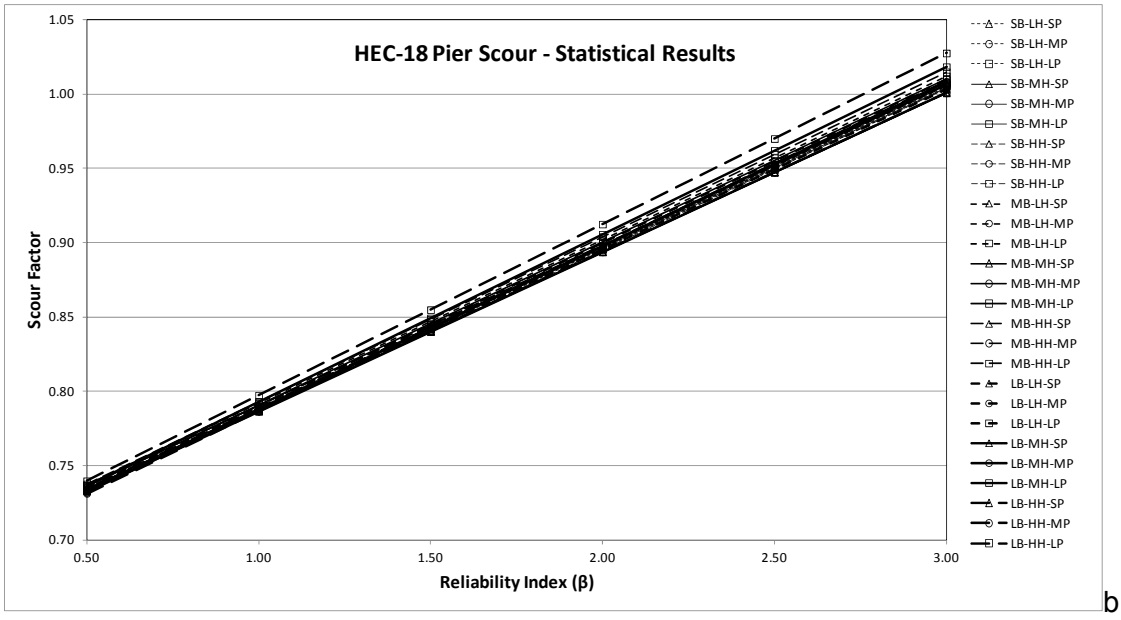

b

Figure 6.1. Scour Factors for the HEC-18 Pier Scour Equation.

Figure 6.2 shows the scour factors for the FDOT equation. There is very little difference in the scour factors among the 27 runs and very little difference between the Monte Carlo results (Figure 6.2a) and the statistics (Figure 6.2b). The scour factors for FDOT are slightly higher than for the HEC-18 equation, indicating slightly lower conservatism in the design equation. For a β of 2.5, the FDOT equation would require a scour factor of only 1.09.

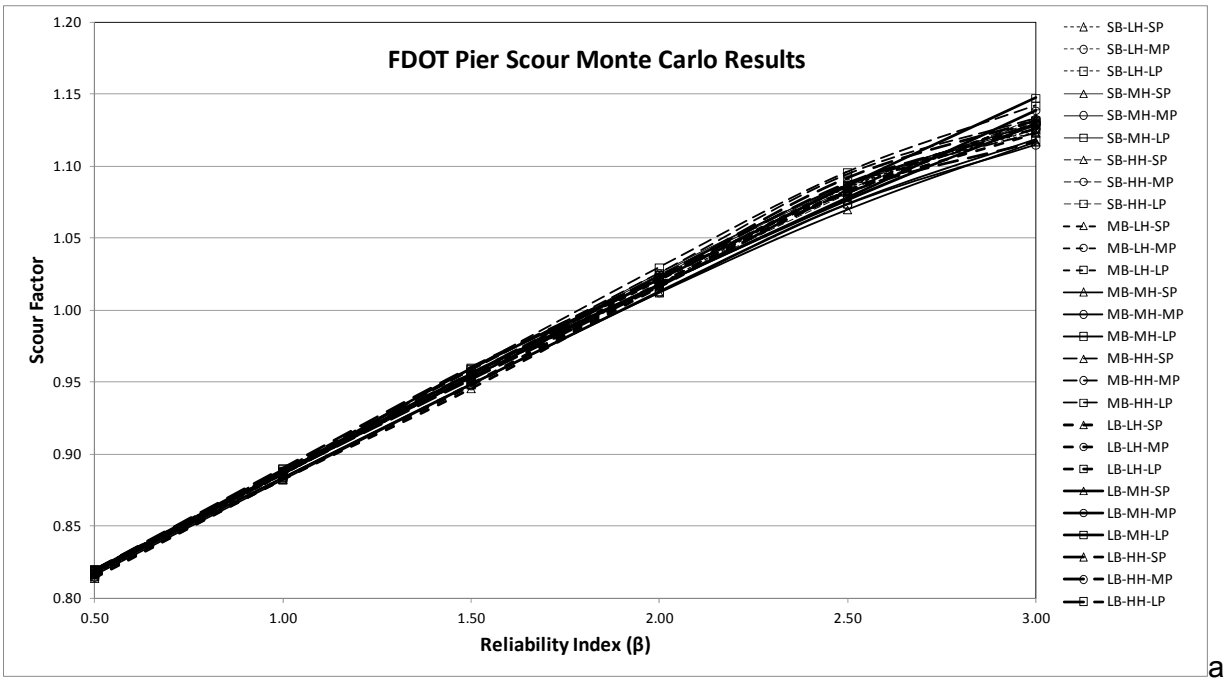

a

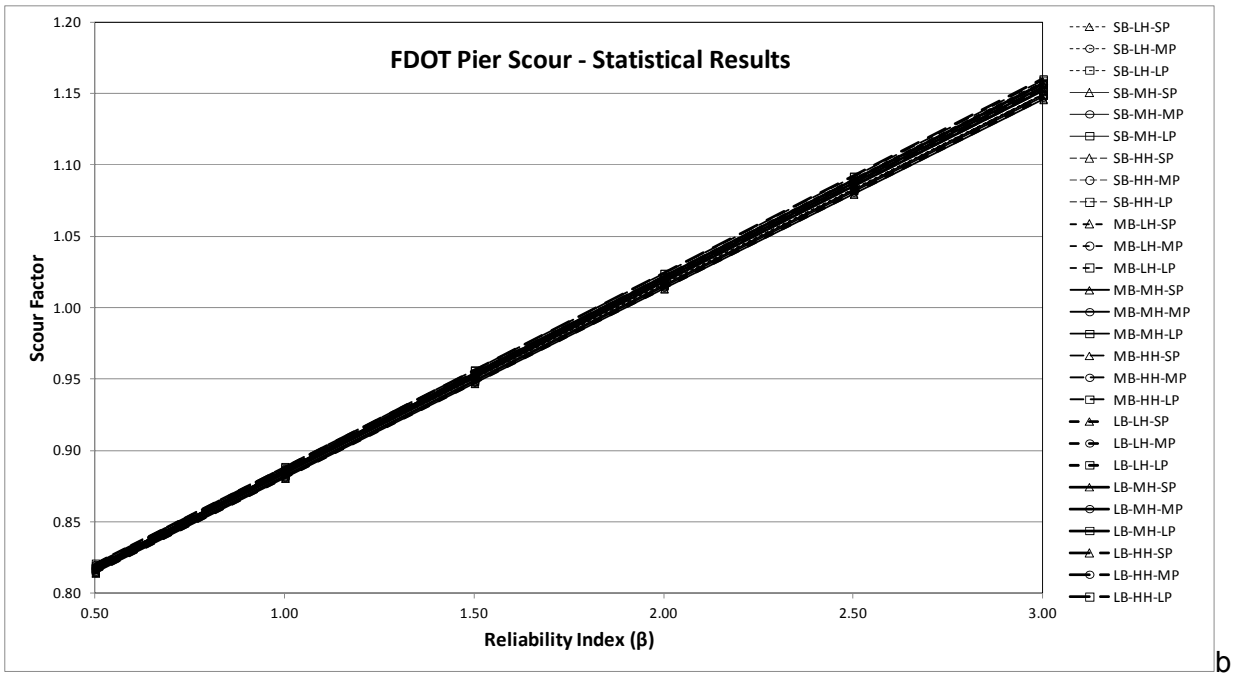

b

Figure 6.2. Scour Factors for the FDOT Pier Scour Equation.

Tables 6.4 and 6.5 show the bias and COV for HEC-18 and FDOT pier scour equations and all 27 Monte Carlo simulations. These tables demonstrate that 3 significant figures are required to discern any difference in these statistics, except for COV of the large bridge, large pier, medium and high hydrologic uncertainty conditions for the HEC-18 equation. Therefore, the pier scour bias and COV can be summarized and were applied as shown in **Table 6.6**, which are the same values as the laboratory data.

Table 6.4. HEC-18 Pier Scour Bias and COV from Monte Carlo Analysis.

		Pier Scour Bias (HEC-18)								
		Small Bridge			Medium Bridge			Large Bridge		
		S-Pier	M-Pier	L-Pier	S-Pier	M-Pier	L-Pier	S-Pier	M-Pier	L-Pier
Hydrologic Uncertainty	Low	0.680	0.679	0.679	0.680	0.680	0.682	0.680	0.679	0.680
	Medium	0.680	0.679	0.680	0.680	0.680	0.681	0.679	0.677	0.680
	High	0.679	0.678	0.679	0.682	0.682	0.682	0.680	0.676	0.682
		Pier Scour COV (HEC-18)								
		Small Bridge			Medium Bridge			Large Bridge		
		S-Pier	M-Pier	L-Pier	S-Pier	M-Pier	L-Pier	S-Pier	M-Pier	L-Pier
Hydrologic Uncertainty	Low	0.159	0.160	0.160	0.159	0.159	0.162	0.158	0.161	0.162
	Medium	0.159	0.160	0.160	0.157	0.157	0.161	0.158	0.163	0.166
	High	0.158	0.160	0.161	0.159	0.159	0.163	0.157	0.164	0.169

Table 6.5. FDOT Pier Scour Bias and COV from Monte Carlo Analysis.

		Pier Scour Bias (FDOT)								
		Small Bridge			Medium Bridge			Large Bridge		
		S-Pier	M-Pier	L-Pier	S-Pier	M-Pier	L-Pier	S-Pier	M-Pier	L-Pier
Hydrologic Uncertainty	Low	0.751	0.751	0.751	0.750	0.750	0.750	0.748	0.748	0.748
	Medium	0.751	0.751	0.751	0.748	0.749	0.749	0.750	0.750	0.750
	High	0.750	0.750	0.750	0.752	0.753	0.754	0.751	0.752	0.752
		Pier Scour COV (FDOT)								
		Small Bridge			Medium Bridge			Large Bridge		
		S-Pier	M-Pier	L-Pier	S-Pier	M-Pier	L-Pier	S-Pier	M-Pier	L-Pier
Hydrologic Uncertainty	Low	0.177	0.177	0.177	0.181	0.181	0.181	0.178	0.178	0.179
	Medium	0.180	0.180	0.180	0.177	0.177	0.178	0.179	0.180	0.181
	High	0.179	0.179	0.179	0.178	0.179	0.180	0.178	0.180	0.181

Table 6.6. Pier Scour Equation Bias and COV From Monte Carlo.

	Pier Scour	
Equation	Bias	COV
HEC-18	0.68	0.16
FDOT	0.75	0.18

Figure 6.3 shows the scour factors for contraction scour. Pier size was considered a secondary influence with contraction scour; therefore, the nine conditions represent bridge size and hydrologic uncertainty. Because the contraction scour equation is a predictive equation and is significantly influenced by the variability of flow distribution resulting from hydraulic uncertainty, the scour factors are significantly greater than for pier scour. Figure 6.3a shows the scour factors directly from the Monte Carlo results and Figure 6.3b shows the scour factors from the statistics (bias and COV).

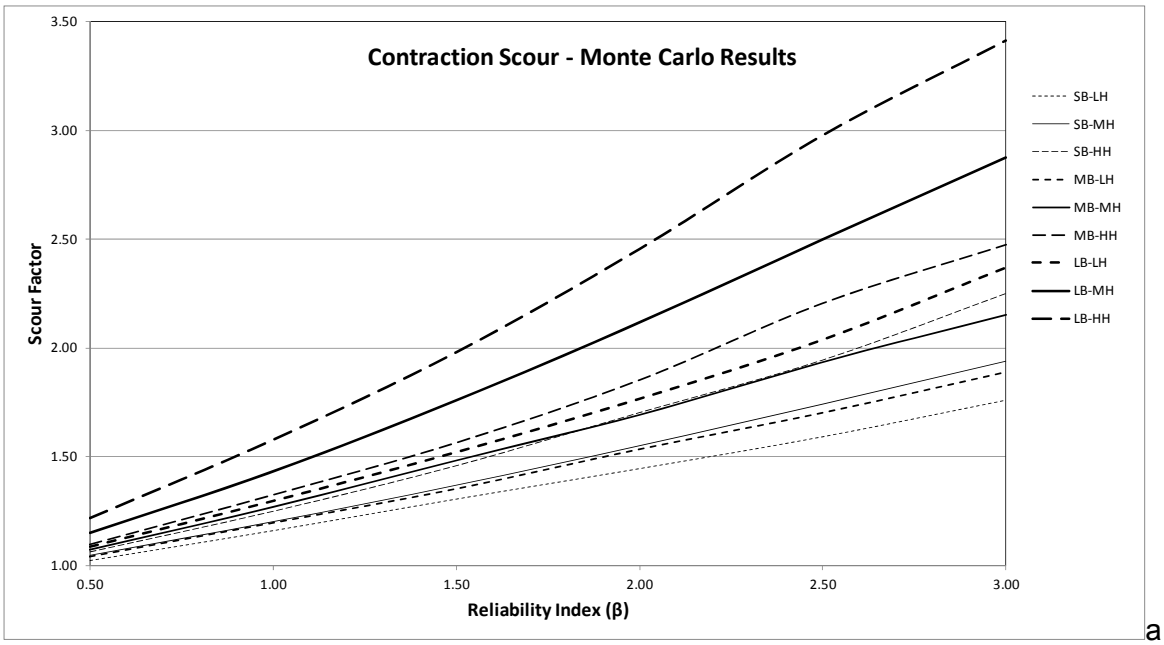

a

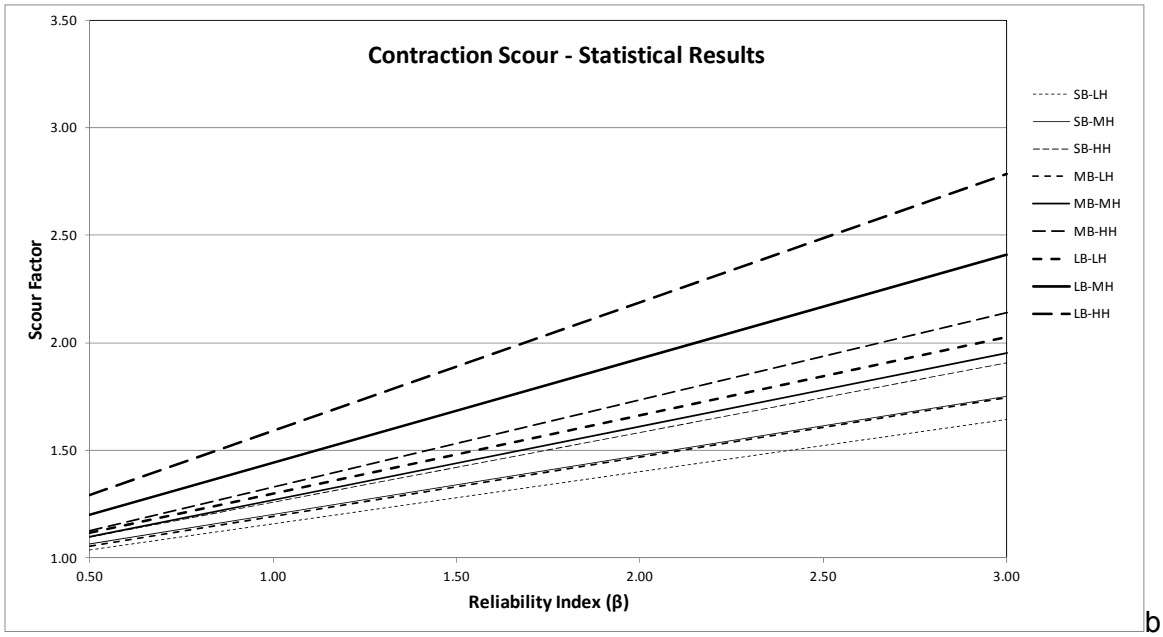

b

Figure 6.3. Scour Factors for Contraction Scour.

Up to β of 1.5 there is little difference in the two plots, but the curves diverge for higher levels of β. This indicates that there is positive skew in the distribution, as is shown in Figure 5.9. Had a log-normal distribution been used, the degree of curvature would have exceeded what is shown in Figure 6.3a. Also shown in Figure 5.9 is an example of the reduced extreme values of contraction scour when relief from road overtopping is included. Extreme flows are most likely to create overtopping, but also produce the greatest contraction scour in the Monte Carlo simulation (which excludes overtopping).

Table 6.7 shows the bias and COV for contraction scour Monte Carlo runs and the laboratory results. The bias is very consistent and similar to the laboratory results with the exception of the large bridge with medium to high hydrologic uncertainty, where the bias ranges from 0.96 to 0.99. A value of 0.93 is reasonable for all other cases. COV increases with bridge size and hydrologic uncertainty and is considerably greater than the laboratory value.

Table 6.7. Contraction Scour Bias and COV.

		Contraction Scour Bias Bridge Size			Contraction Scour COV Bridge Size		
		Small	Medium	Large	Small	Medium	Large
Hydrologic Uncertainty	Low	0.92	0.92	0.93	0.26	0.30	0.39
	Medium	0.93	0.93	0.96	0.29	0.37	0.50
	High	0.93	0.92	0.99	0.35	0.44	0.60
Lab Data		0.92			0.21		

Abutment scour results are very similar to the contraction scour results. **Figure 6.4** shows the scour factors, which are less than those for contraction scour but greater than for pier scour. **Table 6.8** shows that the bias is similar to the laboratory results with increased values for the large bridge. COV also increases with bridge size and hydrologic uncertainty. The level of bias is lower for abutment scour because the amplification factors developed for abutment scour in the NCHRP 24-20 method enveloped the data (see Section 4.3.2).

Table 6.8. Abutment Scour Bias and COV.

		Abutment Scour Bias Bridge Size			Abutment Scour COV Bridge Size		
		Small	Medium	Large	Small	Medium	Large
Hydrologic Uncertainty	Low	0.74	0.74	0.76	0.24	0.26	0.39
	Medium	0.74	0.75	0.78	0.24	0.28	0.51
	High	0.75	0.75	0.80	0.26	0.31	0.61
Lab Data		0.74			0.23		

6.3 Level II Analysis and Results

6.3.1 Overview

As indicated in Section 6.1.4, when a bridge does not fit any of the 27 bridge categories of the Level I approach, it is more appropriate to execute site-specific probabilistic or reliability analyses of scour depths using site-specific statistical data for each variable that is used to compute scour. This may be required if the hydraulic uncertainty parameters exceed the values used in Level I or if other parameters not considered in Level I are deemed to be significant in the design.

The process described in detail in Chapter 5 (see Section 5.4) and in the following section would need to be followed to perform a Level II analysis. This process includes performing a Monte Carlo analysis using a hydraulic model with validated uncertainty parameters including, but not necessarily limited to, hydrologic uncertainty, flow resistance uncertainty, and boundary condition uncertainty. The scour equation bias and COV from the laboratory data as described in Chapter 4 would be used in conjunction with the hydraulic modeling results to develop the distribution of scour components and total scour. If other scour equations are used, then the individual bias and COV of these equations would also need to be determined.

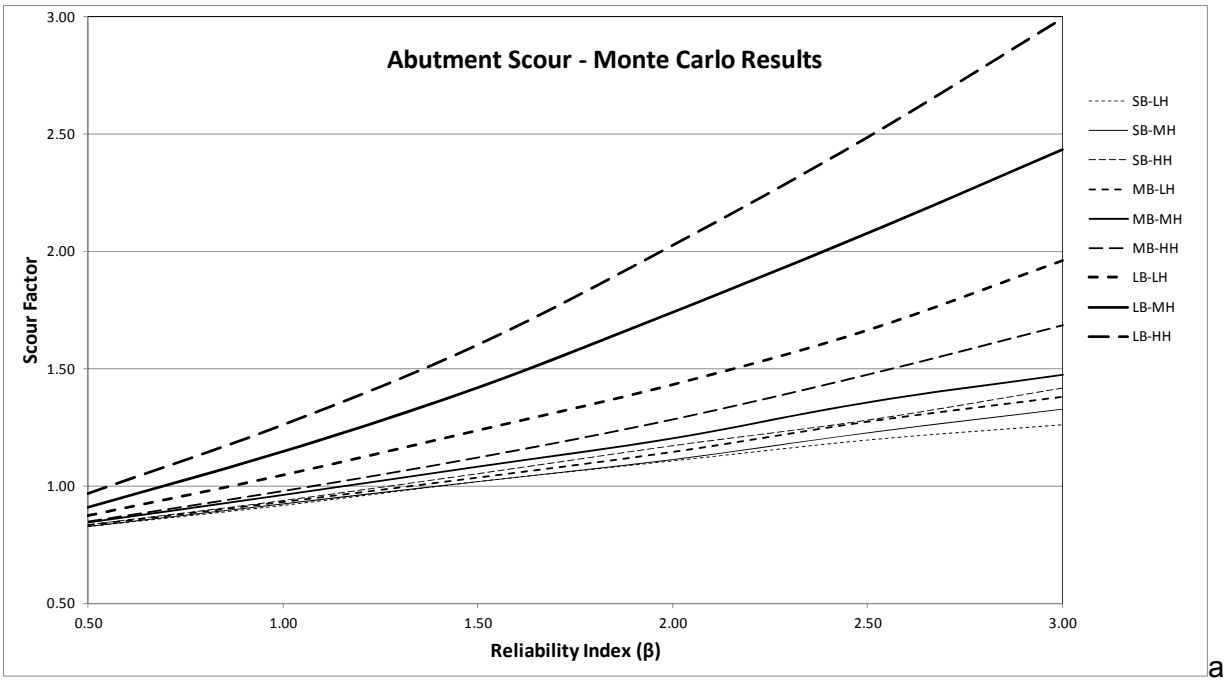

a

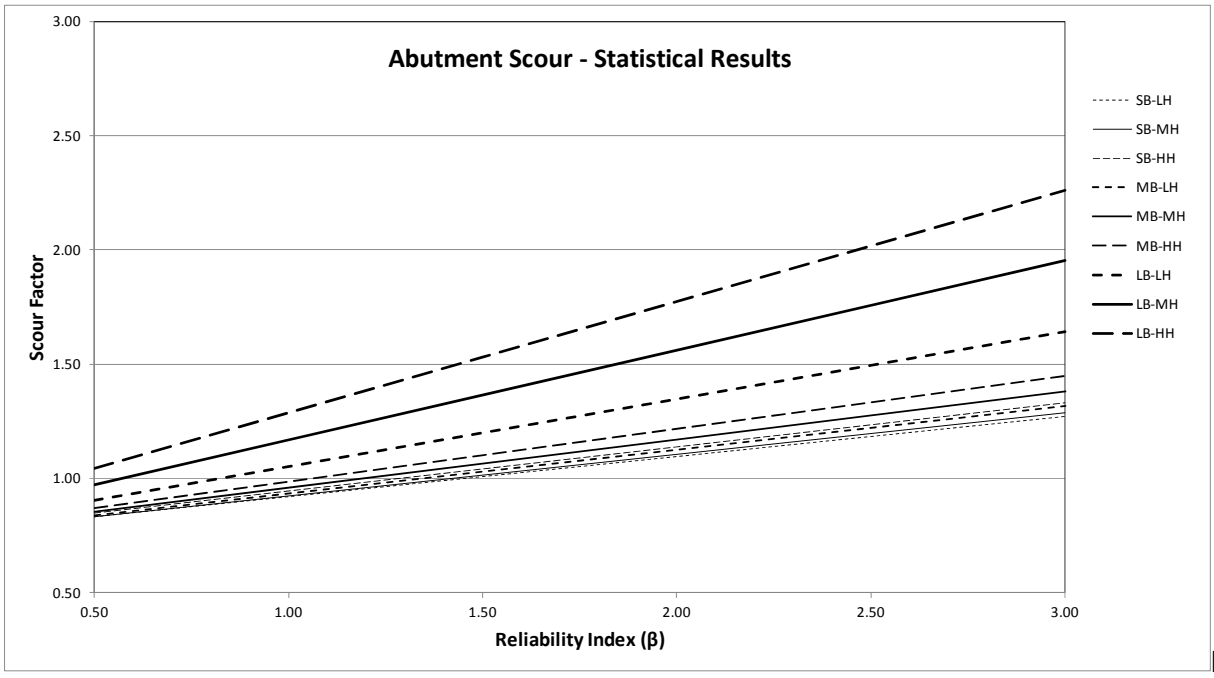

b

Figure 6.4. Scour Factors for the NCHRP Abutment Scour Equation.

6.3.2 Step-By-Step Procedure for Level II Analysis

A Level II analysis involves developing the statistical distribution of each scour component and total scour at a particular bridge site. This type of analysis may be required if the site conditions differ significantly from the conditions used to develop the Level I tables presented in Appendix A. A Level II analysis is useful if (1) the bridge has hydrologic or hydraulic uncertainties that are not reasonably represented by the range of Level I conditions, (2) site conditions require the use of other scour equations than were tested in Chapter 4, or (3) the bridge is considered to be significantly important and a more detailed, site-specific analysis is warranted. Not all the steps outlined below would necessarily be required for a Level II analysis. For example, if the standard scour equations apply at the bridge site, then the model (equation) bias and COV developed in Chapter 4 would apply.

The Level II steps described below follow the approach used in Sections 6.1 and 6.2 to develop the Level I scour factors. Therefore, familiarity with the rest of this document is useful if a Level II analysis is performed. For many of the steps, a prior or subsequent chapter or section in this report is provided as reference material. Steps are provided to determine the statistical distribution of scour for a specific event, such as the 100-year event, and therefore address conditional probabilities. The Monte Carlo simulation can be run for other events (as described in Chapter 8) to evaluate scour exceedance over the life of the bridge (unconditional probability). The steps of the Level II procedure are as follows:

Step 1. Develop a Site Specific Hydraulic Model

a. Develop a four cross section HEC-RAS hydraulic model of the bridge site (see Section 5.1). The Monte Carlo analysis was developed for a four cross section HEC-RAS model. If a large extent model is required, then modification of the Monte Carlo software (e.g., rasTool©) would be required.

b. Make best estimates of Manning n for the channel and overbank areas. Because the Monte Carlo analysis will vary Manning n around the starting estimate, it is important to **not** use conservative values (high or low) of Manning n, as doing so will bias the results. Calibrated values should be used if observed water surface data are available.

c. Make a best estimate of starting water surface boundary condition. It is recommended that the energy slope boundary condition be used, as doing so will vary the starting water surface for the various discharge values that will be applied in the Monte Carlo analysis. As with Manning n, a best estimate of the boundary condition should be used rather than a conservatively high or low value.

d. Evaluate site-specific hydrologic uncertainty (see Section 5.3.2). The Level I analysis used a range of hydrologic uncertainties for each bridge size. For a Level II analysis, the best estimate of hydrologic uncertainty should be developed and applied. The preferred approach is to perform gage analysis and apply Bulletin 17B (Log-Pearson Type III) procedures to determine the target discharge and confidence limits.

   Notes: (1) When applying the HEC-RAS model to a wide range of conditions it may be necessary to limit road overtopping to produce more stable models. If the model is stable for road overtopping conditions, it is recommended that road overtopping be allowed, as this will provide more representative contraction scour results. (2) As described in Step 3 (Perform Monte Carlo Analysis), the model results should be evaluated to determine that the variability of water surface is reasonable for the site conditions.

Step 2. Determine Scour Equation (Model) Uncertainty (Bias and COV)

a. If the standard scour equations are used (HEC-18 pier scour, FDOT pier scour, HEC-18 live-bed or clear-water contraction scour, NCHRP Project 24-20 abutment scour), then the model uncertainties (Bias and COV) from the laboratory data analysis presented in Chapter 4 should be used.

b. If another scour equation is used (such as vertical contraction scour, coarse-bed pier scour, scour in cohesive or erodible rock materials, etc.), then the model uncertainties (Bias and COV) from these alternative equations should be developed following the procedure in Chapter 4. The laboratory data for developing these equations should be used as they are from controlled conditions. HEC-18 (Arneson et al. 2012) includes references to research reports describing the development of several alternative equations.

Step 3. Perform Monte Carlo Analysis

a. Test the Monte Carlo simulation software for the bridge site (see Section 5.3) using the target (best estimate) values of discharge, channel and overbank Manning n, and starting energy slope and the uncertainties (COV) associated with these three input parameters. Determine the COV of the discharge using Equations 5.1 through 5.5. The COV for Manning n should be 0.015, and uncertainty related to Manning n should be determined using Equations 5.9 through 5.11. The COV of starting slope should be 0.10. However, as described in Section 5.3.3, the hydraulic results of the simulations should be reviewed to determine if the results are representative for the site. The tests should include holding discharge constant and varying only Manning n, only starting slope, and both variables. If the water surface varies much more or less than is expected and reasonable, then adjust the COV for Manning n and starting slope to better represent the site conditions. Do not adjust the discharge COV, as this was determined through statistical analysis.

b. Run the Monte Carlo simulation software using the target values of discharge, Manning n, and starting slope and the appropriate values of COV for these input variables. The number of cycles should be large enough to fully represent the range of possible hydraulic results. Because HEC-RAS executes quickly, a 10,000 cycle simulation can be achieved in less than 2 hours and should be sufficient.

Notes: (1) The rasTool© Monte Carlo simulation software developed for this project is a research tool. It was not developed for distribution nor is it thoroughly documented or supported for general use. It is, however, considered robust and could be applied to a range of bridge and/or open channel applications. (2) If a different hydraulic model will be used, then a specific software tool will need to be developed to control the random number generation for the input parameters and to run the number of required cycles in the Monte Carlo simulation. Given the relatively longer simulation times for 2-D models, it is unlikely that the number of cycles could be large enough for their application with standard office computers, and high-performance (supercomputer) technology would need to be used.

Step 4. Compute Component Scour and Total Scour

a. The output from the Monte Carlo simulation software is a text file table that includes the number of requested cycles of the hydraulic variables needed to perform scour calculations. This table is intended to be imported into a spreadsheet for calculating scour components and total scour. Alternatively, the results could be read by other software to calculate scour.

b. For each scour component, the computed scour should be determined by directly applying the appropriate equation. This scour value includes any level of conservatism (Bias) included in the development of the equation. The variability of scour results in this step is based on the variability of the hydraulic results. See pier scour example and Figure 5.5 in Section 5.4.1.

c. The computed scour from Step 4b is adjusted to determine expected scour distribution by multiplying the computed scour by a random number with mean equal to the model bias (0.68 in the case of HEC-18 pier scour) and standard deviation (SD) equal to the model bias times COV (0.16 in the case of HEC-18 pier scour resulting in a standard deviation of 0.68 x 0.16 = 0.109). The Monte Carlo simulation software includes four normally-distributed random numbers (R) of mean equal to zero and standard deviation equal to 1.0, so the desired random number set for a specific scour equation is (R x SD) + Bias. The results of the component scour (pier, contraction, and abutment) are then multiplied by the random number to provide the component scour distribution. See pier scour example and Figure 5.6 in Section 5.4.1.

d. At a pier, total scour is contraction scour plus local scour. The distribution of total scour is computed by adding the individual contraction and pier scour values including the Bias and COV adjustments from Step 4c. For abutment scour using the NCHRP Project 24-20 method, the result is total scour at the abutment. If a different abutment scour equation is used, the evaluation of total scour must be consistent with the development of the equation.

e. Based on the distribution of total scour, the designer should select the level of scour that achieves the desired probability of scour exceedance.

The results of Step 4 are the distributions of scour for a given return period event (conditional probability). Steps 3 and 4 can be repeated for several events to evaluate the unconditional probability of scour exceedance over the life of a bridge. As described in Chapter 8, performing the Monte Carlo analysis for the 50-, 100-, and 500-year events and combining the scour results will provide data to evaluate scour reliability for a 75-year bridge life. Note that the 50-year hydrologic uncertainty would be less than the 100-year hydrologic uncertainty because the 90 percent confidence limits would be closer to the expected value for the smaller event. Conversely, the uncertainty would be greater for the 500-year return period event. As described in Chapter 8, other sets of events would need to be evaluated for other bridge design lives.

The Level II process is illustrated in Section 5.4 using the same Sacramento River bridge that was used to validate the HEC-RAS/Monte software in Section 5.3.3. The Level I application for this bridge is illustrated in Chapter 7 (Section 7.4 Illustrative Example #3).

CHAPTER 7

7. ILLUSTRATIVE EXAMPLES

7.1 Overview

This chapter provides detailed illustrative examples to demonstrate the full range of applicability of the Level I probability-based scour estimates using the procedures presented in Chapter 6. Given the unique nature of any bridge-stream intersection, these examples illustrate application of the the methodology for a wide variety of bridge-stream scenarios in a range of physiographic regions across the country. The five bridge sites selected cover a wide variety of situations, including bridges over navigable waterways where pier scour predominates, single-span bridges where contraction and/or abutment scour occur, and bridges where all three scour components are evident. **Although these are realistic examples using actual bridges, some conditions have been changed for purposes of illustration**.

7.2 Example Bridge #1 - Maryland Piedmont Region

Location:	Maryland
Physiographic region:	Piedmont
Bridge length:	Existing bridge: 44 ft Replacement bridge: 55 ft
No. spans:	1
ADT:	7,801
Main channel width:	33 feet
River planform:	Meandering, moderately sinuous (1.06 - 1.25)
100-year discharge:	4,530 ft^3/sec
100-year depth:	7.5 feet approach flow depth in main channel 7.7 feet at upstream face, main channel
100-year velocity:	5.9 ft/sec approach velocity in main channel upstream 10.7 ft/sec at the upstream internal bridge section
Hydraulic model:	1-Dimensional (HEC-RAS)
Pier type/geometry:	N/A
Bed material:	Gravel
Abutment type/location:	Vertical/South Abutment is set back 5 feet; North Abutment is in the low flow channel. Replacement abutments will be wing-wall configuration.
Purpose of Study:	Bridge replacement

a. Upstream channel

b. Downstream face

Figure 7.2.1. Example Bridge No. 1.

This example applies the Level I analysis method to provide probability values and scour factors for a bridge located in the Piedmont physiographic region of Maryland. The site currently consists of a single-span, two-lane bridge with a history of contraction and abutment scour. The bridge has been rated as scour critical, has scour countermeasures, and is scheduled for replacement. For the new bridge, no overtopping or pressure flow occurs in the 100-year scour design event. For the 100-year scour design event, a desired total scour reliability index, β, of 3.0 is assumed for this example. This β corresponds to a 99.86% probability of non-exceedance during the design event. The calculations presented in this example are for the proposed replacement bridge.

Step 1. Perform hydrologic, hydraulic, and design-equation scour computations using appropriate methods.

a. Hydrologic analysis: USGS regional regression relationships for the Maryland Piedmont and Blue Ridge regions were used to develop the estimate of the 100-year design flood. For the 100-year event, the regression equation is:

$$Q_{100} = 1{,}471.1(DA)^{0.617}(LIME+1)^{-0.154}(FOR+1)^{-0.045}$$

where:

Q_{100} = Estimate of 100-year flood discharge, cfs
DA = Watershed drainage area, square miles
LIME = Percentage of carbonate/limestone rock in watershed, percent
FOR = Percentage of forest cover in watershed, percent

Using the USGS regression equation presented above and the watershed characteristics upstream of the bridge, the 100-year design discharge at this site is estimated to be 4,530 cubic feet per second.

b. Compute abutment scour: The NCHRP 24-20 live-bed approach for estimating total scour at the abutment was used to determine a scour depth of 8.6 feet. The NCHRP approach includes contraction scour plus the local scour at the abutment toe. Because both abutments of the new bridge will be in close proximity to the channel banks, the total scour depth is approximately the same for the left and right sides.

c. Compute pier and contraction scour: The replacement bridge will be a single-span structure; therefore, there are no pier scour or contraction scour components (other than the contraction scour at the abutments) to calculate at this site.

d. Summarize scour calculations:

Table 7.2.1. 100-Year Design Scour Depths.

Pier Scour, ft		Contraction Scour, ft	Total Scour, ft		Abutment Total Scour, ft	
HEC-18	FDOT		HEC-18	FDOT	Left	Right
n/a	n/a	n/a	n/a	n/a	8.6	8.6

Step 2. Determine the appropriate Bridge Size, Hydrologic Uncertainty, and Pier Size corresponding to standard scour factor table values.

a. Bridge Size: The bridge is 55 feet long. From the guidance presented in Section 6.1.3, this bridge is considered a Small Bridge.

b. Hydrologic Uncertainty: The USGS regional regression equation for the 100-year flood for the Maryland Piedmont and Blue Ridge regions has a standard error of 37.5%. From the guidance presented in Section 5.3.2, standard errors greater than 30% are considered to have High Hydrologic Uncertainty.

c. Pier Size: Not applicable - the replacement bridge will be a single span structure similar to the existing bridge.

Step 3. Determine scour factors.

Once we have classified the bridge, we can enter **Appendix A, Table A.7** to determine appropriate bias and scour factors as a function of the desired β.

Table 7.2.2 corresponds to a Small Bridge, High Hydrologic Uncertainty, Small Pier Configuration (note: pier size is not applicable for in this example).

Table 7.2.2. Scour Factors for β = 3.0 (using Monte Carlo results).

	Pier Scour		Contraction Scour	Abutment Total Scour	
	HEC-18	FDOT		Left	Right
Bias	n/a	n/a	n/a	0.75	0.75
Scour Factor	n/a	n/a	n/a	1.42	1.42

Step 4. Apply the Bias and Scour Factors and determine total design scour.

Applying the recommended bias and scour factors for β = 3.0 for all components produces the results shown in **Table 7.2.3**. The individual scour component design scour values are multiplied by the applicable bias to determine the expected scour. The component scour for β = 3.0 is the design scour times the scour factor. By definition for β = 3.0, the difference between the component scour and the expected scour is 3.0 standard deviations from the expected scour. The total scour for the target β is the expected plus the difference.

Table 7.2.3. 100-Year Scour Results for β = 3.0 (using Monte Carlo results).

	Pier Scour		Contraction Scour	Total Scour		Abutment Total Scour	
	HEC-18	FDOT		HEC-18	FDOT	Left	Right
Design Scour (ft)	n/a	n/a	n/a	n/a	n/a	8.6	8.6
Bias						0.75	0.75
Expected Scour (ft)						6.5	6.5
Scour Factor						1.42	1.42
Component Scour for β = 3.0 (ft)						12.2	12.2
Difference from Expected (ft)						5.7	5.7
Total Scour for β = 3.0 (ft)						12.2	12.2

7.3 Example Bridge #2 - Nevada Great Basin Subregion

Location:	Nevada
Physiographic region:	Intermontane Basins and Plateaus – Great Basin Subregion
Bridge length:	210 ft
No. spans:	3
ADT:	1,300 (2001)
Main channel width:	208 ft
River planform:	Sinuous (1.06-1.25)
100-year discharge:	31,150 ft^3/s
100-year depth:	19.6 ft
100-year velocity:	11.7 ft/s
Hydraulic model:	1-Dimensional (HEC-RAS)
Pier type/geometry:	1.7 ft wide by 44 ft long concrete wall piers on 19 ft wide pile caps (exposed)
Bed material:	Sand with gravel
Abutment type/location:	Spill-through abutments at channel banks
Purpose of Study:	Scour evaluation and countermeasure selection for a Plan of Action

Figure 7.3.1. Example Bridge No. 2 (looking downstream).

This example applies the Level I analysis method to provide probability values and scour factors for a bridge located in the Great Basin physiographic region of Nevada. The example bridge is a 210 foot long bridge with two concrete wall piers on spread footings. Due to long-term degradation at this site, the spread footings are now exposed above the stream bed. The abutments are of spill-through configuration located at the channel banks. No overtopping or pressure flow occurs in the 100-year scour design event. For the 100-year scour design event, a desired total scour reliability index, β, of 2.5 is assumed for this example. This β corresponds to a 99.38% probability of non-exceedance during the design event.

Step 1. Perform hydrologic, hydraulic, and design-equation scour computations using appropriate methods.

a. Hydrologic analysis: Bulletin 17B methods were used to determine the design scour event discharge, the expected value of the natural logarithm transform of discharge, and the standard deviation of the uncertainty about that expected value for a given recurrence interval. The resulting discharges and summary statistics are presented in **Table 7.3.1**.

Table 7.3.1. Hydrologic Data from Bulletin 17B Analysis of Bridge Site (N = 17 years).				
Annual Exceedance		Discharge, cfs		
p(X>x)	T (years)	Bulletin 17B Estimate	95% confidence Limits	
			Lower	Upper
0.1	10	10,400	6,720	18,530
0.04	25	17,300	10,560	34,110
0.02	50	23,690	13,910	49,970
0.01	100	31,150	17,630	69,810
0.005	200	39,720	21,740	94,050
0.002	500	52,810	27,750	133,500

b. Design equation scour computations using the HEC-18 method for pier scour, the HEC-18 method for contraction scour, and the NCHRP 24-20 method as presented in HEC-18 for abutment scour were computed for this example. **Table 7.3.2** presents the results of these computations.

Table 7.3.2. 100-Year Design Scour Depths.				
Pier Scour, ft	Contraction Scour, ft	Total Scour, ft	Abutment Total Scour, ft	
			Left	Right
28.9	1.7	30.6	2.4	3.3

Step 2. Determine the appropriate Bridge Size, Hydrologic Uncertainty, and Pier Size corresponding to standard scour factor table values.

a. Bridge Size: The example bridge is 210 ft long. From the guidance presented in Section 6.1.3, this bridge is best represented as a Medium Bridge.

b. Hydrologic Uncertainty: To establish the relative hydrologic uncertainty of this bridge, we must estimate the COV associated with the uncertainty of the discharge estimate for the design scour event.

1. The lognormal distribution of hydrologic uncertainty is determined from the 95% confidence limit discharge values as follows. The hydrologic uncertainty of a given Bulletin 17B discharge estimate is assumed to be log-normally distributed. Consequently, given the 95% upper and 95% lower confidence limits, (see Section 5.3.2),

$$\mu = \frac{\ln(Q_{upper}) + \ln(Q_{lower})}{2}$$

$$\sigma = \frac{\ln(Q_{upper}) - \ln(Q_{lower})}{2Z_c}$$

$$COV = \frac{\sigma}{\mu}$$

2. For a 95% confidence limit, Z_c = 1.645 (see Appendix C, Glossary). From the hydrologic analysis presented above, the upper and lower 95% confidence limits for the 1% exceedance probability event (i.e., the 100-year flood) are:

   Q_{upper} = 69,810 cfs;

   Q_{lower} = 17,360 cfs; and

   Z_c = 1.645

3. Substituting values for Q_{upper}, Q_{lower}, and Z_c into the equations above,

$$\mu = \frac{\ln(69{,}810) + \ln(17{,}360)}{2} = 10.46$$

$$\sigma = \frac{\ln(69{,}810) - \ln(17{,}360)}{2(1.645)} = 0.423$$

$$\text{COV} = \frac{0.423}{10.46} = 0.0404$$

   Compare the computed COV with **Table 7.3.3** (reproduced from Table 5.3) for the 1% exceedance probability event:

Table 7.3.3. Hydrologic Uncertainty as Function of Annual Exceedance Probability (Reproduced from Table 5.3).

Annual Exceedance		Discharge COV (lognormal)		
p(X>x)	T (years)	Low	Medium	**High**
0.04	25	0.009	0.014	0.018
0.02	50	0.010	0.015	0.019
0.01	**100**	0.011	0.016	**0.021**
0.005	200	0.012	0.017	0.022
0.002	500	0.013	0.018	0.023

   This bridge has High Hydrologic Uncertainty.

c. Pier Size: Because the pile caps are exposed above the stream bed, their width (19 feet) is compared to the values in **Table 7.3.4** (Reproduced from Table 6.1). This bridge has Large Piers for a bridge of its type.

Table 7.3.4. Representative Bridge Pier Size as a Function of Bridge Type (Reproduced from Table 6.1).

Bridge Type	Pier Size, ft		
	Small	Medium	**Large**
Small	1	2	3
Medium	1.5	3	**4.5**
Large	3	6	9

Consequently, this bridge is best classified as a Medium Bridge, High Hydrologic Uncertainty, Large Pier Size for the Level I Analysis. However, the 19 ft wide pile cap is significantly larger than the 4.5 ft large pier assumed for a Medium Bridge, suggesting that this bridge may be a candidate for a Level II analysis.

Step 3. Determine Scour Factors.

Once we have classified the bridge, we can enter **Appendix A, Table A.18** to determine appropriate bias and scour factors as a function of the desired β.

Table 7.3.5 corresponds to a Medium Bridge, High Hydrologic Uncertainty, Large Pier Size.

Table 7.3.5. Scour Factors for β = 2.5 (using Monte Carlo results).

	Pier Scour	Contraction Scour	Abutment Total Scour	
			Left	Right
Bias	0.68	0.92	0.75	0.75
Scour Factor	0.97	2.21	1.48	1.48

Step 4. Apply the Bias and Scour Factors and determine total design scour.

Applying the recommended bias and scour factors for β = 2.5 for all components produces the results shown in **Table 7.3.6**. The individual scour component design scour values are multiplied by the applicable bias to determine the expected scour. Total expected scour is the sum of expected pier and contraction scour. The component scour for β = 2.5 is the design scour times the scour factor. By definition for β = 2.5, the difference between the component scour and the expected scour is 2.5 standard deviations from the expected scour.

The total scour difference from expected is the square root of the sum of the squares of the component scour differences (pier and contraction scour). The total scour for the target β is the expected plus the difference as shown in Table 7.3.6.

Table 7.3.6. 100-Year Scour Results for β = 2.5 (using Monte Carlo results).

	Pier Scour	Contraction Scour	Total Scour	Abutment Total Scour	
				Left	Right
Design Scour (ft)	28.9	1.7	30.6	2.4	3.3
Bias	0.68	0.92		0.75	0.75
Expected Scour (ft)	19.7	1.6	21.3	1.8	2.5
Scour Factor	0.97	2.21		1.48	1.48
Component Scour for β = 2.5 (ft)	28.0	3.8		3.6	4.9
Difference from Expected (ft)	8.3	2.2	8.6	1.8	2.4
Total Scour for β = 2.5 (ft)			29.9	3.6	4.9

7.4 Example Bridge #3 - California Pacific Mountains Subregion

Location:	California
Physiographic region:	Pacific Mountains - Great Valley Subregion
Bridge length:	1200 ft
No. spans:	10
ADT:	11,800 (2009)
Main channel width:	607 ft
River planform:	Meandering, highly sinuous (>1.26)
100-year discharge:	140,000 ft^3/s
100-year depth:	24 ft
100-year velocity:	12.04 ft/s
Hydraulic model:	1-Dimensional (HEC-RAS)
Pier type/geometry:	2 column bents, 6-foot diameter columns @ 24 ft OC
Bed material:	Fine to coarse sand
Abutment type/location:	Spill-through abutments set back on floodplain
Purpose of Study:	Scour evaluation

Figure 7.4.1. Example Bridge No. 3 (looking upstream).

This example applies the Level I analysis method to provide probability values and scour factors for a bridge located in the Pacific Mountain physiographic region of California. The example bridge is a 1,200 foot long bridge with 6 foot-diameter drilled shaft interior bents and set back, spill-through type abutments. No overtopping or pressure flow occurs in the 100-year scour design event. For the 100-year scour design event, a desired total scour reliability index, β, of 2.5 is assumed for this example. This β corresponds to a 99.38% probability of non-exceedance during the design event.

Note: For illustrative purposes, in this example pier scour is calculated using both the HEC-18 and Florida DOT (FDOT) methods.

Step 1. Perform hydrologic, hydraulic, and design-equation scour computations using appropriate methods.

a. Hydrologic analysis: Bulletin 17B methods were used to determine the design scour event discharge, the expected value of the natural logarithm transform of discharge, and the standard deviation of the uncertainty about that expected value for a given recurrence interval. The resulting discharges and summary statistics are presented in **Table 7.4.1**.

Table 7.4.1. Hydrologic Data from Bulletin 17B Analysis of Bridge Site (N = 49 years).

Annual Exceedance		Discharge, cfs		
p(X>x)	T (years)	Bulletin 17B Estimate	95% confidence Limits	
			Lower	Upper
0.1	10	92,050	79,470	110,600
0.04	25	112,000	94,920	138,700
0.02	50	126,300	105,700	159,500
0.01	100	140,000	115,800	179,900
0.005	200	153,300	125,500	200,200
0.002	500	170,300	137,700	226,600

b. Design equation scour computations using the HEC-18 and FDOT methods for pier scour, the HEC-18 method for contraction scour, and the NCHRP 24-20 method as presented in HEC-18 for abutment scour were computed for this example. **Table 7.4.2** presents the results of these computations.

Table 7.4.2. 100-Year Design Scour Depths.

Pier Scour, ft		Contraction Scour, ft	Total Scour, ft		Abutment Total Scour, ft	
HEC-18	FDOT		HEC-18	FDOT	Left	Right
13.7	11.2	5.3	19.0	16.5	11.0	6.7

Step 2. Determine the appropriate Bridge Size, Hydrologic Uncertainty, and Pier Size corresponding to standard scour factor table values.

a. Bridge Size: The example bridge is 1,200 ft long. From the guidance presented in Section 6.1.3, this bridge is best represented as a Large Bridge.

b. Hydrologic Uncertainty: To establish the relative hydrologic uncertainty of this bridge, we must estimate the COV associated with the uncertainty of the discharge estimate for the design scour event.

1. The lognormal distribution of hydrologic uncertainty is determined from the 95% confidence limit discharge values as follows. The hydrologic uncertainty of a given Bulletin 17B discharge estimate is assumed to be log-normally distributed. Consequently, given the 95% upper and 95% lower confidence limits, (see Section 5.3.2),

$$\mu = \frac{\ln(Q_{upper}) + \ln(Q_{lower})}{2}$$

$$\sigma = \frac{\ln(Q_{upper}) - \ln(Q_{lower})}{2Z_c}$$

$$COV = \frac{\sigma}{\mu}$$

2. For a 95% confidence limit, Z_c = 1.645 (see Appendix C, Glossary). From the hydrologic analysis presented above, the upper and lower 95% confidence limits for the 1% exceedance probability event (i.e., the 100-year flood) are:

   Q_{upper} = 179,900 cfs;

   Q_{lower} = 115,800 cfs; and

   Z_c = 1.645

3. Substituting values for Q_{upper}, Q_{lower}, and Z_c into the equations above,

$$\mu = \frac{\ln(179{,}900) + \ln(115{,}800)}{2} = 11.88$$

$$\sigma = \frac{\ln(179{,}900) - \ln(115{,}800)}{2(1.645)} = 0.1339$$

$$COV = \frac{0.1339}{11.88} = 0.0113$$

Compare the computed COV with **Table 7.4.3** (reproduced from Table 5.3) for the 1% exceedance probability event:

Table 7.4.3. Hydrologic Uncertainty as Function of Annual Exceedance Probability (Reproduced from Table 5.3).

Annual Exceedance		Discharge COV (lognormal)		
p(X>x)	T (years)	**Low**	Medium	High
0.04	25	0.009	0.014	0.018
0.02	50	0.010	0.015	0.019
0.01	**100**	**0.011**	0.016	0.021
0.005	200	0.012	0.017	0.022
0.002	500	0.013	0.018	0.023

This bridge has Low Hydrologic Uncertainty.

c. Pier Size: Compare the bridge pier size (6 ft diameter) to **Table 7.4.4** (Reproduced from Table 6.1). This bridge has Medium Piers for a bridge of its type.

Table 7.4.4. Representative Bridge Pier Size as a Function of Bridge Type (Reproduced from Table 6.1).

Bridge Type	Pier Size, ft		
	Small	**Medium**	Large
Small	1	2	3
Medium	1.5	3	4.5
Large	3	**6**	9

Consequently, this bridge is best classified as a Large Bridge, Low Hydrologic Uncertainty, Medium Pier Size for the Level I Analysis.

Step 3. Determine Scour Factors.

Once we have classified the bridge, we can enter **Appendix A, Table A.20** to determine appropriate bias and scour factors as a function of the desired β.

Table 7.4.5 corresponds to a Large Bridge, Low Hydrologic Uncertainty, Medium Pier Size.

Table 7.4.5. Scour Factors for β = 2.5 (using Monte Carlo results).					
	Pier Scour		Contraction Scour	Abutment Total Scour	
	HEC-18	FDOT		Left	Right
Bias	0.68	0.75	0.93	0.76	0.76
Scour Factor	0.95	1.08	2.04	1.66	1.66

Step 4. Apply the Bias and Scour Factors and determine total design scour.

Applying the recommended bias and scour factors for β = 2.5 for all components produces the results shown in **Table 7.4.6**. The individual scour component design scour values are multiplied by the applicable bias to determine the expected scour. Total expected scour is the sum of expected pier and contraction scour. The component scour for β = 2.5 is the design scour times the scour factor. By definition for β = 2.5, the difference between the component scour and the expected scour is 2.5 standard deviations from the expected scour.

The total scour difference from expected is the square root of the sum of the squares of the component scour differences (pier and contraction scour). The total scour for the target β is the expected plus the difference as shown in Table 7.4.6.

Table 7.4.6. 100-Year Scour Results for β = 2.5 (using Monte Carlo results).							
	Pier Scour		Contraction Scour	Total Scour		Abutment Total Scour	
	HEC-18	FDOT		HEC-18	FDOT	Left	Right
Design Scour (ft)	13.7	11.2	5.3	19.0	16.5	11.0	6.7
Bias	0.68	0.75	0.93			0.76	0.76
Expected Scour (ft)	9.3	8.4	4.9	14.2	13.3	8.4	5.1
Scour Factor	0.95	1.08	2.04			1.66	1.66
Component Scour for β = 2.5 (ft)	13.0	12.1	10.8			18.3	11.1
Difference from Expected (ft)	3.7	3.7	5.9	7.0	7.0	9.9	6.0
Total Scour for β = 2.5 (ft)				21.2	20.3	18.3	11.1

7.5 Example Bridge #4 - Missouri Interior Lowlands Subregion

Location:	Missouri
Physiographic region:	Interior Lowlands - Dissected Till Plains Subregion
Bridge length:	1,715 ft
No. spans:	7
ADT:	94,470 (2006)
Main channel width:	1013 ft
River planform:	sinuous (>1.25)
100-year discharge:	401,000 ft^3/s
100-year depth:	55.1 ft
100-year velocity:	9.8 ft/s (avg. channel)
Hydraulic model:	1-dimensional (HEC-RAS)
Pier type/geometry:	Proposed Bridge: 11 ft dia. drilled shafts w/cap
Bed material:	Poorly graded sand (SP)
Abutment type/location:	Spill-through abutments on floodplain
Purpose of Study:	New bridge

Figure 7.5.1. Example Bridge No. 4 (looking upstream).

This example applies the Level I analysis method to provide probability values and scour factors for a new bridge located in the Interior Lowlands - Dissected Till Plains physiographic subregion of Missouri. The bridge will be a 1,715 foot long cable-stayed bridge with a large pylon in the main channel and approach bents on the overbanks. The abutments are of spill-through configuration set well back from the main channel. No overtopping or pressure flow occurs during the 100-year scour design event. For the 100-year scour design event, a desired total scour reliability index, β, of 3.0 is assumed for this example. This β corresponds to a 99.86% probability of non-exceedance during the design event.

Step 1. Perform hydrologic, hydraulic, and design-equation scour computations using appropriate methods.

a. Hydrologic analysis: The Missouri River and its major tributaries are highly regulated by a large number of water supply, flood control, and navigation projects constructed over the last century and operated by various state and federal agencies. In 2004, the U.S. Army Corps of Engineers completed the *Upper Mississippi River System Flow Frequency Study* (USACE, 2004). That study developed methodologies to allow the USACE to reconstruct a 100-year period of annual peak flows at selected locations in the system as if all the currently-existing projects were in place and operating since the year 1898.

The USACE study used data from numerous gages, reservoir operation rules, reservoir routing, and unsteady channel flow routing procedures to develop an annual peak flow series at the bridge. Appendix E, "Kansas City District Hydrology and Hydraulics" of that study provides the reconstructed flow series for the Missouri River at Kansas City for the 100-year period from 1898 through 1997.

For this special study, site-specific methods were used to determine the flood frequency relationships for floods of various return periods. The 100-year discharges and summary statistics are presented in **Table 7.5.1**.

Table 7.5.1. Hydrologic Data from Site-Specific Analysis of Bridge Site (N = 100 years).

Annual Exceedance		Discharge, cfs		
			95% confidence Limits	
p(X>x)	T (years)	Special Study Estimate	Lower	Upper
0.01	100	401,000	350,000	458,000

b. Design equation scour computations using the HEC-18 method for pier scour, the HEC-18 method for contraction scour, and the NCHRP 24-20 method as presented in HEC-18 for abutment scour were computed for the 100-year design flood in this example. The pier scour calculations are calculated for the large pylon in the main channel. Both left and right abutments are located outside the existing levees; therefore, no abutment scour is anticipated. **Table 7.5.2** presents the results of these computations.

Table 7.5.2. 100-Year Design Scour Depths.

Pier Scour (ft)	Contraction Scour (ft)	Total Scour (ft)	Abutment Total Scour (ft)	
			Left	Right
44.1	2.3	46.4	0.0	0.0

Step 2. Determine the appropriate Bridge Size, Hydrologic Uncertainty, and Pier Size corresponding to standard scour factor table values.

a. Bridge Size: The example bridge is 1,715 ft long. From the guidance presented in Section 6.1.3, this bridge is best represented as a Large Bridge.

b. Hydrologic Uncertainty: To establish the relative hydrologic uncertainty of this bridge, we must estimate the COV associated with the uncertainty of the discharge estimate for the design flood event.

1. The lognormal distribution of hydrologic uncertainty is determined from the 95% confidence limit discharge values as follows. The hydrologic uncertainty of a given discharge estimate (in this case, from a special study which does not correspond to a strict Bulletin 17B analysis) is assumed to be log-normally distributed. Consequently, given the 95% upper and 95% lower confidence limits, (see Section 5.3.2),

$$\mu = \frac{\ln(Q_{upper}) + \ln(Q_{lower})}{2}$$

$$\sigma = \frac{\ln(Q_{upper}) - \ln(Q_{lower})}{2Z_c}$$

$$COV = \frac{\sigma}{\mu}$$

2. For a 95% confidence limit, Z_c = 1.645 (see Appendix C, Glossary). From the hydrologic analysis presented above, the upper and lower 95% confidence limits for the 1.0% exceedance probability event (i.e., the 100-year design flood) are:

Q_{upper} = 458,000 cfs;

Q_{lower} = 350,000; and

Z_c = 1.645

3. Substituting values for Q_{upper}, Q_{lower}, and Z_c into the equations above,

$$\mu = \frac{\ln(458{,}000) + \ln(350{,}000)}{2} = 12.90$$

$$\sigma = \frac{\ln(458{,}000) - \ln(350{,}000)}{2(1.645)} = 0.082$$

$$COV = \frac{0.082}{12.90} = 0.0064$$

Compare the computed COV with **Table 7.5.3** (reproduced from Table 5.3) for the 1.0% exceedance probability event:

Table 7.5.3. Hydrologic Uncertainty as Function of Annual Exceedance Probability (Reproduced from Table 5.3).				
Annual Exceedance		Discharge COV (lognormal)		
p(X>x)	T (years)	**Low**	Medium	High
0.04	25	0.009	0.014	0.018
0.02	50	0.010	0.015	0.019
0.01	**100**	**0.011**	0.016	0.021
0.005	200	0.012	0.017	0.022
0.002	500	0.013	0.018	0.023

This bridge has Low Hydrologic Uncertainty.

c. Pier Size: The 11 ft width of the drilled shaft piles beneath the main channel pylon is compared to the values in **Table 7.5.4** (Reproduced from Table 6.1). This bridge has Large Piers for a bridge of its type.

Table 7.5.4. Representative Bridge Pier Size as a Function of Bridge Type (Reproduced from Table 6.1).			
Bridge Type	Pier Size, ft		
	Small	Medium	**Large**
Small	1	2	3
Medium	1.5	3	4.5
Large	3	6	**9**

Consequently, this bridge is best classified as a Large Bridge, Low Hydrologic Uncertainty, Large Pier Size for the Level I Analysis.

Step 3. Determine Scour Factors.

Once we have classified the bridge, we can enter **Appendix A, Table A.21** to determine appropriate bias and scour factors as a function of the desired β.

Table 7.5.5 corresponds to a Large Bridge, Low Hydrologic Uncertainty, Large Pier Size.

Table 7.5.5. Scour Factors for β = 3.0 (using Monte Carlo results).				
	Pier Scour	Contraction Scour	Abutment Total Scour	
			Left	Right
Bias	0.68	0.93	0.76	0.76
Scour Factor	0.99	2.37	1.96	1.96

Step 4. Apply the Bias and Scour Factors and determine total design scour.

Applying the recommended bias and scour factors for β = 3.0 for all components produces the results shown in **Table 7.5.6**. The individual scour component design scour values are multiplied by the applicable bias to determine the expected scour. Total expected scour is the sum of expected pier and contraction scour. The component scour for β = 3.0 is the design scour times the scour factor. By definition for β = 3.0, the difference between the component scour and the expected scour is 3.0 standard deviations from the expected scour.

The total scour difference from expected is the square root of the sum of the squares of the component scour differences (pier and contraction scour). The total scour for the target β is the expected plus the difference as shown in Table 7.5.6.

Table 7.5.6. 100-Year Scour Results for β = 3.0 (using Monte Carlo results).

	Pier Scour	Contraction Scour	Total Scour	Abutment Total Scour	
				Left	Right
Design Scour (ft)	44.1	2.3	46.4	0.0	0.0
Bias	0.68	0.93			
Expected Scour (ft)	30.0	2.1	32.1		
Scour Factor	0.99	2.37			
Component Scour for β = 3.0 (ft)	43.7	5.5			
Difference from Expected (ft)	13.7	3.4	14.1		
Total Scour for β = 3.0 (ft)			46.2		

7.6 Example Bridge #5 - South Carolina Atlantic Coastal Plain Subregion

Location:	South Carolina
Physiographic region:	Atlantic Coastal Plain – Sandhills subregion
Bridge lengths:	Main Channel 1,950 ft, West Relief 520 ft. East Relief 520 ft.
No. spans:	13, 8, 8
ADT:	7,450 (2009)
Main channel width:	320 ft
River planform:	Meandering, low sinuosity (< 1.06)
100-year discharge:	249,100 ft^3/s total (181,900 ft^3/s Main Channel, 36,000 ft^3/s West Relief, and 31,200 ft^3/s East Relief)
100-year depth:	54 ft maximum
100-year velocity:	3.3 ft/s average in main channel bridge opening
Hydraulic model:	2-Dimensional (FESWMS FST-2DH)
Pier type/geometry:	Existing bridge: Drilled shafts with web walls
	Proposed replacement bridge: 7 ft diameter drilled shafts main channel and 20 inch columns at the two relief bridges.
Bed material:	Sandy clay (CL) and sandy silt (ML)
Abutment type/location:	Spill-through abutments set back on floodplains
Purpose of Study:	Bridge replacement

Figure 7.6.1. Example Bridge No. 5 (main channel looking upstream).

This example applies the Level I analysis method to provide probability values and scour factors for a bridge located in the Atlantic Coastal Plain physiographic region of the Sandhills subregion of South Carolina. The site includes a main channel bridge and two relief bridges. No overtopping or pressure flow occurs in the 100-year scour design event. For the 100-year scour design event, a desired total scour reliability index, β, of 2.0 is assumed for this example. This β corresponds to a 97.72% probability of non-exceedance during the design event. **Figure 7.6.2** illustrates the velocity contours from a 2-dimensional hydraulic model of the 100-year flood at this site, showing the main bridge and the two relief bridges.

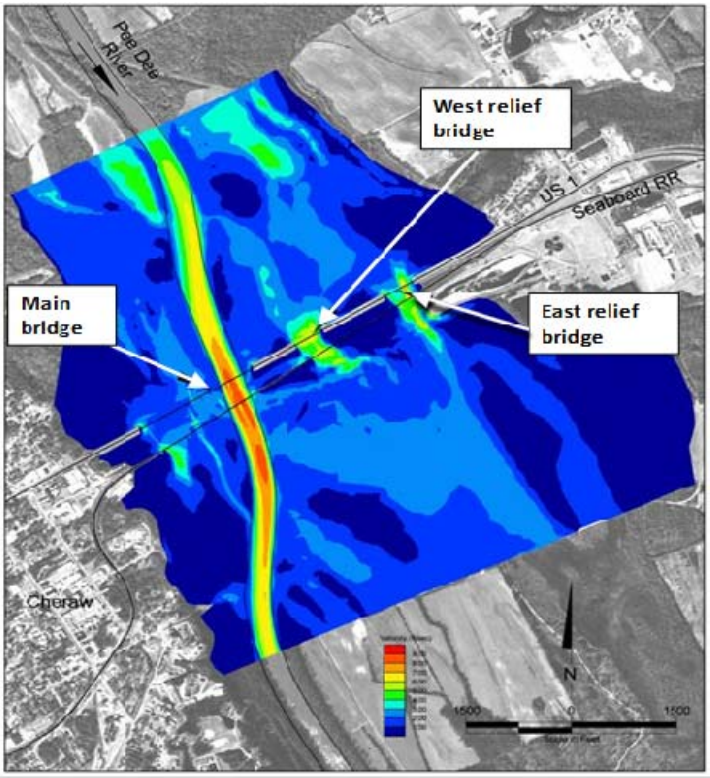

Figure 7.6.2. Two-dimensional model of bridge site (velocity contours shown).

Step 1. Perform hydrologic, hydraulic, and design-equation scour computations using appropriate methods.

a. Hydrologic analysis: Bulletin 17B methods were used to determine the design scour event discharge, the expected value of the natural logarithm transform of discharge, and the standard deviation of the uncertainty about that expected value for a given recurrence interval. The resulting discharges and summary statistics are presented in **Table 7.6.1.**

Table 7.6.1. Hydrologic Data from Bulletin 17B Analysis of Bridge Site (N = 75 years).

Annual Exceedance		Discharge, cfs		
p(X>x)	T (years)	Bulletin 17B Estimate	95% confidence Limits	
			Lower	Upper
0.1	10	139,000	125,000	157,000
0.04	25	178,800	159,000	206,000
0.02	50	212,400	185,000	252,000
0.01	100	249,100	214,000	301,000
0.005	200	287,800	244,000	354,000
0.002	500	351,800	293,000	443,000

b. Design-equation scour computations using the HEC-18 method for pier scour, the HEC-18 method for contraction scour, and the NCHRP 24-20 method as presented in HEC-18 for abutment scour were computed for this example. **Table 7.6.2** presents the results of these computations.

Table 7.6.2. 100-Year Design Scour Depths					
Bridge	Pier Scour, ft	Contraction Scour, ft	Total Scour, ft	Abutment Total Scour, ft	
				Left	Right
Main	9.9	3.4	13.3	4.6	8.8
West Relief	5.4	3.7	9.1	14.5	9.8
East Relief	5.8	4.5	10.3	12.8	15.5

Step 2. Determine the appropriate Bridge Size, Hydrologic Uncertainty, and Pier Size corresponding to standard scour factor table values.

a. Bridge Size: The example bridges are 1,200, 520, and 520 ft long. From the guidance presented in Section 6.1.3, each bridge is best represented as a Large Bridge.

b. Hydrologic Uncertainty: To establish the relative hydrologic uncertainty of this bridge, we must estimate the COV associated with the uncertainty of the discharge estimate for the design scour event.

1. The lognormal distribution of hydrologic uncertainty is determined from the 95% confidence limit discharge values as follows. The hydrologic uncertainty of a given Bulletin 17B discharge estimate is assumed to be log-normally distributed. Consequently, given the 95% upper and 95% lower confidence limits (see Section 5.3.2),

$$\mu = \frac{\ln(Q_{upper}) + \ln(Q_{lower})}{2}$$

$$\sigma = \frac{\ln(Q_{upper}) - \ln(Q_{lower})}{2Z_c}$$

$$COV = \frac{\sigma}{\mu}$$

2. For a 95% confidence limit, Z_c = 1.645 (see Appendix C, Glossary). From the hydrologic analysis presented above, the upper and lower 95% confidence limits for the 1% exceedance probability event are:

Q_{upper} = 301,000 cfs;

Q_{lower} = 214,000 cfs; and

Z_c = 1.645

3. Substituting values for Q_{upper}, Q_{lower}, and Z_c into the equations above,

$$\mu = \frac{\ln(301{,}000) + \ln(214{,}000)}{2} = 12.4443$$

$$\sigma = \frac{\ln(301{,}000) - \ln(214{,}000)}{2(1.645)} = 0.103688$$

$$COV = \frac{0.103688}{12.4443} = 0.0083$$

Compare the computed COV with **Table 7.6.3** (reproduced from Table 5.3) for the 1% exceedance probability event:

Table 7.6.3. Hydrologic Uncertainty as Function of Annual Exceedance Probability (Reproduced from Table 5.3).				
Annual Exceedance		Discharge COV (lognormal)		
p(X>x)	T (years)	**Low**	Medium	High
0.04	25	0.009	0.014	0.018
0.02	50	0.010	0.015	0.019
0.01	**100**	**0.011**	0.016	0.021
0.005	200	0.012	0.017	0.022
0.002	500	0.013	0.018	0.023

This Bridge has Low Hydrologic Uncertainty.

c. Compare the Bridge pier size (7 ft diameter and 20 inch diameter) to **Table 7.6.4** (Reproduced from Table 6.1). The main channel bridge has Medium Piers and the two relief bridges have Small Piers.

Table 7.6.4. Representative Bridge Pier Size as a Function of Bridge Type (Reproduced from Table 6.1).			
Bridge Type	Pier Size, ft		
	Small	**Medium**	Large
Small	1	2	3
Medium	1.5	3	4.5
Large	**3**	**6**	9

Consequently, the main channel bridge is best classified as a Large Bridge, Low Hydrologic Uncertainty, Medium Pier Size, and the two relief bridges are best classified as Large Bridge, Low Hydrologic Uncertainty, Small Pier Size for the Level I Analysis.

Step 3. Determine Scour Factors.

Once we have classified the bridge, we can enter **Appendix A, Tables A.19 and A.20** to determine appropriate bias and scour factors as a function of the desired β.

Table 7.6.5 provides bias and scour factors corresponding to a Large Bridge, Low Hydrologic Uncertainty, Medium Pier Size (for the main bridge) and also for a Large Bridge, Low Hydrologic Uncertainty, Small Pier Size (for the relief bridges).

Table 7.6.5. Scour Factors for β = 2.0 (using Monte Carlo results).					
	HEC-18 Pier Scour		Contraction Scour	Abutment Total Scour	
	LB, LH, MP	LB, LH, SP		Left	Right
Bias	0.68	0.68	0.93	0.76	0.76
Scour Factor	0.90	0.89	1.77	1.43	1.43

Step 4. Apply the Bias and Scour Factors and determine total design scour.

Applying the recommended bias and scour factors for β = 2.0 for all components produces the results shown in **Tables 7.6.6 (a), (b) and (c)** for the specific bridges. The individual scour component design scour values are multiplied by the applicable bias to determine the expected scour. Total expected scour is the sum of expected pier and contraction scour. The component scour for β = 2.0 is the design scour times the scour factor. By definition for β = 2.0, the difference between the component scour and the expected scour is 2.0 standard deviations from the expected scour.

The total scour difference from expected is the square root of the sum of the squares of the component scour differences (pier and contraction scour). The total scour for the target β is the expected scour plus the difference as shown in Table 7.6.6.

Table 7.6.6 (a). 100-Year Scour Results for Main Channel Bridge and β = 2.0.

	HEC-18 Pier Scour	Contraction Scour	Total Scour	Abutment Total Scour	
				Left	Right
Design Scour (ft)	9.9	3.4	13.3	4.6	8.8
Bias	0.68	0.93		0.76	0.76
Expected Scour (ft)	6.7	3.2	9.9	3.5	6.7
Scour Factor for target β	0.90	1.77		1.43	1.43
Component Scour for target β (ft)	8.9	6.0		6.6	12.6
Difference from Expected (ft)	2.2	2.8	3.6	3.1	5.9
Total Scour for target β (ft)			13.5	6.6	12.6

Table 7.6.6 (b). 100-Year Scour Results for West Relief Bridge and β = 2.0.

	HEC-18 Pier Scour	Contraction Scour	Total Scour	Abutment Total Scour	
				Left	Right
Design Scour (ft)	5.4	3.7	9.1	14.5	9.8
Bias	0.68	0.93		0.76	0.76
Expected Scour (ft)	3.7	3.4	7.1	11.0	7.5
Scour Factor for target β	0.89	1.77		1.43	1.43
Component Scour for target β (ft)	4.8	6.6		20.7	14.0
Difference from Expected (ft)	1.1	3.2	3.4	9.7	6.5
Total Scour for target β (ft)			10.5	20.7	14.0

Table 7.6.6 (c). 100-Year Scour Results for East Relief Bridge and β = 2.0.

	HEC-18 Pier Scour	Contraction Scour	Total Scour	Abutment Total Scour	
				Left	Right
Design Scour (ft)	5.8	4.5	10.3	12.8	15.5
Bias	0.68	0.93		0.76	0.76
Expected Scour (ft)	3.9	4.2	8.1	9.7	11.8
Scour Factor for target β	0.89	1.77		1.43	1.43
Component Scour for target β (ft)	5.2	8.0		18.3	22.2
Difference from Expected (ft)	1.2	3.8	4.0	8.6	10.4
Total Scour for target β (ft)			12.1	18.3	22.2

(page intentionally left blank)

CHAPTER 8

8. CALIBRATION OF SCOUR FACTORS FOR A TARGET RELIABILITY

8.1 Approach

8.1.1 Background

The calculations performed for the Probability-Based scour estimates described in Chapter 6 are for a single discharge rate which corresponds to a design return period (e.g., the discharge rate having a return period of 100 years). Thus, the probability-based scour estimate obtained in Chapter 6 is a conditional probability of exceedance which is conditioned on the occurrence of the design discharge rate and can be expressed symbolically as follows for a 100-year discharge rate:

$$P_{ex} / 100 - \text{yr rate} \tag{8.1}$$

During its service life, T_n, a bridge might be exposed to a large range of possible discharge rates. Some of these discharge rates may exceed the one used for the design return period. Many others will be smaller but they are still capable of causing scour at the bridge within the service life. Each of these possible discharge rates will have a probability of occurrence, P_i. Therefore, the unconditional probability of exceedance should account for the probabilities of exceedance for all the possible discharge rates along with their probability of occurrence.

8.1.2 Reliability Analysis

Several methods can be used to calculate the unconditional probability of exceeding the design scour depth within a service life, T_n. One method consists of performing the conditional probability-based scour estimates described in Chapter 6 for a whole set of return periods and associating each conditional probability of exceedance with the probability of occurrence, P_i - that is the probability that the maximum discharge rate within the service life will equal that of the selected return period, which is labeled as P_i. The final unconditional probability of exceedance will be the sum of the products of the probability of exceedance for each discharge rate times the probability of the occurrence of the discharge rate for which the probability of exceedance is calculated. This can be expressed as:

$$P_{ex}(T_n) = \sum_{\text{all return years}} \left(P_{ex} / i^{th} - \text{yr rate}\right) \times P_i \tag{8.2}$$

Where $P_{ex}(T_n)$ is the probability of exceeding the design scour within a service life period T_n, $\left(P_{ex} / i^{th} - \text{yr rate}\right)$ is the probability of exceeding the design scour given that the hydraulic event corresponds to that of a return period equal to i-years, and P_i is the probability that the maximum discharge rate within the service life of the bridge has a probability of occurrence equal to that of the discharge rate having the return period i-years corresponding to the i^{th} hydraulic event. Although there are an infinite number of hydraulic events, these can be combined into discrete segments where each segment has a probability of occurrence P_i. Note that the sum of all the hydraulic event probabilities, P_i, must add up to 1.0:

$$\sum_{\text{all return years}} P_i = 1.0 \tag{8.3}$$

It is common in the probabilistic evaluation of bridge safety to use the reliability index, β, as a measure of safety. The reliability index, β, is inversely related to the probability of scour depth exceedance through the normal cumulative distribution function, Φ:

$$P_{ex}(T_n) = \Phi(-\beta) \quad (8.4)$$

8.1.3 Reliability Calculation Process

The process for calculating the reliability for a given design scour depth can be summarized as follows:

1. Find the design scour for a bridge using current methods.
2. Divide the set of possible discharge rates that could occur within the service life, T_n, of the bridge into a limited number of representative discrete sets of discharge rates. These discharge rates can be identified based on the return period they are associated with.
3. Find the probability of occurrence, P_i, that the maximum discharge expected to occur within the service life will be equal to each of the discharge rates, i, selected in Step 2.
4. Use the approach described in Chapter 6 to find P_{ex} / i^{th} - yr which gives the conditional probability of exceeding the design scour for each of the discharge rates, i, selected in Step 2.
5. Multiply P_{ex} / i^{th} - yr calculated in Step 4 by the probability P_i of Step 3
6. Repeat Steps 3, 4, and 5 to cover the entire set of representative discharge rates.
7. Add all the results from Step 6 to give P_{ex} (T_n) which is the overall probability of exceedance in the service life T_n
8. Find the reliability index, β using the normal cumulative distribution function, ϕ

8.1.4 Calibration of Design Equations

A properly calibrated design scour methodology should provide a reliability index, β, that meets a target value as closely as possible for the range of applicable bridge geometries and channel conditions. If the current design methodology does not meet the target reliability level, adjustments to the scour design methodology must be made. One possible approach is to apply a scour factor on the results of the design scour calculations to ensure that the reliability levels obtained after adjustment meet the target reliability levels.

8.1.5 Simplified Example

In this section, an example set of calculations is performed and the probabilities are obtained as shown in **Table 8.1**. It is assumed that the current design method will stipulate a design scour depth of 15 feet. The table illustrates the application of Equation (8.2) when the probability of exceedance for a service period T_n = 1-year is desired. The calculations assume that the entire range of hydraulic events can be divided into seven discrete segments represented by the seven return periods T_r = 5-, 20-, 50-, 75-, 100-, 200-, and 500-year. The probability of occurrence corresponding to each segment, Pi, is calculated to cover all the probabilities between the different return periods. The probability of exceedance within a one-year period is calculated to be $P_{ex}(T_n = 1-\text{yr})$ = 1.681e-3. Note that the return period T_r serves to specify the hydraulic event to be used. This is different than the service life T_n which defines the period for which the bridge will be in service.

Table 8.1. Example Calculations for Determining Probability of Design Scour Exceedance Within a One-Year Period.				
Return Period, T_r	$P=1/T_r$	Probability of Occurrence P_i	Conditional Probability of Exceeding Design Scour	Product of P_i Times Conditional Probability
5 years	0.2	0.875	6.82e-4	5.97e-4
20 years	0.05	0.09	5.06e-3	4.55e-4
50 years	0.02	0.0183	1.22e-2	2.24e-4
75 years	0.0133	0.005	1.65e-2	0.83e-4
100 years	0.01	0.00567	2.02e-2	1.14e-4
200 years	0.005	0.0035	3.14e-2	1.10e-4
500 years	0.002	0.0025	3.92e-2	0.98e-4
Sum		$\sum P_i = 1.0$		$P_{ex}(T_n = 1-\text{yr})$ =1.681e-3

Using a similar approach for the case when T_n = 75-year, the probability of exceedance within a 75-year design life is $P_{ex}(T_n = 75-\text{yr})$ = 12.1%. The reliability index for the 75-year design life is found to be β = 1.18. To obtain a reliability index β = 1.5, the design scour depth will have to be increased by a scour factor SC = 1.10 or in other words, the design scour must be increased from 15 to 16.5 feet.

The integration approach for calculating the reliability index as described in this section, based on Equations (8.2) through (8.4), provides a simplified approach for calibrating scour factors for a target reliability consistent with LRFD procedures used by structural and geotechnical engineers as discussed in Section 2.6. The example in Table 8.1 uses seven return periods. See Section 8.2 for a discussion of the number of return periods that can be used for the integration to obtain an optimum balance between accuracy and calculation efficiency.

8.2 Validation of the Simplified Procedure

8.2.1 Overview of the Procedure

This section describes an algorithm for the calculation of the reliability of design scour depth exceedance using a limited number of return periods. The validity of the proposed approach is verified by comparing the results from a full-fledged Monte Carlo simulation to those of the evaluation at discrete return periods. The comparison shows that it is sufficient to perform Monte Carlo simulations for five return periods or fewer to obtain good estimates of the mean and standard deviation of the actual scour depth. The statistics of the actual scour depth can subsequently be used to estimate the probability of exceeding the design scour depth. A list of suggested return periods to check for various service lives is provided in **Table 8.2**.

Table 8.2. Proposed Return Periods for Use in Estimating the Scour Reliability for Different Service Lives.					
Service Period, T_n	Return Period 1	Return Period 2	Return Period 3	Return Period 4	Return Period 5
5 years	3-year	5-year	8-year	15-year	50-year
20 years	10-year	20-year	30-year	60-year	200-year
75 years	50-year	100-year	500-year		

As mentioned earlier, there are several methods that can be used to find the reliability of a bridge that may be subject to scour. The most basic approach consists of performing a Monte Carlo Simulation (MCS) to find the probability that the maximum scour depth around a bridge foundation will exceed the scour design depth at any time within the service life of the bridge. The full-fledged Monte Carlo Simulation requires a heavy computational effort that cannot be accommodated within the time, budget, and computer tools available for this project (see Chapter 9, Identification of Research Needs). As outlined in Section 8.1, a simplified approach was developed whereby the Monte Carlo Simulation (MCS) is executed at only a limited number of discrete return periods and the results integrated to obtain estimates of the reliability of the bridge over the entire service period.

The objective of the reliability analysis is to find the reliability index, β, which as defined in Equation (8.4) is related to the probability of design scour depth exceedance within a service period, $P_{ex}(T_n)$. This can also be expressed as:

$$P_{ex}(T_n) = Pr\left(y_{max\ expected} \geq y_{sc\ design}\right) = \Phi(-\beta) \tag{8.5}$$

Where $y_{max\ expected}$ is the expected maximum scour depth during the service life of the bridge, $y_{sc\ design}$ is the design scour depth, Φ is the Cumulative Distribution Function (CDF) for the normal distribution. Note also that $y_{sc\ design}$ is deterministic, computed from the HEC-18 equation (or any appropriate design equation) and $y_{max\ expected}$ is determined from the Monte Carlo simulation, as described below, based on uncertainty and the expected discharges occurring over the service life of the bridge.

To verify that it is possible to obtain accurate results for the reliability index without performing a full-fledged Monte Carlo simulation, a comparison between the results of the two methods is performed in this section for scour around piers. **For simplicity, the analysis is executed using the HEC-18 equation for a simple problem involving local pier scour around a circular column set in a rectangular channel.** This simplified problem is used because scour can be evaluated using closed form expressions which do not require calls to advanced programs such as HEC-RAS (see Chapter 5). The observation from this comparison should be applicable for the more advanced scour analysis steps.

Based on comparisons between the scour depth predicted by the HEC-18 equation and laboratory and field measurements, the maximum expected scour depth can be obtained from an equation of the form:

$$y_{max\ expected} = 2\lambda_{sc} y_0 K_1 K_2 K_3 \left(\frac{a}{y_0}\right)^{0.65} F_R^{0.43} \tag{8.6}$$

Where λ_{sc}, is the modeling bias which accounts for the conservativeness of the HEC-18 equation and the variability between the measured and predicted values, y_0 is the depth of flow just upstream of the bridge pier excluding local scour. K_1, K_2, and K_3, are coefficients that account for the nose shape of the pier, the angle between the direction of the flow and the direction of the pier, and the streambed conditions. The pier diameter is (a) and (F_R) is the Froude number of the approach flow.

Because of the large uncertainties associated with estimating the maximum expected scour depth, the parameters that are used in Eq. (8.6) should be treated as random variables. As an example, **Table 8.3** gives a list of the random variables and their statistics that have been proposed in previous research. **These values are used in this example simply to illustrate the proposed methodology. The actual implementation in Section 8.3 uses the full HEC-RAS/MCS results provided in earlier chapters of this report.**

Table 8.3. Assumed Input Data for Hypothetical Example Illustrating the Reliability Analysis for Scour.				
Variable	Mean Value	COV	Distribution Type	Reference
Q- discharge rate	Depends on channel data	Depends on channel data	Lognormal	Based on data from USGS web site or other information
λ_Q – modeling variable for Q	1.0	5%	Normal	Based on data from USGS web site
λ_{sc}- modeling variable for scour	1.0/1.42	48%	$1/\lambda_{SC}$ is Lognormal	
n- Manning roughness	0.025	28%	Lognormal	USACE (1986)
K_3- bed condition factor	1.1	5%	Normal	Johnson (1995)

The process of finding the probability of design scour depth exceedance and the reliability index, β, involves the following steps.

1. Find the design scour for the bridge, $y_{sc\ design}$, from the as-built conditions or by using typical design equations such as the HEC-18 equations for the 100-year discharge rate.
2. Use the discharge rate data to find the statistics of the maximum expected discharge rate within the remaining service life of the bridge. For example, knowing the probability distribution for the yearly discharge rate, $F_Q(x)$, the maximum flood discharge in a service period, T_n, has a cumulative probability distribution, $F_{QTn}(x)$, related to the probability distribution of the 1-year maximum discharge by:

   $$F_{Q\,Tn}(x) = F_Q(x)^{Tn} \qquad (8.7)$$

3. Apply $F_{QTn}(x)$ and the data in Table 8.3 into a Monte Carlo simulation to find the statistics of $y_{max\ expected}$ for different possible values of the scour within a service period T_n.
4. Determine the percentage of cases for which $y_{max\ expected}$ exceeds $y_{sc\ design}$ and find the reliability index from Eq. (8.5).

Because of the numerical difficulties associated with covering the whole range of possible values of the Cumulative Distribution Function, $F_{QTn}(x)$, a limited number of discharge rates were used to estimate the probability of scour depth exceedance. Through different comparisons between the full-fledged MCS and simulations that used a limited number of discharge rates, it was determined that good accuracy can be achieved when the simulations are executed for five different return periods or fewer. The higher the service life, T_n, the lower is the number of return periods needed for Q. This is because as T_n increases, QT_n evaluated from Equation (8.7) will have a lower Coefficient of Variation (COV). **Figure 8.1** provides a flow chart for evaluating the reliability index β using the simplified procedure.

8.2.2 Case Studies for Validation

To verify the validity of the simplified approach, several comparisons between the results obtained from the approach described in Figure 8.1 and a full-fledged MCS were performed. The analysis assumes that a bridge is constructed over a 220-foot wide rectangular river channel. To obtain realistic results for the effect of scour, different possible discharge rate data from a selected set of rivers are used and design scour depths are calculated for each of these river discharge rates. The simplified approach reproduces the full-fledged MCS results quite well for the five rivers used to assess the procedure.

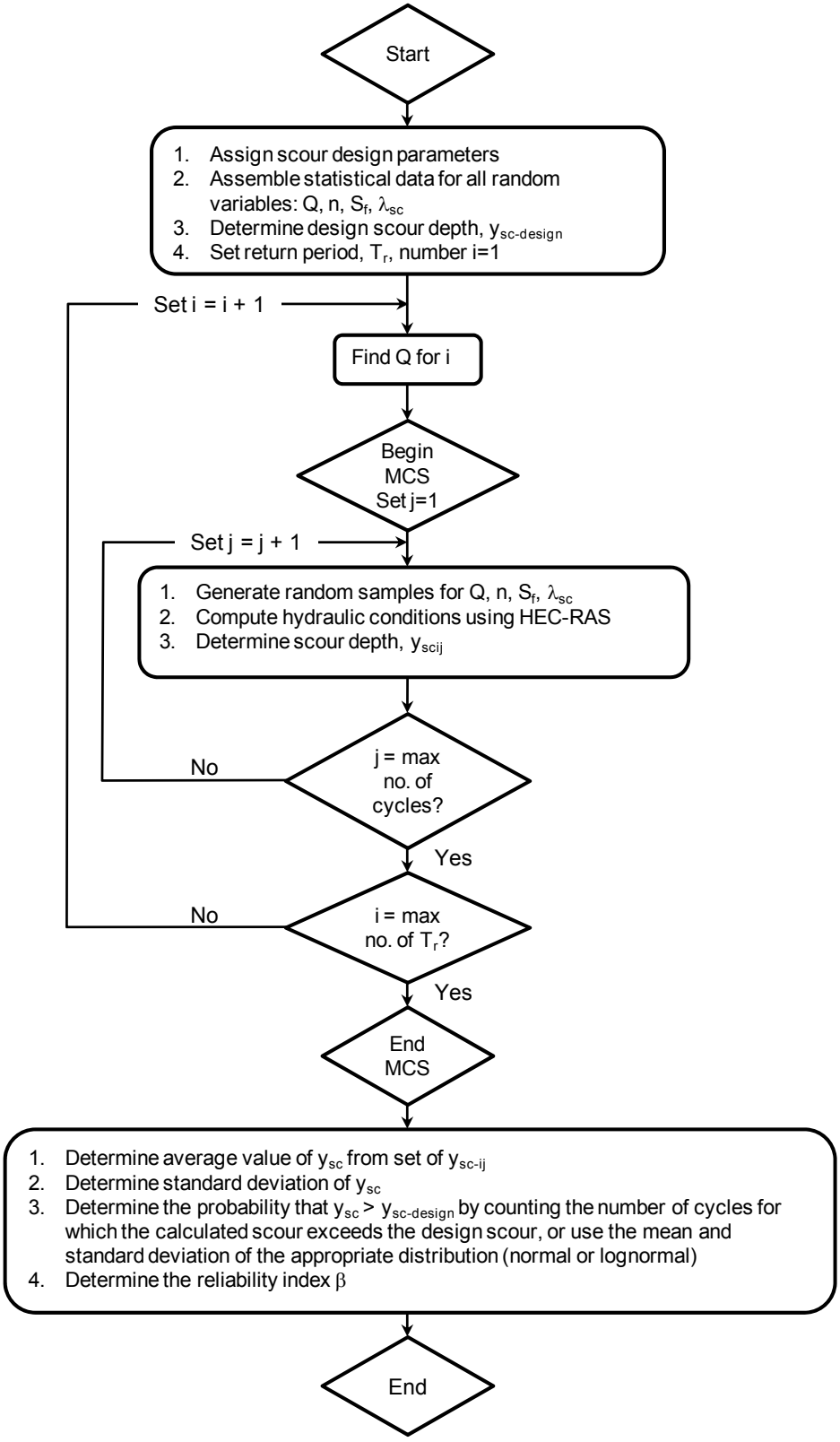

Figure 8.1. Flow chart of simplified method for determining the reliability index for scour depth exceedance.

The rivers chosen for this analysis consist of the following: (1) Schoharie Creek in upstate New York, (2) Mohawk River in Upstate New York, (3) Cuyahoga River in Northern Ohio, (4) Rocky River in Ohio, and (5) Sandusky River in Ohio. Data on the peak annual discharge rates for each of the five rivers were obtained from the USGS web site. Lognormal probability plots and Kolmogorov-Smirnov (K-S) goodness of fit tests showed that the peak annual discharge rate, Q, for all five rivers can be reasonably well modeled by lognormal probability distributions. The mean of the natural log Q and its standard deviation, $S_{\log Q}$, were calculated using a maximum likelihood estimator. These data are provided in columns (1) and (2) of **Table 8.4**.

Column (3) gives the discharge rate for the 100-year return period. Assuming a slope S_0 = 0.2% and a Manning roughness coefficient n = 0.025, the design scour depth for a 100-year return period, $y_{sc\ design}$, is calculated from the HEC-18 equations for the 220-foot rectangular channel and a circular bridge pier with a diameter, a = 6 ft. The design scour depth for the 1-column bent bridge for each river data is obtained as shown in column (4) of Table 8.4. The expected maximum Q given in column (5) of Table 8.4 represents the average value of the maximum discharge rate expected during a 75-year service period. The COV of Q_{75} listed in Column (6) represents the coefficient of variation of the maximum discharge rate expected in a 75-year service life. These are obtained using Eq. (8.7) from the mean and standard deviation of the logarithm of the yearly Q shown in columns (1) and (2) of Table 8.4.

Table 8.4. Annual Discharge Rate Statistics and Corresponding Design Scour and Maximum 75-Year Statistics for Hypothetical Example for Illustration.

River	(1) Ln Q	(2) $S_{\log Q}$	(3) Q 100-Year (ft^3/sec)	(4) $Y_{sc\ design}$, Design Scour Depth (ft)	(5) Expected 75-Year Q, Q_{75} (ft^3/sec)	(6) COV of Q_{75}
Schoharie	9.925	0.578	78,146	17.34	85,000	29%
Mohawk	9.832	0.243	32,747	13.99	34,000	12%
Sandusky	9.631	0.372	36,103	14.33	38,000	18%
Cuyahoga	9.108	0.328	19,299	12.26	20,000	16%
Rocky River	9.012	0.378	19,693	12.32	21,000	19%

The reliability index, β, is calculated using the algorithm described in Figure 8.1 and compared to the value obtained from a full MCS for different river discharge rates. The simplified approach uses a discrete number of return periods and the corresponding values of Q rather than integrating over all possible values of Q. The preset return periods are established based on dividing the distribution function of the maximum discharge rate QT_n into segments of equal probabilities. For example, if 5 return periods are to be used, then each return period is selected to represent a domain of hydraulic events having a probability of occurrence equal to 20% within the service period. Dividing the probability distribution into segments of equal probabilities is the basis of the well-established Latin Hypercube Simulation (LHS) method and is found to be valid for this problem. Thus, the simplified approach may be considered a hybrid of the LHS in combination with conditional MCS for a set of specific return periods. The conditional MCS follows the method outlined in Chapter 6.

Several different cases are analyzed to verify that the simplified approach will yield results which are reasonably similar to those from a full-fledged MCS. In the first case, summarized in **Table 8.5**, the reliability index for each of the five rivers listed in Table 8.4 is determined (assuming six different service lives). The input data are listed in Tables 8.3 and 8.4. The results show that the reliability indexes from the two approaches are on the average within 1.5% with a range varying between 7.33% and -2.82%. These differences are quite acceptable for this level of reliability index values. For the design of new bridges, a service life T_n= 75 years is generally used. However, the calculations presented in Table 8.5 and plotted in **Figure 8.2** are performed for several different service lives to demonstrate how the reliability index approaches asymptotic values as the service period increases from 5 years to 200 years. This trend is illustrated in Figure 8.2.

Table 8.5. Comparison of the Results from Proposed Approach and MCS.

Service Life, T_n	Return Periods, T_r Used to Simulate the Reliability Index for Each Service Life	River No.	Reliability Index β Proposed Approach	Reliability Index β MCS
5 years	3-, 5-, 8-, 15-, and 50-year	1	0.870	0.871
		2	0.677	0.671
		3	0.760	0.743
		4	0.728	0.720
		5	0.754	0.750
20 years	10-, 20-, 30-, 60-, and 200-year	1	0.664	0.655
		2	0.591	0.583
		3	0.612	0.590
		4	0.610	0.599
		5	0.620	0.614
75 years	45-, 110-, and 400-year	1	0.502	0.496
		2	0.516	0.531
		3	0.507	0.506
		4	0.508	0.507
		5	0.512	0.503
100 years	75- and 350-year	1	0.473	0.472
		2	0.506	0.499
		3	0.488	0.487
		4	0.491	0.482
		5	0.485	0.471
150 years	110- and 500-year	1	0.439	0.409
		2	0.493	0.485
		3	0.466	0.467
		4	0.462	0.455
		5	0.459	0.459
200 years	150- and 700-year	1	0.403	0.380
		2	0.475	0.475
		3	0.440	0.429
		4	0.454	0.453
		5	0.439	0.439

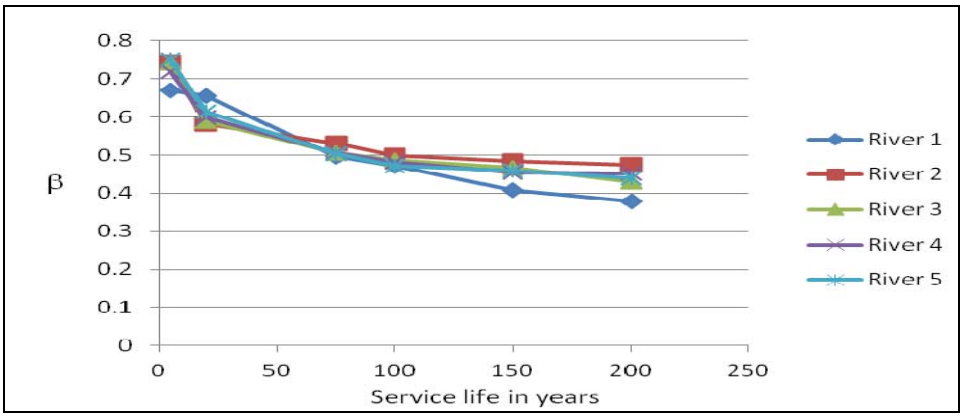

Figure 8.2. Reliability Index, β, versus service life in years, T.

A sensitivity analysis was also performed to investigate the effect of the modeling variable on the reliability index β. Specifically, the COV of the modeling variable λ_{sc} covers a range of 10% to 50%. This analysis was performed for only a service life of 75 years. The results are summarized in **Table 8.6** and plotted in **Figure 8.3**. The results illustrate the importance of the modeling variable on the reliability results and also demonstrate that the simplified approach yields similar results as those of the MCS with a maximum difference of 5% in the reliability index.

Table 8.6. Change of Reliability Index with COV of Modeling Variable.

COV of λ_{sc}	River No.	Reliability Index β Proposed Approach	Reliability Index β MCS
10%	1	2.49	2.37
	2	2.69	2.68
	3	2.64	2.55
	4	2.66	2.60
	5	2.63	2.56
15%	1	1.88	1.81
	2	1.97	1.98
	3	1.95	1.90
	4	1.96	1.93
	5	1.94	1.91
20%	1	1.46	1.43
	2	1.51	1.53
	3	1.50	1.47
	4	1.51	1.49
	5	1.50	1.48
30%	1	0.955	0.942
	2	0.982	1.000
	3	0.973	0.962
	4	0.975	0.968
	5	0.975	0.963
40%	1	0.663	0.655
	2	0.680	0.697
	3	0.671	0.668
	4	0.673	0.670
	5	0.676	0.666
50%	1	0.468	0.462
	2	0.482	0.474
	3	0.472	0.474
	4	0.474	0.473
	5	0.478	0.469

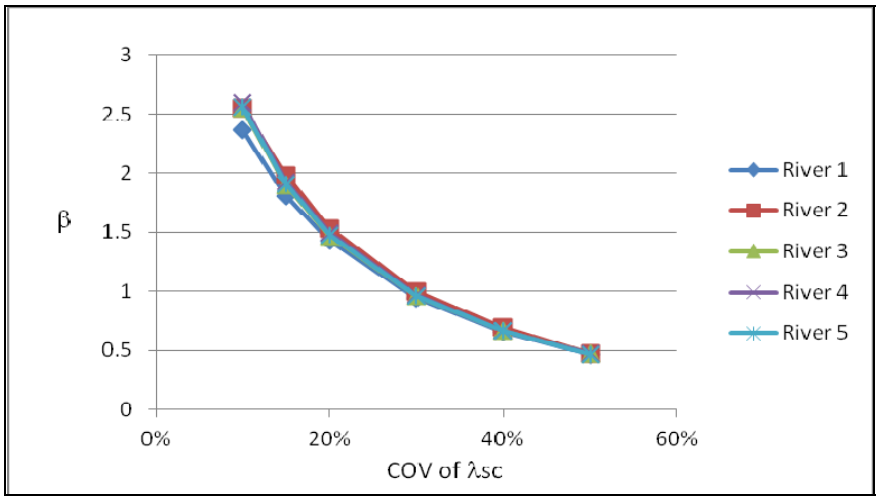

Figure 8.3. Change of Reliability Index, β, with COV of modeling variable, λ_{sc}.

In the procedure described above, a number of simplifying assumptions were made for the purpose of illustrating the process by which the reliability is calculated. In particular, the values of the hydraulic variables used as input to the scour calculations, including slope, Manning n, and channel shape and dimensions, were assumed. In the actual procedure, these would not be assumed, but rather would be provided as output from the HEC-RAS runs associated with hypothetical or case-study streams (see Chapter 5). **Thus, it is important to realize that the results presented in Tables 8.4, 8.5, and 8.6 while realistic, are for illustration purposes only. That is, these are highly simplified examples in that the channel dimensions were simple trapezoids, did not include floodplain flow, and used only Manning's equation rather than HEC-RAS.**

In this section, the proposed procedure was illustrated for pier scour only and did not include contraction or abutment scour. These other scour components are included in the overall study as explained in Sections 8.3 and 8.4. The analysis was conducted in the same manner for all scour components.

8.3 Implementation of Reliability Analysis for Sacramento River Bridge Data

The analysis procedure presented in Section 8.2 was demonstrated using simplified examples. The procedure is now implemented for a reliability analysis for the Sacramento River bridge analyzed in Chapter 5 for the following cases:

1. Pier scour when the foundation is designed using the HEC-18 method,
2. Pier scour when the foundation is designed using the FDOT method,
3. Contraction scour using the HEC-18 equation
4. Combined pier and contraction scour when the foundation is designed using the HEC-18 method for the pier scour component
5. Combined pier and contraction scour when the foundation is designed using the FDOT method for the pier scour component
6. Abutment scour using the NCHRP 24-20 approach as recommended in HEC-18 (5th Edition)

The reliability analysis for the 75-year service life was executed in Section 8.2 using the following three return periods T_r = 45-, 110-, and 400-year. However, during the implementation process it was decided to use the slightly modified set of typical return periods T_r= 50-, 100-, and 500-year because hydraulic engineers use these return periods on a regular basis and their values are more readily available. A sensitivity analysis on a random set of cases has shown that using the modified set of return periods does not lead to noticeable differences in the results of the simplified examples presented in Section 8.2.

8.3.1 Pier Scour Designed Using the HEC-18 Method

As a first step, the simulations are executed to find the pier scour that would be obtained if no modeling bias is assumed (i.e., assuming that the HEC-18 equation gives on the average good estimates of the actual pier scour depth). The results assuming that the bridge is subjected to the hydraulic event corresponding to each of the three return periods T_r = 50-, T_r=100-, and T_r=500-year are presented in **Figure 8.4**.

Given that the HEC-18 design scour for this bridge is 13.7 feet (see Section 5.4.1), the results show that if the 50-year event were to occur, the scour around the bridge pier would have a 27.64% probability of exceeding the 13.7-ft design scour, corresponding to a reliability index β=0.59. If the 100-year event were to occur, the scour around the bridge pier would have a 58.84% probability of exceeding the 13.7-ft design scour (β=-0.22); and if the 500-year event were to occur, the scour around the bridge pier would have a 93.73% probability of exceeding the 13.7-ft design scour (β=-1.5). Using the combined results from the 50-, 100-, and 500-year return period, the bridge would have a probability of 60.07% of exceeding the design scour within a 75-year service period for a reliability index β=-0.25. Such reliability levels are certainly very low compared to acceptable levels.

Fortunately, as demonstrated in Chapter 4, the HEC-18 pier scour equation is <u>not</u> a predictive model of scour depth but instead contains on average some level of conservatism with an average Bias=0.68. In other words, based on laboratory and field data, the actual scour for a given hydraulic discharge rate is 0.68 times the scour depth predicted by the HEC-18 equation. On the other hand, Chapter 4 has shown a large level of variability in the bias around the 0.68 value with a spread around the mean represented by a standard deviation equal to 0.109 (COV=16%). This spread around the bias will offset some of conservatism of the HEC-18 equations by a certain level that can be evaluated using the simulation described above while accounting for the modeling bias and its COV.

The results of the simulation accounting for the bias=0.68 and the COV=16% are presented in **Figure 8.5**. The results in Figure 8.5 demonstrate the dominance of the bias on the results which tends to pull the histograms for the three return periods closer together. The combination of the three histograms is also illustrated in Figure 8.5 which also shows that the maximum scour depth expected within the 75-year service life approaches that of a normal distribution. The effect of the bias leads to a significant increase in the reliability of the bridge design such that the probability that the actual scour will exceed the HEC-18 design scour depth of 13.7 feet is 0.38% with a reliability index β=2.67. This value is more in line with the reliability index that has been deemed acceptable for some bridges under extreme events such as earthquakes or for the rating of existing bridges under vehicular loading as discussed in Section 2.6.3.

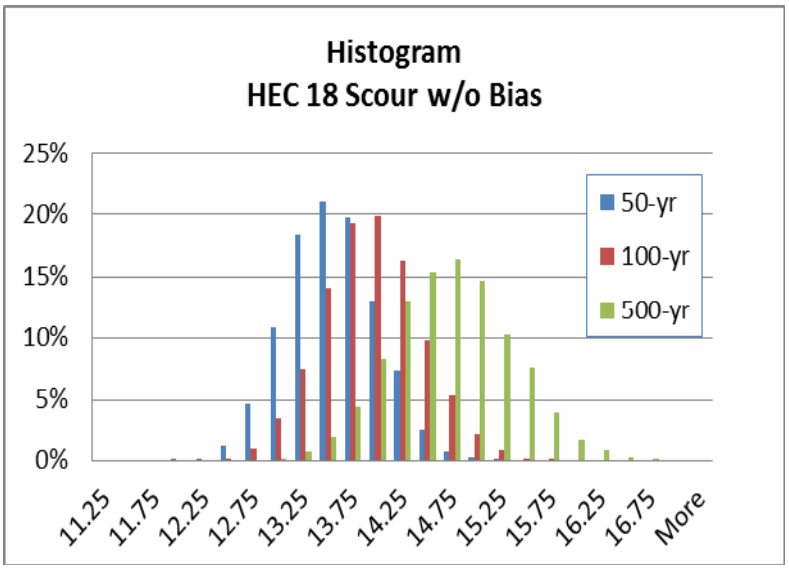

Figure 8.4. Pier scour depth histogram without bias calculated based on HEC-18.

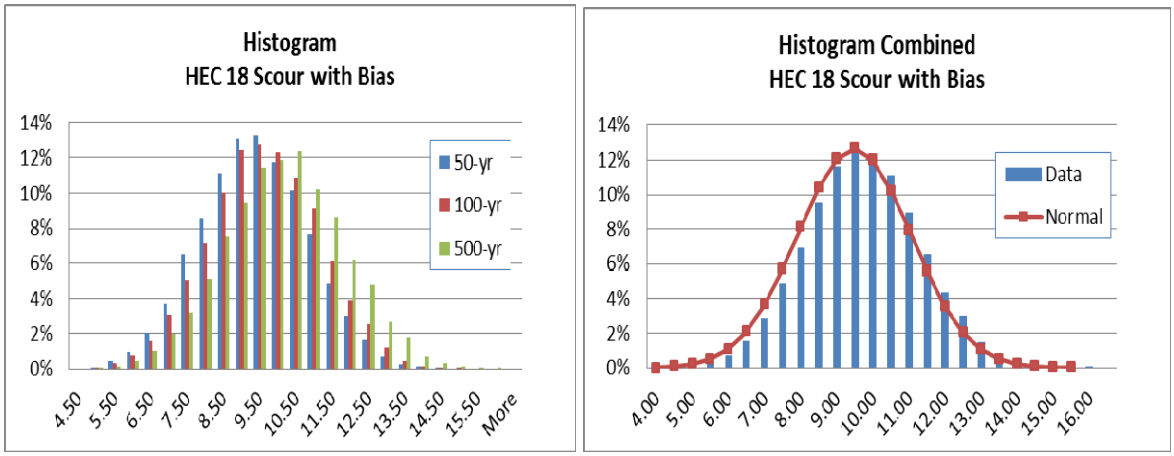

Figure 8.5. Pier scour depth histogram with bias calculated based on HEC-18.

8.3.2 Pier Scour Designed Using FDOT Method

The approach was executed to find the pier scour that would be obtained if the bridge foundation is designed for the scour depth determined using the FDOT pier scour equation. The FDOT method leads to a design scour depth equal to 11.2 feet (see Section 5.4.1). For the FDOT equation, the average Bias=0.75 and the COV=18%. The results of the simulation are presented in **Figure 8.6**. The results in Figure 8.6 show that the maximum scour depth expected within the 75-year service life approaches that of a normal distribution. The probability that the actual scour will exceed the FDOT design scour depth of 11.2 feet is 3.80% with a reliability index β=1.77. This value is somewhat on the low side compared to typical reliability indexes that have been deemed acceptable for bridges under extreme events.

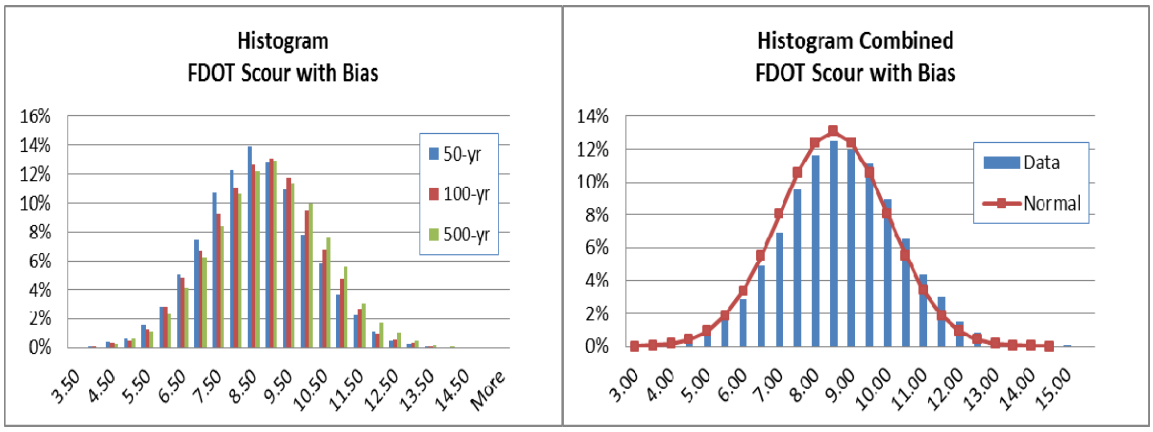

Figure 8.6. Pier scour depth histogram with bias calculated based on the FDOT method.

8.3.3 Contraction Scour Designed Using the HEC-18 Method

The approach was executed to find the contraction scour that would be obtained if the bridge foundation is designed for the scour depth determined using the HEC-18 method. The HEC-18 method leads to a contraction design scour depth equal to 5.3 feet (see Section 5.4.2). For the contraction scour, the average Bias=0.916 and the COV=20.9%. This high bias indicates that the HEC-18 contraction scour equations were developed to be predictive equations rather than more conservative design equations. This high bias in combination with the high COV will lead to low reliability levels. The results of the simulation are presented in **Figure 8.7** which shows that the maximum scour depth expected within the 75-year service life approaches that of a lognormal distribution. The probability that the actual scour will exceed the design contraction scour depth of 5.3 feet is 47.1% with a reliability index β=0.07. This value is very low compared to typical reliability indexes that have been deemed acceptable for bridges under extreme events.

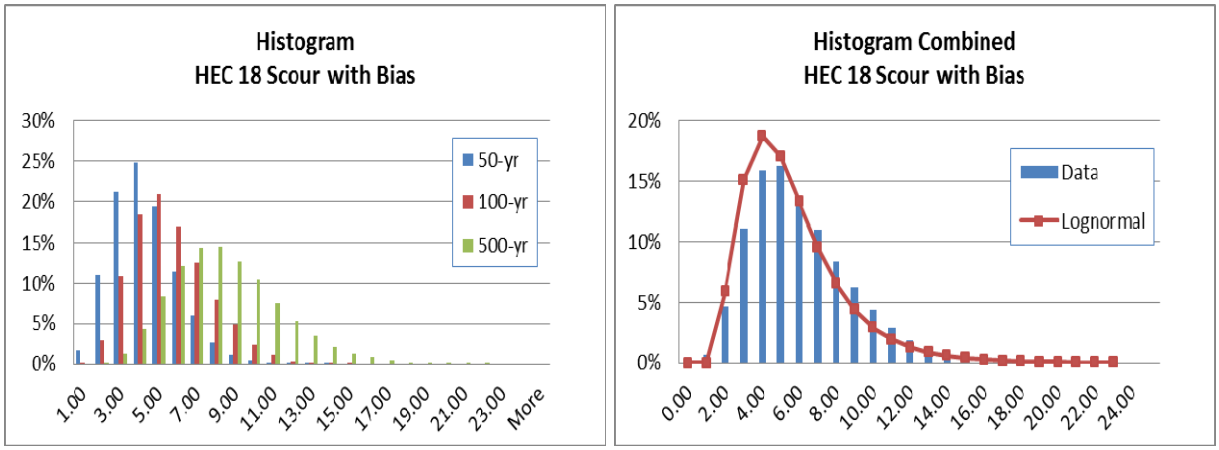

Figure 8.7. Contraction scour depth histogram with bias calculated based on HEC-18.

8.3.4 Total Pier and Contraction Scour Using HEC-18

The simulations were performed to find the combined (total) pier and contraction scour that would be obtained if the bridge foundation is designed for the scour depth determined using the HEC-18 methods for pier and contraction scour. The HEC-18 methods lead to a design total scour depth equal to 19 feet. The results of the simulation are presented in **Figure 8.8**

which shows that the maximum scour depth expected within the 75-year service life approaches that of a lognormal distribution but not too different from a normal distribution. The probability that the actual scour will exceed the total design scour depth of 19 feet is 13.6% with a reliability index β=1.10. This value is low compared to typical reliability indexes that have been deemed acceptable for bridges under extreme events.

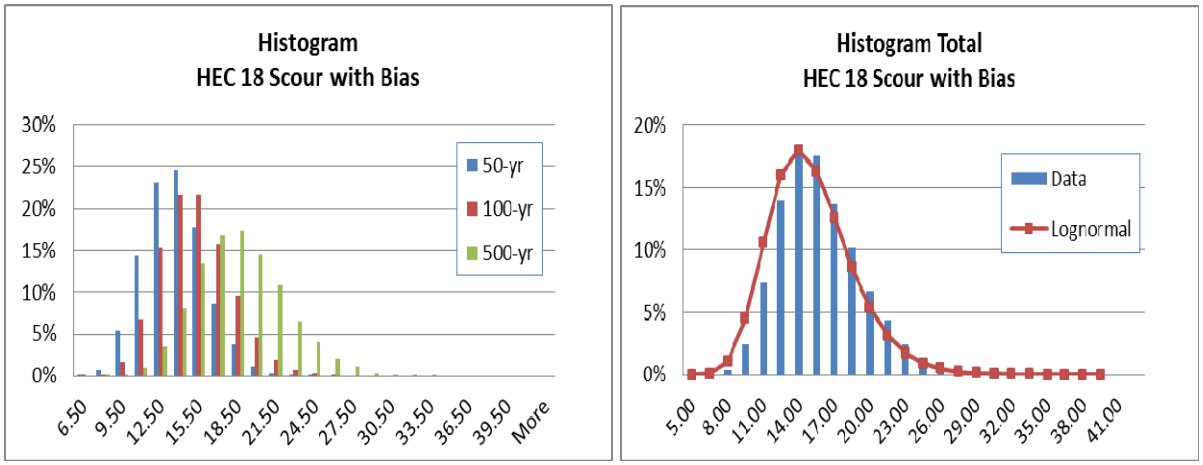

Figure 8.8. Total pier and contraction scour depth histogram calculated using HEC-18.

8.3.5 Total Pier and Contraction Scour Using the FDOT Method

The simulations were performed to find the combined (total) pier and contraction scour that would be obtained if the bridge foundation is designed for the scour depth determined using the FDOT method for pier scour. Since the FDOT method does not provide an equation for the contraction scour, the analysis looks at the design pier scour using the FDOT equation while the contraction scour is obtained from the HEC-18 method. This leads to a design total scour depth equal to 16.5 feet. The results of the simulation presented in **Figure 8.9** show that the maximum scour depth expected within the 75-year service life approaches that of a lognormal distribution. The probability that the actual scour will exceed the total design scour depth of 16.5 feet is 21.75% with a reliability index β=0.78. This value is very low compared to typical reliability indexes that have been deemed acceptable for bridges under extreme events.

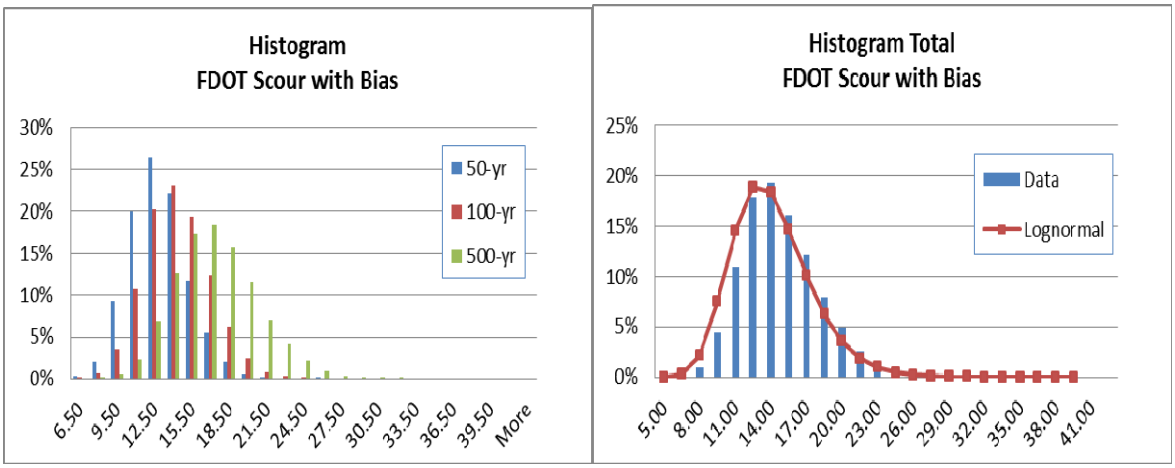

Figure 8.9. Total pier and contraction scour depth histogram calculated using FDOT.

8.3.6 Total Scour at an Abutment Using the NCHRP 24-20 Method

The approach was executed to find the abutment scour that would be obtained if the bridge foundation is designed for the scour depth determined using the NCHRP 24-20 method as described and recommended in the latest edition of HEC-18. **Note that this method includes both the effect of the abutment scour and the contraction scour at the end of the abutment, and therefore is an estimate of total scour at that location**. The method leads to a design abutment scour depth equal to 11 feet (see Section 5.4.3). For the abutment scour, the average Bias=0.74 and the COV=23%. The results of the simulation are presented in **Figure 8.10** which shows that the maximum scour depth expected within the 75-year service life approaches that of a lognormal distribution. The probability that the actual scour will exceed the abutment design scour depth of 11 feet is 30.58% with a reliability index β=0.51. This value is very low compared to typical reliability indexes that have been deemed acceptable for bridges under extreme events.

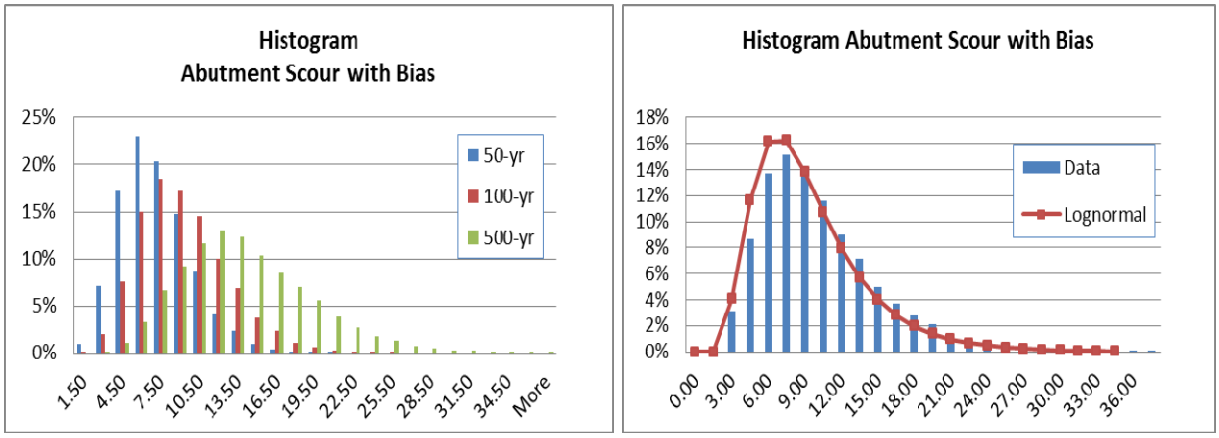

Figure 8.10. Total abutment scour depth histogram using NCHRP 24-20 method. (HEC-18, 5th Ed.)

8.3.7 Summary

The results of the reliability analysis for a 75-year service life of the Sacramento River bridge are summarized in **Table 8.7**. The results demonstrate how the reliability index values vary considerably for the different types of scour and the different equations that can be used to determine the design scour depth. The results demonstrate the dominant effect of the bias and its COV on the reliability index which varies from an acceptable value of 2.67 for the case when the HEC-18 pier scour equation is used to design the foundation to the very low value of 0.07 obtained when the HEC-18 equations are used for designing the foundation for contraction scour. The results are based on the bias and COV obtained by comparing the results from different equations to laboratory data. Results from the field may produce slightly different biases and COV. However, field data are generally considered less reliable due to the various difficulties discussed in Chapter 4.

Table 8.7. Summary of Reliability Analysis Results for 75-Year Service Life Based on Sacramento River Bridge Data.

Scour Type	Design Scour (ft)	Bias	COV	Probability of Exceedance	Reliability Index, β
Pier scour (HEC-18)	13.7	0.68	16%	0.38%	2.67
Pier scour (FDOT)	11.2	0.75	18%	3.80%	1.77
Contraction scour	5.3	0.92	21%	47.1%	0.07
Total HEC-18 pier and contraction scour	19	As shown above		13.6%	1.10
Total FDOT pier and contraction scour	16.5	As shown above		21.8%	0.78
Abutment scour	11.0	0.74	23%	30.6%	0.51

8.4 Calibration of Scour Factors

8.4.1 Calibration Methodology

The reliability analysis performed in Section 8.3 and summarized in Table 8.7 reveals large variations in the reliability levels obtained for the different types of scour. In most cases the reliability index obtained for the bridge is low compared to the level obtained for bridges designed for other extreme events. This low reliability is primarily due to the bias and COV of the existing contraction and abutment scour equations. Other causes for the variability include the hydrologic uncertainty of the discharge rates expected over the service life of the bridge, variability in soil and sediment properties, and the geometric and roughness conditions of the channel and overbank areas.

One approach that can be used to increase the reliability of existing scour equations is to apply a safety factor on the design scour calculated from current procedures so that bridges designed using the safety factor produce reliability levels that meet an acceptable target reliability index β. The target reliability index must be set by the code writing authorities and bridge owners to provide a balance between safety and cost. As indicated earlier, most current bridge LRFD specifications have used a target reliability level that varies between β = 2.5 and 4.0 depending on the types of loads, the consequences of exceeding the target reliability levels, the construction costs, and past histories of successful designs (see Section 2.6.3). In this section, a set of scour factors are calibrated to reach different reliability levels for each scour type. The final decision on which target reliability should be used must be determined by the appropriate code writing authorities. A trial and error process is used to find the scour factors presented in **Table 8.8** required to reach different target reliability levels. The analyses performed in Table 8.8 are based on the scour depths generated directly from the Monte Carlo simulations for the Sacramento River bridge referenced in Section 8.3. Section 8.4.2 compares the results of the calibration based on the generated scour depths to the results obtained using fitted probability distributions.

Table 8.8. Scour Factors to Meet Different Target Reliability Levels for 75-Year Service Life Based on Sacramento River Bridge Data.

Target Reliability Index β	Scour Factor					
	Pier Scour Using HEC-18	Pier Scour Using FDOT	Contraction Scour Using HEC-18	Total Scour Using HEC-18	Total Scour Using FDOT	Abutment Scour
1.50	N/A	N/A	1.95	1.10	1.18	1.60
2.00	N/A	1.03	2.35	1.23	1.33	1.95
2.50	N/A	1.10	2.77	1.37	1.47	2.31
3.00	1.04	1.15	3.20	1.50	1.60	2.75

The calibration of the scour factors performed in this section assumes a 75-year service life and is based on the data for the Sacramento River bridge assuming that these data are representative of typical bridge conditions. Before actual implementation into a design code, similar analyses should be performed for numerous and varied bridges to confirm the consistency of the results.

For the case analyzed, the scour factors shown in Table 8.8 indicate that no additional safety factors would be required for the HEC-18 pier scour equation if the target reliability index is set at 2.50 or lower. A scour factor equal to 1.04 would be needed to reach a target reliability index equal to 3.0. Similarly, only modest scour factors need to be applied to the FDOT pier scour equation to achieve reasonable target reliabilities. Table 8.8 also shows that the current contraction scour equations would need significant additional safety factors to reach acceptable reliability levels. A modest reliability index target of 1.50 would require an additional safety factor equal to 1.95. Only slightly lower safety factors would be needed to improve the reliability of bridges designed using the NCHRP 24-20 abutment scour equation.

The safety factors obtained in Table 8.8 are quite modest for the HEC-18 and FDOT pier scour equations. However, larger factors are needed to offset the large variability observed between the scour depths measured in the laboratory compared to those predicted from the current contraction and abutment scour equations. Additional analyses are recommended to confirm the consistency of the results for different bridge and channel configurations and hydraulic conditions.

8.4.2 Analysis Using Fitted Distributions

The calculations of the probability of exceedance performed in Section 8.4.1 were based on the results of the Monte Carlo simulations by counting the number of generated cases that exceed the design scour. This was possible because of the large number of simulation cycles executed. When it is not possible to generate sufficient numbers of simulation runs because of the heavy computational requirements that the HEC-RAS analysis may need for complicated channel and bridge configurations and high levels of reliability, an alternative approach should be used.

The proposed alternative approach consists of using the results of a limited number of Monte Carlo Simulation runs to obtain the mean and standard deviation of the expected scour and then use those statistics to estimate the probability of exceedance from probability distribution functions. A statistical analysis can be used to select an appropriate probability distribution function. In general, however, the most common probability distribution function used in engineering applications is the normal probability function which assumes a symmetric bell shape distribution around the mean value. When the distribution is skewed to the right as observed in some of the cases studied in Section 8.3 and depicted in Figures 8.5 to 8.10, the distribution may approach a lognormal distribution, which implies that the logarithm of the random variable is normal. In this section, the calculations of the probability of exceedance are evaluated using the mean and standard deviations generated from the Monte Carlo simulations rather than from a direct count of the number of cases that exceed the design scour. Four different cases are considered:

- Simulated scour depths for each return period are assumed to follow normal distributions
- Simulated scour depths for each return period are assumed to follow lognormal distributions
- Combined simulated scour depths from all three return periods (50-, 100-, and 500-year) are assumed to follow normal distributions
- Combined simulated scour depths from all three return periods (50-, 100-, and 500-year) are assumed to follow lognormal distributions

The results for all four cases are compared to those obtained from the direct count to study the probability of exceeding the design scour obtained from current procedures, to find the design scour required to meet different reliability targets, and to determine the scour factor necessary to meet the target reliability levels.

Probability Distributions Independently Fitted to Results of Each Return Period

The results obtained by fitting the generated scour depths from each return period into normal and lognormal distribution functions are compared to those obtained by directly counting the number of generated scour depths that exceed the design scour in **Table 8.9**.

Table 8.9. Probability of Exceeding the 100-Year Event Design Scour Based on Fitted Distributions and a 75-Year Service Life.

			Statistics for Each Return Period		From Direct Count		From Normal Distributions			From Lognormal Distributions		
Scour Type (1)	Design Scour (2)	Return Period (3)	Mean (4)	Standard Deviation (5)	Prob. of Exceed. (6)	Reliability Index, β (7)	Cumulat. Prob. (8)	Prob. of Exceed. (9)	Reliability Index, β (10)	Cumulat. Prob. (11)	Prob. of Exceed. (12)	Reliability Index, β (13)
Pier Scour HEC 18	13.7-ft	50-yr	9.14	1.48	0.38%	2.67	99.90%	0.44%	2.62	99.53%	1.04%	2.31
		100-yr	9.39	1.51			99.78%			99.26%		
		500-yr	9.92	1.62			99.01%			98.07%		
Pier Scour FDOT	11.2-ft	50-yr	8.34	1.48	3.80%	1.77	97.34%	3.78%	1.78	96.11%	4.99%	1.65
		100-yr	8.50	1.51			96.35%			95.13%		
		500-yr	8.66	1.55			94.95%			93.80%		
Contraction Scour	5.3-ft	50-yr	3.83	1.67	47.10%	0.07	81.14%	49.07%	0.02	83.87%	46.19%	0.10
		100-yr	5.09	2.00			54.14%			61.61%		
		500-yr	7.92	2.80			17.50%			15.94%		
Combined HEC18 Pier and Contraction Scour	19.1-ft	50-yr	12.97	2.36	13.60%	1.10	99.48%	13.99%	1.08	98.64%	13.57%	1.10
		100-yr	14.48	2.68			95.43%			94.22%		
		500-yr	17.83	3.48			63.13%			66.44%		
Combined FDOT Pier and Contraction Scour	16.5-ft	50-yr	12.17	2.29	21.80%	0.78	97.08%	22.22%	0.76	95.79%	21.39%	0.79
		100-yr	13.59	2.56			87.16%			87.08%		
		500-yr	16.57	3.27			49.09%			52.98%		
Total Abutment Scour (NCHRP 24-20)	11.0-ft	50-yr	6.45	2.73	30.60%	0.51	95.22%	31.76%	0.47	93.55%	29.57%	0.54
		100-yr	8.51	3.40			76.82%			80.50%		
		500-yr	13.25	5.02			32.68%			37.23%		

In Table 8.9, the generated scour depths for each return period are used to find the mean and standard deviation as shown in columns (4) and (5). Then, assuming a normal distribution, the cumulative probability for all the scour depths that fall below the design scour is obtained for each return period independently as shown in column (8). The probability of exceeding the design scour shown in column (2) is obtained for each return period and the average of the three values is given in column (9) and the corresponding reliability index, β, is given as shown in column (10). This process is repeated for all scour types analyzed as listed in column (1) which consist of pier scour designed using the HEC-18 method, pier scour designed using the FDOT method, contraction scour, combined HEC-18 pier and contraction scour, combined FDOT pier scour plus contraction scour, and abutment scour.

The same analysis process is repeated assuming that the scour depths follow lognormal distributions. Column (11) gives the cumulative distribution for all scour depths that fall below the design scour for each return period independently. Column (12) gives the average probability of exceeding the design scour and column (13) gives the corresponding reliability index for each scour type.

The results obtained from the normal distributions in column (10) and those from the lognormal distributions of column (13) are compared to those obtained from the direct count of the scour depths generated by the Monte Carlo simulation of column (7) showing good agreement for both the normal and lognormal distributions. The similarities are mostly due to the low levels of reliability observed for contraction and abutment scour, in which cases the type of the probability distribution is not very important as long as good estimates of the means and standard deviations are obtained.

Probability Distributions Fitted to the Combined Results from Three Return Periods

The results obtained by fitting the combined scour depths generated for all three return periods into normal and lognormal distribution functions are compared to those obtained by directly counting the number of generated scour depths that exceed the design scours in **Table 8.10**. In Table 8.10, the generated scour depths for each return period are used to find the mean and standard deviation as shown in columns (3) and (4). Then, assuming a normal distribution, the probability of exceeding the design scour shown in column (2) is obtained for the combined return periods as given in column (7) and the corresponding reliability index, β, is given as shown in column (8). This process is repeated for all scour types analyzed as listed in column (1) which consist of pier scour designed using the HEC-18 method, pier scour designed using the FDOT method, contraction scour, combined HEC-18 pier and contraction scour, combined FDOT pier scour plus contraction scour, and abutment scour. The same analysis process is repeated assuming that the scour depths follow lognormal distributions. Column (9) gives the probability of exceeding the design scour and column (10) gives the corresponding reliability index for each scour type.

The results obtained from the normal distributions in column (8) and those from the lognormal distributions of column (10) are compared to those obtained from the direct count of the scour depths generated by the Monte Carlo simulation of column (6) showing good agreement for both the normal and lognormal distributions. These results are also similar to those of Table 8.9. Here again, the similarities are mostly due to the low levels of reliability observed for contraction and abutment scour, in which cases, the type of the probability distribution is not very important as long as good estimates of the means and standard deviations are obtained.

Table 8.10. Probability of Exceeding the 100-Year Design Scour Based on Fitted Distributions of the Combined Return Periods and a 75-Year Service Life.									
		Statistics for Combined Return Periods		From Direct Count		From Normal Distributions		From Lognormal Distributions	
Scour Type (1)	Design Scour (2)	Mean (3)	Standard Deviation (4)	Prob. of Exceed. (5)	Reliability Index, β (6)	Prob. of Exceed. (7)	Reliability Index, β (8)	Prob. of Exceed. (9)	Reliability Index, β (10)
Pier Scour HEC-18	13.7-ft	9.48	1.57	0.38%	2.67	0.36%	2.69	1.02%	2.32
Pier Scour FDOT	11.2-ft	8.50	1.52	3.80%	1.77	3.78%	1.78	5.01%	1.64
Contraction Scour	5.3-ft	5.61	2.79	47.10%	0.07	54.42%	-0.11	45.46%	0.11
Combined HEC-18 Pier and Contraction Scour	19.1-ft	15.09	3.52	13.60%	1.10	13.33%	1.11	13.22%	1.12
Combined FDOT Pier and Contraction Scour	16.5-ft	14.11	3.30	21.80%	0.78	23.45%	0.72	21.38%	0.79
Total Abutment Scour (NCHRP 24-20)	11.0-ft	9.40	4.78	30.60%	0.51	36.89%	0.33	28.52%	0.57

Scour Factors and Design Scour Required to Meet Different Target Reliabilities

The fitted normal and lognormal distributions can also be used to calibrate the required scour factors and the required scour depths needed to meet a given target reliability index and compared to those calibrated from the direct count of the data generated by the Monte Carlo simulations. The results are presented in **Table 8.11**. The comparison shows that the normal fit gives a good match to the calibration for the pier scour factors. The lognormal model gives a better match for the contraction and abutment scour equations. These comparisons are consistent with the histograms plotted in Figures 8.5 through 8.10. The histograms in Figures 8.5 and 8.6 for pier scour follow a bell shaped curve and show good fits with the normal distribution functions. Figures 8.7, 8.8., 8.9 and 8.10 for contraction, combined contraction and pier, and for abutment scour show a skew to the right which is consistent with the lognormal model. The independent fit to each return period gives a slightly better match with the direct count than the case where the fit is executed on the combined set of data because the independent fit per return period is consistent with the simulation method of generating the simulated scour data for the three specific return periods of 50-, 100-, and 500-year. The fit of the entire data set is meant to smooth out the limitation of the rough discretization process which used only three return periods to represent the entire set of possible discharge rates expected to occur within a bridge's design life.

Table 8.11. Calibration to Meet Different Target Reliability Levels for 75-Year Service Life Based Sacramento Bridge Data.						
Scour non-exceedance (ft) based on Monte Carlo results						
Target Reliability Index β	Pier Scour Using HEC-18	Pier Scour Using FDOT	Contraction Scour Using HEC-18	Total Scour Using HEC-18	Total Scour Using FDOT	Total Abutment Scour
β=1.50	11.89	10.79	10.32	20.98	19.55	17.54
β=2.00	12.67	11.62	12.43	23.46	22.04	21.37
β=2.50	13.46	12.41	14.65	26.13	24.36	25.32
β=3.00	14.32	12.97	16.93	28.61	26.51	30.14
Scour factor based on Monte Carlo results						
β=1.50	0.86	0.96	1.95	1.10	1.18	1.60
β=2.00	0.92	1.03	2.35	1.23	1.33	1.95
β=2.50	0.98	1.10	2.77	1.37	1.47	2.31
β=3.00	1.04	1.15	3.20	1.50	1.60	2.75
	Scour non-exceedance (ft) based on normal fit to each return period independently					
Target Reliability Index β	Pier Scour Using HEC-18	Pier Scour Using FDOT	Contraction Scour Using HEC-18	Total Scour Using HEC-18	Total Scour Using FDOT	Total Abutment Scour
β=1.50	11.85	10.79	10.31	20.86	19.47	17.55
β=2.00	12.67	11.54	12.08	23.05	21.48	20.74
β=2.50	13.49	12.31	13.75	25.08	23.40	23.71
β=3.00	14.33	13.08	15.32	27.06	25.25	26.51
	Scour factor based on normal fit to each return period independently					
β=1.50	0.86	0.96	1.95	1.09	1.18	1.60
β=2.00	0.92	1.02	2.28	1.21	1.30	1.89
β=2.50	0.98	1.09	2.60	1.32	1.41	2.16
β=3.00	1.04	1.16	2.90	1.42	1.52	2.42
	Scour non-exceedance (ft) based on lognormal fit to each return period independently					
Target Reliability Index β	Pier Scour Using HEC-18	Pier Scour Using FDOT	Contraction Scour Using HEC-18	Total Scour Using HEC-18	Total Scour Using FDOT	Total Abutment Scour
β=1.50	11.99	10.92	10.28	20.88	19.52	17.38
β=2.00	13.02	11.93	12.64	23.47	21.90	21.67
β=2.50	14.14	13.04	15.37	26.22	24.50	26.73
β=3.00	15.36	14.24	18.60	29.18	27.31	32.78
Scour factor based on lognormal fit to each return period independently						
β=1.50	0.87	0.97	1.94	1.09	1.18	1.59
β=2.00	0.95	1.06	2.39	1.23	1.32	1.98
β=2.50	1.03	1.16	2.91	1.37	1.48	2.44
β=3.00	1.12	1.26	3.52	1.53	1.65	2.99
Scour non-exceedance (ft) based on normal fit to combined generated data from all three return periods						
Target Reliability Index β	Pier Scour Using HEC-18	Pier Scour Using FDOT	Contraction Scour Using HEC-18	Total Scour Using HEC-18	Total Scour Using FDOT	Total Abutment Scour
β=1.50	11.84	10.79	9.81	20.37	19.06	16.56
β=2.00	12.62	11.54	11.18	22.14	20.71	18.98
β=2.50	13.40	12.30	12.59	23.88	22.36	21.34
β=3.00	14.19	13.06	13.99	25.65	24.01	23.76
Scour factor based on normal fit to combined generated data from all three return periods						
β=1.50	0.86	0.96	1.85	1.07	1.15	1.51
β=2.00	0.92	1.02	2.11	1.16	1.25	1.73
β=2.50	0.97	1.09	2.38	1.25	1.35	1.95
β=3.00	1.03	1.16	2.64	1.35	1.45	2.17
Scour non-exceedance (ft) based on lognormal fit to combined generated data from all three return periods						
Target Reliability Index β	Pier Scour Using HEC-18	Pier Scour Using FDOT	Contraction Scour Using HEC-18	Total Scour Using HEC-18	Total Scour Using FDOT	Total Abutment Scour
β=1.50	11.97	10.92	10.18	20.77	19.40	17.22
β=2.00	12.99	11.93	12.85	23.28	21.78	21.89
β=2.50	14.11	13.04	16.27	26.13	24.47	27.83
β=3.00	15.32	14.24	20.56	29.32	27.47	35.31
Scour factor based on lognormal fit to combined generated data from all three return periods						
β=1.50	0.87	0.97	1.92	1.09	1.17	1.57
β=2.00	0.94	1.06	2.43	1.22	1.31	2.00
β=2.50	1.02	1.16	3.08	1.37	1.48	2.54
β=3.00	1.11	1.26	3.89	1.54	1.66	3.22

(page intentionally left blank)

CHAPTER 9

9. IDENTIFICATION OF RESEARCH NEEDS

This chapter identifies and discusses research needs that involve topics beyond the scope of this study that would extend the results and usefulness of this research. The research needs are presented in order of priority considering limiting factors encountered during this research and the opportunities for the most significant contribution to the state of practice in hydraulic engineering. The highest priority research need - conducting a properly designed contraction scour laboratory study is supported by a fully developed Research Problem Statement in Appendix B.

9.1 Conduct a Properly-Designed Contraction Scour Study

This research has demonstrated quite clearly that, in terms of the reliability index β, the HEC-18 contraction scour procedure exhibits the most uncertainty. This necessitates multiplying the design contraction scour depth by a large scour factor in order to provide an acceptable level of reliability.

However, this does not mean that the fault lies with the HEC-18 clear-water and live-bed contraction scour equations themselves, which are based on sediment transport theory. We ran into three major issues during the analysis of the contraction scour data sets:

1. None of the published data sets from contraction scour studies actually measured the depth of flow in the contracted section before scour occurs (y_0). This value had to be calculated using the method described in Chapter 4, and this calculation was confounded by the choking phenomenon. Therefore, in our analysis, this flow depth is an estimate, not a measurement.

2. All but one of the published studies assumed that the depth of flow in the contracted section prior to scour (y_0) was the same as the depth of flow in the approach section (y_1), thereby ignoring the importance of hydraulic drawdown in the contraction. In some cases the researchers actually measured the depth of scour by taking bed elevation measurements, which was a reliable measurement. In other cases the researchers simply assumed that the scour depth was the difference between y_2 (the depth of flow in the contracted section after scour has reached equilibrium) and y_1. These data sets had to be thrown out entirely.

3. All the studies were done under clear-water conditions. We had no data at all with which to assess the HEC-18 live-bed contraction scour equation.

A properly-designed contraction scour study should be performed to provide accurate and reliable data on scour in long contractions, using a range of contraction ratios, flow rates, and grain sizes. To the extent possible, the choking phenomenon should be avoided or minimized. Such a study would provide much more reliable data to accurately assess the bias and COV of the HEC-18 contraction scour equations, and would either: (1) lead to better values of the reliability index β, or (2) result in a better equation for contraction scour design, not best-fit prediction. **A fully developed Research Problem Statement suitable for submittal to AASHTO is provided in Appendix B.**

9.2 Expand Level I Scour Factors

The scour factors developed for use with the Level I approach in Section 6.2 were derived from comprehensive HEC-RAS/Monte Carlo analysis of three representative bridges (small, medium, and large), each with a representative range of pier sizes and hydrologic uncertainties associated with a 100-year design event. This resulted in a 3 x 3 x 3 matrix for a combination of 27 bridge categories as described in Section 6.1.3.

To support implementation of FHWA's risk-based scour design philosophy for new bridges, as promulgated in HEC-18 (5th Edition), similar scour factor tables should be developed for a range of return period flood events. Chapter 2 of HEC-18 (Table 2.1) recommends a scour design approach based on the application of three flood frequencies for scour design: a hydraulic design flood, a scour design flood, and a scour design check flood. To enable a Level I risk-based design for scour for all new bridges, additional scour factor tables should be developed for the Q_{25}, Q_{50}, Q_{200}, and Q_{500} return period floods.

The procedure outlined in Chapters 5 and 6 of this document using the HEC-RAS/Monte Carlo software, the rasTool©, and the off-line scour calculation spread sheets would need to be applied to develop four additional sets of scour factor tables similar to the Q_{100} scour factors in Appendix A. In the process, a wider range of hydrologic uncertainty, bridge size, and pier size could be investigated. These additional scour factor tables would also support development of procedures to calculate bridge-life reliability from Level I calculations as described in Section 9.3, below. In addition, before the results of this research can be implemented into a design code, similar analyses should be performed for a wider range of bridge and channel conditions across various physiographic regions of the United States.

9.3 Develop Procedures to Calculate Bridge-Life Reliability From Level I Calculations

The Monte Carlo simulations used to develop the Level I scour factors also generate Bias and COV values for the various scour components over a range of bridge sizes, pier sizes and hydrologic conditions. The results are the basis for calculating a conditional probability of scour exceedance for the occurrence of a specific event. Chapter 8 shows that normal and log-normal distributions can be fitted to the scour component data to estimate bridge-life reliability for a specific bridge, but does not provide a generally applicable method similar to the Level I approach to estimate bridge-life reliability. This recommended research would simplify the Chapter 8 approach by applying Level I methods to the required return period results and determine the service-life reliability without Monte Carlo analysis. The approach would be generalized for total abutment scour and any relative combination of pier and contraction scour amounts for total scour reliability. It would provide guidance for pre-defined bridge service lives and for user-specified service lives. The research would include application of normal and log-normal distributions to provide the results that are most compatible with the Monte Carlo analysis. This process would be only a moderate level of additional effort compared to the overall effort of performing a Level II analysis.

9.4 Develop User-Friendly HEC-RAS/Monte Carlo Software

The HEC-RAS/Monte Carlo simulation software ("rasTool©") was developed specifically for the purposes of this research project. It has proven to be an extremely useful and powerful computational engine and without it, this research could not have achieved the results it has.

However, in its current configuration, rasTool© would be extremely difficult for anyone other than its developers to use.

Not only would user-friendly rasTool© software permit expanding the Level I scour factors as suggested in the Section 9.2, it would also be extremely useful to any practitioner desiring to perform a site-specific Level II analysis as described in Chapter 6. The scour calculations could also be embedded within rasTool© and produce tables similar to those in Appendix A. Additional effort should be put towards developing rasTool© into a user-friendly Windows-based software package for general use.

9.5 Extremal Analysis as a Substitute for Monte Carlo Simulation

It is possible that the analysis of design scour exceedance could be performed using extremal analysis techniques as a substitute for full Monte Carlo simulation. In theory, the concept is sound but needs to be validated against MCS in a proof-of-concept set of trials. From the practitioner's perspective, if this concept is proven to be a reliable substitute, the ease and efficiency of performing probability-based scour estimates would be significantly enhanced.

Therefore, the introduction of these research results into mainstream practice would occur much more rapidly, and could be applied by a much wider community of bridge and hydraulic design engineers, agency personnel, and code writing authorities. This is an avenue that should be explored in order to enhance the results and usefulness of this research project.

9.6 Probability Analysis for Scour from Debris Loading on a Bridge Pier

NCHRP Report 653, "Effects of Debris on Bridge Pier Scour" provides an approach to computing the increased scour potential at piers with debris (Lagasse et al. 2010). That study also provided an extensive data base from laboratory studies of debris clusters with a range of shapes, geometry, and locations in the water column. The scour equations developed from that study are deterministic, and essentially provide a transform from a pier with debris to an equivalent wider pier. With all the information available from that study, it would be possible to conduct a detailed probability analysis of the calculation procedures for debris loading on a bridge pier.

The laboratory testing program for NCHRP 24-26 was designed and conducted to develop information on a variety of factors related to debris accumulations at piers that was shown to have a significant effect on the depth of scour at the pier. The factors examined included the following:

- Shape: Rectangular or triangular
- Size: Width, length, and thickness
- Location: Surface (floating), mid-depth, or bed (partially buried)
- Roughness: Smooth or roughened
- Porosity: Impermeable or 25% porosity
- Approach velocity: V/V_c ratios of 0.70 and 1.0

The variation of debris parameters from the laboratory studies, possibly buttressed with field data, could be used to develop the statistical parameters to characterize debris loading on bridges. A probability-based procedure would certainly extend the usefulness of the NCHRP 24-26 work.

9.7 Calibration of Scour Factors for Unconditional Target Reliability

The probabilistic analyses performed as part of this research have served to calculate the probability that the actual scour at a bridge site will exceed the design scour assuming that the bridge is subjected to the 100-year flood. The analyses accounted for the hydrologic uncertainties as well as the hydraulic and scour modeling uncertainties. The results are used to calibrate scour factors that will meet a target reliability conditional on the occurrence of the 100-year flood. However, within a bridge's service life, there is a high probability that the design flood will be exceeded and therefore, the 100-year flood may not necessarily lead to conservative designs. In fact, there is a 53% probability of exceeding the 100-year flood within 75 years and 63% probability of exceeding the 100-year flood in 100 years.

To account for the wide range of possible flood events, the same type of calculations performed for this project should be extended to cover the entire probability distribution of discharge rates to investigate how well the probability of exceeding the 100-year scour will represent the unconditional probability of design scour exceedance. This is especially important for the types of scour that are very sensitive to the distribution of flow between the main channel and the floodplain such as contraction and abutment scour. The results of the unconditional probability analyses could then be used to calibrate scour factors to meet target reliability levels that will reflect the true probability of design scour exceedance. Following modern performance-based design methods, the target reliability levels should be based on risk-benefit criteria whereby the cost of the foundation should balance the consequences of scour exceedance and the probability that exceeding the design scour will lead to bridge collapse. This implies that different reliability targets should be allowed depending on the bridge topology and foundation type.

The objectives of the proposed research would be to develop scour factors so that the probabilities of design scour exceedances meet target reliability levels accounting for the complete probability distribution of flood events. The research project would entail the following tasks:

- Assemble data on several representative bridge configurations in typical river channels.
- Develop probability models for all the relevant random variables accounting for hydrologic, hydraulic, geometric, soil and modeling uncertainties.
- Obtain reliability indexes for designs that meet current scour design procedures.
- Establish appropriate target reliabilities by studying successful previous designs and comparing the costs to improve foundation designs and the consequences of failure.
- Recommend scour factors to adjust current method to meet the target reliability indexes.

9.8 Calibration of LRFD Methods for Foundation Scour Design

This research developed procedures and assembled statistical data to estimate the probability that the actual scour depth around a bridge foundation will exceed the design scour. However, a high probability of design scour exceedance will not necessarily lead to a high probability of bridge failure. This is because the design of bridge foundations is usually based on a conservative combination of hazards and includes a number of explicit and implicit safety factors that may offset the relatively high probability of design scour exceedance. In fact, the current AASHTO LRFD suggests that the design of bridge foundations should account for the full design scour depth in combination with the same code-factored permanent and live loads

that are applied for dry land foundations. Furthermore, the AASHTO LRFD specifies that shallow foundations should be designed with a resistance factor of at least 0.50 and that pile foundations be designed with even lower resistance factors for most soil conditions and pile analysis models implying a safety factor of 2.0 or higher in most cases to offset the probability that the actual foundation strength may be lower than that estimated using the current analysis models.

The specified foundation resistance factors are further augmented by load factors on the applied permanent and traffic live loads that would offset the probability that the actual load will exceed the design loads. Because of the low probability that a relatively weak bridge foundation will be subjected to gravity loads that exceed the design loads while simultaneously being subjected to a scour depth that exceeds the design scour, the reliability of foundations designed for the AASHTO specified combination of events is expected to be higher than implied by the current AASHTO LRFD. It has been suggested that it is the AASHTO LRFD conservative combination of extreme events that is leading to the design of over-conservative and costly bridge foundations rather than the HEC-18 scour design equations. Research is needed to assess the reliability of current AASHTO bridge design criteria and adjust the load combination safety factors as necessary to account for the low probability of the simultaneous occurrence of extreme events.

The objectives of this proposed research would be to study the reliability of foundations designed for the combination of gravity loads and scour as specified in the current AASHTO codes and propose adjustments to the extreme events load and resistance factors to reflect the lower probability of their simultaneous occurrence. The research project would entail the following tasks:

- Assemble data on several representative bridge configurations in typical river channels.
- Develop probability models for all the relevant random variables accounting for hydrologic, hydraulic, geometric, soil and modeling uncertainties, foundation strength as well as permanent and live loads.
- Obtain reliability indexes for designs that meet current bridge foundation design procedures for the combination of scour and gravity loads.
- Establish appropriate target reliabilities by studying successful previous designs and comparing the costs to improve foundation designs and the consequences of failure.
- Recommend scour factors to adjust current foundation methods to meet the target reliability index.

(page intentionally left blank)

CHAPTER 10

10. CONCLUSIONS, OBSERVATIONS, AND IMPLEMENTATION

10.1 Conclusions

This research accomplished its basic objectives of developing a risk/reliability-based methodology that can be used in calculating bridge pier, abutment, contraction, and total scour at waterway crossings so that scour estimates can be linked to a probability. The developed probabilistic procedures are consistent with LRFD approaches used by structural and geotechnical engineers.

There is wide-spread belief within the bridge engineering community that unaccounted- for biases, and input parameter and hydraulic modeling uncertainty lead to overly conservative estimates of scour depths. The perception is that this results in design and construction of costly and unnecessarily deep foundations. This research project closed the gap between perception and reality and provides risk/reliability-based confidence bands for bridge scour estimates that align the hydraulic design approach with the design procedures currently used by structural and geotechnical engineers. Hydraulic engineers now have the option of and ability to perform scour calculations that incorporate probabilistic methods into the hydraulic design of bridges.

The primary purpose of this project was to analyze the probability of scour depth exceedance, not the probability of bridge failure. The latter requires advanced analyses of the weakened foundation under the effects of the expected applied loads which was beyond the scope of this project.

This research project produced significant results of practical use to the bridge engineering community. The final outcome of this project was the development of a "Level I" approach that consists of a set of tables of probability values or scour factors that can be used to associate an estimated scour depth provided by the hydraulic engineer with a probability of exceedance for simple pier and abutment geometries. For complex foundation systems and channel conditions, or for cases requiring special consideration, this project provided a "Level II" approach that consists of a step-by-step procedure that hydraulic engineers can follow to provide probability-based estimates of site-specific scour factors. In order to develop the probability-based estimates or scour factor tables for each scour component and to develop the Level II approach, an understanding of the uncertainties associated with the prediction of individual scour components was required.

The goals of this study were achieved. A methodology is now available that can be used to link scour depth estimates to a conditional probability and determine the risk associated with scour depth exceedance for a given design event. The probability linkage considers the propagation of uncertainties among the parameters that are used to quantify the confidence of scour estimates for a specific design event (e.g., a 100-year flood) based on the uncertainty of input parameters and considering model uncertainty and bias. In addition, these uncertainties were incorporated into a reliability analysis framework to provide an initial estimate of an unconditional target reliability for the design life of a bridge consistent with LRFD approaches used by structural and geotechnical engineers. This Final Report is supplemented by a separate "Reference Guide" to aid practitioners in applying the results of this research.

The Level I approach to determine the conditional probability of exceedance of design scour depth for a 100-year design event can be applied using the 27-element matrix of Appendix A if a bridge fits the criteria of one of the 27 bridge categories reasonably well. In total, more than 300,000 HEC-RAS/Monte Carlo simulations were required to produce the statistics on which the 27 tables in Appendix A are based. In addition, more than 300,000 scour calculations for each of the scour equations were completed off-line (i.e., more than 1.2 million off-line scour calculations). However, for more complex bridge or hydraulic situations, or for different return period design events, a Level II approach will be required. A Level II approach will also be necessary if the unconditional probability of exceeding design scour depths to meet a target reliability over the life of a bridge is desired.

This implies that the design engineer must implement a HEC-RAS/Monte Carlo simulation using software similar to that developed for this research project (rasTool©). It must be noted that the rasTool© interface is a research-level software engine requiring considerable insight on the part of the user for application of the processes used in this study for Level II conditional and unconditional probability analyses. Specifically, the Monte Carlo simulation software was not developed for distribution nor is it thoroughly documented or supported for general use. It is, however, considered robust and could be applied to a range of bridge and/or open channel applications. Development of user-friendly HEC-RAS/Monte Carlo Simulation Software is listed as a high priority research need in Chapter 9.

10.2 Observations

During the course of this research project, the research team encountered a number of issues, considerations, and results which merit further discussion.

1. Data Analysis Issues: Observations on data sets used for the analysis of scour equations for pier, contraction, and abutment scour are provided below:

   Pier Scour: There exists a plethora of data on pier scour from many sources, including both laboratory and field studies. The data sets include both clear-water and live-bed conditions. Both the HEC-18 and FDOT pier scour equations were developed as design equations, not best-fit prediction equations, and thus have a degree of conservatism built in. As such, the equations do not underpredict observed scour very often, and the reliability indexes for pier scour compare favorably with those used by structural and geotechnical engineers in LRFD applications for bridges.

   Contraction Scour: In contrast with the pier scour equations, the HEC-18 contraction scour equations are essentially predictive, given that they are derived from sediment transport principles and theory. Therefore, underpredictions of observed scour are much more common, and the resulting reliability is very low compared to typical target values used in LRFD applications. Only studies which used long contracted sections were analyzed, because short contractions include an abutment scour effect. Available data were limited to just the clear-water condition.

   Abutment Scour: The final report for NCHRP Project 24-20, "Estimation of Scour Depth at Bridge Abutments," (Ettema et al., 2010) was published as this study was getting under way, and the results of that research have been formally incorporated into HEC-18, 5th Edition (Arneson et al. 2012).

   There are many data sets in the literature that deal with abutment scour. Unfortunately, most of those data sets do not contain sufficient information regarding the distribution of

flow between the main channel and the overbank area to allow analysis using the NCHRP 24-20 approach. The equations for live-bed abutment scour ("Scour Condition A") and clear-water abutment scour ("Scour Condition B") both use a calculation for contraction scour and then apply an amplification factor to account for the additional scour caused by local effects at the tip of the abutment. Therefore the scour predicted by this method is the total scour at the abutment.

Because the amplification factors were developed as envelope curves to the observed scour depths, the equations are considered to be design equations and therefore have a degree of built-in conservatism. The reliability of the abutment scour equations was found to be intermediate between those of the pier scour and contraction scour equations.

2. Importance of Hydrologic and Hydraulic Uncertainty:

   The HEC-RAS/Monte Carlo simulations proved to be very enlightening with respect to quantifying the effect that hydrologic and hydraulic uncertainties have on scour estimates. Using standard Water Resources Council Bulletin 17-B methodology, the uncertainty in the design discharge is easily quantified using the upper and lower 95% confidence limits. Obviously, the confidence interval decreases with increasing periods of record. Using the confidence limits from flood frequency analyses showed that hydrologic uncertainty can have a major influence on scour variability.

   Given any particular discharge, a hydraulic model (such as HEC-RAS) is necessary to develop hydraulic conditions such as depth and velocity which are then used as input to the scour equations. A striking result of this research effort was the effect of the Manning n resistance coefficient on the distribution of flow between the main channel and the overbank areas, and the resulting effect on the different types of scour. For pier scour, both the HEC-18 and FDOT equations were shown to be relatively insensitive to changes in flow distribution. In contrast, the contraction and abutment scour equations were very sensitive to this effect. Calibrating a hydraulic model to high water marks observed for various floods is crucial to reducing hydraulic uncertainty and thus reducing uncertainty in contraction and abutment scour depths.

3. Roadway Overtopping:

   When roadway overtopping is incorporated in the hydraulic model, contraction scour is considerably reduced. Of course, roadway overtopping will result in road closure and often results in damage to the approach embankments and possibly the road surface as well. However, the bridge itself benefits from the relief of flow afforded by the overtopping condition. This effect has important implications for the design of new bridges as well as the analysis of existing bridges. Where overtopping is likely, the hydraulic model should reflect this as accurately as possible because of the benefit it provides in reducing contraction scour. However, for developing the scour factors in Chapter 6 and the service life target reliability analysis in Chapter 8, the effects of roadway overtopping were not included. The total discharge was routed through the bridge opening in all the Monte Carlo Simulation runs.

4. Total Scour:

   The combined effect of pier plus contraction scour was investigated to develop reliability indexes for the probability that the total design scour would be exceeded during the design life of the bridge (as noted previously, the NCHRP 24-20 abutment scour equations predict total scour at the abutment). NCHRP Project 24-37 is now underway to determine whether total scour can be accurately estimated as simply a superposition of the individual components. Presumably, that study will include the case where a pier is within the abutment scour zone. The results of that project will have implications for the probability-based total scour investigation performed during this study.

10.3 Implementation Plan

10.3.1 The Product

As described in more detail in the preceding sections, the product of this research was practical reliability-based methodologies for linking scour estimates to a probability.

10.3.2 The Market

The market or audience for the results of this research will be hydraulic engineers, bridge engineers, and geotechnical engineers in state, federal, and local agencies with a bridge-related responsibility. These would include:

State Highway Agencies
Federal Highway Administration
City/County Bridge Engineers
Railroad Bridge Engineers
U.S. Army Corps of Engineers
U.S. Bureau of Land Management
National Park Service
U.S. Forest Service
Bureau of Indian Affairs
Any other governmental agency with bridges under their jurisdiction
Consultants to the agencies above

10.3.3 Impediments to Implementation

A serious impediment to successful implementation of results of this research will be difficulties involved in reaching a diverse audience scattered among numerous agencies and institutions; however, this can be countered by a well-planned technology transfer program. Because of the complexity and geographic scope of the bridge scour problem, a major challenge will be to present the results in a format that can be applied by agencies with varying levels of engineering design capabilities. Presenting the guidelines and methods in a format familiar to bridge owners, who are the target audience, will facilitate their use of the results of this research. Using an AASHTO LRFD format will help ensure successful implementation that will be compatible with procedures currently used by structural and geotechnical engineers.

10.3.4 Leadership in Application

FHWA. Because of its broad-based mission to provide guidance to the state highway agencies, the Federal Highway Administration generally takes a leading role in disseminating the results of research products such as this. Through the National Highway Institute and its training courses, FHWA has the program in place to reach a diverse and decentralized target audience.

TRB. The Transportation Research Board through its annual meetings and committee activities, and publications such as the Transportation Research Record, as well as periodic international bridge conferences can also play a leading role in disseminating the results of this research to the target audience.

AASHTO. The American Association of State Highway and Transportation Officials (AASHTO) is the developer and sanctioning agency for standards, methods, and specifications. Thus, it will be important that the research results be formally adopted through the AASHTO process. As a collective representation of individual state DOTs, AASHTO can also suggest any needed training to be developed by FHWA or others. The AASHTO committee on bridges and structures could provide centralized leadership through the involvement of all State DOT Bridge Engineers.

ASCE. Professional societies such as the American Society of Civil Engineers (ASCE) host conferences and publish peer reviewed journals through which the latest advances in engineering research and applications reach a wide audience, including many state, federal, and local hydraulic engineers. For example, the ASCE Task Committee on Bridge Management for Scour Safety hosted a bridge scour symposium at every Water Resources (Hydraulics) Engineering specialty conference between 1991 and 1998. The results of these conferences were made available to bridge practitioners world-wide through the publication of the ASCE Compendium on Stream Stability and Scour at Highway Bridges (Richardson and Lagasse eds. 1999) under the auspices of the Committee.

Regional Bridge Conferences. Regional bridge conferences, such as the Western Bridge Engineer Conference or the International Bridge Engineering Conferences, reach a wide audience of bridge engineers, consultants, and contractors. These groups would have an obvious interest in a reliability-based approach to bridge scour and their acceptance of the results of this research will be key to implementation by bridge owners.

10.3.5 Activities for Implementation

The activities necessary for successful implementation of the results of this research relate to technology transfer activities, as discussed above, and the activities of appropriate AASHTO committees.

"Ownership" of the LRFD approach to scour prediction by AASHTO will be key to successful implementation. Although the procedures that result from this research will be considered and hopefully adopted by AASHTO, it is essential that the various technical committees in AASHTO accept and support these results and use the committee structure to implement them in appropriate AASHTO publications.

10.3.6 Criteria for Success

The best criteria for judging the success of this implementation plan will be acceptance and use of the probabilistic approaches for scour that result from this research by state highway agency engineers and others with responsibility for design, maintenance, rehabilitation, or inspection of highway facilities. Progress can be gaged by peer reviews of technical presentations and publications and by the reaction of state DOT personnel during presentation of results at NHI courses. A supplemental critique sheet could be used during NHI courses to provide feedback on the applicability of the guidelines and suggestions for improvement.

10.4 Applicability of Results to Highway Practice

Approximately 83% of the 583,000 bridges in the National Bridge Inventory (NBI) are built over waterways. Many, especially those on more active streams, will experience problems with scour, bank erosion, and channel instability during their useful life (Lagasse et al. 2012). The magnitude of these problems is demonstrated by the estimated average annual flood damage repair costs of approximately $50 million for bridges on the Federal aid system.

In the U.S. approximately 20,200 highway bridges are currently rated scour critical for Item 113. Each of these bridges must have a Plan of Action developed that could involve monitoring, scour countermeasures, or, possibly bridge replacement. As the bridge owners evaluate their scour-critical bridges, the availability of a risk-based approach for scour assessments could facilitate, and potentially reduce the cost of corrective action.

Although it is difficult to be precise regarding the actual cost to the nation's highway system that result from over design of bridge foundations, the number is obviously very large. The guidelines for a risk-based methodology resulting from this research provide bridge designers the necessary probabilistic estimates for scour which brings a level of confidence in hydraulic design consistent with current LRFD methods used by structural and geotechnical engineers.

The desirable consequences of this project, when implemented, will be more efficient planning, design, and construction of highway facilities considering the reliability of and risk associated with scour prediction used for bridge foundation design. The ultimate result will be more cost effective structures consistent with the reliability-based design used by structural and geotechnical engineers.

11. REFERENCES CITED

AASHTO (2005). "Guide Manual for Condition Evaluation and Load and Resistance Factor Rating (LRFR) of Highway Bridges," 1st Edition with 2005 Interim Revisions, American Association of State Highway and Transportation Officials, Washington, D.C.

AASHTO (2007). "AASHTO LRFD Bridge Design Specifications: Customary U.S. Units," 4th Edition, American Association of State Highway and Transportation Officials, Washington, D.C.

AASHTO (2008). "AASHTO Manual for Bridge Evaluation," 1st Ed. (MBE 1-M), American Association of State Highway and Transportation Officials.

AASHTO (2009). "Guide Specification and Commentary for Vessel Collision Design of Highway Bridges," 2nd Edition, Washington D.C.

ACI 318-05 (2005). "Building Code Requirements for Structural Concrete and Commentary," American Concrete Institute, Farmington Hills, MI.

AISC 325-05 (2005). "Steel Construction Manual," Thirteenth Edition, American Institute of Steel Construction, Chicago, IL.

Akgul, F. and Frangopol, D.M. (2004). "Lifetime Performance Analysis of Existing Steel Girder Bridge Superstructures," ASCE, *Journal of Structural Engineering*, Vol. 130, No. 12, pp. 1875-1888.

Aktas, E., Moses, F. and Ghosn, M. (2001). "Cost and Safety Optimization of Structural Design Specifications," *Journal of Reliability Engineering and System Safety*, Vol. 73, No. 3, pp. 205-212.

ASCE (2010). "Minimum Design Loads for Buildings and Other Structures," ASCE 7-10, American Society of Civil Engineers, Reston, VA.

Arneson, L.A., Zevenbergen, L.W., Lagasse, P.F., and Clopper, P.E., 2012. "Evaluation Scour at Bridges," Fifth Edition, Federal Highway Administration, Report FHWA-HIF-12-003, Hydraulic Engineering Circular No. 18, U.S. Department of Transportation, Washington, D.C.

ATC/MCEER Joint Venture (2002). "Comprehensive Specifications for the Seismic Design of Bridges," NCHRP Report 472, Transportation Research Board, National Academies of Science, Washington D.C.

Ayyub, B.M. (2003). "Risk Analysis in Engineering Economics," Chapman and Hall/CRC.

Ayyub, B.M. and McCuen, R. (2003). "Probability, Statistics, and Reliability for Engineers and Scientists," Second Edition, Chapman and Hall/CRC.

Ballio, F., Terruzi, A., and Radice, A., 2009. "Constriction Effects in Clear-Water Scour at Abutments," ASCE, *Journal of Hydraulic Engineering*, Vol. 135(2).

Barbe, D.E., Cruise, J.F., and Singh, V.P. (1992). "Probalistic Approach to Local Bridge Pier Scour," Transportation Research Record No. 1350, Hydrology and Bridge Scour.

Brabets, T.P. (1994). "Application of surface geophysical techniques in a study of the geomorphology of the lower Copper River, Alaska," Anchorage, AK, U.S. Geological Survey Water-Resources Investigations Report 94-4165.

Briaud, J.L., Brandimarte, L., Wang, J., and D'Odorico, P. (2007). "Probability of Scour Depth Exceedance Owing to Hydrologic Uncertainty," Georisk: Assessment and Management of Risk for Engineered Systems and Geohazards, Vol. 1, Issue 2, pp. 77 – 88.

Canadian Standards Association (2006). "Canadian Highway Bridge Design Code," 10th Edition, CAN/CSA-S6-2006.

Cesare, M.A. (1991). "First-order Analysis of Open-channel Flow," ASCE, *Journal of Hydraulic Engineering*, Vol. 117, No. 2, pp. 242-247.

Chabert, J. and Engeldinger, P. (1956). "Etude des affouilliments autour des piles de ponts." Laboratorie National d'Hydraulique, Chatou, France (in French).

Chee, R.K.W. (1982). "Local Scour at Bridge Piers," Report No. 290, Department of Civil Engineering, University of Auckland, New Zealand.

Chiew, Y.M. (1984). "Local Scour at Bridge Piers," Report No. 355, Department of Civil Engineering, University of Auckland, New Zealand.

Czarnecki A.A. and Nowak A.S. (2008). "Time-variant Reliability Profiles for Steel Girder Bridges," Structural Safety, Vol. 30, No. 1, pp. 49-64.

Dey, S. and Raikar, R., 2005. "Scour in Long Contractions." ASCE, *Journal of Hydraulic Engineering,* Vol. 131(5).

Dey, S., Bose, S.K., and Sastry, G.L.N. (1995). "Clearwater scour at circular piers - A model," ASCE, *Journal of Hydraulic Engineering*, 121(12), pp. 869-876.

Ellingwood, B., Galambos, T.V., MacGregor, J.G., and Comell C.A. (1980). "Development of a Probability Based Load Criterion for American National Standard A58," National Bureau of Standards, Washington, D.C.

Enright, M.P. and Frangopol, D.M. (1998). "Service-Life Prediction of Deteriorating Concrete Bridges," ASCE, *Journal of Structural Engineering*, Vol. 124(3), pp. 309-317.

Ettema, R. (1976). "Influence of Bed Material Gradation on Local Scour," M.S. thesis, University of Auckland, New Zealand.

Ettema, R. (1980). "Scour at Bridge Piers," Report No. 216, University of Auckland, New Zealand.

Ettema, R., Kirkil, G., and Mostafa, E.A. (2006). "Similitude of Large-Scale Turbulence in Experiments on Local Scour at Cylinders," ASCE, *Journal of Hydraulic Engineering*, 132(1), pp. 33-40.

Ettema, R., Nakato,T., and Muste, M., 2010. "Estimation of Scour Depth at Bridge Abutments," Draft Final Report, NCHRP Project 24-20, Transportation Research Board, National Academies of Science, Washington D.C.

Eurocode 2 (1992). "Design of Concrete Structures – Part 1-1: General – Common Rules for Building and Civil Engineering Structures."

Fischer, E.E. (1995). "Contraction Scour at a Bridge over Wolf Creek, Iowa" in Proceedings: Conference on Water Resources Engineering 1995, San Antonio, Texas, American Society of Civil Engineers.

Flynn, K.M., Kirby, W.H., and Hummel, P.R. (2006). "User's Manual for Program Peak FQ, Annual Flood-Frequency Analysis Using Bulletin 17B Guidelines," U.S. Geological Survey, Techniques and Methods Book 4, Chapter B4, Reston, VA.

Froehlich, D.C. (1988). "Analysis of Onsite Measurements of Scour at Piers," In: ASCE National Hydraulic Engineering Conference, Colorado Springs, Colorado 534-539.

Froehlich, D.C. (2003). "Finite Element Surface-Water Modeling System: Two-Dimensional Flow in a Horizontal Plane," FESWMS-2DH, Version 2, User's Manual, U.S. Department of Transportation, Federal Highway Administration, Research, Development, and Technology, Turner-Fairbank Highway Research Center, McLean, VA.

Gao, D., Posada, G.L., and Nordin, C.F. (1993). "Pier Scour Equations Used in the Peoples Republic of China," FHWA-SA-93-076, Washington, D.C.

Ghosn, M. (2010). "Reliability Based Structural System Performance Indicators for Highway Bridges," Proceedings of ASCE Structures Congress, Orlando FL.

Ghosn, M. and Moses, F. (1986). "Reliability Calibration of a Bridge Design Code," ASCE, *Journal of Structural Engineering*, Vol. 112, No. 4.

Ghosn, M. and Moses, F. (1998). "Redundancy in Highway Bridge Superstructures," NCHRP Report 406, Transportation Research Board, National Academies of Science, Washington, D.C.

Ghosn, M., Moses, F., and Wang, J. (2003). "Design of Highway Bridges for Extreme Events'," NCHRP Report 489, Transportation Research Board, National Academies of Science, Washington D.C.

Gill, M.A., 1981. "Bed Erosion in Rectangular Long Contraction." ASCE, *Journal of the Hydraulics Division*, Vol. 107(3).

Graf (1995). "Load Scour Around Piers," Annual Report, Laboratorie de Recherches Hydrauliques, Ecole Polytechnique Federale de Lausanne, Lausanne, Switzerland, pp. B.

Hancu, S. (1971). "Sur le calcu de affouillements locaux dans la zone des piles des ponts," In: 14th International Association of Hydraulic Research Congress, Paris, France, 299-313.

Helsel, D.R. and Hirsch, R.M. (1992). "Statistical Methods in Water Resources," New York, Elsevier, 326 p.

Hong, S.H. (2005). "Interaction of Bridge Contraction Scour and Pier Scour in a Laboratory River Model," Master of Science Thesis, Department of Civil Engineering, Georgia Institute of Technology.

Hopkins, G.R., Vance, R.W., and Kasraie, B. (1980). "Scour Around Bridge Piers," Report No. FHWA-RD-79-103, Federal Highway Administration, Washington, D.C.

Hwang, U. and Shinozuka, M. (1988). "Reliability Analysis of Code-Designed Structures Under Natural Hazards," Report to MCEER, SUNY Buffalo, NY.

Hydrologic Engineering Center (1986). "Accuracy of Computed Water Surface Profiles," U.S. Army Corps of Engineers, Davis, CA.

Imbsen, R. (2007). "AASHTO Guide Specifications for LRFD Seismic Bridge Design," Report to AASHTO T3 Subcommittee, Washington, D.C.

Jain, S.C. and Fischer, E.E. (1979). "Scour Around Bridge Piers at High Froude Numbers," FHWA-RD-79-104, Federal Highway Administration, U.S. Department of Transportation, Washington, D.C.

Johnson, P.A. (1991). "Advancing Bridge Pier Scour Engineering," ASCE, *Journal of Professional Issues*, 117(1), pp. 48-55.

Johnson, P.A. (1992). "Reliability-Based Pier Scour Engineering," ASCE, *Journal of Hydraulic Engineering*, Vol. 118, Issue 10, pp. 1344-1358.

Johnson, P.A. (1995). "Comparison of Pier Scour Equations Using Field Data," ASCE, *Journal of Hydraulic Engineering,* Vol. 121(8), pp. 626-629.

Johnson, P.A. (1996a). "Uncertainty of Hydraulic Parameters," ASCE, *Journal of Hydraulic Engineering*, Vol. 122(2), pp. 112-115.

Johnson, P.A. (1996b). "Uncertainty in Estimations of Excess Shear Stress," *Proceedings of the Seventh IAHR International Symposium, Mackay, Australia*.

Johnson, P.A. (1999). "Fault Tree Analysis of Bridge Failure Due to Scour and Channel Instability," ASCE, *Journal of Infrastructure Systems*, Vol. 5(1), pp. 35-41.

Johnson, P.A. and Ayyub, B.M. (1992a). "Assessing Time-Variant Bridge Reliability due to Pier Scour," ASCE, *Journal of Hydraulic Engineering*, Vol. 118(6), pp. 887-903.

Johnson, P.A. and Ayyub, B.M. (1992b). "Probability of Bridge Failure due to Pier Scour," *Proceedings of the Water Resources Sessions at Water Forum* 1992, ASCE, Baltimore, MD, p. 690.

Johnson, P.A. and Ayyub, B.M. (1996). "Modeling Uncertainty in Prediction of Pier Scour," ASCE, *Journal of Hydraulic Engineering*, Vol. 122(2), pp. 66-72.

Johnson, P.A. and Dock, D.A. (1998). "Probabilistic Bridge Scour Estimates," ASCE, *Journal of Hydraulic Engineering*, Vol. 124(7), pp. 750-754.

Johnson, P.A. and Heil, T.M. (1996). "Bridge Scour - A Probabilistic Approach," *Journal of Infrastructure Systems*, 1(4), 24-30.

Johnson, P.A. and McCuen, R.H. (1991). "A Temporal, Spatial Pier Scour Model," Transportation Research Board Record, No. 1319.

Johnson, P.A. and Niezgoda, S.L. (2004). "Risk-based Method for Selecting Scour Countermeasures," ASCE, *Journal of Hydraulic Engineering*, 130(2), pp. 121-128.

Johnson, P.A. and Simon, A. (1995). "Reliability of Bridge Foundations in Unstable Alluvial Channels," *Proceedings of 1995 Specialty Conference on Hydraulic Engineering*, ASCE, San Antonio, TX.

Johnson, P.A. and Simon, A. (1997). "Reliability of Bridge Foundations in Modified Channels," ASCE, *Journal of Hydraulic Engineering*, Vol. 123(7), pp. 648-651.

Johnson, P.A. and Whittington, R.M. (2010). "Assessing Bridge Vulnerability and Risk due to Stream Instability," *5th International Conference on Scour and Erosion*, San Francisco, CA.

Jones, J.S. (1984), "Comparison of Prediction Equations for Bridge Pier and Abutment Scour," Transportation Research Record 950, Second Bridge Engineering Conference, Vol. 2, Transportation Research Board, National Academies of Science, Washington, D.C.

Kayser, J.R. and Nowak A.S. (1989). "Capacity Loss Due to Corrosion on Steel-Girder Bridges," ASCE, *Journal of Structural Engineering*, Vol. 115(6), pp. 1525-1537.

Keaton, J.R., Mishra, S.K., and Clopper, P.E., 2012. "Scour at Bridge Foundations on Rock," NCHRP Report 717, Transportation Research Board, National Academies of Science, Washington, D.C.

Keefer, T.N., McQuivey, R.S., and Simons, D.B. (1980). "Stream Channel Degradation and Aggradation: Causes and Consequences to Highways," Interim Report No. FHWA/RD-80/038, Federal Highway Administration, Washington, D.C.

Komura, S., 1966. "Equilibrium Depth of Scour in Long Constrictions." ASCE, *Journal of Hydraulic Engineering*, Vol. 92(5).

Kothyari, U.C., Garde, R.C.J., and Raju, K.G.R. (1992). "Temporal Variation of Scour Around Circular Bridge Piers," ASCE, *Journal of Hydraulic Engineering*, 118(8), pp. 1091-1106.

Kulicki, J.M., Mertz, D.R., and Nowak, A.S. (2007). "Updating the Calibration Report for AASHTO LRFD Code," NCHRP Project 20-7/186, Transportation Research Board, National Academies of Science, Washington, D.C.

Kulicki, J.M., Wassef, W.G., Kleinhans, D.D., Yoo, C.H., Nowak, A.S., and Grubb, M. (2006). "Development of LRFD Specifications for Horizontally Curved Steel Girder Bridges," NCHRP Report 563, Transportation Research Board, National Academies of Science, Washington, D.C.

Lagasse, P.F., Spitz, W.J., Zevenbergen, L.W., and Zachmann, D.W., (2004). "Handbook for Predicting Stream Meander Migration," NCHRP Report 533, Transportation Research Board, National Academies of Science, Washington, D.C.

Lagasse, P.F., Clopper, P.E., Zevenbergen, L.W., and Girard, L.G., (2007). "Countermeasures to Protect Bridge Piers from Scour," NCHRP Report 593, Transportation Research Board, National Academies of Science, Washington, D.C.

Lagasse, P.F., Clopper, P.E., Zevenbergen, L.W., Spitz, W.J., and Girard, L.G. (2010). "Effects of Debris on Bridge Pier Scour," NCHRP Report 653, Transportation Research Board, National Academies of Science, Washington, D.C.

Lagasse, P.F., Zevenbergen, L.W., Spitz, W.J., and Arneson, L.A. (2012). "Stream Stability at Highway Structures," Hydraulic Engineering Circular No. 20, Fourth Edition, Federal Highway Administration, HIF-FHWA-12-004, Washington, D.C.

Lagasse, P.F. Ghosn, M., Johnson, P.A., Zevenbergen, L.W., and Clopper, P.E. (2013). "Reference Guide for Applying Risk and Reliability-Based Approaches for Bridge Scour Prediction," NCHRP Report 761, Transportation Research Board, National Academies of Science, Washington, D.C.

Landers, M.N. and Mueller, D.S. (1996). "Channel Scour at Bridges in the United States," FHWA-RD-95-184, Federal Highway Administration, Research and Development, Turner-Fairbank Highway Research Center, McLean, VA.

Laursen, E.M. (1970). "Bridge Design Considering Scour and Risk," ASCE, *Journal of the Transportation Engineering Division*, Vol. 96(2), pp. 149-164.

Lim, S.Y., 1993. "Clear Water Scour in Long Contractions." Proc. Inst. Civ. Eng., Waters Maritime Engrg., 101.

Liu, D., Ghosn, M., Moses F., and Neuenhoffer, A. (2001). "Redundancy in Highway Bridge Substructures," NCHRP Report 458, Transportation Research Board, National Academies of Science, Washington D.C.

Mays, L.W. (2005). "Water Resources Engineering," John Wiley and Sons, Hoboken, NJ, pp. 330-334.

Mays, L.W. and Tung, Y.K. (1992). "Hydrosystems Engineering and Management," McGraw-Hill, Inc.

McCollin, C. (1999). "Working Around Failure," Manufacturing Engineering, 78(1), pp. 37-40.

Mechakhchekh A. and Ghosn, M. (2007). "Reliability-based Procedure for Developing LRFD Seismic Bridge Design Specifications," TRR2028, "Design of Structures," Transportation Research Record, pp. 173-179.

Melchers, R.E. (1999). "Structural Reliability: Analysis and Prediction," 2nd Ed., John Wiley & Sons, New York, NY.

Melville, B.W. (1997). "Pier and Abutment Scour: Integrated Approach," ASCE, *Journal of Hydraulic Engineering*, 123(2), pp. 125-136.

Melville, B.W. and Chiew, Y.M. (1999). "Time scale for local scour at bridge piers," ASCE, *Journal of Hydraulic Engineering*, 125(1), pp. 59-65.

Mori, Y. and Ellingwood, B.R. (1994). "Maintaining Reliability of Concrete Structures, I: Role of Inspection/Repair," ASCE, *Journal of Structural Engineering*, Vol. 120(3), pp. 824-845.

Moses, F. (2001). "Calibration of Load Factors for LRFR Bridge Evaluation," NCHRP Report 454, Transportation Research Board, National Academies of Science, Washington, D.C.

Moses F., Schilling, C.G., and Raju K.S. (1987). "Fatigue Evaluation Procedures for Steel Bridges," NCHRP Report 299, Transportation Research Board, National Academies of Science, Washington, D.C.

Mueller, D.S. and Wagner, C.R. (2005). "Field observation and evaluations of streambed scour at bridges," Louisville, KY, U.S. Department of Transportation FHWA-RD-03-052.

Muzzammil, M., Siddiqui, N.A., and Siddiqui, A.F. (2006). "A Reliability Analysis of Bridge Pier Against Local Scour," Water and Energy International, Year : 2006, Vol. 63, Issue: 2.

Muzzammil, M., Siddiqui, N.A., and Siddiqui, A.F. (2008). "Reliability Considerations in Bridge Pier Scouring," Structural Engineering and Mechanics, 28(1), pp. 1-18.

Muzzammil, M., Siddiqui, N.A., and Anwar, M. (2009). "A Reliability-Based Scour Depth Estimation in Indian Alluvial Rivers," Water and Energy International, Year: 2009, Vol. 66, Issue: 1, Print ISSN : 0974-4207, Online ISSN : 0974-4711.

Norman, V.W. (1975). "Scour at selected bridge sites in Alaska," Anchorage, AK, U.S. Geological Survey Water-Resources Investigations Report 32-75.

Nowak. A.S. (1999). "Calibration of LRFD Bridge Design Code," NCHRP Report 368, Transportation Research Board, National Academies of Science, Washington, D.C.

Nowak, A.S. (2009). "Target Reliability Levels for Serviceability and Ultimate Limit States," ASCE Structures Congress, Austin TX.

Nowak, A.S. and Collins, K.R. (2000). "Reliability of Structures," McGraw-Hill, New York, NY.

Nowak, A.S. and Ibrahim, F. (2009). "Development of Live Load for Long Span Bridges," 5th New York Bridge Conference, New York, NY.

Nowak, A.S., Szwed A., Podhorecki P.J., Czarnecki A., Laumet P., and Galambos T.V. (2006). "Calibration of LRFD Design Specifications for Steel Curved Girder Bridges," Appendix C of NCHRP Report 563, Transportation Research Board, National Academies of Science, Washington D.C.

Oben-Nyarko, K. and Ettema, R. (2011). "Pier and Abutment Scour Interaction," ASCE, *Journal of Hydraulic Engineering*, Vol. 137(12), pp. 1598-1605.

Oliveto, G. and Hager, W.H. (2002). "Temporal Evolution of Clear-Water Pier and Abutment Scour," ASCE, *Journal of Hydraulic Engineering*, 128(9), 811-820.

Pearson, D.R., Jones, J.S., and Stein, S.M. (2000). "Risk-based Design of Bridge Scour Countermeasures," Transportation Research Record, 1696, pp. 229-235.

Raikar, 2004. "Local and General Scour of Gravel Beds." Ph.D. Thesis, Department of Civil Engineering, Indian Institute of Technology, Kharagpur, India.

Ravindra, M.K. and Galambos, T.V. (1978). "Load and Resistance Factor Design for Steel," ASCE, *Journal of the Structural Division*, Vol. 104(9), pp. 1337-1353.

Richardson, E.V. and Davis, S.R. (2001). "Evaluating Scour at Bridges," Hydraulic Engineering Circular No. 18, Fourth Edition, Report FHWA NHI 01-001, Federal Highway Administration, U.S. Department of Transportation, Washington, D.C.

Richardson, E.V., Simons, D.B., and Lagasse, P.F. (2001). "River Engineering for Highway Encroachments – Highways in the River Environment," Report No. FHWA NHI 01-004, Hydraulic Design Series No. 6, Federal Highway Administration, Washington, D.C.

Ries, K.G. (2007). "The National Streamflow Statistics Program: A Computer Program for Estimating Streamflow Statistics for Ungaged Sites," U.S. Geological Survey Techniques and Methods 4-A6, Reston, VA.

Rizkalla, S., Mirmiran, A., Zia, A., Russel, H., and Mast, R. (2007). "Application of the LRFD Bridge Design Specifications to High-Strength Structural Concrete: Flexure and Compression Provisions," NCHRP Report 595, Transportation Research Board, National Academies of Science, Washington, D.C.

Shen, H.W., Schneider, V.R., and Karaki, S.S. (1969). "Local Scour Around Bridge Piers," ASCE, *Journal of the Hydraulics Division*, Vol. 95(6), pp. 1919-1940.

Sheppard, D.M. and Miller, W. (2006). "Live-Bed Local Pier Scour Experiments," ASCE, *Journal of Hydraulic Engineering*, 132(7), pp. 635-642.

Sheppard, D.M., Odeh, M., and Glasser, T. (2004). "Large Scale Clear-Water Local Pier Scour Experiments," ASCE, *Journal of Hydraulic Engineering,* 130(10), pp. 957-963.

Sheppard, D.M., Melville, B.W., and Deamir, H. (2011). "Scour at Wide Piers and Long Skewed Piers," NCHRP Report 682, Transportation Research Board, National Academies of Science, Washington, D.C.

Simon, A. (1992). "Energy, Time, and Channel Evolution in Catastrophically Disturbed Fluvial Systems," *Journal Geomorphology*, 5(3-5), pp. 345-372.

Stein, S.M., Young, K.G., Trent, R.E., and Pearson, D.R. (1999). "Prioritizing Scour Vulnerable Bridges Using Risk," *Journal Infrastructure Systems*, Vol. 5, Issue 3, pp. 95-101.

Sturm, T.W., Ettema, R., and Melville, B.W., 2011. "Evaluation of Bridge-Scour Research: Abutment and Contraction Scour Processes and Prediction," Final Report, NCHRP Project 24-27 (02), Web-Only Document 181, Transportation Research Board, National Academies of Science, Washington D.C.

Takada, T., Ghosn, M., and Shinozuka, M. (1989). "Response Modification Factors for Buildings and Bridges," ICOSSAR '89, the 51h International Conference on Structural Safety and Reliability, San Francisco, CA, pp. 415-422.

Thoft-Christensen, P. and Baker, M.J. (1982). "Structural Reliability Theory and its Applications," Springer Verlag, Berlin.

Tse, J. and Ibrahim, F. (2009). "New National LRFD Design Criteria for Long Span Bridges," 5th New York Bridge Conference, New York, NY.

Tung, Y.K. (1990). "Mellin Transform Applied to Uncertainty Analysis in Hydrology/ Hydraulics," ASCE, *Journal of Hydraulic Engineering*, Vol. 116(5), pp. 659-674.

U.S. Army Corps of Engineers (USACE) (1986). "Accuracy of Computed Water Surface Profiles," Research Document No. 26, (Burnham, M. and D.W. Davis), 198 p.

U.S. Army Corps of Engineers (1992). "Reliability Assessment of Navigation Structures," Department of the Army, Engineer Technical Letter No. 1110-2-532.

U.S. Army Corps of Engineers (2004). "Upper Mississippi: River System Flow Frequency Study - Final Report: Appendix E, Kansas City District, Missouri River Hydrology and Hydraulic Analysis, November 2003," U.S. Army Corps of Engineers, Rock Island District, Rock Island, IL.

U.S. Army Corps of Engineers (2010). "HEC-RAS Version 4.1," USACE Hydrologic Engineering Center, Davis, CA.

U.S. Geological Survey (1981). "Guidelines for Determining Flood Flow Frequency," Bulletin #17B of the Hydrology Subcommittee, Interagency Advisory Committee on Water Data, Reston, VA.

Webby, M.G., 1984. "General Scour at a Contraction." *RRU Bulletin 73*, National Roads Board, Bridge Design and Research Seminar, New Zealand.

Wu, B. and Molinas, A. (2005). "Energy Losses and Threshold Conditions for Choking in Channel Contractions," IAHR, *Journal of Hydraulic Research*, Vol. 43, No. 2, pp. 139-148.

Yanmaz, A.M. (2002). "Dynamic Reliability in Bridge Pier Scouring," *Turkish Journal of Engineering Environmental Science*, 26, pp. 367-375.

Yanmaz, A.M. and Altinbilek, H.D. (1991). "Study of Time-Dependent Local Scour Around Bridge Piers," ASCE, *Journal of Hydraulic Engineering*, 117(10), pp. 1247-1268.

Yanmaz, A.M. and Celebi, T. (2004). "A Reliability Model for Bridge Abutment Scour," *Turkish Journal of Engineering Environmental Science*, 28, pp. 67-83.

Yanmaz, A.M. and Cicekdag, O. (2001). "Composite Reliability Model for Local Scour around Cylindrical Bridge Piers," *Canada Journal Civil Engineering* 28(3), pp. 520–535.

Yanmaz, A.M. and Ustun, I. (2001). "Generalized Reliability Model for Local Scour Around Bridge Piers of Various Shapes," *Turkish Journal of Engineering Environmental Science*, 25, pp. 687 - 698.

Yeh, K.C. and Tung, Y.K. (1993). "Uncertainty and Sensitivity Analyses of Pit-Migration Model," ASCE, *Journal of Hydraulic Engineering*, Vol. 119(2), pp. 262-283.

Yevjevich, V. (1972). "Probability and Statistics in Hydrology," Water Resources Publications, Fort Collins, CO.

Zhuravlyov, M.M. (1978). "New Method for Estimation of Local Scour Due to Bridge Piers and Its Substantiation," Transactions, Ministry of Transport Construction, State All Union Scientific Research Institute on Roads, Moscow, Russia.

(page intentionally left blank)

APPENDIX A
Summary of Scour Factors in Tabular and Graphical Form

(page intentionally left blank)

Table A.1	Small Bridge - Low Hydrologic Uncertainty - Small Pier (1 ft)					
	Pier Scour (HEC-18)	Pier Scour (FDOT)	Contraction Scour	Total Scour (HEC-18)	Total Scour (FDOT)	Abutment Scour
Design Scour (ft)	2.40	2.13	1.70	4.10	3.82	4.02
Expected Scour (ft)	1.63	1.60	1.55	3.19	3.15	2.99
Bias	0.68	0.75	0.92	0.78	0.82	0.74
Std. Dev. (ft)	0.26	0.28	0.41	0.49	0.50	0.71
COV	0.16	0.18	0.26	0.15	0.16	0.24
Design Scour β	2.96	1.87	0.35	1.87	1.35	1.46
Non-Exceedance	0.9985	0.9696	0.6356	0.9690	0.9110	0.9281
Scour Non-Exceedance (ft) based on Monte Carlo results						
β = 0.5 (0.6915)	1.76	1.74	1.73	3.41	3.39	3.32
β = 1.0 (0.8413)	1.89	1.88	1.96	3.67	3.65	3.69
β = 1.5 (0.9332)	2.02	2.03	2.21	3.94	3.93	4.09
β = 2.0 (0.9772)	2.15	2.17	2.45	4.22	4.22	4.45
β = 2.5 (0.9938)	2.28	2.31	2.70	4.51	4.49	4.81
β = 3.0 (0.9987)	2.35	2.39	2.98	4.81	4.84	5.07
Scour factors based on Monte Carlo results						
β = 0.5 (0.6915)	0.73	0.82	1.02	0.83	0.89	0.83
β = 1.0 (0.8413)	0.79	0.89	1.16	0.90	0.95	0.92
β = 1.5 (0.9332)	0.84	0.95	1.30	0.96	1.03	1.02
β = 2.0 (0.9772)	0.90	1.02	1.44	1.03	1.10	1.11
β = 2.5 (0.9938)	0.95	1.08	1.59	1.10	1.17	1.20
β = 3.0 (0.9987)	0.98	1.13	1.76	1.17	1.27	1.26
Scour non-exceedance (ft) based on scour mean and standard deviation						
β = 0.5 (0.6915)	1.76	1.74	1.76	3.43	3.40	3.34
β = 1.0 (0.8413)	1.89	1.88	1.96	3.67	3.65	3.69
β = 1.5 (0.9332)	2.02	2.02	2.17	3.92	3.90	4.04
β = 2.0 (0.9772)	2.15	2.16	2.37	4.16	4.15	4.40
β = 2.5 (0.9938)	2.28	2.30	2.58	4.41	4.40	4.75
β = 3.0 (0.9987)	2.41	2.44	2.78	4.65	4.65	5.10
Scour factors based on scour mean and standard deviation						
β = 0.5 (0.6915)	0.73	0.82	1.04	0.84	0.89	0.83
β = 1.0 (0.8413)	0.79	0.88	1.16	0.90	0.95	0.92
β = 1.5 (0.9332)	0.84	0.95	1.28	0.96	1.02	1.01
β = 2.0 (0.9772)	0.90	1.02	1.40	1.02	1.09	1.09
β = 2.5 (0.9938)	0.95	1.08	1.52	1.08	1.15	1.18
β = 3.0 (0.9987)	1.00	1.15	1.64	1.14	1.22	1.27

Table A.2	Small Bridge - Low Hydrologic Uncertainty - Medium Pier (2 ft)					
	Pier Scour (HEC-18)	Pier Scour (FDOT)	Contraction Scour	Total Scour (HEC-18)	Total Scour (FDOT)	Abutment Scour
Design Scour (ft)	4.66	3.78	1.70	6.35	5.47	4.02
Expected Scour (ft)	3.16	2.84	1.55	4.72	4.39	2.99
Bias	0.68	0.75	0.92	0.74	0.80	0.74
Std. Dev. (ft)	0.51	0.50	0.41	0.67	0.65	0.71
COV	0.16	0.18	0.26	0.14	0.15	0.24
Design Scour β	2.95	1.87	0.35	2.46	1.66	1.46
Non-Exceedance	0.9984	0.9696	0.6356	0.9930	0.9517	0.9281
Scour Non-Exceedance (ft) based on Monte Carlo results						
β = 0.5 (0.6915)	3.42	3.08	1.73	5.04	4.71	3.32
β = 1.0 (0.8413)	3.68	3.35	1.96	5.38	5.04	3.69
β = 1.5 (0.9332)	3.92	3.60	2.21	5.73	5.39	4.09
β = 2.0 (0.9772)	4.17	3.84	2.45	6.09	5.75	4.45
β = 2.5 (0.9938)	4.44	4.10	2.70	6.46	6.09	4.81
β = 3.0 (0.9987)	4.57	4.25	2.98	6.81	6.48	5.07
Scour factors based on Monte Carlo results						
β = 0.5 (0.6915)	0.73	0.82	1.02	0.79	0.86	0.83
β = 1.0 (0.8413)	0.79	0.89	1.16	0.85	0.92	0.92
β = 1.5 (0.9332)	0.84	0.95	1.30	0.90	0.99	1.02
β = 2.0 (0.9772)	0.89	1.02	1.44	0.96	1.05	1.11
β = 2.5 (0.9938)	0.95	1.09	1.59	1.02	1.11	1.20
β = 3.0 (0.9987)	0.98	1.13	1.76	1.07	1.18	1.26
Scour non-exceedance (ft) based on scour mean and standard deviation						
β = 0.5 (0.6915)	3.42	3.09	1.76	5.05	4.72	3.34
β = 1.0 (0.8413)	3.67	3.34	1.96	5.38	5.04	3.69
β = 1.5 (0.9332)	3.92	3.59	2.17	5.72	5.37	4.04
β = 2.0 (0.9772)	4.17	3.84	2.37	6.05	5.69	4.40
β = 2.5 (0.9938)	4.43	4.09	2.58	6.38	6.02	4.75
β = 3.0 (0.9987)	4.68	4.34	2.78	6.71	6.35	5.10
Scour factors based on scour mean and standard deviation						
β = 0.5 (0.6915)	0.73	0.82	1.04	0.79	0.86	0.83
β = 1.0 (0.8413)	0.79	0.88	1.16	0.85	0.92	0.92
β = 1.5 (0.9332)	0.84	0.95	1.28	0.90	0.98	1.01
β = 2.0 (0.9772)	0.90	1.02	1.40	0.95	1.04	1.09
β = 2.5 (0.9938)	0.95	1.08	1.52	1.00	1.10	1.18
β = 3.0 (0.9987)	1.00	1.15	1.64	1.06	1.16	1.27

Table A.3	Small Bridge - Low Hydrologic Uncertainty - Large Pier (3 ft)					
	Pier Scour (HEC-18)	Pier Scour (FDOT)	Contraction Scour	Total Scour (HEC-18)	Total Scour (FDOT)	Abutment Scour
Design Scour (ft)	6.06	5.17	1.70	7.76	6.87	4.02
Expected Scour (ft)	4.12	3.89	1.55	5.67	5.44	2.99
Bias	0.68	0.75	0.92	0.73	0.79	0.74
Std. Dev. (ft)	0.66	0.69	0.41	0.79	0.81	0.71
COV	0.16	0.18	0.26	0.14	0.15	0.24
Design Scour β	2.95	1.87	0.35	2.63	1.77	1.46
Non-Exceedance	0.9984	0.9695	0.6356	0.9958	0.9619	0.9281
Scour Non-Exceedance (ft) based on Monte Carlo results						
β = 0.5 (0.6915)	4.45	4.22	1.73	6.06	5.83	3.32
β = 1.0 (0.8413)	4.79	4.58	1.96	6.47	6.24	3.69
β = 1.5 (0.9332)	5.10	4.93	2.21	6.86	6.67	4.09
β = 2.0 (0.9772)	5.42	5.27	2.45	7.29	7.09	4.45
β = 2.5 (0.9938)	5.77	5.61	2.70	7.70	7.51	4.81
β = 3.0 (0.9987)	5.96	5.82	2.98	8.12	7.82	5.07
Scour factors based on Monte Carlo results						
β = 0.5 (0.6915)	0.73	0.82	1.02	0.78	0.85	0.83
β = 1.0 (0.8413)	0.79	0.89	1.16	0.83	0.91	0.92
β = 1.5 (0.9332)	0.84	0.95	1.30	0.89	0.97	1.02
β = 2.0 (0.9772)	0.90	1.02	1.44	0.94	1.03	1.11
β = 2.5 (0.9938)	0.95	1.09	1.59	0.99	1.09	1.20
β = 3.0 (0.9987)	0.98	1.12	1.76	1.05	1.14	1.26
Scour non-exceedance (ft) based on scour mean and standard deviation						
β = 0.5 (0.6915)	4.45	4.23	1.76	6.07	5.84	3.34
β = 1.0 (0.8413)	4.78	4.57	1.96	6.46	6.25	3.69
β = 1.5 (0.9332)	5.10	4.92	2.17	6.86	6.65	4.04
β = 2.0 (0.9772)	5.43	5.26	2.37	7.26	7.05	4.40
β = 2.5 (0.9938)	5.76	5.60	2.58	7.65	7.46	4.75
β = 3.0 (0.9987)	6.09	5.95	2.78	8.05	7.86	5.10
Scour factors based on scour mean and standard deviation						
β = 0.5 (0.6915)	0.73	0.82	1.04	0.78	0.85	0.83
β = 1.0 (0.8413)	0.79	0.88	1.16	0.83	0.91	0.92
β = 1.5 (0.9332)	0.84	0.95	1.28	0.88	0.97	1.01
β = 2.0 (0.9772)	0.90	1.02	1.40	0.94	1.03	1.09
β = 2.5 (0.9938)	0.95	1.08	1.52	0.99	1.09	1.18
β = 3.0 (0.9987)	1.01	1.15	1.64	1.04	1.14	1.27

Table A.4	Small Bridge - Medium Hydrologic Uncertainty - Small Pier (1 ft)					
	Pier Scour (HEC-18)	Pier Scour (FDOT)	Contraction Scour	Total Scour (HEC-18)	Total Scour (FDOT)	Abutment Scour
Design Scour (ft)	2.40	2.13	1.70	4.10	3.82	4.02
Expected Scour (ft)	1.63	1.60	1.58	3.21	3.17	2.99
Bias	0.68	0.75	0.93	0.78	0.83	0.74
Std. Dev. (ft)	0.26	0.29	0.46	0.53	0.55	0.73
COV	0.16	0.18	0.29	0.17	0.17	0.24
Design Scour β	2.96	1.84	0.26	1.67	1.18	1.42
Non-Exceedance	0.9985	0.9674	0.6020	0.9525	0.8819	0.9217
Scour Non-Exceedance (ft) based on Monte Carlo results						
β = 0.5 (0.6915)	1.77	1.74	1.78	3.45	3.42	3.33
β = 1.0 (0.8413)	1.90	1.89	2.04	3.74	3.72	3.72
β = 1.5 (0.9332)	2.02	2.03	2.32	4.04	4.04	4.10
β = 2.0 (0.9772)	2.14	2.18	2.63	4.37	4.35	4.48
β = 2.5 (0.9938)	2.26	2.31	2.95	4.68	4.68	4.94
β = 3.0 (0.9987)	2.35	2.40	3.29	4.94	5.02	5.34
Scour factors based on Monte Carlo results						
β = 0.5 (0.6915)	0.74	0.82	1.05	0.84	0.90	0.83
β = 1.0 (0.8413)	0.79	0.89	1.20	0.91	0.97	0.93
β = 1.5 (0.9332)	0.84	0.95	1.37	0.99	1.06	1.02
β = 2.0 (0.9772)	0.89	1.02	1.55	1.07	1.14	1.11
β = 2.5 (0.9938)	0.94	1.09	1.74	1.14	1.22	1.23
β = 3.0 (0.9987)	0.98	1.13	1.94	1.21	1.31	1.33
Scour non-exceedance (ft) based on scour mean and standard deviation						
β = 0.5 (0.6915)	1.76	1.74	1.81	3.47	3.45	3.35
β = 1.0 (0.8413)	1.89	1.88	2.04	3.74	3.72	3.72
β = 1.5 (0.9332)	2.02	2.03	2.27	4.01	4.00	4.08
β = 2.0 (0.9772)	2.15	2.17	2.50	4.27	4.27	4.44
β = 2.5 (0.9938)	2.28	2.32	2.74	4.54	4.54	4.81
β = 3.0 (0.9987)	2.41	2.46	2.97	4.80	4.82	5.17
Scour factors based on scour mean and standard deviation						
β = 0.5 (0.6915)	0.73	0.82	1.07	0.85	0.90	0.83
β = 1.0 (0.8413)	0.79	0.89	1.20	0.91	0.97	0.92
β = 1.5 (0.9332)	0.84	0.95	1.34	0.98	1.05	1.02
β = 2.0 (0.9772)	0.90	1.02	1.48	1.04	1.12	1.11
β = 2.5 (0.9938)	0.95	1.09	1.61	1.11	1.19	1.20
β = 3.0 (0.9987)	1.00	1.16	1.75	1.17	1.26	1.29

Table A.5	Small Bridge - Medium Hydrologic Uncertainty - Medium Pier (2 ft)					
	Pier Scour (HEC-18)	Pier Scour (FDOT)	Contraction Scour	Total Scour (HEC-18)	Total Scour (FDOT)	Abutment Scour
Design Scour (ft)	4.66	3.78	1.70	6.35	5.47	4.02
Expected Scour (ft)	3.16	2.84	1.58	4.74	4.41	2.99
Bias	0.68	0.75	0.93	0.75	0.81	0.74
Std. Dev. (ft)	0.51	0.51	0.46	0.71	0.70	0.73
COV	0.16	0.18	0.29	0.15	0.16	0.24
Design Scour β	2.95	1.84	0.26	2.27	1.52	1.42
Non-Exceedance	0.9984	0.9673	0.6020	0.9884	0.9352	0.9217
Scour Non-Exceedance (ft) based on Monte Carlo results						
β = 0.5 (0.6915)	3.42	3.10	1.78	5.08	4.75	3.33
β = 1.0 (0.8413)	3.68	3.35	2.04	5.45	5.12	3.72
β = 1.5 (0.9332)	3.93	3.61	2.32	5.84	5.50	4.10
β = 2.0 (0.9772)	4.16	3.87	2.63	6.22	5.87	4.48
β = 2.5 (0.9938)	4.37	4.11	2.95	6.58	6.22	4.94
β = 3.0 (0.9987)	4.57	4.27	3.29	6.91	6.65	5.34
Scour factors based on Monte Carlo results						
β = 0.5 (0.6915)	0.73	0.82	1.05	0.80	0.87	0.83
β = 1.0 (0.8413)	0.79	0.89	1.20	0.86	0.93	0.93
β = 1.5 (0.9332)	0.84	0.95	1.37	0.92	1.01	1.02
β = 2.0 (0.9772)	0.89	1.02	1.55	0.98	1.07	1.11
β = 2.5 (0.9938)	0.94	1.09	1.74	1.04	1.14	1.23
β = 3.0 (0.9987)	0.98	1.13	1.94	1.09	1.21	1.33
Scour non-exceedance (ft) based on scour mean and standard deviation						
β = 0.5 (0.6915)	3.42	3.09	1.81	5.09	4.76	3.35
β = 1.0 (0.8413)	3.67	3.35	2.04	5.45	5.11	3.72
β = 1.5 (0.9332)	3.92	3.60	2.27	5.80	5.46	4.08
β = 2.0 (0.9772)	4.18	3.86	2.50	6.16	5.81	4.44
β = 2.5 (0.9938)	4.43	4.11	2.74	6.52	6.16	4.81
β = 3.0 (0.9987)	4.68	4.37	2.97	6.87	6.51	5.17
Scour factors based on scour mean and standard deviation						
β = 0.5 (0.6915)	0.73	0.82	1.07	0.80	0.87	0.83
β = 1.0 (0.8413)	0.79	0.89	1.20	0.86	0.93	0.92
β = 1.5 (0.9332)	0.84	0.95	1.34	0.91	1.00	1.02
β = 2.0 (0.9772)	0.90	1.02	1.48	0.97	1.06	1.11
β = 2.5 (0.9938)	0.95	1.09	1.61	1.03	1.13	1.20
β = 3.0 (0.9987)	1.01	1.16	1.75	1.08	1.19	1.29

Table A.6	Small Bridge - Medium Hydrologic Uncertainty - Large Pier (3 ft)					
	Pier Scour (HEC-18)	Pier Scour (FDOT)	Contraction Scour	Total Scour (HEC-18)	Total Scour (FDOT)	Abutment Scour
Design Scour (ft)	6.06	5.17	1.70	7.76	6.87	4.02
Expected Scour (ft)	4.12	3.88	1.58	5.70	5.46	2.99
Bias	0.68	0.75	0.93	0.73	0.79	0.74
Std. Dev. (ft)	0.66	0.70	0.46	0.84	0.86	0.73
COV	0.16	0.18	0.29	0.15	0.16	0.24
Design Scour β	2.94	1.84	0.26	2.47	1.65	1.42
Non-Exceedance	0.9983	0.9672	0.6020	0.9932	0.9500	0.9217
Scour Non-Exceedance (ft) based on Monte Carlo results						
β = 0.5 (0.6915)	4.46	4.24	1.78	6.10	5.88	3.33
β = 1.0 (0.8413)	4.79	4.59	2.04	6.53	6.32	3.72
β = 1.5 (0.9332)	5.12	4.94	2.32	6.98	6.77	4.10
β = 2.0 (0.9772)	5.42	5.31	2.63	7.42	7.19	4.48
β = 2.5 (0.9938)	5.70	5.62	2.95	7.84	7.68	4.94
β = 3.0 (0.9987)	5.96	5.84	3.29	8.28	8.09	5.34
Scour factors based on Monte Carlo results						
β = 0.5 (0.6915)	0.74	0.82	1.05	0.79	0.86	0.83
β = 1.0 (0.8413)	0.79	0.89	1.20	0.84	0.92	0.93
β = 1.5 (0.9332)	0.85	0.95	1.37	0.90	0.99	1.02
β = 2.0 (0.9772)	0.89	1.03	1.55	0.96	1.05	1.11
β = 2.5 (0.9938)	0.94	1.09	1.74	1.01	1.12	1.23
β = 3.0 (0.9987)	0.98	1.13	1.94	1.07	1.18	1.33
Scour non-exceedance (ft) based on scour mean and standard deviation						
β = 0.5 (0.6915)	4.45	4.23	1.81	6.11	5.89	3.35
β = 1.0 (0.8413)	4.78	4.58	2.04	6.53	6.32	3.72
β = 1.5 (0.9332)	5.11	4.93	2.27	6.95	6.74	4.08
β = 2.0 (0.9772)	5.44	5.28	2.50	7.37	7.17	4.44
β = 2.5 (0.9938)	5.77	5.63	2.74	7.79	7.60	4.81
β = 3.0 (0.9987)	6.10	5.98	2.97	8.20	8.03	5.17
Scour factors based on scour mean and standard deviation						
β = 0.5 (0.6915)	0.73	0.82	1.07	0.79	0.86	0.83
β = 1.0 (0.8413)	0.79	0.89	1.20	0.84	0.92	0.92
β = 1.5 (0.9332)	0.84	0.95	1.34	0.90	0.98	1.02
β = 2.0 (0.9772)	0.90	1.02	1.48	0.95	1.04	1.11
β = 2.5 (0.9938)	0.95	1.09	1.61	1.00	1.11	1.20
β = 3.0 (0.9987)	1.01	1.16	1.75	1.06	1.17	1.29

Table A.7	Small Bridge - High Hydrologic Uncertainty - Small Pier (1 ft)					
	Pier Scour (HEC-18)	Pier Scour (FDOT)	Contraction Scour	Total Scour (HEC-18)	Total Scour (FDOT)	Abutment Scour
Design Scour (ft)	2.40	2.13	1.70	4.10	3.82	4.02
Expected Scour (ft)	1.63	1.60	1.58	3.21	3.18	3.01
Bias	0.68	0.75	0.93	0.78	0.83	0.75
Std. Dev. (ft)	0.26	0.28	0.55	0.61	0.63	0.78
COV	0.16	0.18	0.35	0.19	0.20	0.26
Design Scour β	2.99	1.87	0.20	1.45	1.03	1.29
Non-Exceedance	0.9986	0.9690	0.5806	0.9259	0.8481	0.9013
Scour Non-Exceedance (ft) based on Monte Carlo results						
β = 0.5 (0.6915)	1.76	1.74	1.80	3.47	3.44	3.37
β = 1.0 (0.8413)	1.89	1.88	2.12	3.81	3.80	3.78
β = 1.5 (0.9332)	2.02	2.03	2.47	4.20	4.17	4.23
β = 2.0 (0.9772)	2.14	2.16	2.89	4.57	4.58	4.71
β = 2.5 (0.9938)	2.26	2.30	3.30	5.04	5.05	5.15
β = 3.0 (0.9987)	2.35	2.41	3.82	5.53	5.56	5.69
Scour factors based on Monte Carlo results						
β = 0.5 (0.6915)	0.73	0.82	1.06	0.85	0.90	0.84
β = 1.0 (0.8413)	0.79	0.89	1.25	0.93	0.99	0.94
β = 1.5 (0.9332)	0.84	0.96	1.46	1.02	1.09	1.05
β = 2.0 (0.9772)	0.89	1.02	1.70	1.11	1.20	1.17
β = 2.5 (0.9938)	0.94	1.08	1.95	1.23	1.32	1.28
β = 3.0 (0.9987)	0.98	1.13	2.25	1.35	1.45	1.42
Scour non-exceedance (ft) based on scour mean and standard deviation						
β = 0.5 (0.6915)	1.76	1.74	1.86	3.52	3.49	3.40
β = 1.0 (0.8413)	1.89	1.88	2.13	3.82	3.81	3.79
β = 1.5 (0.9332)	2.02	2.02	2.41	4.13	4.12	4.18
β = 2.0 (0.9772)	2.15	2.16	2.68	4.43	4.43	4.57
β = 2.5 (0.9938)	2.27	2.31	2.96	4.74	4.74	4.96
β = 3.0 (0.9987)	2.40	2.45	3.24	5.04	5.06	5.35
Scour factors based on scour mean and standard deviation						
β = 0.5 (0.6915)	0.73	0.82	1.10	0.86	0.91	0.85
β = 1.0 (0.8413)	0.79	0.88	1.26	0.93	1.00	0.94
β = 1.5 (0.9332)	0.84	0.95	1.42	1.01	1.08	1.04
β = 2.0 (0.9772)	0.89	1.02	1.58	1.08	1.16	1.14
β = 2.5 (0.9938)	0.95	1.08	1.75	1.16	1.24	1.24
β = 3.0 (0.9987)	1.00	1.15	1.91	1.23	1.32	1.33

Table A.8	Small Bridge - High Hydrologic Uncertainty - Medium Pier (2 ft)					
	Pier Scour (HEC-18)	Pier Scour (FDOT)	Contraction Scour	Total Scour (HEC-18)	Total Scour (FDOT)	Abutment Scour
Design Scour (ft)	4.66	3.78	1.70	6.35	5.47	4.02
Expected Scour (ft)	3.16	2.83	1.58	4.74	4.42	3.01
Bias	0.68	0.75	0.93	0.75	0.81	0.75
Std. Dev. (ft)	0.51	0.51	0.55	0.79	0.77	0.78
COV	0.16	0.18	0.35	0.17	0.17	0.26
Design Scour β	2.97	1.86	0.20	2.05	1.38	1.29
Non-Exceedance	0.9985	0.9688	0.5806	0.9797	0.9154	0.9013
Scour Non-Exceedance (ft) based on Monte Carlo results						
β = 0.5 (0.6915)	3.41	3.09	1.80	5.10	4.77	3.37
β = 1.0 (0.8413)	3.67	3.35	2.12	5.52	5.17	3.78
β = 1.5 (0.9332)	3.93	3.61	2.47	5.98	5.62	4.23
β = 2.0 (0.9772)	4.17	3.86	2.89	6.41	6.07	4.71
β = 2.5 (0.9938)	4.40	4.09	3.30	6.94	6.53	5.15
β = 3.0 (0.9987)	4.61	4.27	3.82	7.49	7.15	5.69
Scour factors based on Monte Carlo results						
β = 0.5 (0.6915)	0.73	0.82	1.06	0.80	0.87	0.84
β = 1.0 (0.8413)	0.79	0.89	1.25	0.87	0.95	0.94
β = 1.5 (0.9332)	0.84	0.96	1.46	0.94	1.03	1.05
β = 2.0 (0.9772)	0.90	1.02	1.70	1.01	1.11	1.17
β = 2.5 (0.9938)	0.95	1.08	1.95	1.09	1.19	1.28
β = 3.0 (0.9987)	0.99	1.13	2.25	1.18	1.31	1.42
Scour non-exceedance (ft) based on scour mean and standard deviation						
β = 0.5 (0.6915)	3.41	3.09	1.86	5.13	4.80	3.40
β = 1.0 (0.8413)	3.66	3.34	2.13	5.53	5.19	3.79
β = 1.5 (0.9332)	3.91	3.59	2.41	5.92	5.57	4.18
β = 2.0 (0.9772)	4.17	3.85	2.68	6.32	5.95	4.57
β = 2.5 (0.9938)	4.42	4.10	2.96	6.71	6.34	4.96
β = 3.0 (0.9987)	4.67	4.35	3.24	7.10	6.72	5.35
Scour factors based on scour mean and standard deviation						
β = 0.5 (0.6915)	0.73	0.82	1.10	0.81	0.88	0.85
β = 1.0 (0.8413)	0.79	0.88	1.26	0.87	0.95	0.94
β = 1.5 (0.9332)	0.84	0.95	1.42	0.93	1.02	1.04
β = 2.0 (0.9772)	0.89	1.02	1.58	0.99	1.09	1.14
β = 2.5 (0.9938)	0.95	1.09	1.75	1.06	1.16	1.24
β = 3.0 (0.9987)	1.00	1.15	1.91	1.12	1.23	1.33

Table A.9	Small Bridge - High Hydrologic Uncertainty - Large Pier (3 ft)					
	Pier Scour (HEC-18)	Pier Scour (FDOT)	Contraction Scour	Total Scour (HEC-18)	Total Scour (FDOT)	Abutment Scour
Design Scour (ft)	6.06	5.17	1.70	7.76	6.87	4.02
Expected Scour (ft)	4.12	3.88	1.58	5.70	5.46	3.01
Bias	0.68	0.75	0.93	0.73	0.80	0.75
Std. Dev. (ft)	0.66	0.70	0.55	0.91	0.92	0.78
COV	0.16	0.18	0.35	0.16	0.17	0.26
Design Scour β	2.94	1.86	0.20	2.25	1.53	1.29
Non-Exceedance	0.9983	0.9684	0.5806	0.9878	0.9369	0.9013
Scour Non-Exceedance (ft) based on Monte Carlo results						
β = 0.5 (0.6915)	4.45	4.23	1.80	6.12	5.90	3.37
β = 1.0 (0.8413)	4.78	4.58	2.12	6.61	6.38	3.78
β = 1.5 (0.9332)	5.13	4.94	2.47	7.12	6.88	4.23
β = 2.0 (0.9772)	5.44	5.29	2.89	7.64	7.38	4.71
β = 2.5 (0.9938)	5.76	5.61	3.30	8.24	7.93	5.15
β = 3.0 (0.9987)	6.02	5.85	3.82	8.85	8.55	5.69
Scour factors based on Monte Carlo results						
β = 0.5 (0.6915)	0.73	0.82	1.06	0.79	0.86	0.84
β = 1.0 (0.8413)	0.79	0.89	1.25	0.85	0.93	0.94
β = 1.5 (0.9332)	0.85	0.96	1.46	0.92	1.00	1.05
β = 2.0 (0.9772)	0.90	1.02	1.70	0.98	1.07	1.17
β = 2.5 (0.9938)	0.95	1.09	1.95	1.06	1.15	1.28
β = 3.0 (0.9987)	0.99	1.13	2.25	1.14	1.24	1.42
Scour non-exceedance (ft) based on scour mean and standard deviation						
β = 0.5 (0.6915)	4.45	4.23	1.86	6.16	5.92	3.40
β = 1.0 (0.8413)	4.78	4.58	2.13	6.61	6.38	3.79
β = 1.5 (0.9332)	5.11	4.92	2.41	7.07	6.84	4.18
β = 2.0 (0.9772)	5.44	5.27	2.68	7.53	7.30	4.57
β = 2.5 (0.9938)	5.77	5.62	2.96	7.98	7.76	4.96
β = 3.0 (0.9987)	6.10	5.97	3.24	8.44	8.22	5.35
Scour factors based on scour mean and standard deviation						
β = 0.5 (0.6915)	0.73	0.82	1.10	0.79	0.86	0.85
β = 1.0 (0.8413)	0.79	0.88	1.26	0.85	0.93	0.94
β = 1.5 (0.9332)	0.84	0.95	1.42	0.91	1.00	1.04
β = 2.0 (0.9772)	0.90	1.02	1.58	0.97	1.06	1.14
β = 2.5 (0.9938)	0.95	1.09	1.75	1.03	1.13	1.24
β = 3.0 (0.9987)	1.01	1.15	1.91	1.09	1.20	1.33

Table A.10	Medium Bridge - Low Hydrologic Uncertainty - Small Pier (1.5 ft)					
	Pier Scour (HEC-18)	Pier Scour (FDOT)	Contraction Scour	Total Scour (HEC-18)	Total Scour (FDOT)	Abutment Scour
Design Scour (ft)	3.60	3.19	8.02	11.62	11.21	15.12
Expected Scour (ft)	2.45	2.39	7.36	9.81	9.75	11.23
Bias	0.68	0.75	0.92	0.84	0.87	0.74
Std. Dev. (ft)	0.39	0.43	2.21	2.25	2.26	2.88
COV	0.16	0.18	0.30	0.23	0.23	0.26
Design Scour β	2.95	1.85	0.30	0.81	0.65	1.35
Non-Exceedance	0.9984	0.9676	0.6170	0.7897	0.7406	0.9113
Scour Non-Exceedance (ft) based on Monte Carlo results						
β = 0.5 (0.6915)	2.65	2.61	8.34	10.80	10.78	12.58
β = 1.0 (0.8413)	2.84	2.84	9.59	12.10	12.01	14.09
β = 1.5 (0.9332)	3.04	3.04	10.84	13.31	13.28	15.66
β = 2.0 (0.9772)	3.23	3.26	12.30	14.75	14.76	17.31
β = 2.5 (0.9938)	3.43	3.46	13.65	16.17	16.15	19.27
β = 3.0 (0.9987)	3.54	3.61	15.15	17.50	17.65	20.87
Scour factors based on Monte Carlo results						
β = 0.5 (0.6915)	0.73	0.82	1.04	0.93	0.96	0.83
β = 1.0 (0.8413)	0.79	0.89	1.20	1.04	1.07	0.93
β = 1.5 (0.9332)	0.85	0.95	1.35	1.15	1.18	1.04
β = 2.0 (0.9772)	0.90	1.02	1.53	1.27	1.32	1.15
β = 2.5 (0.9938)	0.95	1.08	1.70	1.39	1.44	1.27
β = 3.0 (0.9987)	0.98	1.13	1.89	1.51	1.57	1.38
Scour non-exceedance (ft) based on scour mean and standard deviation						
β = 0.5 (0.6915)	2.64	2.61	8.46	10.93	10.88	12.67
β = 1.0 (0.8413)	2.84	2.83	9.57	12.05	12.01	14.11
β = 1.5 (0.9332)	3.04	3.04	10.68	13.18	13.14	15.55
β = 2.0 (0.9772)	3.23	3.26	11.78	14.30	14.27	17.00
β = 2.5 (0.9938)	3.43	3.47	12.89	15.42	15.40	18.44
β = 3.0 (0.9987)	3.62	3.69	14.00	16.55	16.52	19.88
Scour factors based on scour mean and standard deviation						
β = 0.5 (0.6915)	0.73	0.82	1.06	0.94	0.97	0.84
β = 1.0 (0.8413)	0.79	0.89	1.19	1.04	1.07	0.93
β = 1.5 (0.9332)	0.84	0.95	1.33	1.13	1.17	1.03
β = 2.0 (0.9772)	0.90	1.02	1.47	1.23	1.27	1.12
β = 2.5 (0.9938)	0.95	1.09	1.61	1.33	1.37	1.22
β = 3.0 (0.9987)	1.01	1.16	1.75	1.42	1.47	1.32

Table A.11	Medium Bridge - Low Hydrologic Uncertainty - Medium Pier (3 ft)					
	Pier Scour (HEC-18)	Pier Scour (FDOT)	Contraction Scour	Total Scour (HEC-18)	Total Scour (FDOT)	Abutment Scour
Design Scour (ft)	7.20	5.94	8.02	15.22	13.95	15.12
Expected Scour (ft)	4.90	4.45	7.36	12.26	11.81	11.23
Bias	0.68	0.75	0.92	0.81	0.85	0.74
Std. Dev. (ft)	0.78	0.81	2.21	2.34	2.37	2.88
COV	0.16	0.18	0.30	0.19	0.20	0.26
Design Scour β	2.95	1.84	0.30	1.26	0.90	1.35
Non-Exceedance	0.9984	0.9672	0.6170	0.8967	0.8168	0.9113
Scour Non-Exceedance (ft) based on Monte Carlo results						
β = 0.5 (0.6915)	5.29	4.87	8.34	13.31	12.90	12.58
β = 1.0 (0.8413)	5.68	5.27	9.59	14.62	14.20	14.09
β = 1.5 (0.9332)	6.09	5.66	10.84	15.94	15.50	15.66
β = 2.0 (0.9772)	6.46	6.06	12.30	17.42	17.02	17.31
β = 2.5 (0.9938)	6.86	6.45	13.65	18.80	18.47	19.27
β = 3.0 (0.9987)	7.08	6.71	15.15	20.33	20.18	20.87
Scour factors based on Monte Carlo results						
β = 0.5 (0.6915)	0.73	0.82	1.04	0.87	0.92	0.83
β = 1.0 (0.8413)	0.79	0.89	1.20	0.96	1.02	0.93
β = 1.5 (0.9332)	0.85	0.95	1.35	1.05	1.11	1.04
β = 2.0 (0.9772)	0.90	1.02	1.53	1.14	1.22	1.15
β = 2.5 (0.9938)	0.95	1.09	1.70	1.24	1.32	1.27
β = 3.0 (0.9987)	0.98	1.13	1.89	1.34	1.45	1.38
Scour non-exceedance (ft) based on scour mean and standard deviation						
β = 0.5 (0.6915)	5.29	4.86	8.46	13.43	12.99	12.67
β = 1.0 (0.8413)	5.68	5.26	9.57	14.60	14.18	14.11
β = 1.5 (0.9332)	6.07	5.66	10.68	15.77	15.37	15.55
β = 2.0 (0.9772)	6.46	6.06	11.78	16.94	16.55	17.00
β = 2.5 (0.9938)	6.85	6.47	12.89	18.12	17.74	18.44
β = 3.0 (0.9987)	7.24	6.87	14.00	19.29	18.93	19.88
Scour factors based on scour mean and standard deviation						
β = 0.5 (0.6915)	0.73	0.82	1.06	0.88	0.93	0.84
β = 1.0 (0.8413)	0.79	0.89	1.19	0.96	1.02	0.93
β = 1.5 (0.9332)	0.84	0.95	1.33	1.04	1.10	1.03
β = 2.0 (0.9772)	0.90	1.02	1.47	1.11	1.19	1.12
β = 2.5 (0.9938)	0.95	1.09	1.61	1.19	1.27	1.22
β = 3.0 (0.9987)	1.01	1.16	1.75	1.27	1.36	1.32

Table A.12	Medium Bridge - Low Hydrologic Uncertainty - Large Pier (4.5 ft)					
	Pier Scour (HEC-18)	Pier Scour (FDOT)	Contraction Scour	Total Scour (HEC-18)	Total Scour (FDOT)	Abutment Scour
Design Scour (ft)	10.35	8.44	8.02	18.37	16.45	15.12
Expected Scour (ft)	7.06	6.33	7.36	14.41	13.69	11.23
Bias	0.68	0.75	0.92	0.78	0.83	0.74
Std. Dev. (ft)	1.14	1.15	2.21	2.57	2.53	2.88
COV	0.16	0.18	0.30	0.18	0.18	0.26
Design Scour β	2.89	1.84	0.30	1.54	1.09	1.35
Non-Exceedance	0.9981	0.9670	0.6170	0.9380	0.8632	0.9113
Scour Non-Exceedance (ft) based on Monte Carlo results						
β = 0.5 (0.6915)	7.62	6.92	8.34	15.59	14.87	12.58
β = 1.0 (0.8413)	8.21	7.49	9.59	17.00	16.22	14.09
β = 1.5 (0.9332)	8.80	8.05	10.84	18.40	17.59	15.66
β = 2.0 (0.9772)	9.34	8.63	12.30	20.05	19.15	17.31
β = 2.5 (0.9938)	9.90	9.14	13.65	21.50	20.70	19.27
β = 3.0 (0.9987)	10.33	9.55	15.15	23.11	22.34	20.87
Scour factors based on Monte Carlo results						
β = 0.5 (0.6915)	0.74	0.82	1.04	0.85	0.90	0.83
β = 1.0 (0.8413)	0.79	0.89	1.20	0.93	0.99	0.93
β = 1.5 (0.9332)	0.85	0.95	1.35	1.00	1.07	1.04
β = 2.0 (0.9772)	0.90	1.02	1.53	1.09	1.16	1.15
β = 2.5 (0.9938)	0.96	1.08	1.70	1.17	1.26	1.27
β = 3.0 (0.9987)	1.00	1.13	1.89	1.26	1.36	1.38
Scour non-exceedance (ft) based on scour mean and standard deviation						
β = 0.5 (0.6915)	7.63	6.90	8.46	15.70	14.95	12.67
β = 1.0 (0.8413)	8.20	7.48	9.57	16.98	16.21	14.11
β = 1.5 (0.9332)	8.77	8.05	10.68	18.27	17.48	15.55
β = 2.0 (0.9772)	9.34	8.62	11.78	19.56	18.74	17.00
β = 2.5 (0.9938)	9.91	9.20	12.89	20.84	20.00	18.44
β = 3.0 (0.9987)	10.48	9.77	14.00	22.13	21.27	19.88
Scour factors based on scour mean and standard deviation						
β = 0.5 (0.6915)	0.74	0.82	1.06	0.85	0.91	0.84
β = 1.0 (0.8413)	0.79	0.89	1.19	0.92	0.99	0.93
β = 1.5 (0.9332)	0.85	0.95	1.33	0.99	1.06	1.03
β = 2.0 (0.9772)	0.90	1.02	1.47	1.06	1.14	1.12
β = 2.5 (0.9938)	0.96	1.09	1.61	1.13	1.22	1.22
β = 3.0 (0.9987)	1.01	1.16	1.75	1.20	1.29	1.32

Table A.13	Medium Bridge - Medium Hydrologic Uncertainty - Small Pier (1.5 ft)					
	Pier Scour (HEC-18)	Pier Scour (FDOT)	Contraction Scour	Total Scour (HEC-18)	Total Scour (FDOT)	Abutment Scour
Design Scour (ft)	3.60	3.19	8.02	11.62	11.21	15.12
Expected Scour (ft)	2.45	2.39	7.42	9.87	9.81	11.35
Bias	0.68	0.75	0.93	0.85	0.88	0.75
Std. Dev. (ft)	0.39	0.42	2.74	2.78	2.78	3.18
COV	0.16	0.18	0.37	0.28	0.28	0.28
Design Scour β	2.99	1.90	0.22	0.63	0.50	1.18
Non-Exceedance	0.9986	0.9713	0.5857	0.7353	0.6923	0.8818
Scour Non-Exceedance (ft) based on Monte Carlo results						
β = 0.5 (0.6915)	2.64	2.60	8.60	11.07	11.02	12.77
β = 1.0 (0.8413)	2.84	2.82	10.17	12.66	12.61	14.55
β = 1.5 (0.9332)	3.03	3.03	11.89	14.36	14.31	16.38
β = 2.0 (0.9772)	3.22	3.23	13.56	16.08	16.04	18.21
β = 2.5 (0.9938)	3.37	3.41	15.50	18.02	17.89	20.54
β = 3.0 (0.9987)	3.48	3.56	17.24	19.79	19.79	22.31
Scour factors based on Monte Carlo results						
β = 0.5 (0.6915)	0.73	0.82	1.07	0.95	0.98	0.84
β = 1.0 (0.8413)	0.79	0.88	1.27	1.09	1.13	0.96
β = 1.5 (0.9332)	0.84	0.95	1.48	1.24	1.28	1.08
β = 2.0 (0.9772)	0.89	1.01	1.69	1.38	1.43	1.20
β = 2.5 (0.9938)	0.94	1.07	1.93	1.55	1.60	1.36
β = 3.0 (0.9987)	0.97	1.12	2.15	1.70	1.77	1.48
Scour non-exceedance (ft) based on scour mean and standard deviation						
β = 0.5 (0.6915)	2.64	2.60	8.79	11.26	11.20	12.94
β = 1.0 (0.8413)	2.83	2.81	10.16	12.65	12.59	14.53
β = 1.5 (0.9332)	3.02	3.02	11.53	14.03	13.98	16.12
β = 2.0 (0.9772)	3.22	3.23	12.91	15.42	15.37	17.72
β = 2.5 (0.9938)	3.41	3.45	14.28	16.81	16.76	19.31
β = 3.0 (0.9987)	3.60	3.66	15.65	18.20	18.15	20.90
Scour factors based on scour mean and standard deviation						
β = 0.5 (0.6915)	0.73	0.81	1.10	0.97	1.00	0.86
β = 1.0 (0.8413)	0.79	0.88	1.27	1.09	1.12	0.96
β = 1.5 (0.9332)	0.84	0.95	1.44	1.21	1.25	1.07
β = 2.0 (0.9772)	0.89	1.01	1.61	1.33	1.37	1.17
β = 2.5 (0.9938)	0.95	1.08	1.78	1.45	1.50	1.28
β = 3.0 (0.9987)	1.00	1.15	1.95	1.57	1.62	1.38

Table A.14	Medium Bridge - Medium Hydrologic Uncertainty - Medium Pier (3 ft)					
	Pier Scour (HEC-18)	Pier Scour (FDOT)	Contraction Scour	Total Scour (HEC-18)	Total Scour (FDOT)	Abutment Scour
Design Scour (ft)	7.20	5.94	8.02	15.22	13.95	15.12
Expected Scour (ft)	4.89	4.45	7.42	12.31	11.87	11.35
Bias	0.68	0.75	0.93	0.81	0.85	0.75
Std. Dev. (ft)	0.77	0.79	2.74	2.86	2.89	3.18
COV	0.16	0.18	0.37	0.23	0.24	0.28
Design Scour β	2.99	1.89	0.22	1.01	0.72	1.18
Non-Exceedance	0.9986	0.9706	0.5857	0.8444	0.7648	0.8818
Scour Non-Exceedance (ft) based on Monte Carlo results						
β = 0.5 (0.6915)	5.29	4.85	8.60	13.58	13.13	12.77
β = 1.0 (0.8413)	5.68	5.24	10.17	15.18	14.76	14.55
β = 1.5 (0.9332)	6.05	5.63	11.89	16.90	16.47	16.38
β = 2.0 (0.9772)	6.44	6.01	13.56	18.69	18.28	18.21
β = 2.5 (0.9938)	6.73	6.37	15.50	20.73	20.21	20.54
β = 3.0 (0.9987)	6.96	6.62	17.24	22.54	22.19	22.31
Scour factors based on Monte Carlo results						
β = 0.5 (0.6915)	0.73	0.82	1.07	0.89	0.94	0.84
β = 1.0 (0.8413)	0.79	0.88	1.27	1.00	1.06	0.96
β = 1.5 (0.9332)	0.84	0.95	1.48	1.11	1.18	1.08
β = 2.0 (0.9772)	0.89	1.01	1.69	1.23	1.31	1.20
β = 2.5 (0.9938)	0.94	1.07	1.93	1.36	1.45	1.36
β = 3.0 (0.9987)	0.97	1.11	2.15	1.48	1.59	1.48
Scour non-exceedance (ft) based on scour mean and standard deviation						
β = 0.5 (0.6915)	5.28	4.84	8.79	13.75	13.31	12.94
β = 1.0 (0.8413)	5.66	5.23	10.16	15.18	14.75	14.53
β = 1.5 (0.9332)	6.05	5.63	11.53	16.61	16.20	16.12
β = 2.0 (0.9772)	6.43	6.02	12.91	18.04	17.64	17.72
β = 2.5 (0.9938)	6.82	6.42	14.28	19.48	19.08	19.31
β = 3.0 (0.9987)	7.20	6.81	15.65	20.91	20.53	20.90
Scour factors based on scour mean and standard deviation						
β = 0.5 (0.6915)	0.73	0.82	1.10	0.90	0.95	0.86
β = 1.0 (0.8413)	0.79	0.88	1.27	1.00	1.06	0.96
β = 1.5 (0.9332)	0.84	0.95	1.44	1.09	1.16	1.07
β = 2.0 (0.9772)	0.89	1.01	1.61	1.19	1.26	1.17
β = 2.5 (0.9938)	0.95	1.08	1.78	1.28	1.37	1.28
β = 3.0 (0.9987)	1.00	1.15	1.95	1.37	1.47	1.38

Table A.15	Medium Bridge - Medium Hydrologic Uncertainty - Large Pier (4.5 ft)					
	Pier Scour (HEC-18)	Pier Scour (FDOT)	Contraction Scour	Total Scour (HEC-18)	Total Scour (FDOT)	Abutment Scour
Design Scour (ft)	10.35	8.44	8.02	18.37	16.45	15.12
Expected Scour (ft)	7.05	6.32	7.42	14.47	13.74	11.35
Bias	0.68	0.75	0.93	0.79	0.84	0.75
Std. Dev. (ft)	1.13	1.12	2.74	3.13	3.03	3.18
COV	0.16	0.18	0.37	0.22	0.22	0.28
Design Scour β	2.91	1.88	0.22	1.25	0.89	1.18
Non-Exceedance	0.9982	0.9701	0.5857	0.8935	0.8143	0.8818
Scour Non-Exceedance (ft) based on Monte Carlo results						
β = 0.5 (0.6915)	7.64	6.90	8.60	15.86	15.09	12.77
β = 1.0 (0.8413)	8.19	7.46	10.17	17.65	16.79	14.55
β = 1.5 (0.9332)	8.77	8.00	11.89	19.43	18.56	16.38
β = 2.0 (0.9772)	9.34	8.55	13.56	21.32	20.40	18.21
β = 2.5 (0.9938)	9.79	9.06	15.50	23.34	22.41	20.54
β = 3.0 (0.9987)	10.26	9.44	17.24	25.29	24.82	22.31
Scour factors based on Monte Carlo results						
β = 0.5 (0.6915)	0.74	0.82	1.07	0.86	0.92	0.84
β = 1.0 (0.8413)	0.79	0.88	1.27	0.96	1.02	0.96
β = 1.5 (0.9332)	0.85	0.95	1.48	1.06	1.13	1.08
β = 2.0 (0.9772)	0.90	1.01	1.69	1.16	1.24	1.20
β = 2.5 (0.9938)	0.95	1.07	1.93	1.27	1.36	1.36
β = 3.0 (0.9987)	0.99	1.12	2.15	1.38	1.51	1.48
Scour non-exceedance (ft) based on scour mean and standard deviation						
β = 0.5 (0.6915)	7.62	6.88	8.79	16.04	15.26	12.94
β = 1.0 (0.8413)	8.18	7.45	10.16	17.60	16.77	14.53
β = 1.5 (0.9332)	8.75	8.01	11.53	19.16	18.29	16.12
β = 2.0 (0.9772)	9.32	8.57	12.91	20.73	19.80	17.72
β = 2.5 (0.9938)	9.89	9.13	14.28	22.29	21.32	19.31
β = 3.0 (0.9987)	10.45	9.69	15.65	23.86	22.84	20.90
Scour factors based on scour mean and standard deviation						
β = 0.5 (0.6915)	0.74	0.82	1.10	0.87	0.93	0.86
β = 1.0 (0.8413)	0.79	0.88	1.27	0.96	1.02	0.96
β = 1.5 (0.9332)	0.85	0.95	1.44	1.04	1.11	1.07
β = 2.0 (0.9772)	0.90	1.02	1.61	1.13	1.20	1.17
β = 2.5 (0.9938)	0.96	1.08	1.78	1.21	1.30	1.28
β = 3.0 (0.9987)	1.01	1.15	1.95	1.30	1.39	1.38

Table A.16	Medium Bridge - High Hydrologic Uncertainty - Small Pier (1.5 ft)					
	Pier Scour (HEC-18)	Pier Scour (FDOT)	Contraction Scour	Total Scour (HEC-18)	Total Scour (FDOT)	Abutment Scour
Design Scour (ft)	3.60	3.19	8.02	11.62	11.21	15.12
Expected Scour (ft)	2.46	2.40	7.40	9.85	9.80	11.40
Bias	0.68	0.75	0.92	0.85	0.87	0.75
Std. Dev. (ft)	0.39	0.43	3.26	3.28	3.30	3.51
COV	0.16	0.18	0.44	0.33	0.34	0.31
Design Scour β	2.94	1.85	0.19	0.54	0.43	1.06
Non-Exceedance	0.9984	0.9679	0.5754	0.7046	0.6656	0.8553
Scour Non-Exceedance (ft) based on Monte Carlo results						
β = 0.5 (0.6915)	2.65	2.61	8.77	11.22	11.18	12.87
β = 1.0 (0.8413)	2.84	2.83	10.60	13.10	13.05	14.83
β = 1.5 (0.9332)	3.04	3.05	12.52	15.04	15.03	16.99
β = 2.0 (0.9772)	3.24	3.27	14.84	17.33	17.33	19.44
β = 2.5 (0.9938)	3.43	3.47	17.67	20.00	20.00	22.33
β = 3.0 (0.9987)	3.56	3.58	19.84	22.36	22.32	25.51
Scour factors based on Monte Carlo results						
β = 0.5 (0.6915)	0.74	0.82	1.09	0.97	1.00	0.85
β = 1.0 (0.8413)	0.79	0.89	1.32	1.13	1.16	0.98
β = 1.5 (0.9332)	0.84	0.96	1.56	1.29	1.34	1.12
β = 2.0 (0.9772)	0.90	1.02	1.85	1.49	1.55	1.29
β = 2.5 (0.9938)	0.95	1.09	2.21	1.72	1.78	1.48
β = 3.0 (0.9987)	0.99	1.12	2.47	1.93	1.99	1.69
Scour non-exceedance (ft) based on scour mean and standard deviation						
β = 0.5 (0.6915)	2.65	2.61	9.02	11.49	11.45	13.16
β = 1.0 (0.8413)	2.84	2.83	10.65	13.13	13.09	14.91
β = 1.5 (0.9332)	3.04	3.04	12.28	14.77	14.74	16.67
β = 2.0 (0.9772)	3.23	3.25	13.91	16.42	16.39	18.42
β = 2.5 (0.9938)	3.43	3.47	15.54	18.06	18.04	20.18
β = 3.0 (0.9987)	3.62	3.68	17.17	19.70	19.69	21.93
Scour factors based on scour mean and standard deviation						
β = 0.5 (0.6915)	0.74	0.82	1.13	0.99	1.02	0.87
β = 1.0 (0.8413)	0.79	0.89	1.33	1.13	1.17	0.99
β = 1.5 (0.9332)	0.84	0.95	1.53	1.27	1.32	1.10
β = 2.0 (0.9772)	0.90	1.02	1.74	1.41	1.46	1.22
β = 2.5 (0.9938)	0.95	1.09	1.94	1.55	1.61	1.33
β = 3.0 (0.9987)	1.01	1.15	2.14	1.70	1.76	1.45

Table A.17	Medium Bridge - High Hydrologic Uncertainty - Medium Pier (3 ft)					
	Pier Scour (HEC-18)	Pier Scour (FDOT)	Contraction Scour	Total Scour (HEC-18)	Total Scour (FDOT)	Abutment Scour
Design Scour (ft)	7.20	5.94	8.02	15.22	13.95	15.12
Expected Scour (ft)	4.91	4.47	7.40	12.31	11.87	11.40
Bias	0.68	0.75	0.92	0.81	0.85	0.75
Std. Dev. (ft)	0.78	0.80	3.26	3.35	3.41	3.51
COV	0.16	0.18	0.44	0.27	0.29	0.31
Design Scour β	2.94	1.83	0.19	0.87	0.61	1.06
Non-Exceedance	0.9984	0.9667	0.5754	0.8073	0.7295	0.8553
Scour Non-Exceedance (ft) based on Monte Carlo results						
β = 0.5 (0.6915)	5.30	4.86	8.77	13.74	13.32	12.87
β = 1.0 (0.8413)	5.69	5.27	10.60	15.63	15.25	14.83
β = 1.5 (0.9332)	6.07	5.69	12.52	17.62	17.25	16.99
β = 2.0 (0.9772)	6.47	6.09	14.84	19.93	19.60	19.44
β = 2.5 (0.9938)	6.85	6.50	17.67	22.53	22.32	22.33
β = 3.0 (0.9987)	7.13	6.73	19.84	24.89	24.68	25.51
Scour factors based on Monte Carlo results						
β = 0.5 (0.6915)	0.74	0.82	1.09	0.90	0.95	0.85
β = 1.0 (0.8413)	0.79	0.89	1.32	1.03	1.09	0.98
β = 1.5 (0.9332)	0.84	0.96	1.56	1.16	1.24	1.12
β = 2.0 (0.9772)	0.90	1.03	1.85	1.31	1.41	1.29
β = 2.5 (0.9938)	0.95	1.09	2.21	1.48	1.60	1.48
β = 3.0 (0.9987)	0.99	1.13	2.47	1.64	1.77	1.69
Scour non-exceedance (ft) based on scour mean and standard deviation						
β = 0.5 (0.6915)	5.30	4.87	9.02	13.98	13.57	13.16
β = 1.0 (0.8413)	5.69	5.27	10.65	15.66	15.28	14.91
β = 1.5 (0.9332)	6.08	5.67	12.28	17.33	16.98	16.67
β = 2.0 (0.9772)	6.47	6.07	13.91	19.01	18.69	18.42
β = 2.5 (0.9938)	6.86	6.47	15.54	20.69	20.40	20.18
β = 3.0 (0.9987)	7.25	6.87	17.17	22.36	22.10	21.93
Scour factors based on scour mean and standard deviation						
β = 0.5 (0.6915)	0.74	0.82	1.13	0.92	0.97	0.87
β = 1.0 (0.8413)	0.79	0.89	1.33	1.03	1.10	0.99
β = 1.5 (0.9332)	0.84	0.95	1.53	1.14	1.22	1.10
β = 2.0 (0.9772)	0.90	1.02	1.74	1.25	1.34	1.22
β = 2.5 (0.9938)	0.95	1.09	1.94	1.36	1.46	1.33
β = 3.0 (0.9987)	1.01	1.16	2.14	1.47	1.58	1.45

Table A.18	Medium Bridge - High Hydrologic Uncertainty - Large Pier (4.5 ft)					
	Pier Scour (HEC-18)	Pier Scour (FDOT)	Contraction Scour	Total Scour (HEC-18)	Total Scour (FDOT)	Abutment Scour
Design Scour (ft)	10.35	8.44	8.02	18.37	16.45	15.12
Expected Scour (ft)	7.06	6.36	7.40	14.46	13.75	11.40
Bias	0.68	0.75	0.92	0.79	0.84	0.75
Std. Dev. (ft)	1.15	1.14	3.26	3.64	3.56	3.51
COV	0.16	0.18	0.44	0.25	0.26	0.31
Design Scour β	2.87	1.82	0.19	1.08	0.76	1.06
Non-Exceedance	0.9979	0.9658	0.5754	0.8589	0.7756	0.8553
Scour Non-Exceedance (ft) based on Monte Carlo results						
β = 0.5 (0.6915)	7.64	6.92	8.77	16.06	15.30	12.87
β = 1.0 (0.8413)	8.23	7.51	10.60	18.08	17.27	14.83
β = 1.5 (0.9332)	8.78	8.10	12.52	20.21	19.30	16.99
β = 2.0 (0.9772)	9.39	8.69	14.84	22.54	21.72	19.44
β = 2.5 (0.9938)	10.03	9.25	17.67	25.07	24.58	22.33
β = 3.0 (0.9987)	10.45	9.64	19.84	27.20	27.00	25.51
Scour factors based on Monte Carlo results						
β = 0.5 (0.6915)	0.74	0.82	1.09	0.87	0.93	0.85
β = 1.0 (0.8413)	0.79	0.89	1.32	0.98	1.05	0.98
β = 1.5 (0.9332)	0.85	0.96	1.56	1.10	1.17	1.12
β = 2.0 (0.9772)	0.91	1.03	1.85	1.23	1.32	1.29
β = 2.5 (0.9938)	0.97	1.10	2.21	1.36	1.49	1.48
β = 3.0 (0.9987)	1.01	1.14	2.47	1.48	1.64	1.69
Scour non-exceedance (ft) based on scour mean and standard deviation						
β = 0.5 (0.6915)	7.63	6.93	9.02	16.27	15.53	13.16
β = 1.0 (0.8413)	8.21	7.50	10.65	18.09	17.32	14.91
β = 1.5 (0.9332)	8.78	8.07	12.28	19.91	19.10	16.67
β = 2.0 (0.9772)	9.36	8.64	13.91	21.73	20.88	18.42
β = 2.5 (0.9938)	9.93	9.21	15.54	23.55	22.66	20.18
β = 3.0 (0.9987)	10.51	9.78	17.17	25.37	24.44	21.93
Scour factors based on scour mean and standard deviation						
β = 0.5 (0.6915)	0.74	0.82	1.13	0.89	0.94	0.87
β = 1.0 (0.8413)	0.79	0.89	1.33	0.99	1.05	0.99
β = 1.5 (0.9332)	0.85	0.96	1.53	1.08	1.16	1.10
β = 2.0 (0.9772)	0.90	1.02	1.74	1.18	1.27	1.22
β = 2.5 (0.9938)	0.96	1.09	1.94	1.28	1.38	1.33
β = 3.0 (0.9987)	1.01	1.16	2.14	1.38	1.49	1.45

Table A.19	Large Bridge - Low Hydrologic Uncertainty - Small Pier (3 ft)					
	Pier Scour (HEC-18)	Pier Scour (FDOT)	Contraction Scour	Total Scour (HEC-18)	Total Scour (FDOT)	Abutment Scour
Design Scour (ft)	7.20	6.10	5.29	12.49	11.39	10.96
Expected Scour (ft)	4.90	4.56	4.95	9.85	9.51	8.28
Bias	0.68	0.75	0.93	0.79	0.83	0.76
Std. Dev. (ft)	0.78	0.81	1.93	2.08	2.11	3.24
COV	0.16	0.18	0.39	0.21	0.22	0.39
Design Scour β	2.97	1.90	0.18	1.28	0.89	0.83
Non-Exceedance	0.9985	0.9712	0.5711	0.8990	0.8140	0.7961
Scour Non-Exceedance (ft) based on Monte Carlo results						
β = 0.5 (0.6915)	5.29	4.96	5.74	10.74	10.42	9.57
β = 1.0 (0.8413)	5.69	5.38	6.86	11.89	11.59	11.47
β = 1.5 (0.9332)	6.07	5.76	8.05	13.16	12.84	13.56
β = 2.0 (0.9772)	6.44	6.19	9.35	14.46	14.21	15.70
β = 2.5 (0.9938)	6.79	6.60	10.79	15.87	15.65	18.25
β = 3.0 (0.9987)	7.10	6.85	12.55	17.68	17.62	21.51
Scour factors based on Monte Carlo results						
β = 0.5 (0.6915)	0.73	0.81	1.08	0.86	0.91	0.87
β = 1.0 (0.8413)	0.79	0.88	1.30	0.95	1.02	1.05
β = 1.5 (0.9332)	0.84	0.95	1.52	1.05	1.13	1.24
β = 2.0 (0.9772)	0.89	1.02	1.77	1.16	1.25	1.43
β = 2.5 (0.9938)	0.94	1.08	2.04	1.27	1.37	1.66
β = 3.0 (0.9987)	0.99	1.12	2.37	1.41	1.55	1.96
Scour non-exceedance (ft) based on scour mean and standard deviation						
β = 0.5 (0.6915)	5.28	4.96	5.91	10.88	10.56	9.90
β = 1.0 (0.8413)	5.67	5.37	6.88	11.92	11.62	11.52
β = 1.5 (0.9332)	6.06	5.77	7.84	12.96	12.67	13.14
β = 2.0 (0.9772)	6.45	6.18	8.80	14.00	13.73	14.76
β = 2.5 (0.9938)	6.84	6.58	9.76	15.04	14.78	16.39
β = 3.0 (0.9987)	7.22	6.99	10.73	16.07	15.84	18.01
Scour factors based on scour mean and standard deviation						
β = 0.5 (0.6915)	0.73	0.81	1.12	0.87	0.93	0.90
β = 1.0 (0.8413)	0.79	0.88	1.30	0.95	1.02	1.05
β = 1.5 (0.9332)	0.84	0.95	1.48	1.04	1.11	1.20
β = 2.0 (0.9772)	0.90	1.01	1.66	1.12	1.21	1.35
β = 2.5 (0.9938)	0.95	1.08	1.84	1.20	1.30	1.49
β = 3.0 (0.9987)	1.00	1.15	2.03	1.29	1.39	1.64

Table A.20	Large Bridge - Low Hydrologic Uncertainty - Medium Pier (6 ft)					
	Pier Scour (HEC-18)	Pier Scour (FDOT)	Contraction Scour	Total Scour (HEC-18)	Total Scour (FDOT)	Abutment Scour
Design Scour (ft)	13.77	11.28	5.29	19.07	16.57	10.96
Expected Scour (ft)	9.35	8.43	4.95	14.30	13.38	8.28
Bias	0.68	0.75	0.93	0.75	0.81	0.76
Std. Dev. (ft)	1.51	1.50	1.93	2.58	2.50	3.24
COV	0.16	0.18	0.39	0.18	0.19	0.39
Design Scour β	2.94	1.89	0.18	1.85	1.28	0.83
Non-Exceedance	0.9983	0.9707	0.5711	0.9677	0.8990	0.7961
Scour Non-Exceedance (ft) based on Monte Carlo results						
β = 0.5 (0.6915)	10.11	9.18	5.74	15.50	14.56	9.57
β = 1.0 (0.8413)	10.88	9.95	6.86	16.88	15.87	11.47
β = 1.5 (0.9332)	11.62	10.68	8.05	18.30	17.26	13.56
β = 2.0 (0.9772)	12.33	11.47	9.35	19.82	18.81	15.70
β = 2.5 (0.9938)	13.03	12.21	10.79	21.28	20.34	18.25
β = 3.0 (0.9987)	13.57	12.73	12.55	22.99	22.31	21.51
Scour factors based on Monte Carlo results						
β = 0.5 (0.6915)	0.73	0.81	1.08	0.81	0.88	0.87
β = 1.0 (0.8413)	0.79	0.88	1.30	0.89	0.96	1.05
β = 1.5 (0.9332)	0.84	0.95	1.52	0.96	1.04	1.24
β = 2.0 (0.9772)	0.90	1.02	1.77	1.04	1.13	1.43
β = 2.5 (0.9938)	0.95	1.08	2.04	1.12	1.23	1.66
β = 3.0 (0.9987)	0.99	1.13	2.37	1.21	1.35	1.96
Scour non-exceedance (ft) based on scour mean and standard deviation						
β = 0.5 (0.6915)	10.10	9.19	5.91	15.59	14.63	9.90
β = 1.0 (0.8413)	10.86	9.94	6.88	16.88	15.88	11.52
β = 1.5 (0.9332)	11.61	10.69	7.84	18.17	17.13	13.14
β = 2.0 (0.9772)	12.36	11.44	8.80	19.46	18.38	14.76
β = 2.5 (0.9938)	13.12	12.19	9.76	20.75	19.63	16.39
β = 3.0 (0.9987)	13.87	12.94	10.73	22.04	20.88	18.01
Scour factors based on scour mean and standard deviation						
β = 0.5 (0.6915)	0.73	0.81	1.12	0.82	0.88	0.90
β = 1.0 (0.8413)	0.79	0.88	1.30	0.89	0.96	1.05
β = 1.5 (0.9332)	0.84	0.95	1.48	0.95	1.03	1.20
β = 2.0 (0.9772)	0.90	1.01	1.66	1.02	1.11	1.35
β = 2.5 (0.9938)	0.95	1.08	1.84	1.09	1.18	1.49
β = 3.0 (0.9987)	1.01	1.15	2.03	1.16	1.26	1.64

Table A.21	Large Bridge - Low Hydrologic Uncertainty - Large Pier (9 ft)					
	Pier Scour (HEC-18)	Pier Scour (FDOT)	Contraction Scour	Total Scour (HEC-18)	Total Scour (FDOT)	Abutment Scour
Design Scour (ft)	17.93	15.90	5.29	23.22	21.19	10.96
Expected Scour (ft)	12.19	11.89	4.95	17.14	16.84	8.28
Bias	0.68	0.75	0.93	0.74	0.79	0.76
Std. Dev. (ft)	1.97	2.13	1.93	2.93	2.96	3.24
COV	0.16	0.18	0.39	0.17	0.18	0.39
Design Scour β	2.91	1.89	0.18	2.08	1.47	0.83
Non-Exceedance	0.9982	0.9704	0.5711	0.9811	0.9296	0.7961
Scour Non-Exceedance (ft) based on Monte Carlo results						
β = 0.5 (0.6915)	13.18	12.95	5.74	18.55	18.27	9.57
β = 1.0 (0.8413)	14.19	14.03	6.86	20.07	19.79	11.47
β = 1.5 (0.9332)	15.16	15.08	8.05	21.62	21.32	13.56
β = 2.0 (0.9772)	16.11	16.20	9.35	23.31	23.08	15.70
β = 2.5 (0.9938)	17.00	17.21	10.79	25.16	24.93	18.25
β = 3.0 (0.9987)	17.72	17.95	12.55	26.86	26.66	21.51
Scour factors based on Monte Carlo results						
β = 0.5 (0.6915)	0.74	0.81	1.08	0.80	0.86	0.87
β = 1.0 (0.8413)	0.79	0.88	1.30	0.86	0.93	1.05
β = 1.5 (0.9332)	0.85	0.95	1.52	0.93	1.01	1.24
β = 2.0 (0.9772)	0.90	1.02	1.77	1.00	1.09	1.43
β = 2.5 (0.9938)	0.95	1.08	2.04	1.08	1.18	1.66
β = 3.0 (0.9987)	0.99	1.13	2.37	1.16	1.26	1.96
Scour non-exceedance (ft) based on scour mean and standard deviation						
β = 0.5 (0.6915)	13.18	12.95	5.91	18.60	18.32	9.90
β = 1.0 (0.8413)	14.16	14.02	6.88	20.07	19.80	11.52
β = 1.5 (0.9332)	15.15	15.08	7.84	21.53	21.27	13.14
β = 2.0 (0.9772)	16.13	16.14	8.80	23.00	22.75	14.76
β = 2.5 (0.9938)	17.12	17.20	9.76	24.46	24.23	16.39
β = 3.0 (0.9987)	18.10	18.27	10.73	25.93	25.71	18.01
Scour factors based on scour mean and standard deviation						
β = 0.5 (0.6915)	0.73	0.81	1.12	0.80	0.86	0.90
β = 1.0 (0.8413)	0.79	0.88	1.30	0.86	0.93	1.05
β = 1.5 (0.9332)	0.84	0.95	1.48	0.93	1.00	1.20
β = 2.0 (0.9772)	0.90	1.02	1.66	0.99	1.07	1.35
β = 2.5 (0.9938)	0.95	1.08	1.84	1.05	1.14	1.49
β = 3.0 (0.9987)	1.01	1.15	2.03	1.12	1.21	1.64

Table A.22	Large Bridge - Medium Hydrologic Uncertainty - Small Pier (3 ft)					
	Pier Scour (HEC-18)	Pier Scour (FDOT)	Contraction Scour	Total Scour (HEC-18)	Total Scour (FDOT)	Abutment Scour
Design Scour (ft)	7.20	6.10	5.29	12.49	11.39	10.96
Expected Scour (ft)	4.89	4.57	5.09	9.98	9.66	8.50
Bias	0.68	0.75	0.96	0.80	0.85	0.78
Std. Dev. (ft)	0.77	0.82	2.56	2.67	2.72	4.30
COV	0.16	0.18	0.50	0.27	0.28	0.51
Design Scour β	2.99	1.87	0.08	0.94	0.64	0.57
Non-Exceedance	0.9986	0.9691	0.5322	0.8274	0.7379	0.7165
Scour Non-Exceedance (ft) based on Monte Carlo results						
β = 0.5 (0.6915)	5.28	4.99	6.08	11.04	10.76	9.96
β = 1.0 (0.8413)	5.67	5.40	7.58	12.61	12.34	12.57
β = 1.5 (0.9332)	6.06	5.81	9.31	14.32	14.06	15.55
β = 2.0 (0.9772)	6.43	6.20	11.20	16.24	15.93	19.09
β = 2.5 (0.9938)	6.76	6.56	13.22	18.19	18.01	22.78
β = 3.0 (0.9987)	7.04	6.88	15.22	20.40	20.15	26.69
Scour factors based on Monte Carlo results						
β = 0.5 (0.6915)	0.73	0.82	1.15	0.88	0.94	0.91
β = 1.0 (0.8413)	0.79	0.89	1.43	1.01	1.08	1.15
β = 1.5 (0.9332)	0.84	0.95	1.76	1.15	1.23	1.42
β = 2.0 (0.9772)	0.89	1.02	2.12	1.30	1.40	1.74
β = 2.5 (0.9938)	0.94	1.08	2.50	1.46	1.58	2.08
β = 3.0 (0.9987)	0.98	1.13	2.87	1.63	1.77	2.44
Scour non-exceedance (ft) based on scour mean and standard deviation						
β = 0.5 (0.6915)	5.28	4.98	6.37	11.31	11.02	10.65
β = 1.0 (0.8413)	5.66	5.39	7.64	12.64	12.38	12.80
β = 1.5 (0.9332)	6.05	5.80	8.92	13.98	13.74	14.95
β = 2.0 (0.9772)	6.44	6.21	10.20	15.31	15.10	17.10
β = 2.5 (0.9938)	6.82	6.61	11.48	16.64	16.46	19.25
β = 3.0 (0.9987)	7.21	7.02	12.76	17.98	17.82	21.40
Scour factors based on scour mean and standard deviation						
β = 0.5 (0.6915)	0.73	0.82	1.20	0.91	0.97	0.97
β = 1.0 (0.8413)	0.79	0.88	1.44	1.01	1.09	1.17
β = 1.5 (0.9332)	0.84	0.95	1.69	1.12	1.21	1.36
β = 2.0 (0.9772)	0.89	1.02	1.93	1.23	1.33	1.56
β = 2.5 (0.9938)	0.95	1.08	2.17	1.33	1.45	1.76
β = 3.0 (0.9987)	1.00	1.15	2.41	1.44	1.56	1.95

Table A.23	Large Bridge - Medium Hydrologic Uncertainty - Medium Pier (6 ft)					
	Pier Scour (HEC-18)	Pier Scour (FDOT)	Contraction Scour	Total Scour (HEC-18)	Total Scour (FDOT)	Abutment Scour
Design Scour (ft)	13.77	11.28	5.29	19.07	16.57	10.96
Expected Scour (ft)	9.32	8.46	5.09	14.41	13.54	8.50
Bias	0.68	0.75	0.96	0.76	0.82	0.78
Std. Dev. (ft)	1.52	1.52	2.56	3.19	3.09	4.30
COV	0.16	0.18	0.50	0.22	0.23	0.51
Design Scour β	2.93	1.85	0.08	1.46	0.98	0.57
Non-Exceedance	0.9983	0.9681	0.5322	0.9278	0.8365	0.7165
Scour Non-Exceedance (ft) based on Monte Carlo results						
β = 0.5 (0.6915)	10.08	9.23	6.08	15.82	14.87	9.96
β = 1.0 (0.8413)	10.85	10.00	7.58	17.61	16.59	12.57
β = 1.5 (0.9332)	11.63	10.78	9.31	19.50	18.42	15.55
β = 2.0 (0.9772)	12.41	11.48	11.20	21.47	20.44	19.09
β = 2.5 (0.9938)	13.05	12.16	13.22	23.59	22.77	22.78
β = 3.0 (0.9987)	13.76	12.84	15.22	25.70	24.97	26.69
Scour factors based on Monte Carlo results						
β = 0.5 (0.6915)	0.73	0.82	1.15	0.83	0.90	0.91
β = 1.0 (0.8413)	0.79	0.89	1.43	0.92	1.00	1.15
β = 1.5 (0.9332)	0.84	0.96	1.76	1.02	1.11	1.42
β = 2.0 (0.9772)	0.90	1.02	2.12	1.13	1.23	1.74
β = 2.5 (0.9938)	0.95	1.08	2.50	1.24	1.37	2.08
β = 3.0 (0.9987)	1.00	1.14	2.87	1.35	1.51	2.44
Scour non-exceedance (ft) based on scour mean and standard deviation						
β = 0.5 (0.6915)	10.08	9.22	6.37	16.00	15.09	10.65
β = 1.0 (0.8413)	10.84	9.98	7.64	17.60	16.63	12.80
β = 1.5 (0.9332)	11.60	10.74	8.92	19.20	18.18	14.95
β = 2.0 (0.9772)	12.36	11.50	10.20	20.79	19.72	17.10
β = 2.5 (0.9938)	13.12	12.26	11.48	22.39	21.27	19.25
β = 3.0 (0.9987)	13.88	13.02	12.76	23.99	22.81	21.40
Scour factors based on scour mean and standard deviation						
β = 0.5 (0.6915)	0.73	0.82	1.20	0.84	0.91	0.97
β = 1.0 (0.8413)	0.79	0.88	1.44	0.92	1.00	1.17
β = 1.5 (0.9332)	0.84	0.95	1.69	1.01	1.10	1.36
β = 2.0 (0.9772)	0.90	1.02	1.93	1.09	1.19	1.56
β = 2.5 (0.9938)	0.95	1.09	2.17	1.17	1.28	1.76
β = 3.0 (0.9987)	1.01	1.15	2.41	1.26	1.38	1.95

Table A.24	Large Bridge - Medium Hydrologic Uncertainty - Large Pier (9 ft)					
	Pier Scour (HEC-18)	Pier Scour (FDOT)	Contraction Scour	Total Scour (HEC-18)	Total Scour (FDOT)	Abutment Scour
Design Scour (ft)	17.93	15.90	5.29	23.22	21.19	10.96
Expected Scour (ft)	12.20	11.92	5.09	17.28	17.01	8.50
Bias	0.68	0.75	0.96	0.74	0.80	0.78
Std. Dev. (ft)	2.02	2.16	2.56	3.59	3.53	4.30
COV	0.17	0.18	0.50	0.21	0.21	0.51
Design Scour β	2.84	1.84	0.08	1.66	1.18	0.57
Non-Exceedance	0.9977	0.9672	0.5322	0.9510	0.8819	0.7165
Scour Non-Exceedance (ft) based on Monte Carlo results						
β = 0.5 (0.6915)	13.20	13.01	6.08	18.85	18.60	9.96
β = 1.0 (0.8413)	14.23	14.10	7.58	20.84	20.50	12.57
β = 1.5 (0.9332)	15.26	15.25	9.31	22.99	22.53	15.55
β = 2.0 (0.9772)	16.32	16.23	11.20	25.27	24.68	19.09
β = 2.5 (0.9938)	17.26	17.27	13.22	27.52	27.32	22.78
β = 3.0 (0.9987)	18.28	18.24	15.22	29.85	29.60	26.69
Scour factors based on Monte Carlo results						
β = 0.5 (0.6915)	0.74	0.82	1.15	0.81	0.88	0.91
β = 1.0 (0.8413)	0.79	0.89	1.43	0.90	0.97	1.15
β = 1.5 (0.9332)	0.85	0.96	1.76	0.99	1.06	1.42
β = 2.0 (0.9772)	0.91	1.02	2.12	1.09	1.16	1.74
β = 2.5 (0.9938)	0.96	1.09	2.50	1.18	1.29	2.08
β = 3.0 (0.9987)	1.02	1.15	2.87	1.29	1.40	2.44
Scour non-exceedance (ft) based on scour mean and standard deviation						
β = 0.5 (0.6915)	13.21	13.00	6.37	19.08	18.78	10.65
β = 1.0 (0.8413)	14.22	14.08	7.64	20.87	20.54	12.80
β = 1.5 (0.9332)	15.23	15.16	8.92	22.67	22.31	14.95
β = 2.0 (0.9772)	16.24	16.24	10.20	24.46	24.07	17.10
β = 2.5 (0.9938)	17.25	17.32	11.48	26.25	25.84	19.25
β = 3.0 (0.9987)	18.26	18.40	12.76	28.05	27.60	21.40
Scour factors based on scour mean and standard deviation						
β = 0.5 (0.6915)	0.74	0.82	1.20	0.82	0.89	0.97
β = 1.0 (0.8413)	0.79	0.89	1.44	0.90	0.97	1.17
β = 1.5 (0.9332)	0.85	0.95	1.69	0.98	1.05	1.36
β = 2.0 (0.9772)	0.91	1.02	1.93	1.05	1.14	1.56
β = 2.5 (0.9938)	0.96	1.09	2.17	1.13	1.22	1.76
β = 3.0 (0.9987)	1.02	1.16	2.41	1.21	1.30	1.95

Table A.25	Large Bridge - High Hydrologic Uncertainty - Small Pier (3 ft)					
	Pier Scour (HEC-18)	Pier Scour (FDOT)	Contraction Scour	Total Scour (HEC-18)	Total Scour (FDOT)	Abutment Scour
Design Scour (ft)	7.20	6.10	5.29	12.49	11.39	10.96
Expected Scour (ft)	4.90	4.58	5.26	10.16	9.84	8.79
Bias	0.68	0.75	0.99	0.81	0.86	0.80
Std. Dev. (ft)	0.77	0.81	3.16	3.24	3.32	5.33
COV	0.16	0.18	0.60	0.32	0.34	0.61
Design Scour β	2.99	1.86	0.01	0.72	0.47	0.41
Non-Exceedance	0.9986	0.9686	0.5039	0.7642	0.6796	0.6582
Scour Non-Exceedance (ft) based on Monte Carlo results						
β = 0.5 (0.6915)	5.29	5.00	6.45	11.38	11.16	10.63
β = 1.0 (0.8413)	5.67	5.40	8.35	13.30	13.09	13.83
β = 1.5 (0.9332)	6.06	5.80	10.48	15.49	15.28	17.57
β = 2.0 (0.9772)	6.45	6.20	12.99	17.95	17.77	22.21
β = 2.5 (0.9938)	6.82	6.60	15.76	20.66	20.41	27.26
β = 3.0 (0.9987)	7.08	6.81	18.06	23.13	23.10	32.80
Scour factors based on Monte Carlo results						
β = 0.5 (0.6915)	0.73	0.82	1.22	0.91	0.98	0.97
β = 1.0 (0.8413)	0.79	0.89	1.58	1.06	1.15	1.26
β = 1.5 (0.9332)	0.84	0.95	1.98	1.24	1.34	1.60
β = 2.0 (0.9772)	0.90	1.02	2.45	1.44	1.56	2.03
β = 2.5 (0.9938)	0.95	1.08	2.98	1.65	1.79	2.49
β = 3.0 (0.9987)	0.98	1.12	3.41	1.85	2.03	2.99
Scour non-exceedance (ft) based on scour mean and standard deviation						
β = 0.5 (0.6915)	5.28	4.99	6.84	11.78	11.50	11.45
β = 1.0 (0.8413)	5.67	5.40	8.42	13.40	13.16	14.12
β = 1.5 (0.9332)	6.05	5.80	10.00	15.02	14.82	16.79
β = 2.0 (0.9772)	6.44	6.21	11.58	16.65	16.48	19.45
β = 2.5 (0.9938)	6.82	6.62	13.16	18.27	18.13	22.12
β = 3.0 (0.9987)	7.21	7.02	14.74	19.89	19.79	24.78
Scour factors based on scour mean and standard deviation						
β = 0.5 (0.6915)	0.73	0.82	1.29	0.94	1.01	1.04
β = 1.0 (0.8413)	0.79	0.88	1.59	1.07	1.16	1.29
β = 1.5 (0.9332)	0.84	0.95	1.89	1.20	1.30	1.53
β = 2.0 (0.9772)	0.89	1.02	2.19	1.33	1.45	1.77
β = 2.5 (0.9938)	0.95	1.09	2.48	1.46	1.59	2.02
β = 3.0 (0.9987)	1.00	1.15	2.78	1.59	1.74	2.26

Table A.26	Large Bridge - High Hydrologic Uncertainty - Medium Pier (6 ft)					
	Pier Scour (HEC-18)	Pier Scour (FDOT)	Contraction Scour	Total Scour (HEC-18)	Total Scour (FDOT)	Abutment Scour
Design Scour (ft)	13.77	11.28	5.29	19.07	16.57	10.96
Expected Scour (ft)	9.31	8.48	5.26	14.57	13.74	8.79
Bias	0.68	0.75	0.99	0.76	0.83	0.80
Std. Dev. (ft)	1.53	1.52	3.16	3.79	3.68	5.33
COV	0.16	0.18	0.60	0.26	0.27	0.61
Design Scour β	2.92	1.84	0.01	1.19	0.77	0.41
Non-Exceedance	0.9983	0.9672	0.5039	0.8826	0.7796	0.6582
Scour Non-Exceedance (ft) based on Monte Carlo results						
β = 0.5 (0.6915)	10.05	9.24	6.45	16.16	15.29	10.63
β = 1.0 (0.8413)	10.84	10.02	8.35	18.24	17.28	13.83
β = 1.5 (0.9332)	11.63	10.78	10.48	20.62	19.72	17.57
β = 2.0 (0.9772)	12.43	11.53	12.99	23.32	22.25	22.21
β = 2.5 (0.9938)	13.26	12.28	15.76	25.83	24.94	27.26
β = 3.0 (0.9987)	13.79	12.70	18.06	28.62	27.83	32.80
Scour factors based on Monte Carlo results						
β = 0.5 (0.6915)	0.73	0.82	1.22	0.85	0.92	0.97
β = 1.0 (0.8413)	0.79	0.89	1.58	0.96	1.04	1.26
β = 1.5 (0.9332)	0.84	0.96	1.98	1.08	1.19	1.60
β = 2.0 (0.9772)	0.90	1.02	2.45	1.22	1.34	2.03
β = 2.5 (0.9938)	0.96	1.09	2.98	1.35	1.51	2.49
β = 3.0 (0.9987)	1.00	1.13	3.41	1.50	1.68	2.99
Scour non-exceedance (ft) based on scour mean and standard deviation						
β = 0.5 (0.6915)	10.07	9.24	6.84	16.46	15.58	11.45
β = 1.0 (0.8413)	10.84	10.00	8.42	18.36	17.42	14.12
β = 1.5 (0.9332)	11.60	10.76	10.00	20.25	19.25	16.79
β = 2.0 (0.9772)	12.36	11.52	11.58	22.14	21.09	19.45
β = 2.5 (0.9938)	13.13	12.28	13.16	24.03	22.93	22.12
β = 3.0 (0.9987)	13.89	13.04	14.74	25.93	24.77	24.78
Scour factors based on scour mean and standard deviation						
β = 0.5 (0.6915)	0.73	0.82	1.29	0.86	0.94	1.04
β = 1.0 (0.8413)	0.79	0.89	1.59	0.96	1.05	1.29
β = 1.5 (0.9332)	0.84	0.95	1.89	1.06	1.16	1.53
β = 2.0 (0.9772)	0.90	1.02	2.19	1.16	1.27	1.77
β = 2.5 (0.9938)	0.95	1.09	2.48	1.26	1.38	2.02
β = 3.0 (0.9987)	1.01	1.16	2.78	1.36	1.49	2.26

Table A.27	Large Bridge - High Hydrologic Uncertainty - Large Pier (9 ft)					
	Pier Scour (HEC-18)	Pier Scour (FDOT)	Contraction Scour	Total Scour (HEC-18)	Total Scour (FDOT)	Abutment Scour
Design Scour (ft)	17.93	15.90	5.29	23.22	21.19	10.96
Expected Scour (ft)	12.23	11.95	5.26	17.49	17.22	8.79
Bias	0.68	0.75	0.99	0.75	0.81	0.80
Std. Dev. (ft)	2.06	2.16	3.16	4.25	4.11	5.33
COV	0.17	0.18	0.60	0.24	0.24	0.61
Design Scour β	2.76	1.82	0.01	1.35	0.97	0.41
Non-Exceedance	0.9971	0.9658	0.5039	0.9113	0.8335	0.6582
Scour Non-Exceedance (ft) based on Monte Carlo results						
β = 0.5 (0.6915)	13.23	13.03	6.45	19.25	19.02	10.63
β = 1.0 (0.8413)	14.27	14.15	8.35	21.59	21.20	13.83
β = 1.5 (0.9332)	15.35	15.27	10.48	24.36	23.76	17.57
β = 2.0 (0.9772)	16.55	16.27	12.99	27.29	26.54	22.21
β = 2.5 (0.9938)	17.73	17.36	15.76	30.43	29.62	27.26
β = 3.0 (0.9987)	18.69	17.99	18.06	33.56	32.75	32.80
Scour factors based on Monte Carlo results						
β = 0.5 (0.6915)	0.74	0.82	1.22	0.83	0.90	0.97
β = 1.0 (0.8413)	0.80	0.89	1.58	0.93	1.00	1.26
β = 1.5 (0.9332)	0.86	0.96	1.98	1.05	1.12	1.60
β = 2.0 (0.9772)	0.92	1.02	2.45	1.18	1.25	2.03
β = 2.5 (0.9938)	0.99	1.09	2.98	1.31	1.40	2.49
β = 3.0 (0.9987)	1.04	1.13	3.41	1.44	1.55	2.99
Scour non-exceedance (ft) based on scour mean and standard deviation						
β = 0.5 (0.6915)	13.26	13.03	6.84	19.62	19.27	11.45
β = 1.0 (0.8413)	14.29	14.12	8.42	21.74	21.32	14.12
β = 1.5 (0.9332)	15.33	15.20	10.00	23.87	23.38	16.79
β = 2.0 (0.9772)	16.36	16.28	11.58	25.99	25.43	19.45
β = 2.5 (0.9938)	17.39	17.36	13.16	28.11	27.49	22.12
β = 3.0 (0.9987)	18.42	18.45	14.74	30.24	29.54	24.78
Scour factors based on scour mean and standard deviation						
β = 0.5 (0.6915)	0.74	0.82	1.29	0.84	0.91	1.04
β = 1.0 (0.8413)	0.80	0.89	1.59	0.94	1.01	1.29
β = 1.5 (0.9332)	0.85	0.96	1.89	1.03	1.10	1.53
β = 2.0 (0.9772)	0.91	1.02	2.19	1.12	1.20	1.77
β = 2.5 (0.9938)	0.97	1.09	2.48	1.21	1.30	2.02
β = 3.0 (0.9987)	1.03	1.16	2.78	1.30	1.39	2.26

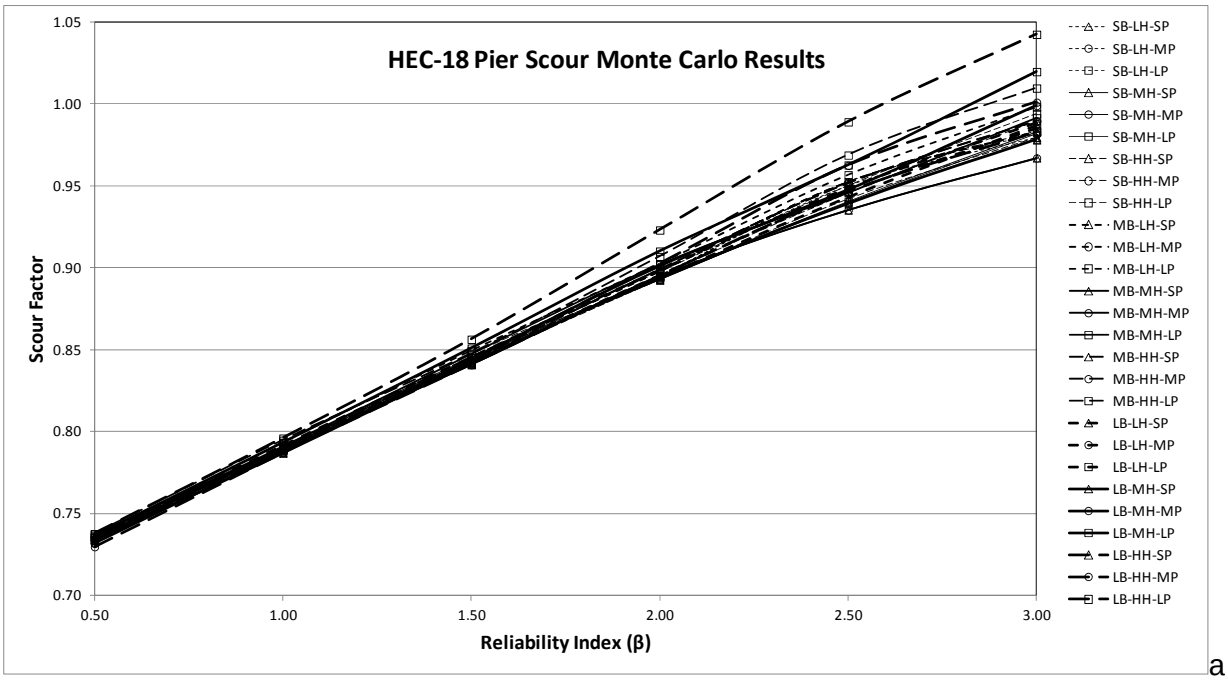

a

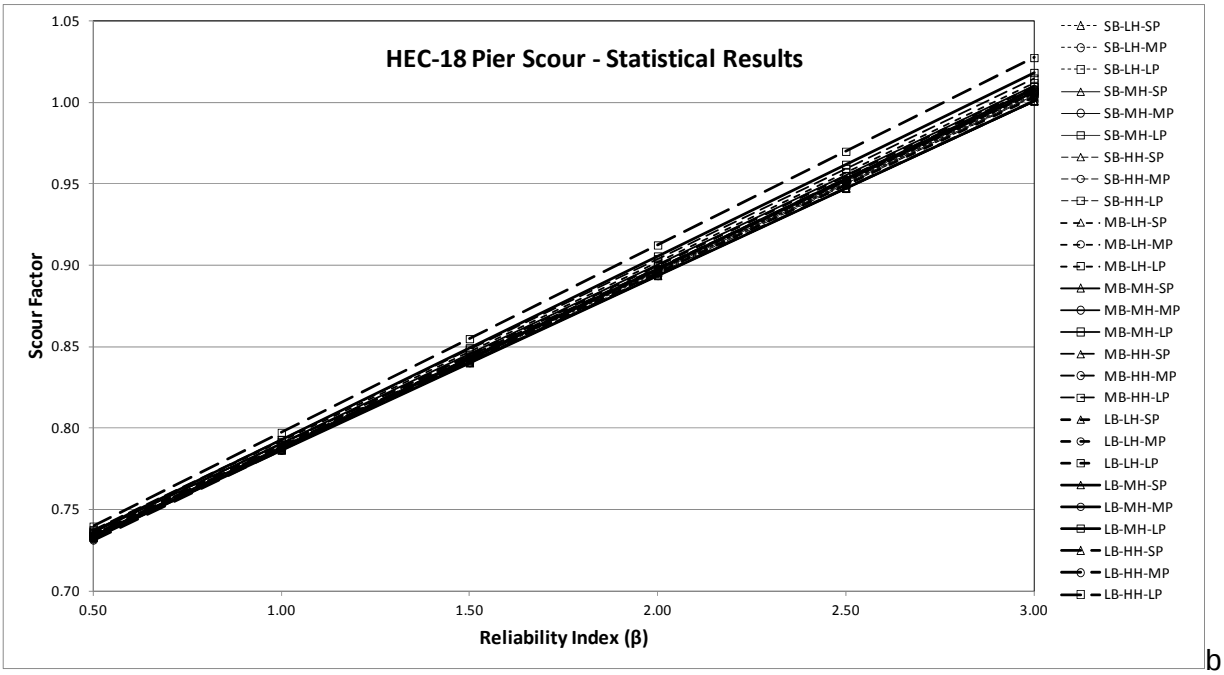

b

Figure A.1. Scour Factors for the HEC-18 Pier Scour Equation.

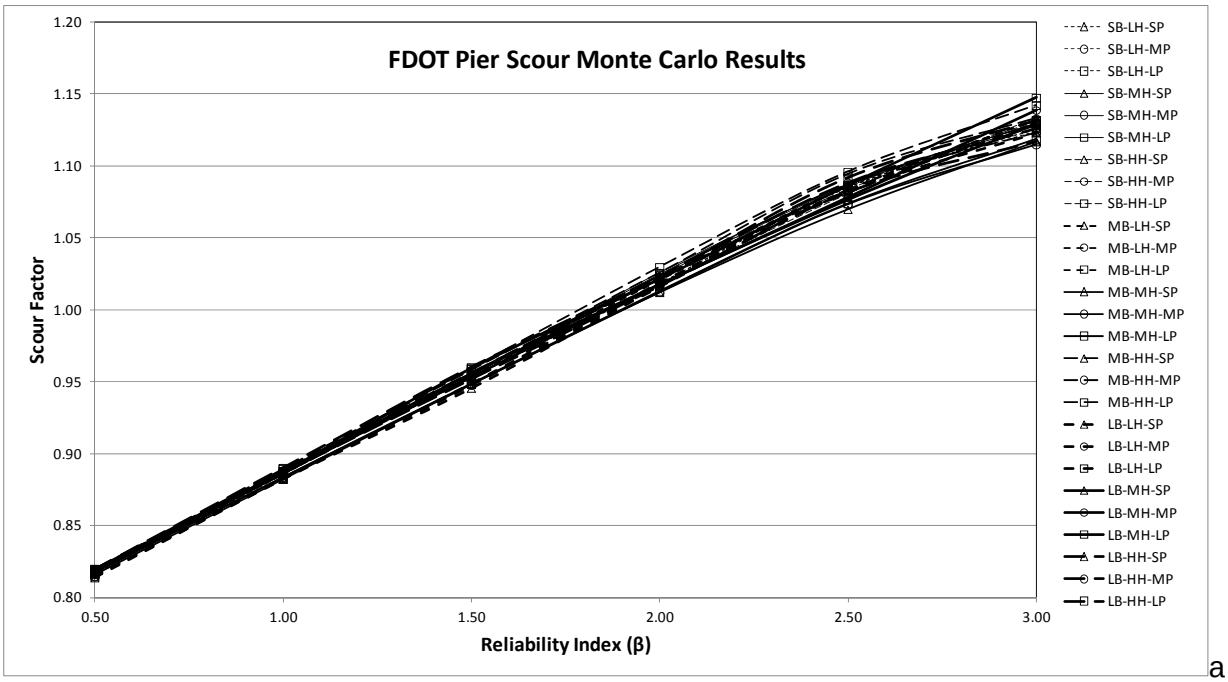

a

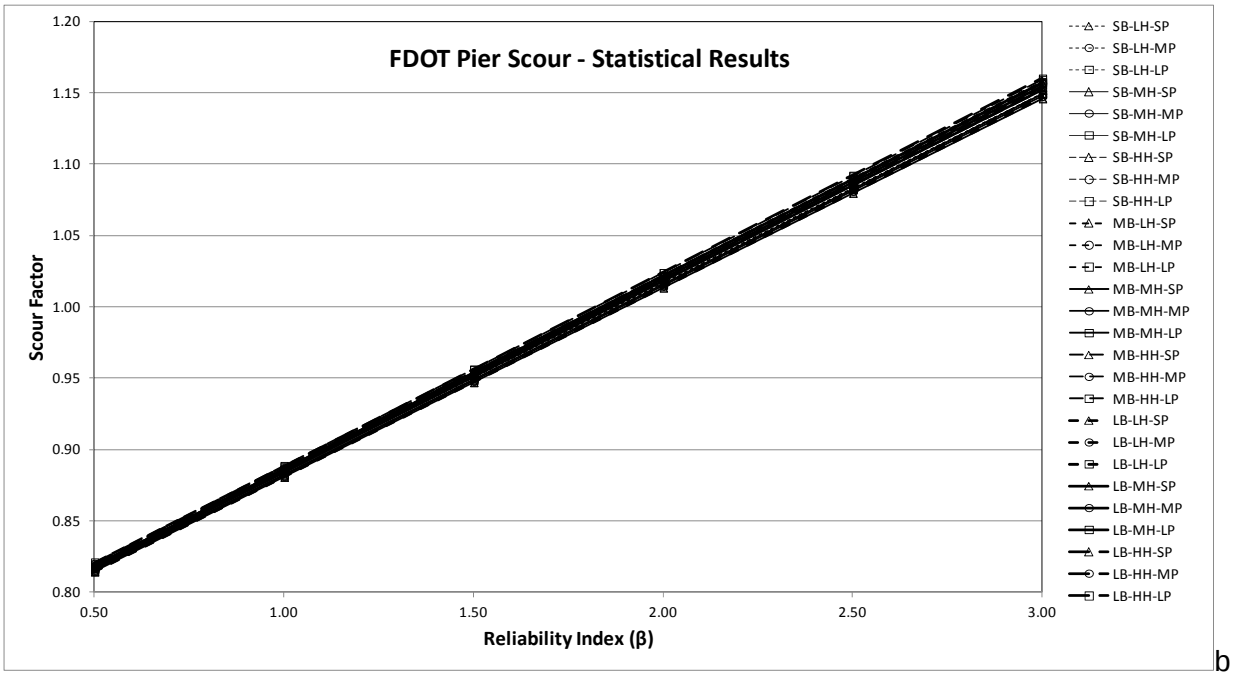

b

Figure A.2. Scour Factors for the FDOT Pier Scour Equation.

a

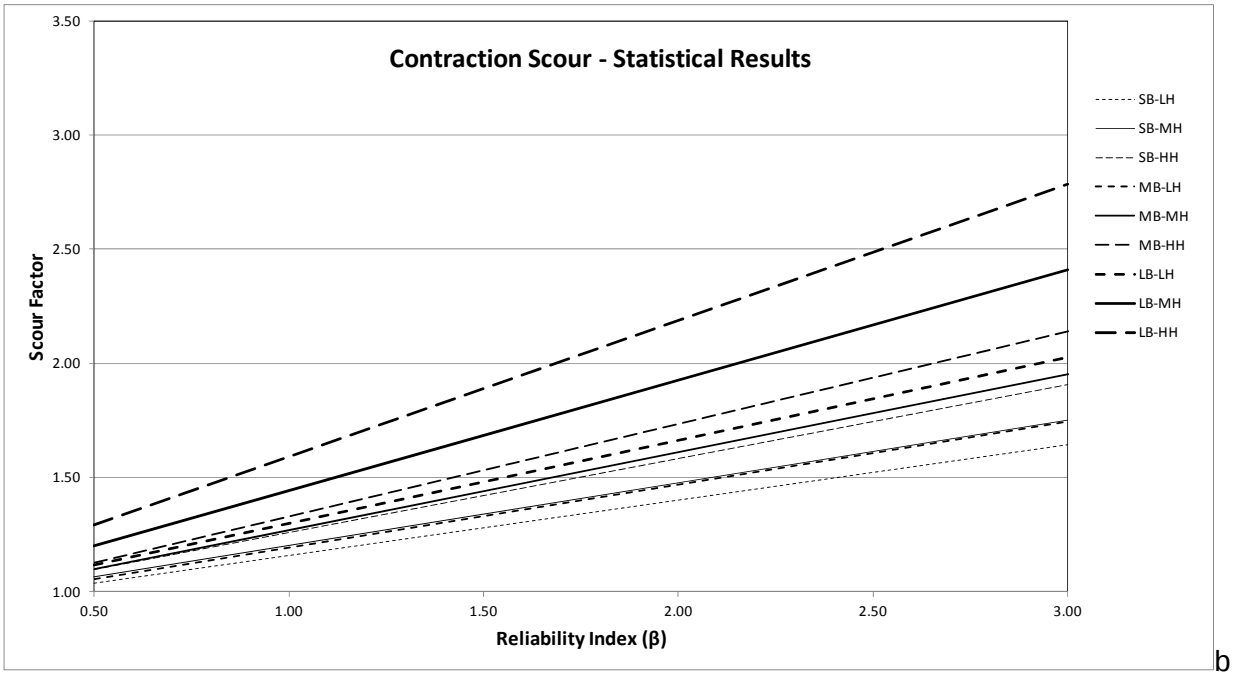

b

Figure A.3. Scour Factors for Contraction Scour.

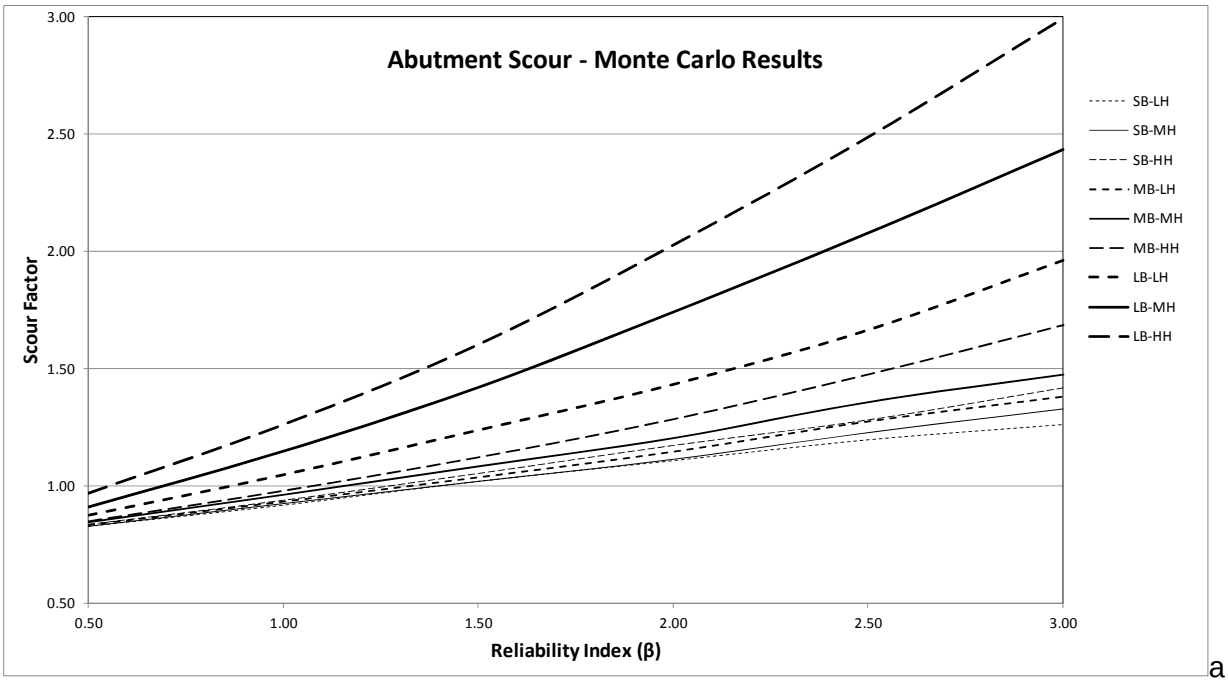

a

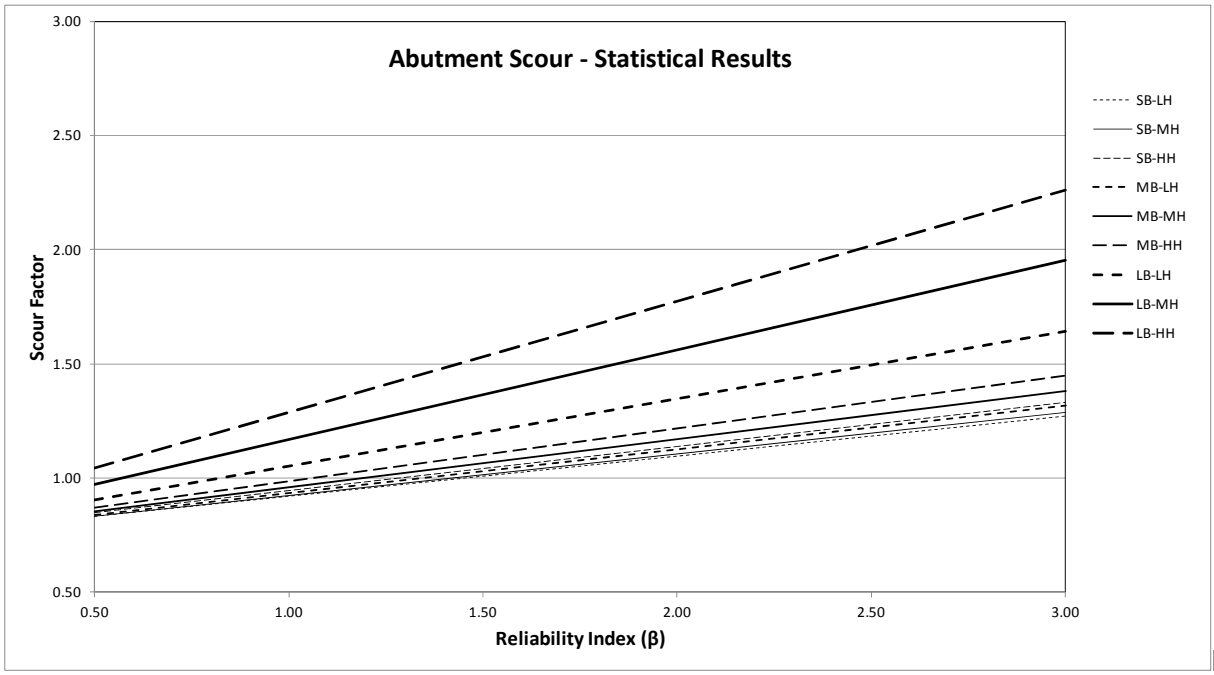

b

Figure A.4. Scour Factors for the NCHRP Abutment Scour Equation.

(page intentionally left blank)

APPENDIX B
Problem Statement for Contraction Scour Study

(page intentionally left blank)

AASHTO STANDING COMMITTEE ON RESEARCH
AMERICAN ASSOCIATION OF STATE HIGHWAY AND TRANSPORTATION OFFICIALS

NCHRP Problem Statement Outline

I. PROBLEM NUMBER

To be assigned by NCHRP staff.

II. PROBLEM TITLE

Clear-Water and Live-Bed Scour in Long Contractions

III. RESEARCH PROBLEM STATEMENT

Current guidance in Hydraulic Engineering Circular No. 18 (HEC-18), "Evaluating Scour at Bridges," (Arneson et al. 2012) provides equations for estimating contraction scour. Existing equations are based on sediment transport theory using approaches developed by Laursen, 1960 (live-bed contraction scour) and Laursen, 1963 (clear-water contraction scour). Both equations assume that the scour is due solely to the contraction effect and that local effects are negligible (i.e., that the contraction is hydraulically "long"), and both solve for the depth of flow y_2 in the contracted section after scour has occurred. The depth of scour of the bed material, y_s, is then calculated as

$$y_s = y_2 - y_0 \quad (1)$$

where y_0 is the depth of flow in the contracted section before scour occurs.

Depending on the ratio of the length of contraction L to the approach channel width b_1, channel contractions are designated as long or short. According to Komura (1966), a contraction becomes long when $L/b_1 > 1$, whereas Webby (1984) considered it as $L/b_1 > 2$. In a short contraction, local scour also occurs throughout the contracted section as a result of large-scale turbulent flow structures created at the entrance to the contraction, and the total scour is the result of both the contraction and local effects.

Analysis of existing laboratory data sets conducted under NCHRP Project 24-34, "Risk-Based Approach for Bridge Scour Prediction" revealed that the clear-water contraction scour equation does not envelope the observed data as a design equation. Rather, it is a predictive equation which is seen to underpredict observed scour relatively frequently compared to pier and abutment scour equations. No laboratory data sets of live-bed contraction scour were identified during the NCHRP 24-34 study; therefore, the live-bed contraction scour equation could not be assessed against observed data.

In addition, the NCHRP 24-34 study found that all of the previous studies suffered from a flaw in the experimental design, as none actually measured the depth of flow y_0 in the contracted section before scour began to occur. Therefore, this value had to be estimated in order to determine the depth of scour using Equation (1). In addition, a number of laboratory studies did not directly measure the depth of scour using bed elevation measurements. Instead, the assumption was made that y_0 was equal to y_1 (the depth of flow in the approach section upstream of the contraction). This assumption ignores the hydraulic drawdown effect in the contraction which occurs during subcritical flow (particularly in a bridge reach).

Lastly, most of the existing laboratory data points were obtained from tests where the contraction ratio W_2/W_1 created a "choked" condition at the entrance to the contraction (Wu and Molinas, 2004). This condition leads to energy losses between the approach and contracted sections, further compounding the difficulty in estimating y_0.

The proposed research would identify, compile, and assess existing laboratory data sets to supplement the NCHRP 24-34 analyses. In addition, laboratory studies should be conducted under both live-bed and clear-water conditions where the physical model setup can be adjusted to examine contraction scour under a range of hydraulic conditions, contraction ratios, and bed material types.

IV. LITERATURE SEARCH SUMMARY

Current guidelines in HEC-18 for determining the total scour prism at a bridge crossing involve the calculation of various scour components (e.g., local scour at piers and abutments, contraction scour, and pressure scour). Using the principle of superposition, the components are considered additive at bridge piers and the scour prism is then drawn as a singular line for each frequency flood event (e.g., 50-year, 100-year and 500-year flood events). The effects of potential long-term degradation over the life of the bridge as determined by methods presented in HEC-20 (Lagasse et al., 2012) are typically included in the total scour prism.

The need for an NCHRP research project on the "Interdependency of Scour Components" was published in the Transportation Research Circular in 1996 (Circular No. 466, December). In particular, the difficulty in distinguishing between contraction and abutment scour was ranked Number 23 in a set of 35 high-priority problem statements that constituted a long-range research program for issues related directly to bridge scour (NCHRP Project 24-8, Parola et al. 1996).

In 2004, NCHRP Project 20-07 (178) (Lagasse and Zevenbergen 2004) identified and evaluated bridge scour research for both riverine and coastal areas initiated or completed since 1997, with the objective of providing guidance to the AASHTO Task Force on Hydrology and Hydraulics in re-formulating the strategic plan for scour research for a 10-year planning period. That project included a comprehensive survey of 131 hydraulic and bridge engineers representing NCHRP, FHWA, state DOTs, academic researchers, and design practitioners. The survey results indicated an overarching recognition of the need for "guidance or models combining scour components and estimating total scour (less conservative than simply adding the components)"

In June 2008, the NCHRP sponsored the "Joint Workshop on Abutment Scour: Present Knowledge and Future Needs." That workshop recommended additional research on the "Interaction of Abutment and Contraction Scour," as reported in NCHRP Research Results Digest No. 334, March 2009. The results of NCHRP 24-27(02) are reported in *NCHRP Web-Only Document 181* (Sturm et al. 2011). With respect to contraction scour prediction equations, NCHRP 24-27(02) established that none of the current methods fully satisfy the following criteria:

- Limitations of equations in design applications with respect to ranges of controlling parameters on which they are based
- Categorization and acceptability of laboratory and research methods
- Attempts to verify and compare equations with other laboratory and field data

NCHRP 24-27(02) concluded that "… much remains to be learned before the more settled and defined state of knowledge that currently exists with respect to pier scour is arrived at for abutment and contraction scour."

NCHRP Project 24-20, "Prediction of Scour at Abutments" (Ettema et al. 2010) considered the complex flow structure around the ends of bridge abutments that interact with a contracted section and observed that "the flow field around an abutment… is not readily delineated as a contraction flow field that is separate from a local flow field limited to the near zone of the abutment." The NCHRP 24-20 procedure for estimating the total scour at an abutment begins with a contraction scour estimate which is then multiplied by an amplification factor to account for local effects at the abutment tip. Clearly, a reliable estimate of contraction scour is key to determining total scour at an abutment using this approach.

NCHRP Project 24-37, "Combining Individual Scour Components to Determine Total Scour" is scheduled to begin in 2013, and is expected to provide recommendations to account for the interdependencies of individual scour components at a bridge crossing.

References Cited:

Arneson, L.A., Zevenbergen, L.W., Lagasse, P.F., and Clopper, P.E., 2012. "Evaluation Scour at Bridges," Fifth Edition, Federal Highway Administration, Report FHWA-HIF-12-003, Hydraulic Engineering Circular No. 18, U.S. Department of Transportation, Washington, D.C.

Ettema, R., Nakato,T., and Muste, M., 2010. "Estimation of Scour Depth at Bridge Abutments," Draft Final Report, NCHRP Project 24-20, Transportation Research Board, Washington D.C., January.

Komura, S., 1966. "Equilibrium Depth of Scour in Long Constrictions." J. Hydraul. Div., ASCE, Vol. 92(5).

Lagasse, P.F., Zevenbergen, L.W., Spitz, W.J., and Arneson, L.A. (2012). "Stream Stability at Highway Structures," Hydraulic Engineering Circular No. 20, Fourth Edition, Federal Highway Administration, HIF-FHWA-12-004, Washington, D.C.

Lagasse, P.F. and L.W. Zevenbergen, 2004. "Evaluation and Update of NCHRP Project 24-08: Scour at Bridge Foundation Research Needs." NCHRP Project 20-07 Task 178, Transportation Research Board of the National Academies, Washington, D.C.

Laursen, E.M., 1960. "Scour at Bridge Crossings." Journal of the Hydraulics Division, ASCE, 86(2), pp. 39-54.

Laursen, E.M., 1963. "An Analysis of Relief Bridge Scour." Journal of the Hydraulics Division, ASCE, 89(3), pp. 93-118.

Parola, A.C., D.J. Hagerty, D.S. Mueller, B.W. Melville, G. Parker and J.S. Usher, 1996. "Draft Strategic Plan for NCHRP Project 24-08: Scour at Bridge Foundations: Research Needs." Transportation Research Board of the National Academies, Washington, D.C.

Sturm, T.W., Ettema, R., and Melville, B.W., 2011. "Evaluation of Bridge-Scour Research: Abutment and Contraction Scour Processes and Prediction," Final Report, NCHRP Project 24-27 (02), Web-Only Document 181, Transportation Research Board, Washington D.C., September.

Webby, M.G., 1984. "General Scour at a Contraction." *RRU Bulletin 73*, National Roads Board, Bridge Design and Research Seminar, New Zealand.

Wu, B. and A. Molinas, 2005. "Energy Losses and Threshold Conditions for Choking in Channel Contractions." Journal of Hydraulic Research, IAHR, Vol. 43, No. 2, pp. 139-148

V. RESEARCH OBJECTIVE

The objectives of this research effort are to: 1) Develop a reliable data base of scour in long contractions under both clear-water and live-bed conditions, and 2) Develop live-bed and clear-water contraction scour equations suitable for use in bridge design, not simply a best-fit prediction. The laboratory studies must be designed specifically to overcome the problems identified in Section III above, and shall be performed for a wide range of hydraulic conditions, contraction ratios, and bed material sizes and gradation uniformities.

To achieve this objective, at a minimum the following tasks must be performed:

1. *Review of existing knowledge*: Much work along these lines has already been done to summarize the existing body of knowledge and the research needed to fill the gaps that are reflected by the current state of practice (see Sections III and IV above).

2. *Identify existing laboratory data sets*: This task will consist of identifying and compiling data from previous laboratory studies where reliable experimental procedures and measurement methods have been employed to determine scour in long contractions. This work will supplement, to the extent possible, the data analyses conducted under NCHRP Project 24-34.

3. *Formulate a work plan and conduct laboratory studies*: This task will establish the experimental design for controlled laboratory testing of contraction scour. Both live-bed and clear-water conditions will be examined using non-cohesive sediments having a wide range of d_{50} sizes and uniformity coefficients. An appropriate experimental design must accommodate issues including the measurement of the flow depth y_0 prior to scour, periodic measurements of flow depth and bed elevations at multiple locations during each test run, and resolution of the effect of choking on energy loss. The laboratory testing plan must be approved by an NCHRP Research Panel prior to commencing the laboratory work.

4. *Develop a methodology appropriate for estimating scour in long contractions*: This task will consist of analyzing and interpreting the laboratory test results to develop a revised approach to estimating contraction scour for both live-bed and clear-water conditions. The revised approach may consist of modifications to the existing Laursen equations, or may be a new methodology. The approach will be validated using other laboratory data sets identified in Task 2.

5. *Final Report*: The final report will be written in two parts. The first part will document the research performed to arrive at the new methodology. The second part will be written in the form of a manual that provides design guidelines for practitioners in the field of bridge scour calculation suitable for incorporation in AASHTO and FHWA guidelines.

VI. ESTIMATE OF PROBLEM FUNDING AND RESEARCH PERIOD

Recommended Funding:

$500,000

Research Period:

30 months

VII. URGENCY, PAYOFF POTENTIAL, AND IMPLEMENTATION

Scour estimates at bridge foundations have been roundly criticized for decades as being overly conservative. The perception is that the equations almost always result in more costly bridge designs, at major expense to taxpayers. A long and ongoing concern has been expressed by bridge engineers regarding the perceived excessive conservatism in predicting bridge scour. This indicates that there is an urgent need to determine the most appropriate and reliable way to estimate the various components of bridge scour in order to estimate total scour for: 1) assessing scour vulnerability of existing bridges, and 2) designing foundations for new bridges.

Research conducted under NCHRP Project 24-34 clearly indicates that of the three primary scour components (pier, contraction, and abutment), the contraction scour equations exhibit, by far, the least amount of reliability in terms of 1) the conditional probability that the contraction scour estimate will be exceeded during the design event, and 2) the unconditional probability that the contraction scour estimate will be exceeded during the life of the bridge. Thus there is a demonstrated and urgent need to decrease the uncertainty of contraction scour estimates so that greater reliability can be achieved.

The payoff potential to bridge owners is significant if bridges currently considered to be scour critical can be reclassified to a lower-risk status, or if foundations for new bridges can be designed for a lesser amount of total scour. Implementation of new guidance would be primarily oriented toward revisions of HEC-18 and the AASHTO Highway Drainage Guidelines.

VIII. PERSON(S) DEVELOPING THE PROBLEM STATEMENT

Peter Lagasse, Ph.D., P.E.
Principal Investigator, NCHRP Project 24-34
Senior Water Resources Engineer
Ayres Associates
3665 JFK Parkway, Building 2, Suite 200
Fort Collins, CO 80525-3152
Phone 970.223.5556
Fax 970.223.5578
LagasseP@AyresAssociates.com

Paul Clopper, P.E.
Director, Applied Technology
Ayres Associates
3665 JFK Parkway, Building 2, Suite 200
Fort Collins, CO 80525-3152
Phone 970.223.5556
Fax 970.223.5578
ClopperP@AyresAssociates.com

IX. PROBLEM MONITOR

To be assigned by NCHRP staff.

X. DATE AND SUBMITTED BY

Submitted on __/__/2013 by:

Steve Ng, P.E.
Chair, NCHRP Project 24-34 Research Panel
Senior Bridge Engineer
California DOT
1801 30th Street
Mail Stop 9-Hyd-1/2i
Sacramento, CA 95816-8041
Phone: 916-227-8018
Fax: 916-227-8031
steve_ng@dot.ca.gov

Larry Arneson, Ph.D., P.E.
Senior Hydraulic Engineer
Federal Highway Administration
FHWA Resource Center
12300 West Dakota Ave., Suite 340
Lakewood, CO 80228
Phone: 720-963-3200
Fax: 720-963-3232
larry.arneson@dot.gov

Please submit completed problem statement to the following e-mail address:

nchrp@nas.edu

Questions on the process can be directed to the same address or cjencks@nas.edu.

APPENDIX C
Glossary

(page intentionally left blank)

APPENDIX C

GLOSSARY

Hydrologic, Hydraulic, and Geomorphic Terms

Aggradation:	General and progressive buildup of the longitudinal profile of a channel bed due to sediment deposition.
Alluvial Channel:	Channel wholly in alluvium; no bedrock is exposed in channel at low flow or likely to be exposed by erosion.
Alluvial Stream:	A stream which has formed its channel in cohesive or noncohesive materials that have been and can be transported by the stream.
Alluvium:	Unconsolidated material deposited by a stream in a channel, floodplain, alluvial fan, or delta.
Annual Flood:	The maximum flow in one year (may be daily or instantaneous).
Average Velocity:	Velocity at a given cross section determined by dividing discharge by cross sectional area.
Backwater:	The increase in water surface elevation relative to the elevation occurring under natural channel and floodplain conditions. It is induced by a bridge or other structure that obstructs or constricts the free flow of water in a channel.
Backwater Area:	The low-lying lands adjacent to a stream that may become flooded due to backwater.
Bank:	The sides of a channel between which the flow is normally confined.
Bank, Left (Right):	The side of a channel as viewed in a downstream direction.
Bankfull Discharge:	Discharge that, on the average, fills a channel to the point of overflowing.
Base Floodplain:	Floodplain associated with the flood with a 100-year recurrence interval.
Bed:	Bottom of a channel bounded by banks.
Bed Form:	A recognizable relief feature on the bed of a channel, such as a ripple, dune, plane bed, antidune, or bar. Bed forms are a consequence of the interaction between hydraulic forces (boundary shear stress) and the bed sediment.

Bed Material:	Material found in and on the bed of a stream (May be transported as bed load or in suspension).
Bed Shear (Tractive Force):	The force per unit area exerted by a fluid flowing past a stationary boundary.
Boulder:	A rock fragment whose diameter is greater than 250 mm.
Boundary Condition (Model):	A specified hydraulic condition such as a water surface elevation or energy slope used as a starting point for a hydraulic model simulation.
Bridge Opening:	The cross-sectional area beneath a bridge that is available for conveyance of water.
Bridge Substructure:	Structural elements supporting a bridge in contact with the stream or channel bed, including bridge abutments, piers, and footings.
Bridge Waterway:	The area of a bridge opening available for flow, as measured below a specified stage and normal to the principal direction of flow.
Catchment:	See Drainage Basin.
Channel:	The bed and banks that confine the surface flow of a stream.
Channel Pattern:	The aspect of a stream channel in plan view, with particular reference to the degree of sinuosity, braiding, and anabranching.
Channel Process:	Behavior of a channel with respect to shifting, erosion and sedimentation.
Choking (of flow):	Excessive constriction of flow which may cause severe backwater effect.
Clay (Mineral):	A particle whose diameter is in the range of 0.00024 to 0.004 mm.
Clear-Water Scour:	Scour at a pier or abutment (or contraction scour) when there is no movement of the bed material upstream of the bridge crossing at the flow causing bridge scour.
Constriction:	A natural or artificial control section, such as a bridge crossing, channel reach or dam, with limited flow capacity in which the upstream water surface elevation is related to discharge.
Contraction:	The effect of channel or bridge constriction on flow streamlines.

Contraction Scour:	Contraction scour, in a natural channel or at a bridge crossing, involves the removal of material from the bed and banks across all or most of the channel width. This component of scour results from a contraction of the flow area at the bridge which causes an increase in velocity and shear stress on the bed at the bridge. The contraction can be caused by the bridge or from a natural narrowing of the stream channel.
Conveyance:	A measure of the carrying capacity of a channel section. In the Manning equation, conveyance K is: $K = \frac{1.486}{n} AR^{2/3} = \frac{Q}{\sqrt{S}}$
Critical Shear Stress:	The minimum amount of shear stress required to initiate soil particle motion.
Critical Velocity (Particle Motion):	The velocity required to initiate motion of a particle of a specified size and weight.
Cross Section:	A section normal to the trend of a channel or flow.
Daily Discharge:	Discharge averaged over one day (24 hours).
Debris:	Floating or submerged material, such as logs, vegetation, or trash, transported by a stream (Drift).
Degradation (Bed):	A general and progressive (long-term) lowering of the channel bed due to erosion, over a relatively long channel length.
Depth of Scour:	The vertical distance a streambed is lowered by scour below a reference elevation.
Design Flow (Design Flood):	The discharge that is selected as the basis for the design or evaluation of a hydraulic structure including a hydraulic design flood, scour design flood, and scour design check flood.
Discharge:	Volume of water passing through a channel during a given time.
Drainage Basin:	An area confined by drainage divides, often having only one outlet for discharge (Catchment, Watershed).
Drift:	Alternative term for vegetative debris.
Energy (Friction) Slope:	Rate of energy loss with distance in the downstream flow direction: S_f = dH/dL where H is total energy and L is streamwise distance.

Ephemeral Stream:	A stream or reach of stream that does not flow for parts of the year. As used here, the term includes intermittent streams with flow less than perennial.
Erosion:	Displacement of soil particles due to water or wind action.
FESWMS:	A 2-dimensional open channel flow model called the Finite Element Surface Water Modeling System developed and supported by the Federal Highway Administration (also referred to as FST-2DH).
Fill Slope:	Side or end slope of an earth-fill embankment. Where a fill-slope forms the streamward face of a spill-through abutment, it is regarded as part of the abutment.
Flood:	Large volumetric rate of discharge in a river or stream that occurs infrequently and is usually associated with inundation and economic damage.
Flood Exceedance Probability:	The statistical chance that a specified discharge rate will be equaled or exceeded in a given year.
Flood Frequency:	The average interval between floods exceeding a given magnitude. For example, a flood having an annual probability of exceedance of 1 percent has a 1/(0.01) = 100-year frequency of recurrence; a flood of this magnitude would be expected to occur on average about once every 100 years.
Flood-Frequency Curve:	A graph indicating the probability that the annual flood discharge will exceed a given magnitude, or the recurrence interval corresponding to a given magnitude.
Floodplain:	A nearly flat, alluvial lowland bordering a stream, that is subject to frequent inundation by floods.
Flood Return Period/Recurrence Interval:	See Flood Frequency.
Flow Skew:	The angle of incidence of flow on a rectangular or long wall pier. Flow aligned with the long axis of a structure has a skew of zero degrees.
Fluvial Geomorphology:	The science dealing with the morphology (form) and dynamics of streams and rivers.
Fluvial System:	The natural river system consisting of (1) the drainage basin, watershed, or sediment source area, (2) tributary and mainstem river channels or sediment transfer zone, and (3) alluvial fans, valley fills and deltas, or the sediment deposition zone.

Freeboard:	The vertical distance above a design stage that is allowed for waves, surges, drift, and other contingencies.
Froude Number:	A dimensionless number that represents the ratio of inertial to gravitational forces in open channel flow.
Gabion:	A basket or compartmented rectangular container made of wire mesh. When filled with cobbles or other rock of suitable size, the gabion becomes a flexible and permeable unit with which flow- and erosion-control structures can be built.
Gaging Station:	Instrumentation on a stream or river that is used for measuring the volumetric rate of flow. Gaging stations exhibit a unique relationship between water surface elevation and flow rate which is periodically calibrated.
Geomorphology/Morphology:	That science that deals with the form of the Earth, the general configuration of its surface, and the changes that take place due to erosion and deposition.
Graded Stream:	A geomorphic term used for streams that have apparently achieved a state of equilibrium between the rate of sediment transport and the rate of sediment supply throughout long reaches.
Gravel:	A rock fragment whose diameter ranges from 2 to 64 mm.
HEC-RAS:	A one-dimensional open channel flow model developed and supported by the U.S. Army Corps of Engineers - Hydrologic Engineering Center.
Headcutting:	Channel degradation associated with abrupt changes in the bed elevation (headcut) that generally migrates in an upstream direction.
Hydraulics:	The applied science concerned with the behavior and flow of liquids, especially in pipes, channels, structures, and the ground.
Hydraulic Model:	A small-scale physical (or mathematical) representation of a flow situation.
Hydrograph:	The graph of stage or discharge against time.
Hydrology:	The science concerned with the occurrence, distribution, and circulation of water on the earth.
Incised Reach:	A stretch of stream with an incised channel that only rarely overflows its banks.
Incised Stream:	A stream which has deepened its channel through the bed of the valley floor, so that the floodplain is a terrace.

Instantaneous Discharge/Peak:	The volumetric rate of flow passing a given cross section on a stream or river at a specific point in time.
Invert:	The lowest point in the channel cross section or at flow control devices such as weirs, culverts, or dams.
Ineffective Flow:	An area of flow where water is not being conveyed in a downstream direction (e.g., ponding above or below an embankment).
Lateral Erosion (Migration):	Erosion in which the removal of material is extended horizontally as contrasted with degradation and scour in a vertical direction.
Live Flow:	Area of flow where water is actively conveyed in a downstream direction (e.g., channel flow and unobstructed floodplain flow.
Live-Bed Scour:	Scour at a pier or abutment (or contraction scour) when the bed material in the channel upstream of the bridge is moving at the flow causing bridge scour.
Local Scour:	Removal of material from around piers, abutments, spurs, and embankments caused by an acceleration of flow and resulting vortices induced by obstructions to the flow.
Longitudinal Profile:	The profile of a stream or channel drawn along the length of its centerline. In drawing the profile, elevations of the water surface or the thalweg are plotted against distance as measured from the mouth or from an arbitrary initial point.
Manning Equation:	Relationship between discharge, channel geometry, and roughness: $Q = \frac{1.486}{n} AR^{2/3} S_f^{1/2}$
Manning Roughness Coefficient (n):	Parameter of the Manning equation that is a measure of the resistance to flow caused by the channel boundary.
Mathematical Model:	A numerical representation of a flow situation using mathematical equations (also computer model).
Meandering Stream:	A stream having a sinuosity greater than some arbitrary value. The term also implies a moderate degree of pattern symmetry, imparted by regularity of size and repetition of meander loops. The channel generally exhibits a characteristic process of bank erosion and point bar deposition associated with systematically shifting migrating meanders.
Median Diameter:	The particle diameter of the 50th percentile point on a size distribution curve such that half of the particles (by weight, number, or volume) are larger and half are smaller ($D_{50.}$)

Migration:	Change in position of a channel by lateral erosion of one bank and simultaneous accretion of the opposite bank.
Nonalluvial Channel:	A channel whose boundary is in bedrock or non-erodible material.
Normal Stage:	The water stage prevailing during the greater part of the year.
Obstructed Flow Area:	Portion of the waterway and/or floodplain blocked by a structure such as a bridge pier or approach roadway embankment.
Overbank Flow:	Water movement that overtops the bank either due to stream stage or to overland surface water runoff.
Overtopping Flow:	Portion of the flood discharge that flows over a roadway embankment or bridge deck.
Perennial Stream:	A stream or reach of a stream that flows continuously for all or most of the year.
Pile:	An elongated member, usually made of timber, concrete, or steel, that serves as a structural component of a river-training structure or bridge.
Pressure Flow/Scour:	See Vertical Contraction Scour.
Probable Maximum Flood:	A very rare flood discharge value computed by hydro-meteorological methods, usually in connection with major hydraulic structures.
Probability Distribution (Log-Pearson Type III):	Statistical probability distribution used to estimate flood frequency characteristics, typically using historical flood peak flows from gaging station records.
Reach:	A segment of stream length that is arbitrarily bounded for purposes of study.
Recurrence Interval:	The reciprocal of the annual probability of exceedance of a hydrologic event (also return period, exceedance interval).
Regression Relationship (Regional):	A method for estimating the magnitude and frequency of floods using watershed characteristics such as drainage area, percent impervious surface, percent forest cover, etc.
Relief Bridge:	An opening in an embankment on a floodplain to permit passage of overbank flow.

Riparian:	Pertaining to anything connected with or adjacent to the banks of a stream (corridor, vegetation, zone, etc.).
Riprap:	Layer or facing of rock or broken concrete dumped or placed to protect a structure or embankment from erosion; also the rock or broken concrete suitable for such use. Riprap has also been applied to almost all kinds of armor, including wire-enclosed riprap, grouted riprap, sacked concrete, and concrete slabs.
Roughness Coefficient:	Numerical measure of the frictional resistance to flow in a channel, as in the Manning or Chezy's formulas.
Sand:	A rock fragment whose diameter is in the range of 0.062 to 2.0 mm.
Scour:	Erosion of streambed or bank material due to flowing water; often considered as being localized (see local scour, contraction scour, total scour).
Scour Prism:	Total volume of stream bed material removed by scour in the bridge reach for design flood conditions.
Sediment or Fluvial Sediment:	Fragmental material transported, suspended, or deposited by water.
Sediment Concentration:	Weight or volume of sediment relative to the quantity of transporting (or suspending) fluid.
Sediment Discharge:	The quantity of sediment that is carried past any cross section of a stream in a unit of time. Discharge may be limited to certain sizes of sediment or to a specific part of the cross section.
Sediment Load (Transport):	Amount of sediment being moved (transported) by a stream.
Sediment Yield:	The total sediment outflow from a watershed or a drainage area at a point of reference and in a specified time period. This outflow is equal to the sediment discharge from the drainage area.
Sediment Size (Median Diameter):	The particle diameter of the 50th percentile point on a size distribution curve such that half of the particles (by weight, number, or volume) are larger and half are smaller (D_{50}).
Shear Stress:	See Unit Shear Force.
Silt:	A particle whose diameter is in the range of 0.004 to 0.062 mm.
Sinuosity:	The ratio between the thalweg length and the valley length of a stream.

Slope (of Channel or Stream):	Fall per unit length along the channel centerline or thalweg.
Slope-Area Method:	A method of estimating unmeasured flood discharges in a uniform channel reach using observed high-water levels.
Spill-Through Abutment:	A bridge abutment having a fill slope on the streamward side. The term originally referred to the "spill-through" of fill at an open abutment but is now applied to any abutment having such a slope.
Spread Footing:	A pier or abutment footing that transfers load directly to the earth.
Stability:	A condition of a channel when, though it may change slightly at different times of the year as the result of varying conditions of flow and sediment charge, there is no appreciable change from year to year; that is, accretion balances erosion over the years.
Stable Channel:	A condition that exists when a stream has a bed slope and cross section which allows its channel to transport the water and sediment delivered from the upstream watershed without aggradation, degradation, or bank erosion (a graded stream).
Stage:	Water-surface elevation of a stream with respect to a reference elevation.
Stream:	A body of water that may range in size from a large river to a small rill flowing in a channel. By extension, the term is sometimes applied to a natural channel or drainage course formed by flowing water whether it is occupied by water or not.
Subcritical, Supercritical Flow:	Open channel flow conditions with Froude Number less than and greater than unity, respectively.
Thalweg:	The line extending down a channel that follows the lowest elevation of the bed.
Toe of Bank:	That portion of a stream cross section where the lower bank terminates and the channel bottom or the opposite lower bank begins.
Total Scour:	The sum of long-term degradation, contraction scour, and local scour.
Tractive Force:	The drag or shear on a streambed or bank caused by passing water which tends to move soil particles along with the streamflow.

Turbulence:	Motion of fluids in which local velocities and pressures fluctuate irregularly in a random manner as opposed to laminar flow where all particles of the fluid move in distinct and separate lines.
Ultimate Scour:	The maximum depth of scour attained for a given flow condition. May require multiple flow events and in cemented or cohesive soils may be achieved over a long time period.
Uniform Flow:	Flow of constant cross section and velocity through a reach of channel at a given time. Both the energy slope and the water slope are equal to the bed slope under conditions of uniform flow.
Unit Discharge:	Discharge per unit width (may be average over a cross section, or local at a point).
Unit Shear Force (Shear Stress):	The force or drag developed at the channel bed by flowing water. For uniform flow, this force is equal to a component of the gravity force acting in a direction parallel to the channel bed on a unit wetted area. Usually in units of stress, Pa (N/m^2) or (lb/ft^2).
Unsteady Flow:	Flow of variable discharge and velocity through a cross section with respect to time.
Velocity:	The time rate of flow usually expressed in m/s (ft/sec). The average velocity is the velocity at a given cross section determined by dividing discharge by cross-sectional area.
Vertical Contraction Scour:	Scour resulting from flow impinging on bridge superstructure elements (e.g., low chord).
Vortex:	Turbulent eddy in the flow generally caused by an obstruction such as a bridge pier or abutment (e.g., horseshoe vortex).
Watershed:	See Drainage Basin.
Waterway Opening Width (Area):	Width (area) of bridge opening at (below) a specified stage, measured normal to the principal direction of flow.

GLOSSARY

Probability and Statistical Terms

Bias: A statistical measure of systematic difference between a predicted value and the population parameter of interest, typically shown as the symbol λ; a measure of consistent overprediction or underprediction.

Box-Muller Transform: A method for generating independent standard normally distributed random numbers given a source of uniformly distributed random numbers.

Chi-Squared Test: A statistical test commonly used to compare observed data with data one would expect to obtain according to a specific hypothesis.

Coefficient of Variation (COV): A measure of the dispersion of a probability distribution defined as the standard deviation divided by the mean:

$$\text{COV} = \frac{\sigma}{\mu}$$

Confidence Limit: An interval estimator of a population parameter used to assess the reliability of an estimate, typically shown as the symbol Z_c. For example, there is a 90% probability that the true value lies between the Upper and Lower 95% confidence limits.

Confidence Limit	Z_c
90%	1.281
95%	1.645
98%	2.054

Cumulative Distribution (Density) Function (CDF): A mathematical expression that quantifies the likelihood (or percent chance) that a quantity will be exceeded.

Data Set Outlier: An observation that is numerically distant from the rest of the data in a sample. Outliers are sometimes considered to be faulty data and are removed from the data set.

Design Life (of Bridge): The useful life over which a structure is planned to perform its intended function without becoming damaged or obsolete. Typically this term refers to new structures.

Deterministic Factor: A parameter which is not variable for a given structure; for example the width of a bridge pier.

Equation (Design): A mathematical relationship that envelopes the observed data in such a way that the results are conservative in nature.

Equation (Predictive):	A mathematical relationship that tends to fit through the cloud of observed data points in such a way that overprediction and underprediction occur with relatively equal magnitude and frequency.
Gaussian Distribution:	The Standard Normal or “bell-shaped” probability distribution function.
Kolmogorov-Smirnov Test:	A nonparametric goodness-of-fit test that compares a probability distribution obtained from a sample to a reference cumulative distribution function, or to a distribution from a second sample.
Latin Hypercube Simulation (LHS):	A statistical method of generating a sample using equally probable intervals, often used in uncertainty analysis.
Level I Analysis/Approach:	A method for accounting for uncertainty in bridge scour estimates that multiplies a scour estimate by a “scour factor” to achieve a desired level of reliability that the resulting scour depth will not be exceeded during a design flood event.
Level II Analysis/Approach:	A method for accounting for uncertainty in bridge scour estimates that uses Monte Carlo simulation to develop scour estimates for a specific bridge using its unique characteristics.
Load and Resistance Factor Design (LRFD):	A structural design method that uses calibrated load factors and prescribed code values to achieve a desired level of reliability against structural failure.
Load and Resistance Factor Rating (LRFR):	A structural rating system used to evaluate bridges based upon calibrated load factors using principles of structural reliability.
Log-Transform:	The natural logarithms of a data series.
Mean:	The average value of a sample or a population, typically shown as the symbol μ.
Monte Carlo Realization:	One simulation out of many where certain variables are allowed to vary within prescribed limits in accordance with specified probability distributions.
Monte Carlo Simulation (MCS):	The net result of performing many individual realizations in order to obtain statistical information about the process or phenomenon being modeled.
Poisson Process:	A stochastic process which counts the number of events and the time that these events occur within a given time interval.

Probability:	A measure or estimate of the likelihood (or percent chance) that an event will occur or that a statement is true ranging from 0 (0% chance or will not happen) to 1 (100% chance, or will happen). Typically the term P_F is the probability of failure and P or P_y symbolize probability.
Probability (Conditional):	The likelihood (percent chance) that a quantity will be exceeded given the condition that another event has occurred or will occur.
Probability Distribution (Density) Function (PDF):	A mathematical expression that quantifies the likelihood that an event will occur or that a quantity will take on a value or fall within a range of values.
Probability Distribution (Log-Normal):	A mathematical expression of the Gaussian or "bell-shaped" probability curve that fits the logarithms of the data points.
Probability Distribution (Normal)	A mathematical expression of the Gaussian or "bell-shaped" probability curve that fits the values of the data points.
Probability of Exceedance:	The likelihood (percent chance) that a quantity will exceed a specified value, typically shown as P_n for n years or P_a for annual probability of exceedance. .
Probability of Non-Exceedance:	The likelihood (percent chance) that a quantity will not exceed a specified value.
Probability (Unconditional):	The likelihood (percent chance) that a design value will be exceeded over the entire remaining service life of a structure.
Random Factor:	A factor is random when the quantities under study are part of a larger population and the goal of the study is to make a statement or conclusion regarding the larger population.
Random Number Generator (RNG)	A computational or physical device designed to generate a sequence of numbers or symbols that lack any pattern.
rasTool© :	The name given to the computer program which links the HEC-RAS hydraulic model to Monte Carlo simulation software.
Reliability:	A branch of statistics which seeks to quantify the ability of a system or component to perform its required functions under stated conditions for a specified period of time.

Reliability Index:	The probability of non-exceedance expressed as the number of standard deviations from the mean, typically shown as the symbol β. For example, the standard Normal distribution has a probability of non-exceedance of 84.13% at β = 1.0, 97.73% at β = 2.0, and 99.87% at β = 3.0.
Risk:	The potential that a chosen action or activity (including the choice of inaction) will lead to a loss (an undesirable outcome). In economic terms, risk is often defined as the product of probability of failure times the cost of failure, and is measured in dollars, typically shown as the symbol R.
Scour Factor:	A safety factor which multiplies a scour estimate to achieve a desired target Reliability Index β.
Service Life (of Bridge):	Similar to Design Life. Refers to the remaining planned life of an existing structure. Typically this term refers to existing structures.
Skew (Distribution):	A measure of the asymmetry of a probability distribution.
Standard Deviation (SD):	In probability and statistics, a measure of the spread or dispersion that exists from the average value, typically shown as the symbol σ.
Standard Error (SE):	A measure of the accuracy of predictions. In hydrology, SE is often reported as the accuracy, in percent, of a discharge estimate developed using regional regression equations.
Stochastic:	A non-deterministic system or process which is characterized both by the system's predictable actions and by a random element.
Target Reliability:	The desired level of probability of non-exceedance. See Reliability Index.
Uncertainty (Aleatory):	Sources of uncertainty which reflect the natural randomness of a process and which cannot be suppressed by making more accurate measurements. Also referred to as statistical uncertainty.
Uncertainty (Epistemic):	Sources of uncertainty that reflect the inaccuracies in the modeling of a process. Also referred to as modeling uncertainty.
Z Limit:	The number of standard deviations from the mean.